

Investigations of the Formation and the *In-Vitro* Hydrolysis of Acyl Chain Oxidation Products Formed Upon Heating of Phytosteryl/-stanyl Fatty Acid Esters

Veronika Maria Stiegler

Vollständiger Abdruck der von der TUM School of Life Sciences der Technischen Universität München zu Erlangung einer

Doktorin der Naturwissenschaften
(Dr. rer. nat.)

genehmigten Dissertation.

Vorsitz: Prof. Dr. Wilfried Schwab

Prüfende der Dissertation:

1. Prof. Dr. Karl-Heinz Engel
2. Prof. Dr. Michael Rychlik

Die Dissertation wurde am 24.07.2024 bei der Technischen Universität München eingereicht und durch die TUM School of Life Sciences am 30.10.2024 angenommen.

ACKNOWLEDGEMENTS

The present work was carried out under supervision of Prof. Karl-Heinz Engel at the Chair of General Food Technology of the Technical University Munich. I want to thank Prof. Engel for the opportunity to work on this subject, for his scientific support and his enduring guidance in completing this thesis.

The support of Prof. Dr. Wolfgang Eisenreich and Christine Schwarz (Department of Chemistry, TUM) in the acquisition of NMR spectra of synthesized compounds is gratefully acknowledged. Prof. Dr. Corinna Dawid and Verena Mittermeier (Chair of Food Chemistry and Molecular Sensory Science, TUM) are thanked for their support regarding the HPLC-ELSD analysis.

Many thanks go to my former colleagues at the Chair of General Food Technology, in particular Dr. Anja Riegel, Dr. Walter Weiss, Dr. Birgit Scholz, Dr. Sophia Goßner, Dr. Christiane Kiske, Dr. Chenguang Zhou, Dr. Stefan Wocheslander, Dr. Ludwig Ziegler, Prof. Motoko Wakabayashi, Dr. Hidehiko Wakabayashi, Verena Breu, Claudia Steinmetz, Iulia Poplacean, Manuela Wilk, and Rudolf Harpaintner. Further, I thank all students, in particular, David Stöttner, Nadia Syam, and Quentin Thiel for their practical assistance.

I am especially grateful for Dr. Anja Riegel's invaluable help and creative inspiration in completing this thesis.

TABLE OF CONTENTS

ACKNOWLEDGEMENTS	I
TABLE OF CONTENTS	II
LIST OF FIGURES	V
LIST OF TABLES	X
ABBREVIATIONS	XII
1. INTRODUCTION AND OBJECTIVES	1
2. BACKGROUND	4
2.1 Sterols and Stanols	4
2.1.1 Structure and Occurrence	4
2.1.2 Biosynthesis	7
2.1.3 Biological Function	9
2.1.4 Metabolism	10
2.1.5 Cholesterol-Lowering Effect	13
2.2 Oxidations	15
2.2.1 Oxidation of the Phytosterol/-stanol Moiety	15
2.2.2 Oxidation of the Fatty Acid Moiety	17
2.2.3 Oxidation of Phytosterol/-stanol Fatty Acid Esters	23
2.2.4 Impact of Oxidation Products on Metabolism	24
2.3 Hydrolysis of Steryl/Stanyl Esters and Their Oxidation Products	24
2.3.1 Hydrolysis of Cholesteryl esters	24
2.3.2 Hydrolysis of Phytosteryl/-stanyl esters	26
2.3.3 Hydrolysis of Oxidized Phytosteryl/-stanyl esters	28
2.4 Analytical Methods	28
2.4.1 Analysis of Phytosterols/-stanols	28
2.4.2 Analysis of Fatty acids	30
2.4.3 Analysis of (Intact) Phytosteryl/-stanyl Esters	31
3. MATERIALS AND METHODS	33
3.1 Materials	33
3.1.1 Chemicals	33
3.1.2 Syntheses of Reference Compounds and Substrates	35

3.1.2.1 Internal Standards for UHPLC-MS/MS-Based Analysis of ACOPs	35
3.1.2.2 Reference Compounds for UHPLC-MS/MS-Based Analysis of ACOPs	36
3.1.2.3. Reference Compounds for GC-Based Analysis of ACOPs	42
3.1.2.4 Substrates for <i>In-Vitro</i> Hydrolyses	43
3.2 Methods.....	46
3.2.1 GC-Based Analysis of Long-Chain ACOPs.....	46
3.2.1.1 Long-Chain ACOPs Formed From Sitostanyl Oleate.....	46
3.2.1.2 Long-Chain ACOPs From Other Oleates.....	47
3.2.1.3 Quantitation of Fatty Acid Methyl Esters with GC-FID	48
3.2.2 <i>In-Vitro</i> Hydrolysis of ACOPs	49
3.2.2.1 <i>In-Vitro</i> Hydrolysis with Cholesteryl Esterase	49
3.2.2.2 Determination of Conversion Rates with GC-FID	51
3.2.3 GC Analysis	52
3.2.3.1 GC-FID	52
3.2.3.2 GC-MS.....	52
3.2.4 Further Analysis	53
3.2.4.1 NMR Spectroscopy	53
3.2.4.2 HPLC-ELSD Analysis	53
4. RESULTS AND DISCUSSION.....	54
4.1 Syntheses of ACOPs Used as Internal Standards and Reference Compounds for UHPLC-MS/MS-Based Analysis.....	54
4.1.1 Introduction	54
4.1.2 Syntheses of Internal Standards	55
4.1.3 Syntheses of Reference Substances	60
4.1.4 ACOPs Formed upon Thermo-oxidation of Sitostanyl Oleate	71
4.1.5 Summary.....	73
4.2 GC-Based Investigations of Long-Chain ACOPs Formed Upon Thermo-oxidation of Sitostanyl Oleate.....	74
4.2.1 Introduction	74
4.2.2 Methodology.....	74
4.2.3 Syntheses of Methyl Esters of Long-Chain ACOPs to be Used as Reference Compounds.....	77
4.2.4 Identification of ACOPs	83

4.2.5 Quantitation of Long-Chain ACOPs	89
4.2.5.1 Approach	89
4.2.5.2 Temperature Dependence of the Formation of Long-Chain ACOPs... ..	91
4.2.5.3 Time Dependence of the Formation of Long-Chain ACOP at 180°C and 200°C.....	94
4.2.5.4 Formation of Long-Chain ACOPs Upon Heating of Other Oleates ...	100
4.2.5.5 Discussion	103
4.2.5.6 Summary	113
4.3 <i>In-Vitro</i> Hydrolyses of Steryl/Stanyl Oleates and Respective ACOPs	115
4.3.1 Introduction	115
4.3.2 Methodology.....	116
4.3.3 Hydrolysis of Unaltered Steryl/Stanyl Oleates.....	119
4.3.4 Hydrolysis of ACOPs Derived from Sitostanyl and Sitosteryl Oleate.....	120
4.3.5 Influence of Cholesteryl Oleate on the Conversions of ACOPs	125
4.3.5.1 <i>In-vitro</i> Hydrolyses of Stanyl ACOPs in the Presence of Cholesteryl Oleate	125
4.3.5.2 <i>In-vitro</i> Hydrolyses of Steryl ACOPs in the Absence/Presence of Cholesteryl Oleate	128
4.3.5.3 Additional Studies on the Influence of Cholesteryl Oleate on the Conversions of Sitostanyl Oleate and Respective ACOPs	131
4.3.6 Influence of ACOPs on the Conversion of Cholesteryl Oleate	134
4.3.6.1 Impact of the <i>In-vitro</i> Hydrolysis Conditions on the Conversion of Cholesteryl Oleate in the Absence/Presence of Sitosteryl 9,10- Dihydroxystearate.....	136
4.3.7 Discussion.....	138
4.3.8 Summary.....	143
5. SUMMARY	144
6. ZUSAMMENFASSUNG	147
7. REFERENCES	150
8. PUBLICATIONS AND PRESENTATIONS.....	165

LIST OF FIGURES

Figure 1: Structure and numbering of steroids according to IUPAC-IUB recommendations (Moss, 1989).	4
Figure 2: Structure of cholesterol.....	5
Figure 3: Examples of phytosterols (a: campesterol, b: sitosterol, c: stigmasterol) and phytostanols (d: campestanol, e: sitostanol).....	6
Figure 4: Simplified pathway outlining principle steps of the biosynthesis of cholesterol and sitosterol.	8
Figure 5: Major metabolic pathways of cholesteryl and phytosteryl/stanyl esters in humans (adapted from Calpe-Berdiel <i>et al.</i> (2009)).....	11
Figure 6: Structures of main phytosterol oxidation products (POPs) derived from sitosterol (a: 7-hydroxysitosterol, b: 7-ketositosterol, c: 5,6-epoxysitosterol, d: 5,6-dihydroxysitosterol).....	17
Figure 7: Structures of hydroperoxides in positions 8, 9, 10, and 11 generated from oleates due to thermo-oxidation.	18
Figure 8: Functional groups in potential long-chain oxidation products of oleate: allylic keto group (a), epoxy group in the position of the former double bond, i.e. 9,10-epoxystearate (b), allylic epoxy group (c), 1,2-dihydroxy group in the position of the former double bond, i.e. 9,10-dihydroxystearate (d), 1,2-dihydroxy group adjacent to the shifted double bond (e), allylic 1,4-dihydroxy group (f).	19
Figure 9: Formation of aldehyde, hydroxy, and olefinic oxidation products from 8-hydroperoxide (A) or 10-hydroperoxide (B) of oleate via homolytic β -scission, resulting in the short-chain oxidation products 8-oxooctanoate, 7-oxoheptanoate, 6-oxohexanoate, 7-hydroxyheptanoate, heptanoate (A) or 10-oxoundecenoate and 9-oxononanoate (B).	22
Figure 10: Structures of unconjugated and conjugated bile acid sodium salts differing in the number of hydroxy groups.	25
Figure 11: Hydrolysis of sitosteryl octanoate to octanoic acid and sitosterol via pancreatic cholesteryl esterase (PCE).....	27
Figure 12: Structures of sitosterol (a) and its silylated (b) or acetylated (c) derivatives.	29
Figure 13: Structures of 8-hydroxyoctadec-9-enoic acid (a) and its actually analyzed derivative (b). Three steps of derivatisation were applied: (i) methylation of the acid group, (ii) silylation of the hydroxy group, and (iii) hydrogenation of double bond. ...	30
Figure 14: UHPLC-MS/MS-based approach for the analysis of ACOPs of sitostanyl oleate (Scholz <i>et al.</i> , 2019).	54
Figure 15: Structures of the synthesized internal standards used for UHPLC-MS/MS-based analysis: cholestanyl heptanoate IS ₁ , cholestanyl oleate IS ₂ , cholestanyl 9-hydroxynonanoate IS ₃ , cholestanyl <i>cis</i> -9,10-epoxystearate IS ₄ , and cholestanyl 6-oxoheptanoate IS ₅	56
Figure 16: Synthesis of cholestanyl heptanoate IS ₁ via Steglich esterification of heptanoic acid and cholestanol.	56
Figure 17: Synthesis of cholestanyl oleate IS ₂ from oleic acid and cholestanol.....	57
Figure 18: Procedure applied to synthesize cholestanyl 9-hydroxynonanoate IS ₃ . ..	58
Figure 19: Synthesis of cholestanyl <i>cis</i> -9,10-epoxystearate IS ₄ via epoxidation of cholestanyl oleate IS ₂	59

Figure 20: Synthesis of cholestanyl 6-oxoheptanoate IS₅ via Steglich esterification of 6-oxoheptanoic acid and cholestanol.	59
Figure 21: Structures of the remaining unaltered sitostanyl oleate 3 and of the short-chain non-polar ACOPs sitostanyl heptanoate 1 and sitostanyl octanoate 2	61
Figure 22: Synthesis of sitostanyl heptanoate 1 via Einhorn-acylation.	61
Figure 23: Structures of ACOPs of sitostanyl oleate containing one or two hydroxy groups in the fatty acid moiety: sitostanyl 7-hydroxyheptanoate 4 , sitostanyl 8-hydroxyoctanoate 5 , sitostanyl 9-hydroxynonanoate 6 , sitostanyl 9,10-dihydroxystearate 7 , and sitostanyl 8/11-hydroxyoctadecen-(9 <i>E</i>)-oate 8a,b	62
Figure 24: Synthesis of sitostanyl 7-hydroxyheptanoate 4	63
Figure 25: Synthesis of 8/11-hydroxyoctadecen-(9 <i>E</i>)-oic acid via allylic hydroxylation of oleic acid.....	63
Figure 26: Synthesis of sitostanyl 9,10-dihydroxystearate 7	63
Figure 27: Structures of sitostanyl <i>cis</i> -9,10-epoxystearate 10a , sitostanyl <i>cis</i> -9,10-epoxyoctadecen-(11 <i>E</i>)-oate 9a , and sitostanyl <i>trans</i> -11,12-epoxyoctadecen-(9 <i>Z</i>)-oate 9b	64
Figure 28: Structures of synthesized ACOPs carrying a keto-group in the fatty acid chain: positional isomers of sitostanyl oxo octadecenoate 22a-d , positional isomers of sitostanyl oxo octadecanoate 23a-d , sitostanyl 6-oxoheptanoate 15 , sitostanyl 5-oxohexanoate 13 , and sitostanyl 4-oxopentanoate 11	66
Figure 29: Oxidation of methyl oleate with <i>t</i> BHP to positional isomers of methyl oxooctadecenoates.	67
Figure 30: Demethylation of methyl 8-oxooctadecen-(9 <i>E</i>)-oate with barium hydroxide.	67
Figure 31: Hydrogenation of methyl oxooctadecenoate.....	68
Figure 32: ACOPs containing an aldehyde group: sitostanyl 10-oxodecanoate 19 , sitostanyl 9-oxononanoate 17 , sitostanyl 8-oxooctanoate 16 , sitostanyl 7-oxoheptanoate 14 , sitostanyl 11-oxoundecene-(9 <i>E</i>)-noate 21 , and sitostanyl 10-oxodecenoate (8 <i>E</i>)-noate 18	69
Figure 33: Demethylation of methyl 10-oxodecanoate.	69
Figure 34: Synthesis of 7-oxoheptanoic acid from heptanone via Baeyer-Villiger-reaction, lactone opening and oxidation with IBX.	70
Figure 35: Wittig-type reaction for synthesis of sitostanyl 11-oxo-undecene-(9 <i>E</i>)-noate 21	70
Figure 36: Procedure applied for the GC-based analysis of long-chain ACOPs formed upon heating of sitostanyl oleate.	75
Figure 37: Structures of internal standards used for the GC-based quantitation of long-chain ACOPs: methyl palmitate IS₆ and methyl ricinoleate IS₇	75
Figure 38: Synthesis of <i>cis</i> -9,10-epoxystearate 34 via epoxidation of methyl oleate.	77
Figure 39: Synthesis of methyl 9,10-dihydroxystearate 36 via ring opening of the epoxide.	78
Figure 40: Products obtained by hydroxylation of methyl oleate with selenium dioxide / <i>t</i> BHP.	79
Figure 41: GC-separation of the products obtained by hydroxylation of methyl oleate with selenium dioxide / <i>t</i> BHP. A: non-silylated, B: after silylation.....	80
Figure 42: Characteristic mass fragments of methyl hydroxyoctadecenoates (29-31) obtained by hydroxylation of methyl oleate with selenium dioxide / <i>t</i> BHP in their (A) non-silylated or (B) silylated form.	81

Figure 43: GC-chromatograms of the transesterified non-polar (A) and polar fraction (B) obtained after heating of sitostanyl oleate (180°C, 60 min.). methyl palmitate IS ₆ , methyl ricinoleate IS ₇ , methyl oleate 28 , methyl 10-hydroxyoctadec-8-enoate 29 , methyl 9-hydroxyoctadec-10-enoate 30 , methyl 8-hydroxyoctadec-9-enoate 31 , methyl 11-hydroxyoctadec-9-enoate 32 , methyl <i>trans</i> -9,10-epoxystearate 33 , methyl <i>cis</i> -9,10-epoxystearate 34 , methyl 8/9/10/11-oxooctadecenoate 35 , methyl 9,10-dihydroxystearate 36 , campestanol 52 , sitostanol 53 . Marked (*) compounds were tentatively assigned based on their GC-FID retention times.....	84
Figure 44: Structures of compounds identified in the transesterified polar fraction of heated (180°C, 60 min.) sitostanyl oleate 3 . Methyl <i>trans</i> -9,10-epoxystearate 33 , methyl <i>cis</i> -9,10-epoxystearate 34 , methyl 9,10-dihydroxystearate 36 , methyl 8-hydroxyoctadec-(9 <i>E</i>)-enoate 31 , methyl 11-hydroxyoctadec-(9 <i>E</i>)-enoate 32 , methyl 10-hydroxyoctadec-8-enoate 29 , and methyl 9-hydroxyoctadec-10-enoate 30	85
Figure 45: Segments of GC-FID chromatograms of the transesterified polar fraction of heated (180°C, 60 min.) sitostanyl oleate. The upper chromatogram corresponds to the non-silylated, the lower to the silylated sample.....	86
Figure 46: Structures of methyl oxooctadecenoates, which could not be separated under the applied conditions.....	88
Figure 47: Structures of tentatively assigned short-chain oxidation products in the transesterified polar fraction of heated (180°C, 60 min.) sitostanyl oleate 3 . Methyl 5-oxohexanoate 24 , methyl 8-hydroxyoctanoate 25 , methyl 7-oxoheptanoate 26 , and methyl 8-oxooctanoate 27	89
Figure 48: Amounts of long-chain ACOPs formed upon heating of sitostanyl oleate for 30 minutes at different temperatures. Values represent means of triplicate experiments and respective standard deviations.	92
Figure 49: Amounts of remaining sitostanyl oleate, in which the acyl chain has not been oxidized, after heating for different periods at 180°C and 200°C, respectively. Values represent means of triplicate experiments and respective standard deviations.....	95
Figure 50: Amounts of ACOPs formed upon heating of sitostanyl oleate for different times from 15 min. to 180 min. A : 180°C, B : 200°C. Values represent means of triplicate experiments and respective standard deviations.	96
Figure 51: Amounts of remaining oleate after heating to 180°C for 30 minutes. The data are based on the quantitation of methyl oleate resulting from transesterification; for the calculation of the value for triolein, the presence of three oleic acid moieties was taken into account. Values represent means of triplicate experiments and respective standard deviations.	101
Figure 52: Long-chain ACOPs determined after heating different oleates for 30 minutes at 180°C. The data are based on the quantitation of methyl esters resulting from transesterification; for the calculation of the value for triolein, the presence of three oleic acid moieties was taken into account. Values represent means of triplicate experiments and respective standard deviations.....	102
Figure 53: Amounts of different classes of long-chain ACOPs in heated (180°C, 30 min.) sitostanyl oleate determined by UHPLC/MS-MS analysis (Scholz <i>et al.</i> , 2019) and by GC, respectively.....	106
Figure 54: Comparison of the decrease of sitostanyl oleate and the increase of sitostanyl long-chain ACOPs upon thermal treatment of sitostanyl oleate at 180°C (A) or 200°C (B) for different durations. Values represent means of triplicate experiments and respective standard deviations.	112

Figure 55: Procedure applied for the <i>in-vitro</i> hydrolyses.....	116
Figure 56: Structures of ACOPs subjected to <i>in-vitro</i> hydrolyses.	118
Figure 57: Conversions determined in PCE-catalyzed hydrolyses of different steryl and stanyl oleates (77 nmol). Values represent means of triplicate experiments and confidence intervals. Different letters indicate statistically significant differences (Games-Howell $p < 0.05$).....	120
Figure 58: Conversions (%) of sitostanyl oleate 3 and respective ACOPs (77 nmol each) upon <i>in-vitro</i> PCE-catalyzed hydrolysis (1h). The substrate numbers and the abbreviations correspond to those in Table 17. The data were assessed by one-way ANOVA; different letters indicate statistically significant differences (Games-Howell test at $p < 0.05$). Values represent means of triplicate experiments and respective confidence intervals.....	121
Figure 59: Conversions (%) of sitosteryl oleate 43 and respective ACOPs (77 nmol each) upon <i>in-vitro</i> PCE-catalyzed hydrolysis (1h). The substrate numbers and the abbreviations correspond to those in Table 17. The data were assessed by one-way ANOVA; different letters indicate statistically significant differences (Games-Howell test at $p < 0.05$). Values represent means of triplicate experiments and respective confidence intervals.....	122
Figure 60: Conversions (%) of sitostanyl oleate 3 and its ACOPs (each 77nmol) upon PCE-catalyzed <i>in-vitro</i> hydrolysis. The grey bars represent sitostanyl esters in the absence of cholesteryl oleate 37 , the white bars represent sitostanyl esters in the presence of an equimolar amount of cholesteryl oleate 37 . The data were assessed by one-way ANOVA; different letters indicate significant differences (Games-Howell test at $p < 0.05$) in the conversions for the series of stanyl esters with and without addition of cholesteryl oleate 37 , respectively. The * indicate a significant difference (Welch-test at $p < 0.05$) at pairwise comparison of the conversions of the respective ACOP without/with added cholesteryl oleate. The peak numbers and the abbreviations correspond to those of Table 17. Values represent means of triplicate experiments and respective confidence intervals.....	126
Figure 61: Conversions (%) of sitosteryl oleate 43 and its ACOPs (each 77nmol) upon PCE-catalyzed <i>in-vitro</i> hydrolysis. The black bars represent sitosteryl esters in the absence of cholesteryl oleate 37 , the shaded bars represent sitosteryl esters in the presence of an equimolar amount of cholesteryl oleate 37 . The data were assessed by one-way ANOVA; different letters indicate significant differences (Games-Howell test, $p < 0.05$) in the conversions for the series of steryl esters with and without addition of cholesteryl oleate 37 , respectively. The * indicate a significant difference (Welch-Test, $p < 0.05$) at pairwise comparison of conversions of the respective ACOP without/with added cholesteryl oleate. The peak numbers and the abbreviations correspond to those of Table 17. Values represent means of triplicate experiments and respective confidence intervals.....	129
Figure 62: Conversion of sitostanyl oleate 3 depending on the amount of cholesteryl oleate 37 added to the hydrolysis mixture. Values represent means of triplicate experiments and respective confidence intervals.	132
Figure 63: Conversions (%) of sitostanyl oleate 3 , sitostanyl 7-oxoheptanoate 14 , sitostanyl heptanoate 1 and sitostanyl 5-oxohexanoate 15 upon <i>in-vitro</i> PCE-catalyzed hydrolysis (1h) in the presence of either cholesteryl oleate or its hydrolysis products oleic acid and cholesterol, respectively. The data were assessed by one-way ANOVA; different letters indicate significant differences (Games-Howell test at $p < 0.05$) in the	

- conversions for the series of different stanyl esters, respectively. Values represent means of triplicate experiments and respective confidence intervals. 134
- Figure 64: Conversions (%) of cholesteryl oleate **37** upon *in-vitro* PCE-catalyzed hydrolysis (1h) in the presence of equimolar amounts (77 nmol each) of (i) intact stanyl/steryl oleates, (ii) ACOPs derived from sitostanyl oleate, and (iii) ACOPs derived from sitosteryl oleate. The data were assessed by one-way ANOVA; different letters indicate significant differences (Games-Howell test at $p < 0.05$). Values represent means of triplicate experiments and respective confidence intervals. 135
- Figure 65: Conversions (%) of 77 nmol cholesteryl oleate **37** without addition of sitosteryl 9,10-dihydroxystearate **44** (shaded bars) or with addition of 105 nmol sitosteryl 9,10-dihydroxystearate **44** (white bars) to the hydrolysis mixture. Experiments were performed using (A) 19-hydroxycholesterol **IS₉** or (B) 5 α -cholestane **IS₈** as internal standard, and sodium desoxycholate (A1, B1) or a bile salt mixture (A2, B2). The data were assessed by one-way ANOVA; different letters indicate significant differences (Games-Howell test at $p < 0.05$). Values represent means of triplicate experiments and respective confidence intervals. 137

LIST OF TABLES

Table 1: Purities of esters used as substrates for <i>in-vitro</i> hydrolyses.	44
Table 2: Amounts of starting substances used for esterification of stanol / sterol and fatty acid under nitrogen atmosphere (Barnsteiner <i>et al.</i> , 2012) and ratio of elution solvents employed for purification with flash chromatography.	45
Table 3: Amounts of starting substances used for esterification of sitosteryl esters via Steglich esterification (Wocheslander <i>et al.</i> , 2016) and ratio of elution solvents employed for purification with flash chromatography.	46
Table 4: Amounts of oleic acid and cholesterol, respectively, added to the hydrolysis mixtures of sitostanyl esters.	50
Table 5: ACOPs formed upon heating (180°C, 30 min.) of sitostanyl oleate determined by Scholz <i>et al.</i> (2019) via UHPLC-MS/MS-analysis, using the synthesized internal standards and reference substances described in sections 4.1.2 and 4.1.3.	72
Table 6: Mass spectral data of methyl <i>trans</i> - and <i>cis</i> -9,10-epoxystearate 33,34	77
Table 7: GC-MS data of methyl 9,10-dihydroxystearate 36	78
Table 8: GC-MS-data of the silylated products obtained by hydroxylation of methyl oleate with selenium dioxide / tBHP.	82
Table 9: Mass spectral data of methyl 8/9/10/11-oxooctadecenoate 35	83
Table 10: GC-MS-data of methyl hydroxyoctadecenoates identified in the transesterified polar fraction of heated (180°C, 60 min.) sitostanyl oleate. The compound numbers correspond to those in Figure 43.	88
Table 11: Limits of detection (LOD), limits of quantitation (LOQ) and relative response factors (RRF) of various methyl esters.	90
Table 12: Recovery rates of sitostanyl oleate 3 , sitostanyl <i>cis</i> 9,10-epoxystearate 10a , and sitostanyl 9,10-dihydroxystearate 7 . Values represent means of triplicate experiments and respective standard deviations.	91
Table 13: Amounts (mol%) of long-chain ACOPs formed upon heating of sitostanyl oleate for 30 minutes at different temperatures. Values represent means of triplicate experiments and respective standard deviations.	93
Table 14: Amounts (mol%) of remaining unaltered ester and of long-chain oxidation products formed upon heating of sitostanyl oleate 3 at 180°C for different time periods. Values represent means of triplicate experiments and respective standard deviations.	98
Table 15: Amounts (mol%) of remaining unaltered ester and of long-chain oxidation products formed upon heating of sitostanyl oleate 3 at 200°C for different time periods. Values represent means of triplicate experiments and respective standard deviations.	99
Table 16: Conversions (%) determined in triplicate experiments performed either on one or on three different days. Values represent means and confidence intervals.	119
Table 17: Conversions (%) of sitostanyl oleate 3 and sitosteryl oleate 43 and their ACOPs (77 nmol each) upon PCE-catalyzed <i>in-vitro</i> hydrolysis. Values represent means of triplicate experiments and respective confidence intervals.	124
Table 18: Conversion (%) of sitostanyl oleate 3 and its ACOPs (each 77nmol) upon PCE-catalyzed <i>in-vitro</i> hydrolyses with and without addition of an equimolar amount of cholesteryl oleate (CO) 37 to the hydrolysis mixtures. Values represent means of triplicate experiments and respective confidence intervals.	128

Table 19: Conversions (%) of sitosteryl oleate **43** and its ACOPs (each 77nmol) upon PCE-catalyzed *in-vitro* hydrolysis with and without addition of an equimolar amount of cholesteryl oleate (CO) **37** to the hydrolysis mixture. Values represent means of triplicate and respective confidence intervals. 131

ABBREVIATIONS

ABCA1	ATP Binding Cassette Subfamily A Member 1
ABCG5/8	ATP Binding Cassette Subfamily G Member 5/8
ACAT2	Acyl-CoA:Cholesterol Acyltransferase 2
ACOP	Acyl Chain Oxidation Product
APCI	Atmospheric Pressure Chemical Ionization
CLA	Conjugated Linoleic Acid
CO	Cholesteryl Oleate
DCM	Dichloromethane
DMAP	4-(Dimethylamino)pyridine
e.g.	exempli gratia
EFSA	European Food Safety Authority
EI	Electron Ionization
ELSD	Evaporative light scattering detector
FA	Fatty Acid
FAME	Fatty Acid Methyl Ester
FID	Flame Ionization Detector
GC	Gas Chromatography
HDL	High Density Lipoprotein
HPMC	Hydroxypropyl Methyl Cellulose
i.e.	id est
IBX	2-Iodoxybenzoic acid
ID	Inner Diameter
IS	Internal Standard

IUPAC	International Union of Pure and Applied Chemistry
LDL	Low Density Lipoprotein
LPL	Lipoprotein Lipase
LXR	Liver X Receptor
MALDI-TOF	Matrix Assisted Laser Desorption/Ionization – Time-of-flight
<i>m</i> -CPBA	3-Chloroperbenzoic acid
MS	Mass Spectrometer
MS/MS	Tandem Mass Spectrometer
MTBE	Methyl <i>tert</i> -Butyl Ether
MTP	Microsomal Triglyceride Transport Protein
NMR	Nuclear Magnetic Resonance
NPC1L1	Niemann-Pick C1 like 1
PBS	Phosphate-Buffered Saline
PCE	Pancreatic Cholesterol Esterase
POP	Phytosteryl Oxidation Products
PSE	Phytosteryl/Phytostanyl Esters
RCT	Reverse Cholesterol Transport
RRT	Relative Retention Time
SPE	Solid Phase Extraction
tBHP	<i>Tert</i> -Butylhydroperoxide
THF	Tetrahydrofuran
TMS	Trimethylsilyl
(U)HPLC	(Ultra) High Performance Liquid Chromatography
UV	Ultra-Violet

VLDL Very Low Density Lipoprotein

1. INTRODUCTION AND OBJECTIVES

An increased plasma low-density lipoprotein (LDL)-cholesterol level is considered as a risk factor for the development of cardiovascular diseases (Esrey *et al.*, 1996). In addition to therapeutic measures, the dietary consumption of phytosterols or phytostanols has been established as approach to reduce LDL-cholesterol levels. A daily intake of 2 - 3 g phytosterols/-stanols has been reported to lower plasma LDL-cholesterol levels by approximately 10 - 12 % (Katan *et al.*, 2003; De Smet *et al.*, 2012; Ras *et al.*, 2014). Consequently, a broad spectrum of foods is being enriched with phytosterols/-stanols (EFSA, 2010; Scholz *et al.*, 2015a). To increase the solubility in fat-based foods, they are mostly not added as free phytosterols/-stanols but as mixtures of esters of fatty acids obtained from sources, such as rapeseed or soybean oil.

Similar to other lipophilic food constituents, phytosteryl and phytostanyl fatty acid esters added to foods are anticipated to undergo oxidation reactions during household-type preparations or storage. Considering their structures, phytosteryl/-stanyl fatty acid esters may be oxidized in the sterol/stanol moieties as well as in the fatty acid chains (Scholz *et al.*, 2015a; Scholz *et al.*, 2019).

There has been extensive research on products resulting from thermo-oxidation of free sterols/stanols or steryl/stanyl moieties in respect to fatty acid esters. The spectrum of so-called POPs (phytosterol oxidation products) comprises keto-, hydroxy-, and epoxy-derivatives of the sterols/stanols. Various reviews on their formation, analysis, consumption and toxicological relevance are available (Otaegui-Arrazola *et al.*, 2010; Garcia-Llatas and Rodriguez-Estrada, 2011; Scholz *et al.*, 2015a; Feng *et al.*, 2020; Evtugin *et al.*, 2023).

There is also a large body of information available on oxidations of unsaturated fatty acid moieties in fats and oils. The decomposition of initially formed hydroperoxides leads to a broad array of chain-shortened as well as long-chain oxidized fatty acyl moieties possessing mainly aldehyde-, keto-, hydroxy- and epoxy groups (Neff and Byrdwell, 1998; Berdeaux *et al.*, 1999a; Velasco *et al.*, 2004b; Marmesat *et al.*, 2008; Brühl, 2014; Koch *et al.*, 2023). However, studies on the formation of acyl chain oxidation products (ACOPs) resulting from thermo-oxidation of the unsaturated fatty acid moieties of phytosteryl/-stanyl esters are scarce. Syntheses and HPLC-ESI-MS/MS-based analyses in heat-treated spreads enriched with phytosteryl esters have only been reported for one type of ACOPs formed upon thermo-oxidation of sitosteryl

oleate, i.e. sitosteryl 9,10-dihydroxystearate and 9,10-dihydroxystearates of 7-oxo, 7-hydroxy- and 5,6-epoxysitosterol (Julien-David *et al.*, 2008; Julien-David *et al.*, 2014). In addition, data from investigations dealing with the identification and quantitation of a limited spectrum of sitostanyl and sitosteryl ACOPs amenable to GC-analysis have been available (Wocheslander *et al.*, 2016; Wocheslander *et al.*, 2017).

The objective of the studies underlying this thesis was to extend this knowledge by elaborating for a broader spectrum of ACOPs formed upon thermo-oxidation of sitostanyl and sitosteryl oleate, respectively, data on their analysis and formation as well as on their fate in the course of *in-vitro* hydrolyses. The studies can be divided into the following parts:

- (i) A previously reported approach based on capillary gas chromatography (GC) resulted in the identification and quantification of ACOPs formed upon heating of phytosteryl/-stanyl oleates and linoleates (Wocheslander *et al.*, 2016; Wocheslander *et al.*, 2017). However, the spectrum of ACOPs covered by the employed methodology was limited to short and medium-chain non-polar alkanoates and polar oxo-, hydroxyalkanoates up to chain length C9 only. The studies performed in the first part of this thesis were embedded in a project aiming at the development of a UHPLC-MS/MS-based analysis covering a broader spectrum of ACOPs resulting from thermo-oxidation of sitostanyl oleate. The goal was to reduce the knowledge gap by particularly covering the anticipated long-chain ACOPs. To this end, the first tasks to be performed in the course of the thesis were syntheses of potential candidates of non-polar and polar (keto-, aldehyde-, hydroxy-) ACOPs expected to be formed upon thermo-oxidation of sitostanyl oleate. The synthesized sitostanyl ACOPs should serve as authentic reference compounds supporting identifications and quantifications in the course of the UHPLC-MS/MS-based analysis; respective cholestanyl analogues should be synthesized for use as internal standards.
- (ii) The representatives of ACOPs synthesized in the first part of this thesis as internal standards and reference compounds, respectively, were employed in the above-mentioned project to develop strategies for the UHPLC-MS/MS-based analysis of different classes of ACOPs resulting from thermo-oxidation of sitostanyl oleate

(Scholz *et al.*, 2019). The study revealed that the long-chain ACOPs sitostanyl *trans*- and *cis*-9,10-epoxystearate, sitostanyl 8- and 11-hydroxyoctadec-9-enoate, and sitostanyl 9,10-dihydroxystearate constituted the majority of the ACOPs determined in sitostanyl oleate subjected to heating at 180°C for 30 minutes. Therefore, the objective of the second part of the thesis was to follow the formation of these principal ACOPs of sitostanyl oleate at different time/temperature combinations reflecting household-type preparation conditions. In these studies, identifications and quantifications should be based on transesterification of the formed sitostanyl ACOPs and GC-analysis of the resulting methyl esters, using synthesized reference compounds.

- (iii) The cholesterol-lowering properties of phytosterols/-stanols are, at least partly, thought to be due to a competition of sterols/stanols with intestinal cholesterol for incorporation into mixed micelles and chylomicrons (De Smet *et al.*, 2012). In order to exert this effect, phytosteryl/stanyl fatty acid esters require hydrolysis by pancreatic cholesteryl esterase to liberate the free sterols/stanols (Piironen *et al.*, 2000; Trautwein *et al.*, 2003; Brown *et al.*, 2010). Scholz *et al.* (2017) demonstrated that *in-vitro* digestion of cholesterol in the presence of thermooxidized phytosteryl/stanyl fatty acid esters resulted in significant increases of cholesterol micellarization. According to Julien-David *et al.* (2009), sitosteryl 9,10-dihydroxystearate acted as non-competitive inhibitor of the PCE-catalyzed *in-vitro* hydrolysis of cholesteryl oleate and sitosteryl oleate. These data indicate a potential impact of the formation of ACOPs on the cholesterol-lowering efficacy of phytosteryl/stanyl fatty acid esters. Therefore, in the final part of the thesis, synthesized sitostanyl and sitosteryl ACOP representatives from different classes were subjected to *in-vitro* hydrolyses catalyzed by porcine cholesteryl esterase, and the conversions rates were compared to those of unaltered sitostanyl and sitosteryl oleate, respectively. In addition, the influence of the presence of cholesteryl oleate on the conversions of ACOPs and the influence of the presence of ACOPs on the conversions of cholesteryl oleate should be studied.

2. BACKGROUND

2.1 Sterols and Stanols

2.1.1 Structure and Occurrence

Sterols belong to the chemical group of steroids. Their nomenclature was standardized based on a recommendation of IUPAC-IUB (Moss, 1989). Steroids consist of a cyclopenta[α]phenanthrene skeleton with methyl groups in positions C-10 and C-13 (Figure 1). Sterols have a hydroxy group in position C-3 and a side chain in position C-17; there can also be methyl groups in positions C-4. Sterols occur in free form or conjugated to sugar moieties, phenolic acids or fatty acids at C-3 (Piironen *et al.*, 2000). Fatty acids in the range from C12 to C22 are known to be linked to sterols. The mainly occurring fatty acids are palmitic, stearic, oleic, linoleic, and linolenic acid (Dyas and Goad, 1993).

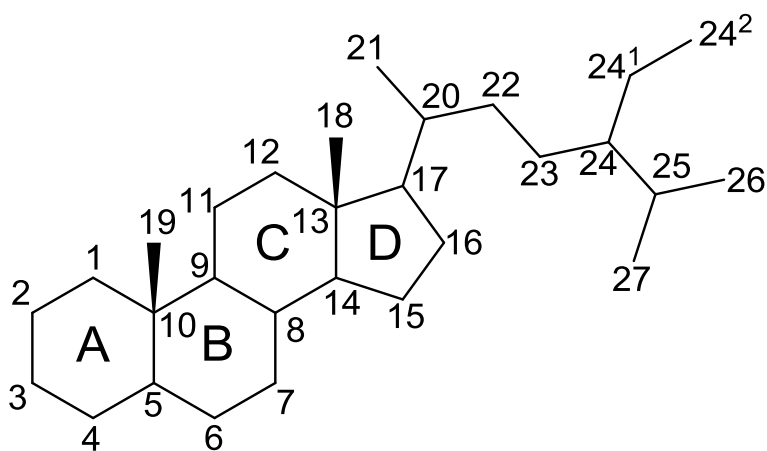


Figure 1: Structure and numbering of steroids according to IUPAC-IUB recommendations (Moss, 1989).

Cholesterol

The side chain of sterols in mammalian sources consists of eight carbon atoms. There is only one major sterol: cholesterol (Figure 2) (Hartmann, 1998). Cholesterol can be synthesized endogenously by mammals as well as be part of the diet. The main source in the diet are mammalian products such as meat, egg yolk, milk products or fish (Matissek and Baltes, 2016). In plants cholesterol is generally found only at low levels,

but there are also some species that are known to contain higher amounts of cholesterol (Moreau *et al.*, 2002).

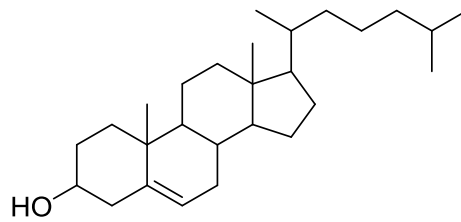


Figure 2: Structure of cholesterol.

Phytosterols

Sterols from plant origin are named phytosterols. The term phytosterol is in some literature used as general term for both plant sterols and stanols. In this thesis, it will be used specifically for plant sterols. There are more than 100 different phytosterols/-stanols known (Moreau *et al.*, 2002). They can be divided in different groups based on their structure. Depending on the presence of methyl groups in position C-4, they are called 4-desmethyl-, 4 α -monomethyl- and 4,4-dimethylsterols. The last mentioned are precursors during the biosynthesis of 4-desmethyl sterols and occur at low levels. A further division of 4-desmethyl sterols can be made based on the positions and the number of double bonds in the B-ring resulting in Δ^5 -sterols, Δ^7 -sterols, and $\Delta^{5,7}$ -sterols (Piironen *et al.*, 2000). The main dietary phytosterols are β -sitosterol (65%), campesterol (30%) and stigmasterol (5%) (Trautwein *et al.*, 2003); they are 4-desmethyl Δ^5 -sterols which have an additional substituent at C-24 (Piironen *et al.*, 2000). β -Sitosterol has an additional ethyl group (C-24¹ and C-24²), campesterol an additional methyl group (C-24¹) in the side chain and stigmasterol an additional ethyl group (C-24¹ and C-24²) and a double bond (Δ^{22}) (Figure 3). The alkylation at C-24 as well as the additional *trans*-configured double bond in Δ^{22} are specific for plant sterols (Piironen *et al.*, 2000).

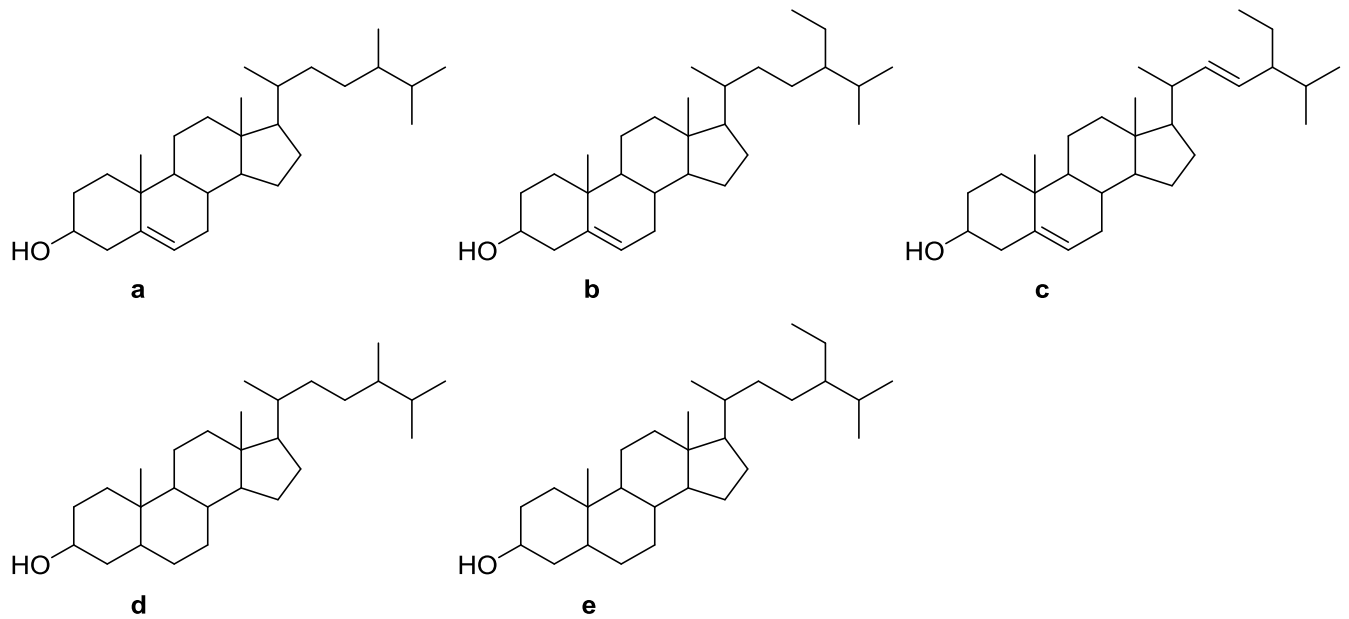


Figure 3: Examples of phytosterols (a: campesterol, b: sitosterol, c: stigmasterol) and phytostanols (d: campestanol, e: sitostanol).

Phytosterols occur in plants in free form, as fatty acid esters, glycosides, or hydroxycinnamates (Garcia-Llatas and Rodriguez-Estrada, 2011). The compositions of phytosterols in plants differ for each type of plant. In the same plant, the compositions found for C3-derivatized sterols are often similar to those of the free sterols (Dyas and Goad, 1993). Apart from being part of plant-based diet, phytosterols are added to foods due to their cholesterol-lowering effect (Scholz *et al.*, 2015a). The European Food Safety Authority (EFSA) initially authorized yellow fat spreads with added phytosteryl/stanyl esters, which are not meant to be used for cooking and baking. Later, the use was extended to other food products with the condition of labeling and limiting consumption to a maximum of 3 g per day (EFSA, 2010). Phytosterols/-stanols are known in a great variety of foods, for example in juices, yoghurts, yellow fat spreads, meat, bakery products, bars, or green teas (Chawla *et al.*, 2016).

Phytostanols

Phytostanols are the saturated (B-ring) form of phytosterols (EFSA, 2008). They occur in a normal diet at about 10% of the total sterol/stanol content (Ostlund, 2002). Among the most occurring members of this group are sitostanol (Figure 3), also known as stigmastanol, and campestanol (Katan *et al.*, 2003; Barnsteiner *et al.*, 2012). The main

sources are cereals, such as wheat, maize, and rye, and the above-mentioned cholesterol-lowering foods to which they are being added (Scholz *et al.*, 2015a).

Mycosterols

Mycosterols are sterols occurring in fungi. Ergosterol, the major representative, contains three double bonds $\Delta^{5,7,22}$ and a methyl group at C-24 (Hartmann, 1998; Garcia-Llatas and Rodriguez-Estrada, 2011).

2.1.2 Biosynthesis

A simplified pathway outlining principle steps of the biosynthesis of cholesterol and phytosterols is shown in Figure 4.

Mammals can synthesize cholesterol starting from acetyl-CoA (Nes, 2011). In several steps of the so-called mevalonate-pathway, squalene is formed as important intermediate which is further transformed to 2,3-oxidosqualene by squalene monooxygenase in a highly specific reaction in the endoplasmic reticulum. In the next step lanosterol synthetase converts linear 2,3-oxidosqualene into cyclic lanosterol. This stereo- and regiospecific mechanism is not fully investigated yet, but it comprises several steps such as protonation of the epoxide, ring formation, shift of hydrides and methyl groups, and deprotonation. Lanosterol is finally converted to cholesterol by several enzymatic reactions. Within the Bloch pathway, the side chain of lanosterol and further reaction products remain unsaturated (Δ^{24}), while within the Kandutsch-Russel pathway the side chain is saturated. The steps involved in the formation of cholesterol are demethylation and reduction at C-14, demethylation at C-4 and multiple-step rearrangement of the double bond in the B-ring. The saturation of the side chain could take place before (Kandutsch-Russel pathway), after (Bloch pathway) or during this reaction steps.

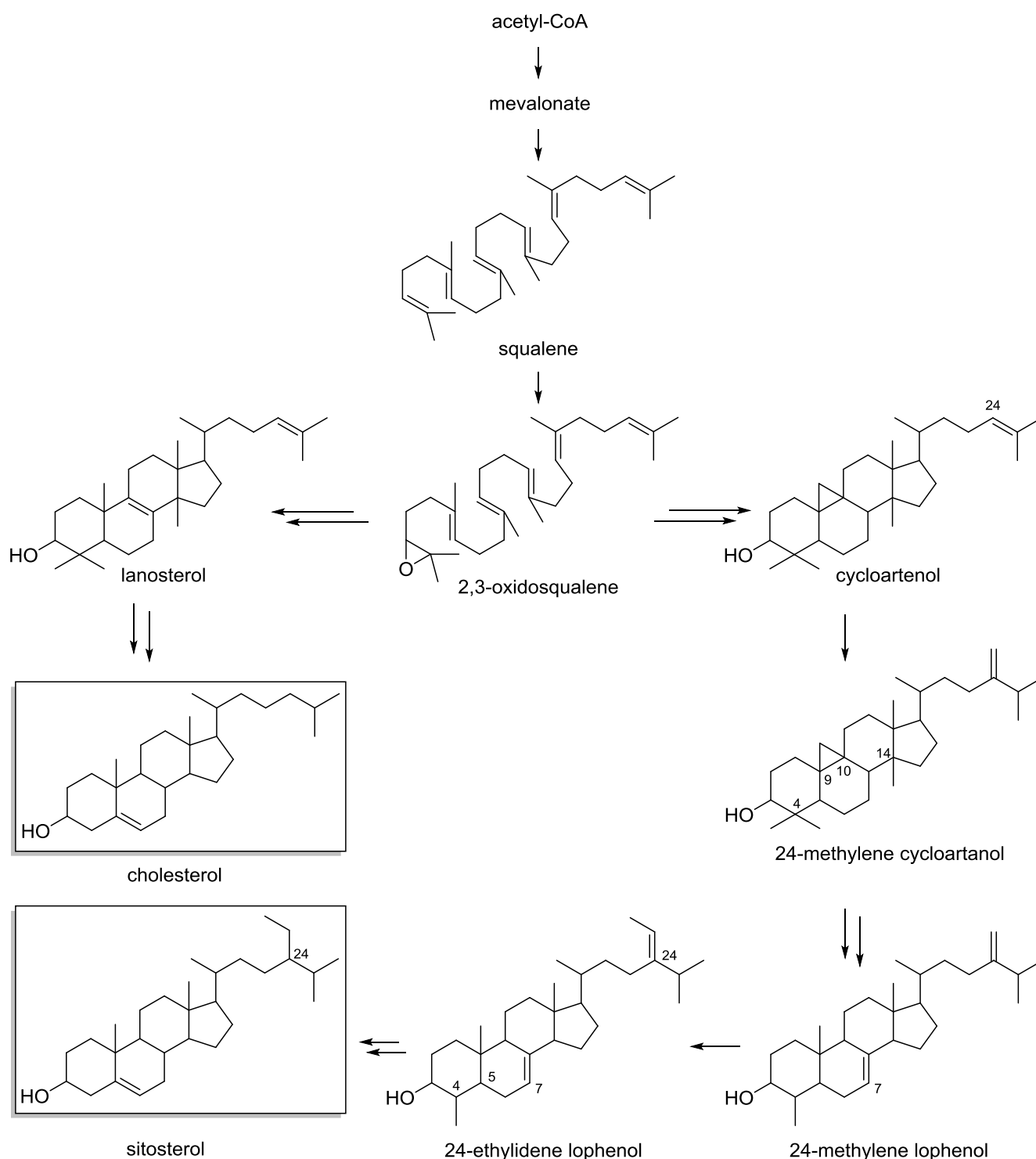


Figure 4: Simplified pathway outlining principle steps of the biosynthesis of cholesterol and sitosterol.

The synthetic pathway leading to sitosterol is similar to that of cholesterol up to the intermediate 2,3-oxidosqualene. In contrast to the route leading to cholesterol, in the next enzymatic step with cyclisation and rearrangement of hydrides and methyl groups, cycloartenol instead of lanosterol is formed. The following series of reactions starts

with methylation of the side chain of cycloartenol at C-24. In contrast to cholesterol biosynthesis, where demethylation starts at C-14, the demethylation starts at C-4 with removal of one methyl group. Subsequently, the cyclopropane ring (C9/10) is opened. Demethylation at C-14, Δ^{14} -reduction and isomerisation of Δ^8 to Δ^7 in the B-ring result in 24-methylene lophenol. At this stage, a second methylation in the side chain (C-24¹) takes place (24-ethylidene lophenol), followed by a demethylation at C-4. The conversion of Δ^7 to Δ^5 happens by an $\Delta^{7,5}$ intermediate. The last step in the synthesis of sitosterol is the reduction of Δ^{24} in the side chain. It is probable that the Δ^{22} bond is inserted at a very late reaction step as stigmasterol could be synthesized from sitosterol. The biosynthesis takes place exclusively in the cytoplasm. The enzymes are mostly located in the membrane of the plant endoplasmic reticulum (Benveniste, 1986; Piironen *et al.*, 2000).

As reviewed by Piironen *et al.* (2000), the biosynthesis of stanols is not well investigated, especially regarding regulation factors and responsible genes. It can be distinguished between sitostanol derived from plant material (5α reduction) and sitostanol derived from reduction by bacteria (5β reduction) in the large bowel (Ostlund, 2002). Some knowledge of stanol biosynthesis could be gained from investigations on biosynthesis of brassinosteroids where the synthesis of campestanol from campesterol is an important synthesis step. By cell feeding experiments it was shown that the multiple step synthesis is performed from campesterol via campest-4-en-3 β -ol, campest-4-en-3-one and campestan-3-one to campestanol (Fujioka and Sakurai, 1997; Noguchi *et al.*, 1999).

2.1.3 Biological Function

Cholesterol occurs in cell membranes and acts as precursor of different compounds such as bile acids, vitamins or steroid hormones. In cell membranes cholesterol provides more rigidity and closer packaging, but it is also involved in other membrane processes such as endocytosis. The polar hydroxy group can interact with polar group of phospholipids, the building blocks of the membranes. The hydrophobic carbon body can interact with the non-polar tails of the phospholipids (Cerqueira *et al.*, 2016). The cholesterol fatty acid esters are used for storage and transport (Garcia-Llatas and Rodriguez-Estrada, 2011).

Phytosterols/-stanols have similar functions in plants as cholesterol in mammals. They affect the fluidity and permeability of membranes and can modulate membrane-associated processes, such as the activity of ATPase. Additionally, they act as precursors of various metabolites, such as brassinosteroids or glycoalkaloids, and play a role in cellular differentiation and proliferation. Phytosteryl-/stanyl esters are also involved in transport and storage (Hartmann, 1998; Piironen *et al.*, 2000; Garcia-Llatas and Rodriguez-Estrada, 2011; Evtuyugin *et al.*, 2023).

2.1.4 Metabolism

Cholesterol

The daily intake of cholesterol in a Western diet is 300 – 600 mg. The minor proportion is provided as cholesteryl fatty acid esters (Trautwein *et al.*, 2003). The smaller amount of cholesterol in the intestinal lumen is from the diet, the more than three-fold amount is available from enterohepatic cycle and secreted *via* the liver and bile into the intestinal lumen. Dietary cholesterol and cholesteryl esters are emulsified by bile salts in the intestinal lumen into mixed micelles. There is a contrary debate, whether the biliary free cholesterol is preferred for incorporation in the micelles as it is already in micellar state or whether uptake of esterified cholesterol from the diet is more efficient due to the activity of pancreatic cholesteryl esterase which is responsible for the hydrolysis of cholesteryl esters (Figure 5). Cholesterol can either be excreted via colon and feces or the micelles interact and dissociate by contact with the apical brush-border membrane of enterocytes, the epithelial cells of the small intestine. For absorption of cholesterol in the enterocytes, the carrier protein Niemann-Pick C1 like 1 (NPC1L1) plays the major role. There are three different ways of further circulation in the enterocytes. Cholesterol can be excreted back in the intestinal lumen by transporters ABCG5 and ABCG8, which are regulated by liver X receptor (LXR). It can also be excreted as HDL-cholesterol by transporter ABCA1 to the lymph. Following the enterohepatic circulation, cholesterol is esterified with fatty acids in the enterocytes by acyl-CoA:cholesterol acyltransferase 2 (ACAT2) to cholesteryl esters. The esters are packed via microsomal triglyceride transport protein (MTP) and excreted as chylomicrons, which contain additionally apolipoprotein B-48, triglycerides or phospholipids, to the lymph and blood circulation. In the blood vessel, the triglycerides are hydrolyzed by endothelial lipoprotein lipase (LPL) and chylomicrons remnants are taken up in the liver.

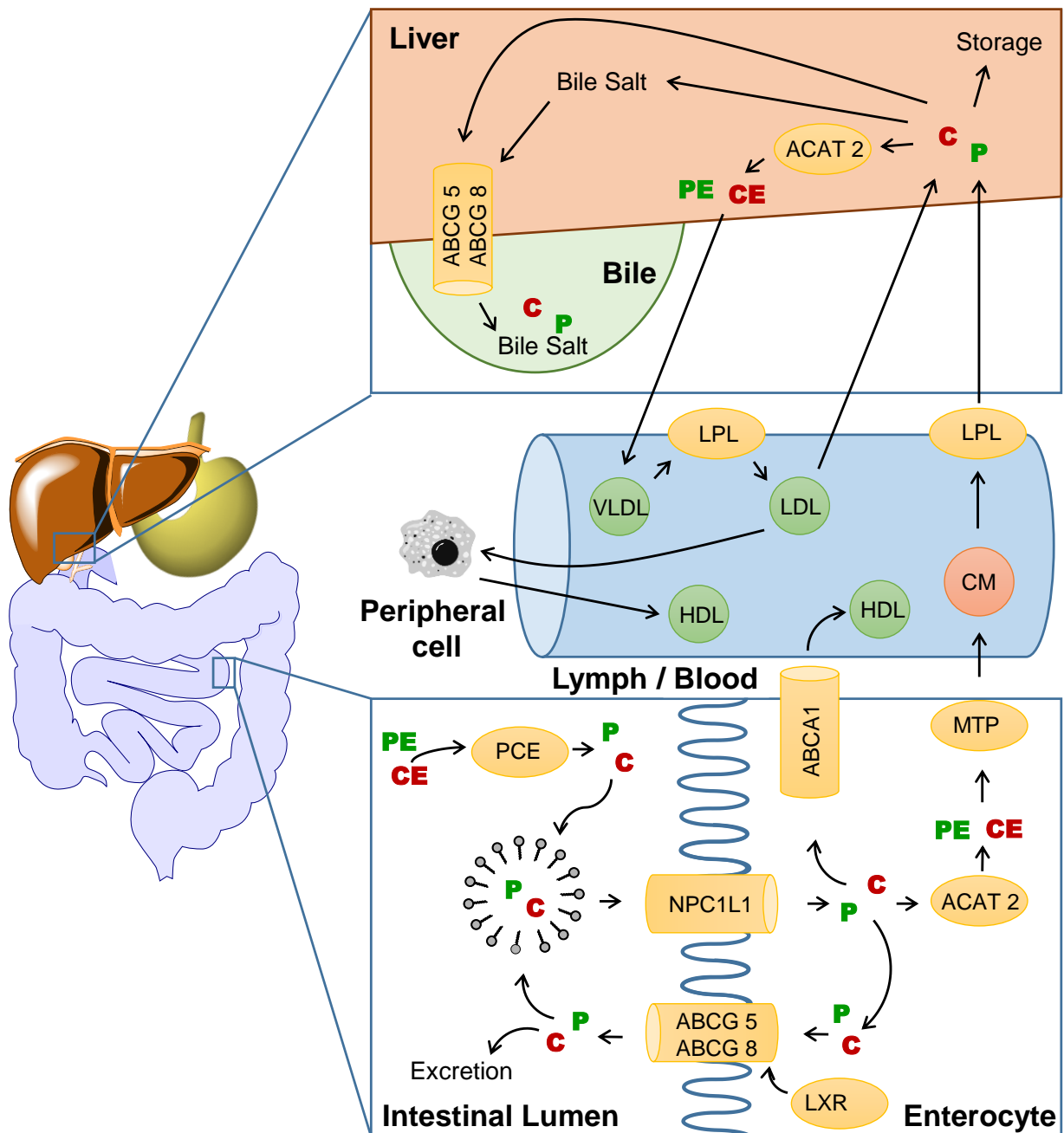


Figure 5: Major metabolic pathways of cholesteryl and phytosteryl/stanyl esters in humans (adapted from Calpe-Berdiel *et al.* (2009)).

ABCG5, ABCG8, ABCA1: adenosine triphosphate-binding cassette G5/G8/A1; ACAT2: acyl-CoA:cholesterol acyltransferase 2; C: cholesterol; CE: cholesteryl ester; PCE: pancreatic cholesteryl esterase; CM: chylomicron; HDL: high-density lipoprotein; LDL: low-density lipoprotein; LPL: lipoprotein lipase; LXR: liver X receptor; MTP: microsomal triglyceride transport protein; NPC1L1: Niemann-Pick C1 like 1 protein; P: phytosterol/phytostanol; PE: phytosteryl/phytostanyl ester; VLDL: very low-density lipoprotein.

In the liver the dietary cholesterol and the *de novo* synthesized cholesterol can go different ways. The regulation of the different ways depends on its intracellular concentration. Cholesterol can be stored in the liver or excreted as free cholesterol or bile salts via ABCG5 and ABCG8 transporter to the bile. From the bile, components are brought back to the intestinal lumen and the circulation process. Most of the cholesterol in the liver is esterified by ACAT2 and secreted as very low density lipoprotein (VLDL). By LPL it is transferred to low density lipoprotein (LDL), which can be transported to peripheral cells. Cholesterol uptake in these cells is regulated by LDL receptors. The transport of cholesterol from peripheral cells to the liver is operated via high density lipoprotein (HDL) particles and is called reverse cholesterol transport (RCT) (Trautwein *et al.*, 2003; von Bergmann *et al.*, 2005; Calpe-Berdiel *et al.*, 2009; Elshourbagy *et al.*, 2014).

Phytosterols/-stanols

The daily intake of phytosterols/-stanols ranges from 150 – 400 mg in free or esterified form, whereby β -sitosterol is the main component with 65% (Trautwein *et al.*, 2003). The absorption process in mammals differs scarcely from that of cholesterol. There is, however, a difference in the absorbed amounts. Approximately 40 – 60% of dietary cholesterol can be absorbed, while only 15% or less of dietary phytosterols/-stanols (De Smet *et al.*, 2012). The first step of metabolism is, as explained for cholesterol, incorporation into mixed micelles (Brufau *et al.*, 2008). Phytosterols/-stanols are subsequently esterified, hydrolyzed and transported with the same enzymes and proteins as cholesterol (Trautwein *et al.*, 2003; Moreau and Hicks, 2004). The main differences are the overall lower absorption of phytosterols/-stanols and that they cannot be transferred to bile salts (Brufau *et al.*, 2008). Additionally, it was found, that the transport particle chylomicron contains in particular cholesteryl esters, which are transported in the core of chylomicrons, and free phytosterols/-stanols, which serve as surface lipids. Comparable to cholesteryl esters, the free phytosterols/-stanols are absorbed by the liver from chylomicron remnants. The phytosterols/-stanols can be excreted by the liver via VLDL. Unlike the chylomicrons, the proportion of esterified phytosterols/-stanols was the same as for cholesterol in VLDL and LDL. Peripheral cells take phytosterols/-stanols and cholesterol equally, depending on their amount in LDL, up and incorporate both in the cells membrane. In the reverse way, the transport

by HDL the proportional amount of phytosterols/-stanols was higher than in LDL or VLDL (Trautwein *et al.*, 2003).

2.1.5 Cholesterol-Lowering Effect

The risk of cardiovascular diseases is correlated with a high level of plasma low-density lipoprotein (LDL)-cholesterol (Esrey *et al.*, 1996; Elshourbagy *et al.*, 2014). As phytosterols/-stanols undergo the same metabolic pathway as cholesterol, they are potential actors in lowering LDL-cholesterol level. A daily intake of 3 g phytosterols/stanols has been shown to lower the serum cholesterol level by 10 – 12%, higher amounts did not efficiently improve the effect (Katan *et al.*, 2003; EFSA, 2010; Ras *et al.*, 2014). The lowering effect is known since the 1950s. The studies started with free phytosterols/-stanols. Later it was found that there was no significant difference for the LDL-cholesterol level reduction whether using free sterols/stanols or their esterified form (De Smet *et al.*, 2012). Therefore, to improve solubility in the food matrix and bioavailability, fatty acid esters of sterols/stanols are used for addition to foods. The liberated free phytosterols/-stanols could lower cholesterol level derived from diet as well as cholesterol from enterohepatic circulation (Brufau *et al.*, 2008).

Within the intestinal absorption process of cholesterol, there are several potential steps at which the influence of phytosterols/-stanols on the LDL-cholesterol level could be explained. The first is co-crystallization of phytosterols/-stanols and cholesterol. Crystalline sterols/stanols have a very low bioavailability. β -Sitosterol was shown to be incorporated in cholesterol crystals; by the formation of these mixed crystals the cholesterol absorption was reduced. When using sitostanol, phase-separation was observed. As in general, β -sitosterol and sitostanol both reduce the LDL-cholesterol level similarly, *in-vivo* co-crystallization of cholesterol and sitostanol may be possible or the co-crystallization may play only a minor role in the reduction of LDL-cholesterol level (Trautwein *et al.*, 2003).

The next potential step, incorporation of sterols/stanols in mixed micelles, has been well investigated. Incorporation is needed as sterols/stanols are hydrophobic and have to be solubilized in micelles for their metabolism. As micelles have limited capacity, dietary cholesterol and phytosterols/-stanols compete for incorporation in mixed micelles. The bile, secreted during the digestion, provides a micellar system in which compounds such as sterols/stanols could be incorporated to be transported as free sterols/stanols. It was shown that the presence of phytosterols/-stanols reduces the

incorporation of cholesterol into mixed micelles and could even displace it. Therefore, less cholesterol was available for the transport and further absorption. This effect can especially take place when cholesterol and phytosterols/-stanols were digested at the same time (Katan *et al.*, 2003; Trautwein *et al.*, 2003). On the other hand, it was found that consumption of phytosterols/-stanols over three meals was as effective in lowering the LDL-cholesterol level as a single time consumption, indicating that incorporation into mixed micelles with a joint diet was not the only mechanism (De Smet *et al.*, 2012). In mixed micelles mainly the free sterols/stanols can be transported. Therefore, esters have to be hydrolyzed by pancreatic cholesteryl esterase (PCE) during digestion. About 20% of dietary cholesterol is present as ester and has to be hydrolyzed before incorporated into mixed micelles. As phytosteryl/stanyl esters are substrates for unspecific pancreatic cholesteryl esterase as well, they can compete with cholesteryl esters regarding hydrolysis. As cholesteryl esters make up only a small amount of dietary cholesterol, this solely cannot be responsible for the cholesterol-lowering effect. Another effect is that owing to a blocking of PCE by phytosteryl/stanyl esters and their reduced hydrolysis, these esters are available as “solvent” that transports lipophilic compounds including cholesterol and bile salts further in the intestinal lumen where absorption is less efficient and could even lead to excretion (Trautwein *et al.*, 2003). This would result in a reduced amount of cholesterol available in the intestinal lumen. It is known that phytosterols/-stanols and cholesterol use the same transport protein (NPC1L1) to pass the epithelial brush border membrane, therefore a competition at this site was conceivable. In NPC1L1-deficient mice, sterol/stanol absorption was reduced by about 90%. Until now, knowledge about this step is low and therefore a reduction potential could neither be explained nor excluded (Trautwein *et al.*, 2003; De Smet *et al.*, 2012).

In the enterocytes the efflux proteins ABCG5 and ABCG8 transport phytosterols/-stanols selectively back in the intestinal lumen, due to that the absorption in further metabolism is low and even more free phytosterols/-stanols are available for competition about incorporation in mixed micelles in the intestinal lumen (Katan *et al.*, 2003). The activation of the liver X-receptor by phytosterols/-stanols is discussed as reason for the greater efflux of phytosterols/-stanols compared to cholesterol by ABCG proteins (Brufau *et al.*, 2008).

Also an interference of phytosterols/-stanols with ACAT, that regulates the esterification in the enterocytes, was suggested; this would inhibit the formation of

chylomicrons and therefore the excretion to the lymph (Brufau *et al.*, 2008). The esterification is less efficient for phytosterols/-stanols and therefore a limiting effect on cholesterol absorption. As the inhibition promotes ACAT production, it is not clear if the blocked esterification could be compensated (Trautwein *et al.*, 2003; De Smet *et al.*, 2012).

The transport from enterocytes to the lymph proceeds via the formation of chylomicrons. They incorporate mostly esterified cholesterol. The lower esterification rates of phytosterols/-stanols limit their incorporation (Trautwein *et al.*, 2003).

There is an ongoing discussion about another possible cholesterol lowering effect. Cholesterol secretion is not only due to reverse cholesterol transport route (RCT), but there is a transintestinal cholesterol excretion (TICE) directly from blood into the intestinal lumen. It is not known which transporters are responsible for this effect and therefore more studies are needed to explain its potential role in the lowering of cholesterol (De Smet *et al.*, 2012; Feng *et al.*, 2020).

In summary, there are many steps in the metabolism of cholesterol where a lowering effect could potentially take place. For several of the steps, there is strong evidence for the involvement of phytosterols/stanols or the respective fatty acid esters in the cholesterol-lowering, but none of these steps on its own could explain the effect. Therefore, it is likely that a complex interplay of the described effects leads to the cholesterol-lowering effect. However, nearly all of the mentioned mechanisms require free phytosterols/-stanols and therefore hydrolysis of the esters is a limiting step (De Smet *et al.*, 2012).

2.2 Oxidations

2.2.1 Oxidation of the Phytosterol/-stanol Moiety

If phytosterols or phytostanols are added to foods, they may undergo autoxidation reactions during household-type cooking or storage like other lipids. Phytostanols are less susceptible to oxidation than phytosterols as they lack the double bond in the B-ring (Soupas *et al.*, 2004a). However, at temperatures above 100°C, radicals formed from hydroperoxides may also induce hydrogen abstraction from saturated compounds (Swern *et al.*, 1948). There are phytostanol oxidation products known with hydroxy groups in positions 7 α , 7 β , 6 α , 5 β , or 15 α ; some contain keto groups in positions C-6 or C-7 (Soupas *et al.*, 2004b). Phytostanyl oxidation products have been investigated

in different matrices using 6 α -hydroxysitostanol and 7 α -hydroxysitostanol as markers for sitostanol oxidation. The oxidation rates were low and required high temperatures (Soupas *et al.*, 2004a). There is one study in which oxidation products of esterified phytosterols were quantified. Phytostanyl fatty acid esters were heated and the formed amounts of phytostanyl oxidation products were compared to the total loss of non-oxidized ester. Oxidation products of the phytostanyl moiety could explain less than 1% of the observed ester loss (Scholz *et al.*, 2016a).

In the phytosterol moiety the most susceptible groups for oxidation are the double bonds in the unsaturated B-ring and in the side chain of some phytosterols (Piironen *et al.*, 2000). Autoxidation at the double bond in the B-ring of phytosterols is initiated by allylic abstraction of hydrogen atom at C-7 under formation of a radical (Piironen *et al.*, 2000). By reaction with triplet oxygen and hydrogen radical, the so-called primary oxidation products 7 α - and 7 β -hydroperoxide are formed (Garcia-Llatas and Rodriguez-Estrada, 2011).

Further reactions lead to so-called secondary oxidation products (Figure 6), such as 7 α -hydroxysterol, 7 β -hydroxysterol and 7-ketosterol (Lehtonen *et al.*, 2011); respective compounds derived from sitosterol are shown in Figure 6. A bimolecular reaction between a hydroperoxide and a non-oxidized sterol may result in 5 α ,6 α - and 5 β ,6 β -epoxides. In acidic environment, 3,5,6-triols could be formed by opening of the epoxide. These groups of polar secondary oxidation products are often summarized in the literature as POPs (phytosterol oxidation products) (Garcia-Llatas and Rodriguez-Estrada, 2011). Other oxidation products resulting from oxidations in the side chain at the tertiary carbon atoms C20, C24, and C25 have also been reported (Yanishlieva *et al.*, 1980; Johnsson and Dutta, 2003).

So-called tertiary oxidation products are conjugated dimers, trimers or polymers resulting from the secondary oxidation products described above (Garcia-Llatas and Rodriguez-Estrada, 2011). Also fragmentations of the sterols followed by reactions to dimers and oligomers (Rudzinska *et al.*, 2010) as well as dienes or trienes formed by abstraction of the hydroxy group in position C3 (Lercker and Rodriguez-Estrada, 2000; Dutta, 2004) have been discussed.

Esterification of phytosterols has an influence on amount and formation of oxidation products in the sterol moiety (Soupas *et al.*, 2005). The type of esterified fatty acid also

has an impact; for example, unsaturation in the fatty acid promotes a higher POP content (Raczyk *et al.*, 2017).

In general, time and intensity of temperature treatment, the presence of oxygen or light as well as the matrix influence the oxidation reaction (Xu *et al.*, 2011). Antioxidants could lower oxidation reactions of phytosterols when added to the matrix (Barriuso *et al.*, 2016).

As the loss of intact phytosterols exceeds the amount of known oxidation products (e.g. secondary oxidation products), there is still an unexplained “gap” (Soupas *et al.*, 2007; Menendez-Carreno *et al.*, 2008).

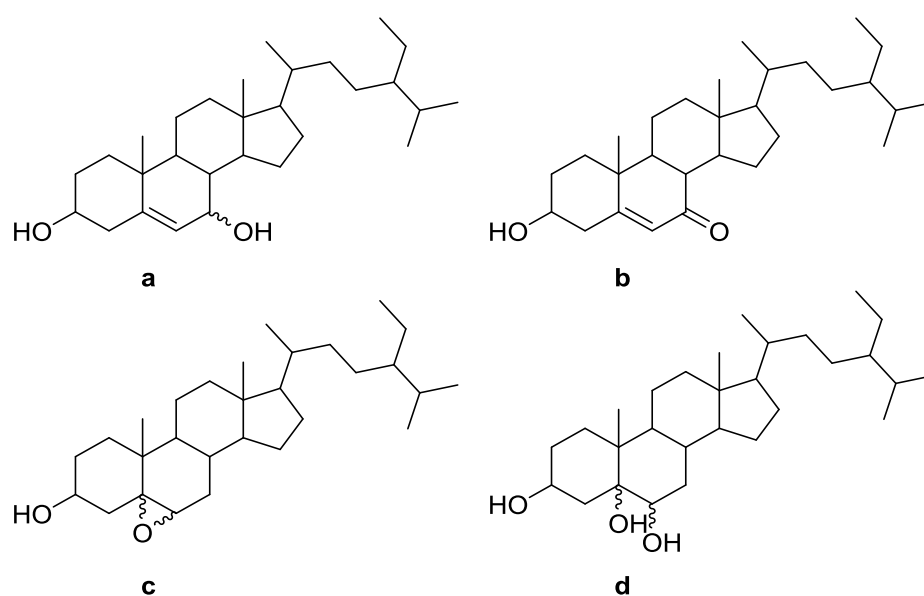


Figure 6: Structures of main phytosterol oxidation products (POPs) derived from sitosterol (a: 7-hydroxysitosterol, b: 7-ketositosterol, c: 5,6-epoxysitosterol, d: 5,6-dihydroxysitosterol).

2.2.2 Oxidation of the Fatty Acid Moiety

Research on oxidation of the fatty acid moiety mainly focused on oleic, linoleic, and linolenic acid and its esterified products in frying fats (Neff and Byrdwell, 1998; Velasco *et al.*, 2004b; Berdeaux *et al.*, 2012). As described for sterols, the double bond was the most susceptible group for oxidative reaction. The first step of oxidation is the reaction to hydroperoxides. In oleic acid, this oxidation can take place in positions 8, 9, 10, or 11 (Figure 7). These hydroperoxides are called primary oxidation products (Frankel, 2005). Quantitations showed that they constitute the main oxidation products in triolein, exposed to 60°C for three weeks (Neff and Byrdwell, 1998).

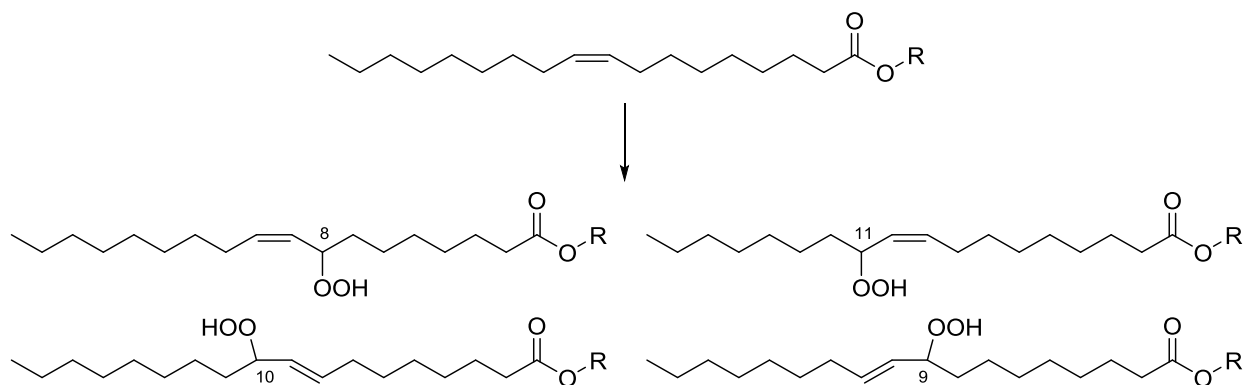


Figure 7: Structures of hydroperoxides in positions 8, 9, 10, and 11 generated from oleates due to thermo-oxidation.

Secondary oxidation products formed from hydroperoxides can be divided in (i) long-chain oxidation products, which have similar molecular weight as the starting unaltered fatty acid, (ii) chain-shortened oxidation products, (iii) dimers and oligomers, and (iv) volatile compounds (Frankel, 2005).

Long-chain oxidation products (Figure 8) are formed in different ways. Dehydration of hydroperoxides from oleic acid leads to allylic keto-octadecenoates, e.g. 8-oxooctadecen-(9)-oate (Frankel, 2005). Two kinds of epoxy-containing compounds can be formed, one with the epoxide in the original position of the double bond and products with epoxides in allylic positions. The first mentioned may be formed by reaction of oleate and the hydroperoxides, the second by cyclization of an alkoxy radical (Neff and Byrdwell, 1998; Frankel, 2005). 1,2- and 1,4-dihydroxyoctadecenoates can also be formed from alkoxy radicals (Frankel, 2005). At temperatures above 200°C, geometrical isomerization takes place in monounsaturated fatty acids. The configuration of the double bond changes from *cis* to *trans* (Berdeaux *et al.*, 2008; Brühl, 2014). *Trans*-fatty acids are related to adverse effects (Mozaffarian *et al.*, 2009). Cyclization in the fatty acid as reported for linoleic and linolenic acid, cannot take place for monounsaturated fatty acids (Berdeaux *et al.*, 2008).

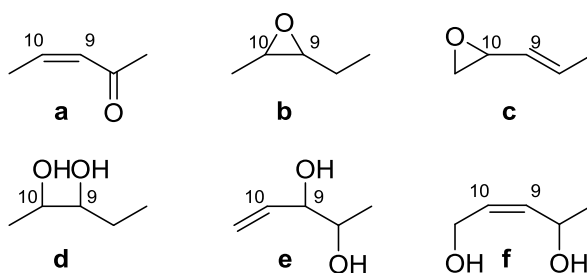


Figure 8: Functional groups in potential long-chain oxidation products of oleate: allylic keto group (a), epoxy group in the position of the former double bond, i.e. 9,10-epoxystearate (b), allylic epoxy group (c), 1,2-dihydroxy group in the position of the former double bond, i.e. 9,10-dihydroxystearate (d), 1,2-dihydroxy group adjacent to the shifted double bond (e), allylic 1,4-dihydroxy group (f).

Long-chain oxidation products have been considered in several studies. Berdeaux *et al.* (2008) found epoxy-containing compounds as the main group of long-chain oxidation products in transesterified sunflower and olive frying oil. Regarding oleic acid, *cis*-9,10- and *trans*-9,10-epoxystearate were identified and quantified. Also for methyl oleate these compounds were identified as the major oxidation products (Berdeaux *et al.*, 1999b; Velasco *et al.*, 2002). It was found that the formation of epoxides was similar for methyl oleate and triolein. Compared to polyunsaturated compounds, the formation of epoxides was more pronounced for monounsaturated compounds. In all investigated cases, more *trans*-epoxy oxidation products than *cis*-epoxy compounds were determined, and this group made up the major oxidation products detected by GC-MS. Additionally, longer heating periods resulted in an increase of epoxy-oxidation products (Berdeaux *et al.*, 1999a). Investigation of heated olive oil, which contained mainly oleic acid as fatty acid moiety, showed double the amount of *trans*-9,10-epoxystearate than *cis*-9,10-epoxystearate. This ratio remained similar over a time period of 5 to 15 hours, whereby the total amount of oxidation products increased (Velasco *et al.*, 2004b). Brühl (2014) reported that in the course of thermo-oxidation the formation of *trans*-epoxy acids was preferred to those possessing *cis*-configuration. As a result, Koch *et al.* (2023) defined the ratio of *cis/trans*-9,10-epoxystearate as a parameter to indicate the degree of oxidation of a heated oil. A ratio greater than 1 indicates low oxidation, meaning that more *cis*-9,10-epoxystearate is present. Significant oxidation is indicated by a ratio less than 1 (Koch *et al.*, 2023). During oxidation, *cis*-9,10-epoxystearate may be further converted into *threo*-9,10-dihydroxystearate, and *trans*-9,10-epoxystearate into *erythro*-9,10-dihydroxystearate.

Despite their significantly lower concentrations compared to epoxystearates, the ratio of *threo/erythro*-9,10-dihydroxystearate was proposed as additional marker to evaluate the oxidation status of oils (Koch *et al.*, 2023).

There are less studies on other long-chain oxidations products such as keto and hydroxy compounds. In heated and transesterified soybean oil the most abundant peak in the range of epoxides was identified as 9,10-epoxystearate. Additionally, in the range of ketones methyl oxooctadecenoate was detected as most abundant, but the position of the keto group could not be identified. Methyl hydroxyoctadecanoate as well as methyl hydroxyoctadecenoate were identified; however, there was no information available on their quantities or the positions of the functional groups (Gardner *et al.*, 1992). In the study of Byrdwell and Neff (1999) triolein was investigated. They found long-chain hydroperoxides, epoxides, ketones, and other oxidation products. The ketone could be identified as keto stearate. Its signals seemed to overlap with signals that could result from epoxy octadecenoate, therefore it could not be excluded that epoxy octadecenoate arised as well in this oxidative study.

Using sunflower oil, rich in oleic acid, quantitation of epoxy, keto, and hydroxy oxidation products was performed using transesterification. The main long-chain oxidation products could be identified as *trans*-9,10-epoxystearate and *cis*-9,10-epoxystearate. The *trans*-configured product was the main mono epoxy-containing compound. Due to many different possibilities for compounds containing keto or hydroxy groups, that have all similar molecular weights, the sample was hydrogenated prior to investigation of the three groups. The total amount of hydroxy-containing compounds was slightly higher than that of the epoxy-containing compounds; the amount of keto-containing compounds was distinctly lower. The three classes made about 50% of the monomeric fraction of polar methyl fatty acid esters (Marmesat *et al.*, 2008).

In another study, oxo-fatty acids and (poly) hydroxy fatty acids were investigated in different frying fats. Using olive oil rich in oleic acid, after transesterification the formed oxidation products were quantified. The amount of hydroxy acids was greater than of that of oxo-acids. Depending on the heating time, for hydroxy acids a maximum amount of oxidation could be found, longer heating period led to a lower content of hydroxy compounds (Schwartz *et al.*, 1994). Zhou *et al.* (2022) also observed that the proportion of hydroperoxides decreased with longer heating times. This effect was found in various oleates, including oleic acid, monoolein, and triolein. However, triolein exhibited steric hindrance, resulting in greater oxidative stability and reaching the

maximum proportion of oxidation products after a longer heating period. Examining the hydroperoxides at different temperatures but with the same heating duration, it was observed that their concentration decreased after initial increase with temperature.

Further secondary oxidation products can be generated by decomposition of monohydroperoxides and homolytic β -scission. They are divided into (i) volatile compounds (e.g. decanal, 2-undecanal, nonanal), which are related to the flavor quality, and (ii) those remaining with the (esterified) acid group, so called short-chain oxidation products. Potential compounds of this group can contain aldehyde, olefine, hydroxy, or alkyl groups (e.g. heptanoate, 8-oxooctanoate, 11-oxoundec-9-enoate). Formation of aldehydes (e.g. 9-oxononanoate) can additionally be explained by the Hock cleavage (Frankel, 2005). The formation of several short-chain oxidation products via homolytic β -scission is depicted in Figure 9.

Berdeaux *et al.* (2008) reported that main oxidation products of triacylglycerols determined in the course of the analysis of short-chain oxidation products after transesterification were methyl heptanoate, methyl octanoate, methyl 8-oxooctanoate and methyl 9-oxononanoate as well as dimethyl suberate (C8 diester) and dimethyl azelate (C9 diester). In a heated sample of methyl oleate, short-chain oxidation products were identified and divided by functional group in (i) aldehyde, (ii) di-acid-monomethyl, (iii) keto, (iv) non-polar, (v) hydroxy, and (vi) volatile compounds. The group of aldehyde fatty acid esters contained methyl 7-oxoheptanoate, 8-oxooctanoate, 9-oxononanoate, 10-oxodecanoate, as well as the monounsaturated methyl 10-oxodec-8-enoate and 11-oxoundec-9-enoate. All these compounds result from β -scission of the four hydroperoxides. Further oxidation of these oxidation products resulted in the formation of diacid monomethyl esters as suberic acid monomethyl ester or led to keto fatty acid esters. The identified compounds were methyl 7-oxooctanoate, 8-oxononanoate, and 9-oxodecanoate. Non-polar fatty acid esters were derived from β -scission as well, and methyl heptanoate, octanoate, nonanoate, and non-8-enoate could be identified. Another group that was formed by β -scission were hydroxy fatty acid esters. For methyl oleate, only methyl 7-hydroxyheptanoate could be identified. The volatile compounds contain different functional groups as well; acids, aldehydes and alcohols with chain lengths from six to ten carbon atoms have been reported (Berdeaux *et al.*, 2012).

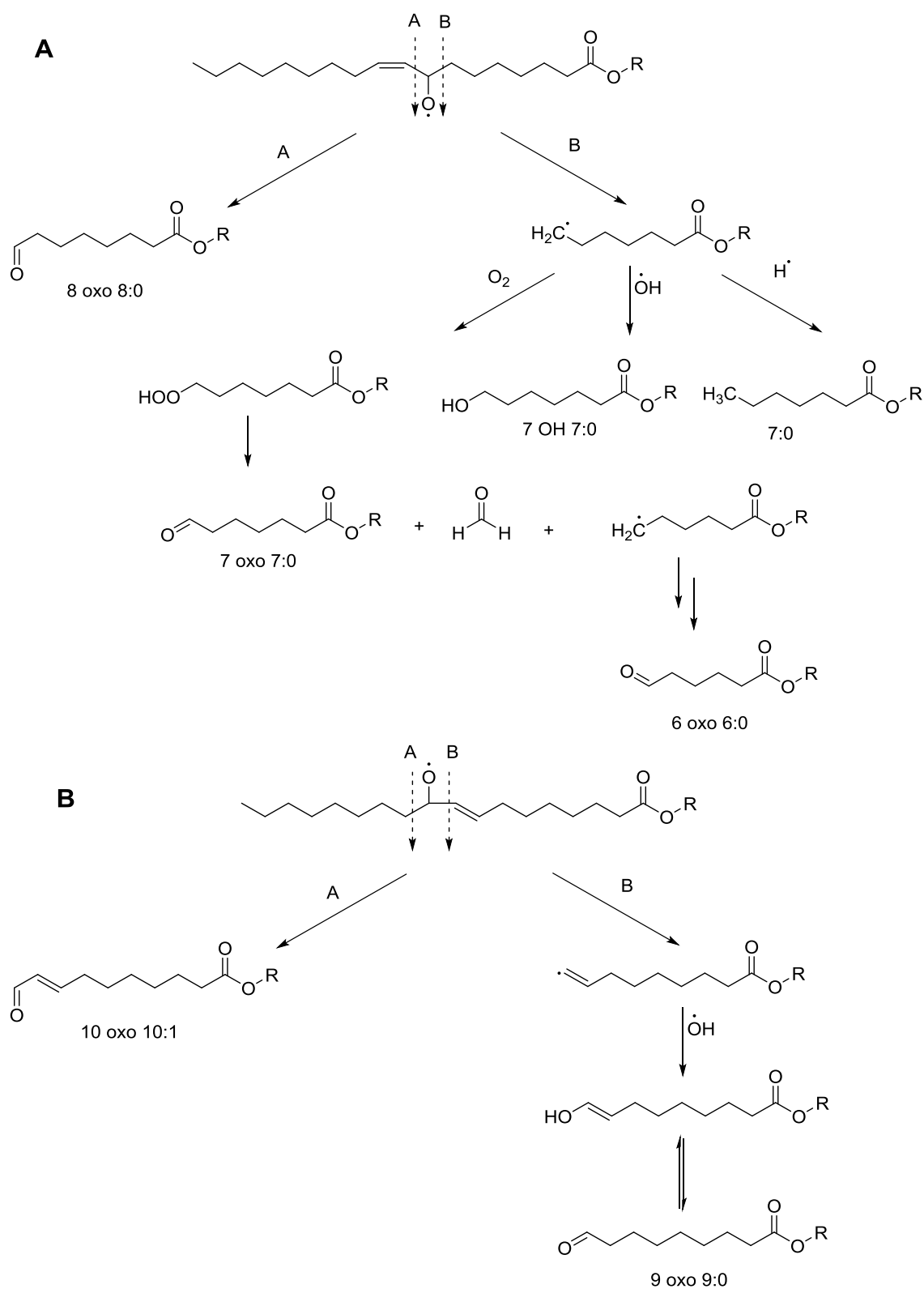


Figure 9: Formation of aldehyde, hydroxy, and olefinic oxidation products from 8-hydroperoxide (A) or 10-hydroperoxide (B) of oleate via homolytic β -scission, resulting in the short-chain oxidation products 8-oxooctanoate, 7-oxoheptanoate, 6-oxohexanoate, 7-hydroxyheptanoate, heptanoate (A) or 10-oxoundecenoate and 9-oxononanoate (B).

The levels of short-chain oxidation products were far below those of the long-chain epoxy-compounds, but as reported for epoxy-compounds, the amount of oxidation product increased with prolonged heating time and was in the same range for methyl oleate and triolein. The highest amounts of short-chain oxidation product were detected for 9-oxononanoate and octanoate. Concentrations of 8-oxooctanoate and heptanoate were lower. C8 or C9 diester were only detected at longer heating times (Berdeaux *et al.*, 2002). In fats such as triolein, hydrolysis could also take place before oxidation due to moisture resulting in diglycerides, monoglycerides, and free fatty acids. These compounds again can undergo oxidation reactions similar to triolein by formation of long-chain, short-chain, and volatile oxidation products (Byrdwell and Neff, 1999; Dobarganes and Márquez-Ruiz, 2007).

The last group of secondary oxidation products consists of dimers or oligomers. These compounds are less amenable to analysis due to their high molecular weights and therefore lower ionization properties; additionally there is a lack of reference compounds. Using gas chromatographic approaches, dimers and oligomers could not be investigated (Berdeaux *et al.*, 2012). Byrdwell and Neff (1999) determined several dimeric compounds in a heated sample of triolein, but only tentative assignments were possible. The formation of broad peaks led to the assumption of formation of a mixture of homologs. Data indicated that dimerization products were formed *via* oxygen-linkage as well as carbon-carbon linkage. The last mentioned seemed to be predominant. Dimers contained polar groups like keto or epoxy or showed a loss of one chain as mentioned above for non-dimerized triolein (Byrdwell and Neff, 1999; Dobarganes and Márquez-Ruiz, 2007). The analysis of higher oligomers is even more difficult; isolation and derivatisation steps are necessary, which lead to loss of information (Dobarganes and Márquez-Ruiz, 2007).

2.2.3 Oxidation of Phytosterol/-stanol Fatty Acid Esters

As described for triolein, the analysis of phytosterol/-stanol fatty acid oxidation products is difficult due to their high molecular weight. One study investigated chain-shortend ACOPs in their esterified form. The investigated esters could be analyzed with GC-FID/MS without derivatisation or transesterification. Using sitostanyl oleate sample, the main quantified ACOP was sitostanyl 9-oxononanoate, followed by sitostanyl 8-oxooctanoate and octanoate. Lower concentrations were detected for sitostanyl

hepanoate, 7-oxoheptanoate, 8-hydroxyoctanoate and 7-hydroxyheptanoate (Wocheslander *et al.*, 2017).

2.2.4 Impact of Oxidation Products on Metabolism

The metabolism is influenced by oxidation products. POPs have a pro-atherogenic and pro-inflammatory effect and are therefore considered undesirable in food (Poudel *et al.*, 2022). Therefore, EFSA has decided against extending the use of phytosterol/stanol-enriched foods to vegetable fat spreads or liquid vegetable fat-based emulsions that can be heated (EFSA, 2020).

In terms of the fatty acid moiety, oligomers of fatty acids could decrease digestibility, and aldehyde fatty acids are known to affect hepatic metabolism (Brühl, 2014).

There is one study that investigated the micellarisation of cholesterol in the presence of thermooxidized phytosteryl or phytostanyl fatty acid esters. Using non-oxidized esters, the incorporation of cholesterol into the micelles was reduced. However, the cholesterol concentration in mixed micelles increased significantly when oxidized phytosteryl/stanyl esters were used for incorporation in mixed micelles. The influence on micellarisation was correlated to the degree of thermo-oxidation (Scholz *et al.*, 2017).

2.3 Hydrolysis of Steryl/Stanyl Esters and Their Oxidation Products

2.3.1 Hydrolysis of Cholesteryl esters

The hydrolysis of steryl/stanyl esters is an essential step in their metabolism, as described in chapter 2.1.4. The hydrolysis of a wide range of cholesteryl esters has been investigated using cholesteryl esterase from rat liver homogenates. Among cholesteryl oleate, linoleate, palmitate, and stearate, the esters with unsaturated fatty acids were hydrolyzed more efficiently than those with saturated fatty acids (Deykin and Goodman, 1962). For unsaturated fatty acid esters, the configuration of the double bond has been shown to have an influence on the hydrolysis; *cis*-configured unsaturated fatty acid esters were hydrolyzed better than the respective *trans*-stereoisomers (Sgoutas, 1968). The hydrolysis rates of cholesteryl octadecenoates also depended on the position of the double bond (Goller *et al.*, 1970). Among cholesteryl esters with saturated fatty acid chains ranging from ethanoic acid (2:0) to eicosanoic acid (20:0) the highest hydrolysis rate was observed for cholesteryl

decanoate. Except for cholesteryl nonanoate, even-chain fatty acid esters were hydrolyzed at higher rates than the odd-chain fatty acid ester with either one more or one less carbon atom (Sgoutas, 1971).

Another investigated aspect was the influence of bile salts and their concentration on cholesteryl esterase activity. Using cholesteryl esterase from hog pancreas to hydrolyze cholesteryl oleate, the use of sodium taurocholate and sodium cholate resulted in the highest hydrolysis rates for cholesteryl oleate. Among sodium cholate (3 hydroxy groups), desoxycholate (2 hydroxy groups), lithocholate (1 hydroxy group) and dehydrocholate (no hydroxy group) (Figure 10), the hydrolysis rate of cholesteryl oleate decreased with decreasing number of hydroxy groups (Swell *et al.*, 1953). Another study even reported no hydrolysis of cholesteryl oleate without cholic acid or its conjugates (Vahouny *et al.*, 1965).

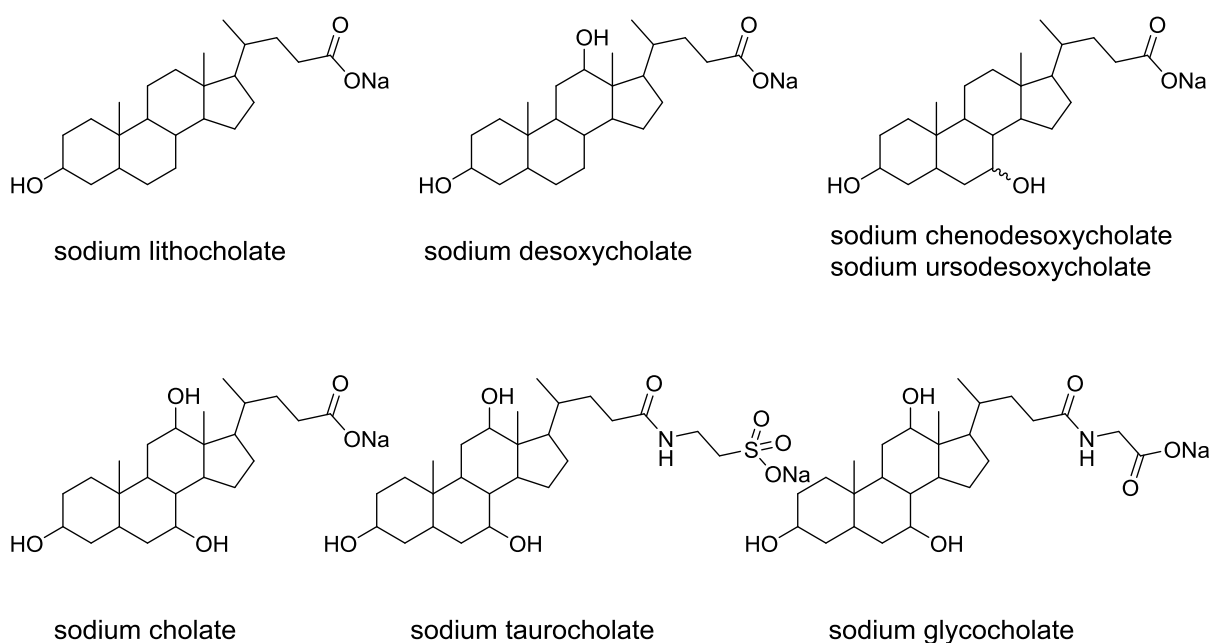


Figure 10: Structures of unconjugated and conjugated bile acid sodium salts differing in the number of hydroxy groups.

The efficiency of the hydrolysis of cholesteryl oleate was investigated in comparison to other cholesteryl esters containing saturated fatty acid moieties. Short-chain esters, such as cholesteryl acetate, were hydrolyzed much more efficiently than cholesteryl oleate. When cholesteryl oleate and cholesteryl acetate were hydrolyzed in a solution containing both esters, it was found that the two esters compete for hydrolysis by pancreatic cholesterol esterase (Swell and Treadwell, 1955). Cholesteryl esters with

branched fatty acid chains were less hydrolyzed than the corresponding *n*-acid esters (Stern and Treadwell, 1958).

2.3.2 Hydrolysis of Phytosteryl/-stanyl esters

Investigations of hydrolyses of phytosteryl/-stanyl esters are rare. Regarding the sterol specificity, pancreatic cholesteryl esterase showed a higher hydrolysis rate for cholesteryl oleate than for sitosteryl oleate and stigmasteryl oleate, the lowest was observed for ergosteryl oleate (Swell *et al.*, 1954).

Brown *et al.* (2010) demonstrated that the hydrolysis rates of steryl and stanyl esters by porcine pancreatic cholesteryl esterase depended on both the sterol/stanol and the fatty acid moieties. For all investigated steryl/stanyl esters, oleates showed the highest hydrolysis rates; those of palmitates and stearates were in the same order of magnitude. For all investigated fatty acid esters, cholesteryl esters were hydrolyzed more effectively than esters containing other sterol/stanol moieties. Stigmastanyl and sitosteryl esters were hydrolyzed to a similar degree; stigmasteryl esters were hydrolyzed the least. Using cholesteryl oleate, the influence of an addition of free sterols/stanols was tested. There was no significant influence on the rate of hydrolysis of cholesteryl oleate upon addition of equimolar amounts of free sterols or fatty acids. Addition of larger amounts of fatty acids resulted in increased hydrolysis rate; this was assumed to be due to the formation of a more native lipid emulsion.

There are several studies on the bioavailability and bioaccessibility of phytosterols (Wang *et al.*, 2023) and on the micellarisation of phytosterols liberated after hydrolysis, from which information can be gained on the hydrolysis properties of phytosteryl/-stanyl esters.

For example, Moran-Valero *et al.* (2012) reported that in intestinal *in-vitro* digestions involving pancreatin extract and cholesteryl esterase, phytosteryl esters of conjugated linoleic acid were hydrolyzed to a similar extent (51%) as those in a commercially available mixture of phytosteryl fatty acid esters (47%), mainly containing sitosteryl linoleate.

Gleize *et al.* (2016) investigated hydrolyses of phytosteryl fatty acid esters in the course of their studies on the impact of the form of phytosterols and the food matrix on their incorporation into mixed cells and cholesterol micellatization. In the employed *in-vitro* systems, the hydrolysis efficiency of phytosteryl esters with pancreatic lipase/colipase was negligible ($\leq 2\%$). The efficiency of hydrolysis with cholesteryl esterase was

dependent on whether the esters were present in mixed micelles or as emulsion. Incorporation in mixed micelles led to higher hydrolysis rate in the order of 44% to 60% versus 7% to 20% after 30 minutes, depending on the type of phytosterol esters. The hydrolysis of esters of octanoic acid (Figure 11) was most efficient compared to other investigated esters of decanoic, oleic, linoleic, or linolenic acid. When comparing analogous esters with either unsaturated (e.g. sitosterol) or saturated (e.g. sitostanol) sterol moiety, esters with unsaturated sterol moiety were hydrolyzed better.

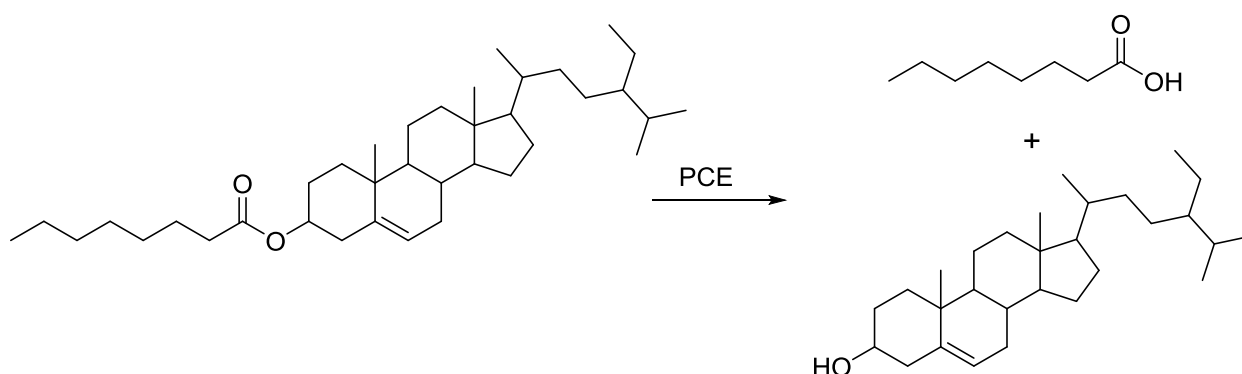


Figure 11: Hydrolysis of sitosteryl octanoate to octanoic acid and sitosterol *via* pancreatic cholesteryl esterase (PCE).

In a study by Vaghini *et al.* (2016), the bioaccessibility of phytosterols from fermented milk beverages containing phytosterol/-stanol esters was determined by investigating the micellar fraction obtained after an *in-vitro* digestion in a model containing a step with hydrolysis by bovine pancreas cholesteryl esterase. The percentage of bioaccessibility can be used as indicator for the hydrolysis efficiencies. For sitostanol, the bioaccessibility ranged from 11% to 14%, depending on the type of used food sample. For sitosterol, the value was in the range of 6% to 17%. In most cases, the bioaccessibility was higher for sterols than stanols. It was also shown to be dependent on the food matrix.

The different digestion systems reported in the literature are rarely comparable. Therefore, the COST INFOGEST network is aiming for a standard protocol for *in-vitro* digestion. Digestion steps from oral, gastric to intestinal were considered (Minekus *et al.*, 2014; Boyd *et al.*, 2021; Miedes *et al.*, 2023). The standard protocol was updated with regard to the addition of enzymes (Brodkorb *et al.*, 2019; Makran *et al.*, 2022) and the exchange of bile salts (Boyd *et al.*, 2022a). Further changes, e.g. the addition of cholesteryl esterase to the assay especially for determination of the bioaccessibility of

phytosteryl/stanyl esters (Boyd *et al.*, 2022b; Makran *et al.*, 2022), are still under discussion. The INFOGEST protocol was used to investigate the influence of bile salts on the *in-vivo* bioaccessibility of phytosteryl esters; inhibition of cholesteryl esterase by monohydroxy and dihydroxy bile acids was suspected (Boyd *et al.*, 2022a).

2.3.3 Hydrolysis of Oxidized Phytosteryl/-stanyl esters

There is only one study in which the hydrolysis properties of oxidized sterol esters have been investigated. Julien-David *et al.* (2009) compared the kinetic parameters *K_m* and *V_{max}* for cholesteryl esterase-catalyzed *in-vitro* hydrolyses of cholesteryl oleate, sitosteryl oleate and the two oxidation products 7-ketositosteryl oleate and sitosteryl 9,10-dihydroxystearate. 7-Ketositosteryl oleate exhibited higher affinity and velocity than the non-oxidized esters and showed the best hydrolysis among the investigated substrates. In contrast, the oxidation in the fatty acid chain resulted in a nearly complete loss of hydrolysis of sitosteryl 9,10-dihydroxystearate. Additional experiments revealed sitosteryl 9,10-dihydroxystearate to be a non-competitive inhibitor of cholesteryl oleate and sitosteryl oleate, respectively in the course of the cholesteryl esterase-catalyzed hydrolysis.

2.4 Analytical Methods

2.4.1 Analysis of Phytosterols/-stanols

Sample Preparation

Sterols/stanols and their esters are in most cases incorporated in foods or fat-based matrices. For their analytical determination, a separation from the matrix and concentration steps are necessary as these components are mostly present in low amounts. Lipids are usually extracted with non-polar solvents (Piironen *et al.*, 2000) followed by alkaline hydrolysis, with the non-saponified fraction containing sterols/stanols (Piironen *et al.*, 2000; Guardiola *et al.*, 2004). For analysis of oxidation products, transesterification was preferred to saponification to avoid artefacts or additional oxidation due to derivatisation (Guardiola *et al.*, 2004).

Depending on the food or fat matrix, further purification steps, e.g. thin layer chromatography (TLC), column chromatography, or solid phase extraction (SPE) can be necessary (Piironen *et al.*, 2000; Dutta, 2004).

Gas chromatography

Gas chromatography equipped with flame ionization detector (FID) or a mass spectrometer as detector is a good and fast analytic method for determination of total sterol/stanol content; it is also applied for the analysis of sterol oxidation products. Derivatisations of the compounds are recommended. The hydroxy group in position C3 may be derivatized to a methyl, trimethylsilyl or acetyl group (Figure 12). Derivatized compounds have higher thermal stability and better volatility, as well as improved chromatographic resolution and peak symmetry (Piironen *et al.*, 2000; Guardiola *et al.*, 2004; Barnsteiner *et al.*, 2012).

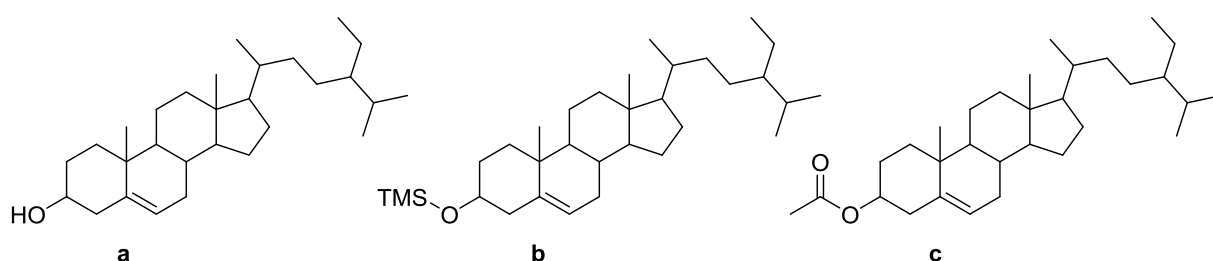


Figure 12: Structures of sitosterol (a) and its silylated (b) or acetylated (c) derivatives.

Liquid chromatography

Besides gas chromatography, reversed phase (RP)-HPLC is the mostly used analytical method to determine sterols/stanols, but it is less suitable than gas chromatography due to lower peak resolutions and less sensitive detectors. The use of mass spectrometers provides an additional tool for identification of the compounds (Piironen *et al.*, 2000; Dutta, 2004). Apart from APCI, MALDI-TOF or EI can be used as ionization method (Moreau *et al.*, 2002; Scholz *et al.*, 2016a).

Online LC-GC

A synergetic effect of gas chromatography and liquid chromatography can be exploited by online LC-GC. With this method a HPLC is linked via a transfer valve to a gas chromatograph. Purification, pre-separation, and concentration of the sample are performed with HPLC; further analysis occurs after on-line transfer to the gas chromatograph (Esche *et al.*, 2013b). Advantages are less sample loss, less degradation of labile oxides and less formation of artefacts compared to off-line processes, such as SPE or TLC (Scholz *et al.*, 2015b).

2.4.2 Analysis of Fatty acids

Sample Preparation

Fatty acids are part of fats and oils from animal or plant origin. They occur mainly as acyl moieties of triacylglycerides, but could also be present in their free form or esterified to phosphorus-containing compounds or sterols/stanols (Belitz *et al.*, 2008). To simplify the analysis, in most cases hydrolysis of the sample combined with a derivatisation, e.g. transesterification, which transfers the fatty acids into their methyl esters, is applied (Figure 13). Hydrogenation is also known as a simplifying step, especially applied for oxidized long-chain fatty acids (Berdeaux *et al.*, 1999a; Dobarganes and Márquez-Ruiz, 2007; Marmesat *et al.*, 2008). Using methyl linoleate, it was shown, that transesterification has no influence on tested oxidized fatty acid methyl esters. Different transesterification procedures have been described (Berdeaux *et al.*, 1999b). Dimers and oligomers cannot be transesterified (Dobarganes and Márquez-Ruiz, 2007).

For analysis of oxidized fatty acids a further pre-concentration step and separation from non-polar fatty acid methyl esters and other sample components has been achieved by silica column chromatography (Velasco *et al.*, 2002; Marmesat *et al.*, 2008; Berdeaux *et al.*, 2012).

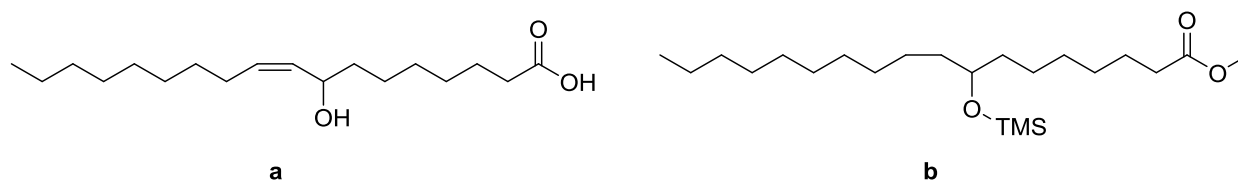


Figure 13: Structures of 8-hydroxyoctadec-9-enoic acid (a) and its actually analyzed derivative (b). Three steps of derivatisation were applied: (i) methylation of the acid group, (ii) silylation of the hydroxy group, and (iii) hydrogenation of double bond.

Gas chromatography

Many studies used gas chromatography for quantitative or qualitative analyses of fatty acid methyl esters (FAME) (Toschi *et al.*, 1997; Lercker *et al.*, 2002; Velasco *et al.*, 2002; Marmesat *et al.*, 2008; Berdeaux *et al.*, 2012; Xia and Budge, 2018). More specialized derivatisation reagents, such as *N*-methyl-pyridinium-3-methanamine (NMPA) or *N*-(4-aminomethylphenyl)-pyridinium (AMPP), have been used (Young *et al.*, 2022). Despite pre-concentration steps and derivatisations, the analysis of oxidized

fatty acids remains challenging. The broad spectrum of potential oxidation products on the one hand and their similarities, e.g. in terms of molecular weights, on the other hand, render analyses difficult (Dobarganes and Márquez-Ruiz, 2007).

Liquid chromatography

Normal phase HPLC has been applied for quantitative analysis of methyl fatty acid esters as well as for triacylglycerides by using a DAD detector (Velasco *et al.*, 2018). The use of an ELSD detector has also been described for the analysis of FAME from vegetable oils (Morales *et al.*, 2014). By using a mass spectrometer as detector unit, different types of oxidation products of a triacylglyceride could be distinguished and identified (Neff and Byrdwell, 1998).

2.4.3 Analysis of (Intact) Phytosteryl/-stanyl Esters

Analysis of intact phytosteryl-/stanyl esters is a challenge due to broad spectrum of very similar compounds, which only differ in saturation of the sterol B-ring or in the structures of the sterol side chain or the fatty acid part (Scholz *et al.*, 2014). Separation via saponification, for example, of sterol/stanol and fatty acid moiety simplifies analysis, while information due to composition will be lost (Barnsteiner *et al.*, 2012).

Sample Preparation

Depending on the sample, different sample preparation steps may be useful. For fat-based samples separation of steryl/stanyl esters from triacylglycerides is necessary. This separation could be efficiently achieved with aminopropyl SPE (Esche *et al.*, 2012; Oelschlägel *et al.*, 2012). For complex food matrices, more steps may be required (Esche *et al.*, 2013a).

Efficient separation procedure were required if high amounts of non-oxidized / non-polar components and very low amounts of oxidized / polar components were present (Neff and Byrdwell, 1998; Kuksis, 2007; Hutchins *et al.*, 2011; Wocheslander *et al.*, 2017). The separation of non-polar and polar products could be achieved with silica SPE (Marmesat *et al.*, 2008; Lehtonen *et al.*, 2011; García-González *et al.*, 2017; Wocheslander *et al.*, 2017). For qualitative identification also thin layer chromatography was used for separation and pre-concentration from the matrix (Kamido *et al.*, 1992).

Gas chromatography

Gas chromatographic analysis of intact esters is limited by the low volatility of the compounds, as well as co-elution and thermal degradation due to high boiling points of the esters (Barnsteiner *et al.*, 2012). Compared to HPLC, gas chromatography shows better separation and sensitivity for non-oxidized steryl/stanyl esters (Caboni *et al.*, 2005; Barnsteiner *et al.*, 2011). Phytostanyl ester of palmitic acid, stearic, oleic, linolic, linolenic, or arachidic acid could be detected and separated using gas chromatography (Barnsteiner *et al.*, 2011). Steryl/stanyl esters with (oxidized) short fatty acid chains could be analyzed as well. For some compounds, an additional derivatisation step was helpful to improve volatility and stability in the analytical process, e.g. silylation of hydroxy-containing compounds (Wocheslander *et al.*, 2016).

Liquid chromatography

For analysis of intact steryl/stanyl esters, various methods based on liquid chromatography have been developed using different detection techniques such as UV/Vis, APCI-MS, ESI-MS or ELSD (Billheimer *et al.*, 1983; Caboni *et al.*, 2005; Scholz *et al.*, 2014). Steryl/stanyl esters in heated enriched margarine were analyzed by liquid chromatography using triple quadrupole mass spectrometry (Julien-David *et al.*, 2014). Using APCI as ionization technique, which was especially suitable for non-polar compounds such as steryl/stanyl esters, complete in-source fragmentation takes place and may challenge the analysis (Kostiainen and Kauppila, 2009; Scholz *et al.*, 2014; Scholz *et al.*, 2016b). Using ESI as ionization technique, addition of ammonium acetate has been shown to be helpful to the generation of molecular adduct ions (Caboni *et al.*, 2005; Hutchins *et al.*, 2011; Scholz *et al.*, 2019); identification via lithium adducts has also been reported (Julien-David *et al.*, 2014). Additional derivatisations helpful for identifications of oxidation products included derivatizations of aldehydes with 2,4-dinitrophenylhydrazine (DNPH) (Kamido *et al.*, 1993) or their conversion into methoximes, as well silylation of hydroxy-containing compounds (Hutchins *et al.*, 2011). Regarding analysis of hydroperoxides, in addition to mass spectrometry evaporative light scattering detector (ELSD) has been used (Lehtonen *et al.*, 2011; Lehtonen *et al.*, 2012).

3. MATERIALS AND METHODS

3.1 Materials

3.1.1 Chemicals

Steroids

A mixture of phytosterols/-stanols named “ β -sitosterol” consisting of 75% sitosterol, 12% sitostanol, 10% campesterol, 2% campestanol, and 1% others was purchased from Acros Organics (Morris Plains, NJ, USA). A mixture of phytostanols, consisting of 91.2% sitostanol and 8.2% campestanol (Reducol® Stanol Powder), was obtained from Cognis GmbH (Illertissen, Germany). These mixtures will be referred to as “sitosterol” and “sitostanol”, respectively, in the further course of this thesis.

Cholestanol (96%) and cholesterol (95%) and were purchased from Sigma-Aldrich (Steinheim, Germany). 19-Hydroxycholesterol was provided by Steraloids (Rhode Island, USA).

Sodium cholate hydrate (99%) was from Alfa Aesar GmbH & Co. KG (Karlsruhe, Germany). Bile salts (cholic acid sodium salt, ~50%; desoxycholic acid sodium salt, ~50%), 5 α -cholestane (99%), and sodium desoxycholate (\geq 98%) were purchased from Sigma-Aldrich (Steinheim, Germany).

Fatty acids / Fatty acid esters

Cholesteryl oleate (\geq 98%), conjugated linoleic acid (9Z,11E) (\geq 96%), glycerin trioleate (triolein) (\geq 99%), methyl oleate (99%), methyl 10-oxodecanoate (95%), methyl ricinoleate (\geq 99%), 1-monooleoyl-*rac*-glycerol (C18:1, *cis*-9) (monoolein), oleic acid (\geq 99%), and 5-oxohexanoic acid (97%) were purchased from Sigma-Aldrich (Steinheim, Germany). 4-Oxopentanoic acid (98%) was provided by Frey+Lau GmbH (Henstedt-Ulzburg, Germany). 6-Oxoheptanoic acid (96%) was ordered from Alfa Aesar (Karlsruhe, Germany). Methyl *trans*-9,10-epoxystearate (10 mg/mL in methanol, >99%) was purchased from Larodan (Solna, Sweden). Methyl palmitate (99%) was ordered from Carl Roth GmbH (Karlsruhe, Germany). Aleuritic acid (9,10,16-trihydroxypalmitic acid (\geq 94%) was from Santa Cruz Biotechnology (Heidelberg, Germany).

Further chemicals

Acetic acid ($\geq 99.8\%$, p.a.), *tert*-butyl hydroperoxide solution (*t*BHP) (5.0-6.0 M in decane), celite, 3-chloroperbenzoic acid (*m*-CPBA) ($\geq 77\%$), copper(I) iodide ($\geq 99.0\%$), cycloheptanone ($\geq 98\%$), cyclohexane (puriss, p.a., $\geq 99\%$), cyclooctanone ($\geq 98\%$), diethylether (DEE) (extrapure), ethyl acetate (puriss, p.a., $\geq 99.5\%$), *n*-heptane (puriss, p.a., $>99\%$), *n*-hexane (puriss, p.a., $\geq 99\%$), hydrochloric acid (25%), hydroxypropyl methyl cellulose (HPMC) (meets USP testing specifications), 2-iodoxybenzoic acid (45 wt-%), manganese(III) acetate dihydrate (97%), 70% perchloric acid (99.999%), potassium hydroxide ($\geq 85\%$), potassium periodate (99.8%), pyridine (99.8%), selenium dioxide ($\geq 99.9\%$), sodium borohydride ($\geq 96\%$), sodium chloride, sodium hydrogen carbonate ($\geq 95\%$), sodium hydroxide ($\geq 98.0\%$, p.a.), sodium thiosulfate ($\geq 98.0\%$, p.a.), tetrahydrofuran (puriss.), and (triphenylphosphoranylidene)acetaldehyde (95%) were purchased from Sigma-Aldrich (Steinheim, Germany). Boron trifluoride (10% in methanol), dicyclohexylcarbodiimide (DCC) (1M in DCM, $>99\%$), 4-(dimethylamino)pyridine (DMAP, puriss.), and magnesium sulfate ($\geq 98\%$, water-free) were ordered from Fluka Analytical (Steinheim, Germany). Methyl *tert*-butyl ether (MTBE) was provided by Evonik Industries AG (Essen, Germany). Citric acid (anhydrous, for synthesis), dimethylsulfoxide (DMSO) ($>99\%$, for synthesis), 1,4-dioxane (EMSURE, p.a.), sodium methylate (30% solution in methanol, for synthesis), sodium sulfite ($\geq 98.0\%$, p.a.), and sulfuric acid (98%) were purchased from Merck (Darmstadt, Germany). Chloroform (99.3%), dichloromethane (DCM) (AnalaR Normapur), ethanol (99%), *n*-hexane (AnalaR Normapur), methanol (HiPerSolv, Chromanorm, LC-MS), petroleum ether (technical, 40-65°C), and sodium sulfate (anhydrous) were purchased from VWR International (Darmstadt, Germany). Ethyl acetate (EtOAc) and methanol (both Rotisolv, LC-MS) were from Carl Roth GmbH (Karlsruhe, Germany). Magnesium sulfate (anhydrous, $\geq 99.5\%$) and petroleum ether (30/60, HPLC grade) were ordered from Alfa Aesar (Karlsruhe, Germany). SPE Tubes Strata NH₂ (55 μ m, 70Å) were purchased from Phenomenex (Aschaffenburg, Germany), and Supelclean™ LC-Si SPE Tubes (500 mg, 3mL) were from Supelco (Bellefonte, PA, USA).

Enzyme

Cholesterol esterase from porcine pancreas (29.5 U/mg) was purchased from Sigma-Aldrich (Steinheim, Germany).

3.1.2 Syntheses of Reference Compounds and Substrates

3.1.2.1 Internal Standards for UHPLC-MS/MS-Based Analysis of ACOPs

Cholestanyl heptanoate IS₁. Cholesterol (198 mg), heptanoic acid (203 mg), and DMAP (5.3 mg) were dissolved in 4 ml DCM. After addition of 1 mL 1M DCC solution, the mixture was stirred for 24h at room temperature. After cooling in a freezer for five minutes, the mixture was filtrated (0.45 µm). After addition of 10 ml DCM, the mixture was washed with 15 ml 0.5M hydrochloric acid and 15 ml saturated sodium hydrogen carbonate solution. The organic layer was dried over magnesium sulfate and the solvent removed with a gentle stream of nitrogen. Flash chromatography was used for final purification (petroleum ether/ethyl acetate 9/1) and resulted in 94% purity (GC-FID).

Cholestanyl oleate IS₂. Cholesterol (100 mg) and oleic acid (300 mg) were heated at 180°C under nitrogen atmosphere for 25h. To the reaction mixture 2.5 ml *n*-hexane/MTBE (3/2, v/v) and 2.5 ml 1M KOH-solution were added. The mixture was vortexed, centrifuged, and the upper organic layer was collected in a second tube. The extraction process was repeated twice. The collected organic layers were dried with a gentle stream of nitrogen, resulting in 96 mg cholestanyl oleate IS₂ (purity 57%). For further purification, the residue was dissolved in *n*-hexane and purified over a Si-SPE Tube, which was conditioned with *n*-hexane. Elution of cholestanyl oleate IS₂ was done with *n*-hexane/MTBE (98/2, v/v). This led to 87% purity (GC-FID).

Cholestanyl 9-hydroxynonanoate IS₃. In the first step, 9-oxononanoic acid was synthesized in accordance with the procedure described by Wochezlander *et al.* (2016). Aleuritic acid (4 g) was dissolved in 200 ml methanol/water (1/1, v/v) and the solution was warmed to 40°C. A solution of 3 g potassium periodate in 150 ml 1M sulfuric acid was added and the mixture stirred for 10 minutes. After cooling down to 15°C in a methanol/ice bath, the mixture was extracted twice with 200 ml diethyl ether. The organic layer was extracted twice with 50 ml saturated sodium hydrogen carbonate. The aqueous layer was acidified with concentrated hydrochloric acid and extracted twice with 50 ml diethyl ether. The organic layer was washed twice with 50 ml 10% sodium chloride and dried over magnesium sulfate. The raw product obtained

after removal of the solvent with a gentle stream of nitrogen was used for the subsequent synthesis of cholestanyl 9-oxononanoate.

Cholesterol (402 mg) and 409 mg 9-oxononanoic acid were esterified using 10.9 mg DMAP and 1.5 mL 1M DCC. The raw product (65 mg) was dissolved in 1 ml THF, cooled in an ice bath and reduced by addition of 65 mg sodium borohydride. After 10 minutes stirring with a spatula, crushed ice was added for quenching. The mixture was extracted twice with 3 ml *n*-hexane/MTBE (3/2, v/v) and dried over magnesium sulfate. The solvent was removed with a gentle stream of nitrogen. Further purification with Si-SPE tube led to 82% purity (GC-FID, TMS-derivative).

Cholestanyl 6-oxoheptanoate **IS**₅. Cholesterol (399 mg), 6-oxoheptanoic acid (402 mg), and DMAP (11.0 mg) were dissolved in 8 ml DCM and 2 mL 1M DCC solution were added. The reaction mixture was stirred for 25h at room temperature, filtrated and washed as described above for cholestanyl heptanoate **IS**₁. For further purification, the residue was dissolved in *n*-hexane and put on an Si-SPE tube pre-conditioned with *n*-hexane. Elution of cholestanyl 6-oxoheptanoate **IS**₅ was done with *n*-hexane/MTBE (98/2, v/v). This purification resulted in 91% purity (GC-FID).

Cholestanyl *cis*-9,10-epoxystearate **IS**₄. Cholestanyl oleate **IS**₂ (51 mg) was dissolved in 1 mL DCM, and 20 mg *m*-CPBA was added (Aerts and Jacobs, 2004). After stirring for 20 min. and addition of 4 mL DCM, the solution was washed with 4 mL water. The organic layer was dried over magnesium sulfate, and after evaporation of the solvent via a gentle stream of nitrogen, 53 mg of **IS**₄ were obtained. Flash chromatography was used for final purification (petroleum ether/ethyl acetate 9/1) and resulted in 35 mg with 79% purity (HPLC-ELSD).

3.1.2.2 Reference Compounds for UHPLC-MS/MS-Based Analysis of ACOPs

Sitostanyl oleate **3**. Sitostanol (100 mg) and oleic acid (300 mg) were placed into a brown glass vial. After flushing with nitrogen, the vial was sealed and heated at 180°C for 25h. Purification as described above for cholestanyl oleate yielded in 96 mg sitostanyl oleate **3** (purity 57%). Further purification with a Si-SPE Tube using *n*-hexane led to 87% purity (GC-FID).

Sitostanyl 4-oxopentanoate 11. Sitostanol (100 mg) and 4-oxopentanoic acid (98 mg) were esterified using 2.9 mg DMAP and 0.5 mL 1M DCC solution. Flash chromatography was used for final purification (petroleum ether/ethyl acetate 7/3) and resulted in 99% purity (GC-FID).

Sitostanyl 5-oxohexanoate 13. Sitostanol (102 mg) and 5-oxohexanoic acid (99 mg) were esterified using 3.3 mg DMAP and 0.5 mL 1M DCC solution. Flash chromatography was used for final purification (petroleum ether/ethyl acetate 7/3) and resulted in 97% purity (GC-FID).

Sitostanyl 6-oxoheptanoate 15. Sitostanol (201 mg) and 6-oxoheptanoic acid (196 mg) were esterified using 5.4 mg DMAP and 1 mL 1M DCC solution. Flash chromatography was used for final purification (petroleum ether/ethyl acetate 8/2) and resulted in 95% purity (GC-FID).

Sitostanyl 7-oxoheptanoate 14. 7-Oxoheptanoic acid was synthesized in accordance with the approach described by Wocheslander *et al.* (2016). Cycloheptanone (3.1 g) was dissolved in 15 ml DCM. After addition of 3.3 g *m*-CPBA, the mixture was stirred for twelve days at room temperature. The reaction was quenched by addition of 500 μ l saturated sodium thiosulfate solution. The organic layer was washed three times with 25 ml saturated sodium hydrogen carbonate solution and twice with 25 ml 10% sodium chloride solution, and then dried over magnesium sulfate. The solvent was removed with a gentle stream of nitrogen. For lactone opening, the residue was dissolved in 3 ml dioxane and after addition of 25 ml 3M sodium hydroxide solution stirred over night at room temperature. The aqueous layer was washed with 25 ml ethyl acetate and afterwards the pH was adjusted to 3.5 with 25% hydrochloric acid. The aqueous layer was extracted twice with 30 ml ethyl acetate. The extract was washed twice with 30 ml saturated sodium chloride solution and dried over magnesium sulfate. After removal of the solvent with a gentle stream of nitrogen, 7-hydroxyheptanoic acid was obtained. For oxidation 108 mg raw product were dissolved in 3.7 ml DMSO. After addition of 68 mg IBX, the mixture was stirred for 4h at room temperature. The reaction was quenched with 5 ml distilled water, filtrated and extracted twice with 15 ml ethyl acetate. After drying with magnesium sulfate and removal of the solvent by a gentle stream of nitrogen, 7-oxoheptanoic acid was obtained. The synthesis of sitostanyl 7-

oxoheptanoate **14** was performed using 105 mg sitostanol, 243 mg raw product of 7-oxoheptanoic acid, 2.7 mg DMAP and 0.5 mL 1M DCC solution. Flash chromatography was used for final purification (petroleum ether/ethyl acetate 8/2) and resulted in 95% purity (GC-FID).

Sitostanyl 8-oxooctanoate **16**. 8-Oxooctanoic acid was synthesized in analogy to the procedure described above for 7-oxoheptanoic acid. Cyclooctanone (2.07 g) was converted into the respective lactone by reaction with *m*-CPBA (2.1 g). For lactone opening, 25 ml 3M sodium hydroxide solution was used, and oxidation to 8-oxooctanoic acid was performed with 118 mg 8-hydroxyoctanoic acid using 202 mg IBX. Sitostanyl 8-oxooctanoate **16** was obtained via Steglich esterification using 200 mg sitostanol, 182 mg raw product of 8-oxooctanoic acid, 4.3 mg DMAP and 1 mL 1M DCC solution. Flash chromatography was used for final purification (petroleum ether/ethyl acetate 8/2) and resulted in 94% purity (GC-FID).

Sitostanyl 9-oxononanoate **17**. Sitostanol (200 mg) and 240 mg 9-oxononanoic acid were esterified using 5.4 mg DMAP and 1 mL 1M DCC solution. Flash chromatography was used for final purification (petroleum ether/ethyl acetate 9/1) and resulted in 98% purity (GC-FID).

Sitostanyl 10-oxodecanoate **19**. First, 10-oxodecanoic acid was obtained via demethylation of methyl 10-oxodecanoate according to the procedure described by Julien-David *et al.* (2008). Methyl 10-oxodecanoate (303 mg) was dissolved in 50 mL methanol, and 833 mg barium sulfate was added. The mixture was stirred for two hours at 50°C, the solvent was evaporated, and the residue suspended in 15 mL water. The suspension was acidified with 25% hydrochloric acid until it became transparent and subsequently extracted with 15 mL dichloromethane. The extract was washed with 15 mL water and 15 ml saturated sodium chloride. After drying with magnesium sulfate and evaporation of the solvent, 67 mg raw product of 10-oxodecanoic acid was obtained. The synthesis of sitostanyl 10-oxodecanoate **19** was performed via Steglich esterification using 50 mg sitostanol, the raw product of 10-oxodecanoic acid, 1.6 mg DMAP and 0.25 mL 1M DCC solution. Flash chromatography was used for final purification (petroleum ether/ethyl acetate 95/5) and resulted in 94% purity (GC-FID).

Sitostanyl heptanoate 1. Sitostanol (52 mg) was dissolved in 6 mL pyridine at 0°C. Heptanoyl chloride (247 µL) was slowly added, the mixture was thawed, and stirred for further 90 minutes at room temperature (Carvalho *et al.*, 2011). Pyridine was evaporated as azeotrope with heptane using a rotary evaporator. The residue was dissolved in 20 mL diethyl ether/hexane 1/1 and washed with 5% hydrochloric acid, sodium hydrogen carbonate and water (20 mL each). After drying with sodium sulfate, the solvent was evaporated. Flash chromatography was used for final purification (petroleum ether/ethyl acetate 95/5) of 165 mg and resulted in 95% purity (GC-FID).

Sitostanyl octanoate 2. Sitostanol (50 mg) was dissolved in 6 mL pyridine and 296 µL octanoyl chloride were added as described for sitostanyl heptanoate 1. Flash chromatography was used for final purification (petroleum ether/ethyl acetate 95/5) of 155 mg and resulted in 95% purity (GC-FID).

Sitostanyl 7-hydroxyheptanoate 4. The raw product of sitostanyl 7-oxoheptanoate 14 (51 mg) was reduced using 51 mg sodium borohydride as described for cholestanyl 9-hydroxynonanoate **IS₃**. Flash chromatography was used for final purification (petroleum ether/ethyl acetate 8/2) and resulted in 58% purity (GC-FID, TMS-derivative).

Sitostanyl 8-hydroxyoctanoate 5. The raw product of sitostanyl 8-oxooctanoate 16 (45 mg) was reduced using 19 mg sodium borohydride as described for cholestanyl 9-hydroxynonanoate **IS₃**. Flash chromatography was used for final purification (petroleum ether/ethyl acetate 85/15) and resulted in 96% purity (GC-FID, TMS-derivative).

Sitostanyl 9-hydroxynonanoate 6. The raw product of sitostanyl 9-oxononanoate 17 (30 mg) was reduced using 10 mg sodium borohydride as described for cholestanyl 9-hydroxynonanoate **IS₃**. Flash chromatography was used for final purification (petroleum ether/ethyl acetate 8/2) and resulted in 98% purity (GC-FID, TMS-derivative).

Sitostanyl *cis*-9,10-epoxystearate 10. Sitostanyl oleate 3 (67 mg) was dissolved in 1 mL DCM, and 20 mg *m*-CPBA was added (Aerts and Jacobs, 2004). After stirring for

20 min. and adding 4 mL DCM, the solution was washed with 4 mL water. The organic layer was dried over magnesium sulfate, and after evaporation of the solvent via a stream of nitrogen, 68 mg of **10** were obtained. Flash chromatography was used for final purification (petroleum ether/ethyl acetate 9/1) and resulted in 94% purity (GC-FID).

Sitostanyl 9,10-dihydroxystearate **7**. Sitostanyl *cis*-9,10-epoxystearate **10** (68 mg) was suspended in 2.5 mL H₂O/THF (1:3, v/v), and 310 µL perchloric acid (10%) was added. The mixture was stirred for 20h at room temperature and extracted with 2.5 mL DEE; the organic phase was washed with 2.5 mL saturated sodium hydrogen carbonate solution (Ahn *et al.*, 2011). After evaporation of the solvent via a stream of nitrogen, 51 mg of **7** was obtained. Flash chromatography was used for final purification (petroleum ether/ethyl acetate 8/2) and resulted in 92% purity (GC-FID).

Sitostanyl 10-oxo-dec-8(*E*)-enoate **18** and sitostanyl 11-oxo-undec-9(*E*)-enoate **21**. Sitostanyl 8-oxooctanoate **16** (30 mg) and sitostanyl 9-oxononanoate **17** (30 mg), respectively, and (triphenylphosphoranylidene)acetaldehyde (18.2 mg) were dissolved in 200 µL chloroform, and the solution was stirred for 48h at 70 °C (Lin *et al.*, 2007). The sample was loaded onto a 500 mg silica SPE column, pre-conditioned with 6 mL *n*-hexane, and eluted with 5 mL *n*-hexane/DEE (2:1, v/v). After removal of the solvent, 82 mg of **18** and 53 mg of **21** were obtained.

Sitostanyl 8/11-hydroxyoctadec-9(*E*)-enoate **8 a,b**. A mixture of 19 mg selenium dioxide dissolved in 400 µL DCM and 75 µL of a 5M *tert*-butyl-hydroperoxide solution in *n*-decane was stirred (30 min; room temperature). Oleic acid (90 µL) and DCM (100 µL) were added, and the solution was stirred again (24h; room temperature). After addition of 300 µL H₂O and a spatula tip of citric acid, the mixture was extracted with 500 µL ethyl acetate (Knothe *et al.*, 1993; Yokoi *et al.*, 2010). After removing the solvent under nitrogen, the raw product (185 mg) was esterified with sitostanol (83 mg) in the presence of 2.0 mg DMAP and DCC (0.4 mL, 1M in DCM), resulting in 47 mg of **8 a,b**.

Sitostanyl 9,10-epoxyoctadec-11-enoate/11,12-epoxyoctadec-9-enoate **9 a,b**. A solution (5 mL) of *m*-CPBA in DCM (8 mg/mL) was added to 50 mg conjugated linoleic acid (9*Z*,11*E*); the mixture was stirred (4h; room temperature), washed with saturated

sodium hydrogencarbonate and saturated sodium chloride solution (4 mL each), and the solvent was removed via a stream of nitrogen (Toschi *et al.*, 1997). This intermediate (119 mg) was esterified with sitostanol (112 mg) in the presence of 3.0 mg DMAP and DCC (0.5 mL, 1M in DCM), resulting in 206 mg of **9 a,b**.

Sitostanyl 8/9/10/11-oxooctadecenoate (E) **22 a-d**. Methyl oleate (520 mg in 5 mL EtOAc), 1.7 mL 5M *tert*-butyl-hydroperoxide solution in *n*-decane and 300 mg 3 Å molecular sieves were stirred for 30 min. at room temperature; after addition of 50 mg manganese(III) acetate dihydrate, the solution was stirred for another 48 h at room temperature (Dang *et al.*, 2008). After dilution with diethyl ether (50 mL), the mixture was filtered through celite, and the filtrate was concentrated via a stream of nitrogen. For demethylation (Julien-David *et al.*, 2008), the crude product was dissolved in 17 mL methanol, 280 mg barium hydroxide octahydrate was added and the mixture was stirred at 50°C for 2h. After removal of the solvent under reduced pressure, the residue was redissolved in 10 mL water and acidified with 37% HCl (1.5 mL). The solution was extracted with DCM, and the organic layer was washed with water and saturated sodium chloride solution. After drying with sodium sulfate, the solvent was removed via a stream of nitrogen resulting in 97 mg raw product. Esterification with sitostanol (116 mg) in the presence of 2.9 mg DMAP and DCC (0.5 mL, 1M in DCM) resulted in 204 mg of **22 a-d**.

Sitostanyl 8/9/10/11-oxooctadecanoate **23 a-d**. A mixture of methyl 8/9/10/11-oxooctadecenoate **22 a-d** was obtained via oxidation of methyl oleate as described above. Methyl 8/9/10/11-oxooctadecenoate (100 mg) **22 a-d** was dissolved in 7 mL methanol. After addition of 50 mg 10% Pd/C, the mixture was stirred under hydrogen atmosphere for 2h at room temperature and subsequently filtered through celite (Dang *et al.*, 2008). The solvent was removed via a gentle stream of nitrogen. The subsequent demethylation (Julien-David *et al.*, 2008) was also performed as described for the synthesis of **22 a-d**. Upon esterification of the raw product (35 mg) with sitostanol (36 mg) in the presence of 0.8 mg DMAP and DCC (0.25 mL, 1M in DCM), 80 mg of sitostanyl oxooctadecanoate **23 a-d** was obtained.

3.1.2.3. Reference Compounds for GC-Based Analysis of ACOPs

Sitosteryl oleate 43. The esterification of sitosterol and oleic acid was performed as described above for sitostanyl oleate **3**.

Methyl cis-9,10-epoxystearate 34. *m*-CPBA (62 mg) was added to a solution of 65 mg methyl oleate in 2 mL DCM, and the mixture was stirred for 20 minutes at room temperature. After addition of 4 mL dichloromethane, the organic layer was washed with 4 mL water and dried with magnesium sulfate (Aerts and Jacobs, 2004). Flash chromatography with petroleum ether/ethyl acetate (92/8, v/v) was used for final purification of 109 mg raw product and resulted in 57 mg **34** with a purity of 99% (GC-FID).

Methyl 8/11-hydroxyoctadecenoate 31, 32. Selenium dioxide (19 mg), 75 μ L *t*BHP and 100 μ L DCM were stirred for 30 minutes at room temperature. After addition of 75 mg methyl oleate in 400 μ L dichloromethane, the solution was stirred for 24 hours at room temperature. After addition of 1 mL water, it was extracted three times with 1 mL *n*-hexane/MTBE (3/2, v/v). The combined organic layer was washed three times with 1 mL water and twice with 1 mL saturated sodium chloride solution and dried over magnesium sulfate (Knothe *et al.*, 1993; Yokoi *et al.*, 2010). Flash chromatography with petroleum ether/ethyl acetate (6/4, v/v and 8/2, v/v) was used for final purification of 171 mg raw product (purity 58%) and resulted in 16 mg **31, 32** with a purity of 88% (GC-FID).

Methyl 8/9/10/11-oxooctadecenoate 35. *t*BHP (7 mL) was added to 1.9 g oleic acid in 20 mL ethyl acetate. The solution was stirred for 30 minutes at room temperature. After addition of 198 mg manganese(III) acetate dihydrate, the solution was stirred for 48 hours. The solution was filtered through celite with 150 mL diethyl ether. Flash chromatography with petroleum ether/ethyl acetate (6/4, v/v) was used for purification of 420 mg of 3.1 g raw product and resulted in 142 mg oxo octadecenoic acid (Dang *et al.*, 2008). The acid was methylated (Ichihara and Fukubayashi, 2010) with 10 mL of 10% boron trifluoride solution in methanol. The mixture was shaken for 20 minutes at 37°C and after addition of 20 mL water extracted three times with 10 mL *n*-hexane. Flash chromatography with petroleum ether/ethyl acetate (8/2, v/v) was used for final

purification of 108 mg raw product (purity 37%) and resulted in 18 mg **35** with a purity of 77% (GC-FID).

Methyl 9,10-dihydroxystearate **36**. Methyl *cis*-9,10-epoxystearate **34** (200 mg) was suspended in 8 ml water/THF (1/3, v/v). After addition of 480 μ L 10% perchloric acid the solution was stirred for 20 hours at room temperature. The solution was extracted with 10 mL diethyl ether and the organic layer washed with 10 mL saturated sodium hydrogen carbonate and dried with magnesium sulfate (Ahn *et al.*, 2011). Flash chromatography with petroleum ether/ethyl acetate (6/4, v/v) was used for final purification of 214 mg raw product (purity 46%) and resulted in 43 mg **36** with a purity of 94% (GC-FID).

Methyl 5-oxohexanoate **24**. Sitostanyl 5-oxohexanoate **13** (18 mg) was weight into a reaction vessel and dissolved in 180 μ L MTBE. To the solution 30 μ L of 30% sodium methylate were added. The mixture was shaken for three minutes and left standing for two minutes. The reaction mixture was neutralized with 90 μ L 0.5M methanolic sulfuric acid and 400 μ L water was added. After shaking, 20 μ L of MTBE phase was diluted with 980 μ L *n*-hexane/MTBE (3/2, v/v) for GC-analysis.

Methyl 8-hydroxyoctanoate **25**. Sitostanyl 8-hydroxyoctanoate **5** (18 mg) was treated as described for methyl 5-oxohexanoate **24**.

Methyl 7-oxoheptanoate **26**. Sitostanyl 7-oxoheptanoate **14** (18 mg) was treated as described for methyl 5-oxohexanoate **24**.

Methyl 8-oxooctanoate **27**. Sitostanyl 8-oxooctanoate **16** (18 mg) was treated as described for methyl 5-oxohexanoate **24**.

3.1.2.4 Substrates for *In-Vitro* Hydrolyses

Eleven representatives of sitostanyl ACOPs, the respective sitosteryl ACOPs as well as sitostanyl, sitosteryl, cholesteryl and cholestanyl oleate were synthesized and purified by flash chromatography. The purities of the esters used as substrates for the *in-vitro* hydrolyses are given in Table 1.

Table 1: Purities of esters used as substrates for *in-vitro* hydrolyses.

no.	compound	purity [%]
37	cholesteryl oleate	97
38	cholestanyl oleate	98
3	sitostanyl oleate	97
39	sitostanyl nonanoate	98
2	sitostanyl octanoate	99
1	sitostanyl heptanoate	98
17	sitostanyl 9-oxononanoate	97
16	sitostanyl 8-oxooctanoate	98
14	sitostanyl 7-oxoheptanoate	98
15	sitostanyl 6-oxoheptanoate	99
13	sitostanyl 5-oxohexanoate	99
11	sitostanyl 4-oxopentanoate	99
10	sitostanyl <i>cis</i> -9,10-epoxystearate	83
7	sitostanyl 9,10-dihydroxystearate	96 ^a
43	sitosteryl oleate	97
42	sitosteryl nonanoate	99
41	sitosteryl octanoate	98
40	sitosteryl heptanoate	99
51	sitosteryl 9-oxononanoate	95
50	sitosteryl 8-oxooctanoate	98
48	sitosteryl 7-oxoheptanoate	97
49	sitosteryl 6-oxoheptanoate	96
47	sitosteryl 5-oxohexanoate	97
46	sitosteryl 4-oxopentanoate	96
45	sitosteryl <i>cis</i> -9,10-epoxystearate	93
44	sitosteryl 9,10-dihydroxystearate	96 ^a

^a determined after silylation

The syntheses and purifications of the sitostanyl ACOPs **1**, **2**, **7**, **10**, **11**, **13**, **14**, **15**, **16** and **17** were carried out according to the protocols described in section 3.1.2.2. In addition, sitostanyl nonanoate **39** was synthesized according to Barnsteiner *et al.*

(2012); the amounts of starting substances and the purification conditions are given in Table 2.

Table 2: Amounts of starting substances used for esterification of stanol / sterol and fatty acid under nitrogen atmosphere (Barnsteiner *et al.*, 2012) and ratio of elution solvents employed for purification with flash chromatography.

no.	compound	amount of		flash chromatography
		stanol / sterol (mg)	acid (mg)	petroleum ether / ethyl acetate
39	sitostanyl nonanoate	198	342	95/5
43	sitosteryl oleate	281	112	9/1
42	sitosteryl nonanoate	101	212	95/5
41	sitosteryl octanoate	102	203	95/5
40	sitosteryl heptanoate	104	177	95/5

Sitosteryl oleate **43** and the sitosteryl ACOPs **40** - **42** were also synthesized according to Barnsteiner *et al.* (2012); synthesis and purification conditions are given in Table 2.

The sitosteryl oxo-ACOPs **46** - **51** were obtained by Steglich esterification using sitosterol and the respective oxo-fatty acids which were either available (4-oxopentanoic acid, 5-oxohexanoic acid, and 6-oxoheptanoic acid) or synthesized according to the procedures described for the corresponding sitostanyl esters. Amounts of starting substances and purifications conditions are presented in Table 3.

Sitosteryl *cis*-9,10-epoxystearate **45**. Oleic acid (307 mg) was stirred for 1 h with 162 mg *m*-CPBA in 26 mL DCM. The solution was quenched with 20 mL saturated sodium thiosulfate. The aqueous phase was separated and the organic layer washed with 20 mL water (Aerts and Jacobs, 2004). After drying with magnesium sulfate the peroxide free raw product was used for esterification to sitostanyl *cis*-9,10-epoxystearate **45** (Table 3).

Sitosteryl 9,10-dihydroxystearate **44**. Sitosteryl *cis*-9,10-epoxystearate **45** (52 mg) was suspended in 2.5 mL water/THF (1/3, v/v) and 310 μ L perchloric acid was added. Flash

chromatography was used for final purification (petroleum ether/ethyl acetate, 92/8) (Ahn *et al.*, 2011).

Table 3: Amounts of starting substances used for esterification of sitosteryl esters via Steglich esterification (Wocheslander *et al.*, 2016) and ratio of elution solvents employed for purification with flash chromatography.

no.	compound	amount of				flash
		sterol (mg)	acid (mg)	DMAP (mg)	DCC (mL)	chromatography petroleum ether/ ethyl acetate
51	sitosteryl 9-oxononanoate	300	295	8.7	1.5	9/1
50	sitosteryl 8-oxooctanoate	490	396	7.5	2.0	85/15
48	sitosteryl 7-oxoheptanoate	232	203	5.4	1.0	85/15
49	sitosteryl 6-oxoheptanoate	209	197	5.0	1.0	8/2
47	sitosteryl 5-oxohexanoate	202	201	4.7	1.0	8/2
46	sitosteryl 4-oxopentanoate	202	189	4.9	1.0	7/3
45	sitosteryl <i>cis</i> -9,10-epoxystearate	251	457	7.1	1.25	92/8

3.2 Methods

3.2.1 GC-Based Analysis of Long-Chain ACOPs

3.2.1.1 Long-Chain ACOPs Formed From Sitostanyl Oleate

Thermal Treatment

Sitostanyl oleate (18.0 ± 0.1 mg) was weighed into a 1.5 mL brown glass vial. The vial was placed without a lid into a heating block (VLM Metal, Bielefeld, Germany) for defined time periods (from 15 to 180 minutes) at different temperatures (from 120°C to 200°C).

Solid-Phase Extraction

Methyl palmitate **IS**₆ (3.3 mg) and methyl ricinoleate **IS**₇ (0.35 mg) were added as internal standards to the heat-treated sitostanyl oleate, the mixture was dissolved in 3 ml of cyclohexane and the solution was loaded onto a Supelclean LC-Si SPE tube

(500 mg) which had been pre-conditioned with 6 mL *n*-hexane. The non-oxidized sitostanyl oleate and the non-polar oxidation products were eluted with 50 mL cyclohexane, the polar oxidation products with 10 mL MTBE. From both fractions the solvents were removed with a gentle stream of nitrogen.

Transesterification

For both fractions, the residues were dissolved in 180 μ L MTBE, and 30 μ L of 30% sodium methylate were added. The non-polar fraction was shaken for one minute and left standing for two minutes. The polar fraction was shaken for three minutes and left standing for two minutes. The reaction mixtures were neutralized with 90 μ L 0.5M methanolic sulfuric acid and 400 μ L water was added. After shaking, the mixtures were diluted for GC-analysis. The non-polar fraction (10 μ L of MTBE phase) was mixed with 9.99 mL *n*-hexane/MTBE (3/2, v/v) and 1 mL was transferred to a GC vial. The polar fraction (20 μ L of MTBE phase) was mixed with 980 μ L *n*-hexane/MTBE (3/2, v/v) in a GC vial.

3.2.1.2 Long-Chain ACOPs From Other Oleates

Thermal Treatment

Sitosteryl oleate, triolein, monoolein, and methyl oleate, respectively, (26.42 μ mol each) were weighed into a 1.5 mL brown glass vial. The vial was placed without a lid into a heating block (VLM Metal, Bielefeld, Germany) for 30 minutes at 180°C.

Transesterification

Methyl palmitate **IS₆** (3.3 mg or 6.6 mg for heated triolein) and methyl ricinoleate **IS₇** (0.35 mg) were added as internal standards to the heat-treated sample. The samples were dissolved in 180 μ L MTBE, and 30 μ L (60 μ L for triolein) of 30% sodium methylate were added. The sample was shaken for three minutes and left standing for two minutes. The reaction mixtures were neutralized with 90 μ L (180 μ L for triolein) 0.5M methanolic sulfuric acid and 400 μ L water was added. 100 μ L of the MTBE fraction was taken for SPE-separation. Transesterification was not performed for heated methyl oleate.

Solid-Phase Extraction

The (transesterified) sample was dissolved in 3 ml of cyclohexane and the solution was loaded onto a Supelclean LC-Si SPE tube (500 mg) which had been pre-conditioned with 6 mL *n*-hexane. The non-polar fraction was eluted with 70 mL (triolein, monoolein) or 90 mL (methyl oleate, sitosteryl oleate) cyclohexane, the polar fraction with 10 mL MTBE. From non-polar fraction the solvent was removed with a gentle stream of nitrogen, the residue was dissolved in 5 ml *n*-hexane/MTBE (3/2, v/v), and 100 µl of that solution was diluted with 900 µl *n*-hexane/MTBE (3/2, v/v) and transferred to a GC vial. The polar fraction was transferred in a GC vial without further dilution.

3.2.1.3 Quantitation of Fatty Acid Methyl Esters with GC-FID

The quantitation was based on a comparison of the area of the internal standard to that of the respective fatty acid methyl ester. Methyl palmitate **IS₆** was used as internal standard for quantitation of fatty acid methyl esters in the non-polar phase. Methyl ricinoleate **IS₇** was used as internal standard for quantitation of fatty acid methyl esters in the polar phase.

The limits of detection (LOD) and limits of quantification (LOQ) were determined according to Vogelgesang and Hädrich (1998). For their determination, dilution series (concentrations from 0.0001 mg/mL to 0.005 mg/mL) were prepared for methyl *trans*-9,10-epoxystearate **33**, methyl *cis*-9,10-epoxystearate **34**, methyl 9,10-dihydroxystearate **36**, the mixture of methyl hydroxyoctadecenoates **29-32**, and methyl oleate **28**, in triplicate.

An extended dilution series (concentrations from 0.00001 mg/ml to 0.1 mg/ml) was used to determine the Relative Response Factors (RRF) of the mentioned compounds. They were determined in triplicate experiments performed for the different concentrations and calculated as follows:

$$RRF_C = \frac{m_C \cdot A_{IS} \cdot P_{IS}}{m_{IS} \cdot A_C \cdot P_C}$$

A: area, C: compound, IS: internal standard, m: mass, P: purity, RRF: relative response factor

Recoveries were determined with a sample containing a mixture of 15 mg sitostanyl oleate, 2.5 mg sitostanyl epoxystearate, and 0.5 mg sitostanyl dihydroxystearate.

The percentage molar amount of an ACOP in the heated mixture was calculated as follows:

$$m(ACOP)[mg] = \frac{m(IS) \cdot A(ACOP) \cdot RRF_{standard\ to\ ACOP}}{A(IS)}$$

$$n(ACOP)[\mu mol] = \frac{1000 \cdot m(ACOP)}{M(ACOP)}$$

$$amount\ of\ ACOP\ after\ heating\ [mol\%] = \frac{100 \cdot n(ACOP)}{n(inserted\ sitostanyl\ oleate)}$$

A: area, ACOP: methyl ester of acyl chain oxidation product, IS: internal standard, m: mass, M: molecular weight, n: amount of substance, RRF: relative response factor

Results reported as [μ g/mg sitostanyloleate] were calculated in the same way. Only the last calculation step differed, as follows:

$$m\ (sitostanyl\ ACOP)\ [\mu g] = M(sitostanyl\ ACOP) \cdot n(ACOP)$$

$$amount\ [\mu g\ Ester/mg\ sitostanyl\ oleate] = \frac{m\ (sitostanyl\ ACOP)}{18\ mg\ sitostanyl\ oleate}$$

ACOP: methyl ester of acyl chain oxidation product, m: mass, M: molecular weight, n: amount of substance, RRF: relative response factor, sitostanyl ACOP: sitostanyl ester of acyl chain oxidation product

3.2.2 *In-Vitro* Hydrolysis of ACOPs

3.2.2.1 *In-Vitro* Hydrolysis with Cholesteryl Esterase

The hydrolysis conditions were adapted from Julien-David *et al.* (2009). Stock solutions (1 mg/mL) of steryl/stanyl esters, sterols/stanols, 5 α -cholestane **IS₈**, 19-hydroxycholesterol **IS₉** and oleic acid were prepared in ethyl acetate or chloroform. Cholesteryl esterase (0.08 mg/mL) was dissolved in PBS buffer (43 g/l KH₂PO₄, adjusted to pH 7.0 with 1M KOH). All solutions were stored at -20°C until use.

Standard Procedure

Stock solution containing 77 nmol of ester was placed into a 11 mL glass tube and 1-25 μ L stock solution of 5 α -cholestane **IS₈** was added; the amount of internal standard was adjusted based on the conversion of the ester estimated in a preliminary experiment. After removal of the solvent with a gentle stream of nitrogen and addition of 100 μ L bile salt solution (150 mg/mL in water) and 760 μ L of HPMC solution (20 mg/mL in water), the mixture was subjected four times to a procedure comprising

alternating sonication and vortexing (each for two min.). After addition of 2.1 mL PBS buffer (43 g/l KH_2PO_4 , adjusted to pH 7.0 with 1M KOH), and 40 μL freshly thawed cholesteryl esterase solution, the mixture was incubated at 37°C under shaking at 200 rpm in an incubation shaker (SW-20C/2 from Julabo Labortechnik GmbH, Seelbach, Germany). The hydrolysis was stopped after one hour by addition of *n*-heptane and following three times extraction each with 8 mL *n*-heptane. The solvent of the organic layer was removed with a rotary evaporator. The residue was transferred with *n*-hexane/MTBE (3/2, v/v) into a 1.5 mL GC vial. After evaporation with a gentle stream of nitrogen and dissolution in 500 μL *n*-hexane/MTBE (3/2, v/v) the sample was analyzed with GC-FID.

Hydrolyses of Two Esters at the Same Time

Except for the addition of 77 nmol of a second ester, the standard procedure was not modified.

Hydrolyses of Sitostanyl Esters in the Presence of the Products Resulting from the Hydrolysis of Steryl/-stanyl Oleates

The products resulting from hydrolysis of cholesteryl oleate, i.e. oleic acid and cholesterol, were added to the hydrolysis mixtures of sitostanyl esters in the amounts given in Table 4. Otherwise, the standard procedure was not modified.

Table 4: Amounts of oleic acid and cholesterol, respectively, added to the hydrolysis mixtures of sitostanyl esters.

Ester (each 77 nmol)	Conversion of cholesteryl oleate ^a (%)	Oleic acid (nmol)	Cholesterol (nmol)
Sitostanyl oleate	62	48	48
Sitostanyl 7-oxoheptanoate	73	56	56
Sitostanyl heptanoate	73	56	56
Sitostanyl 5-oxohexanoate	68	52	52

^a this conversion determined for the hydrolysis of cholesteryl oleate in the presence of the respective ester (see Figure 64) was used to calculate the added amounts (nmol) of oleic acid and cholesterol.

In additional experiments, hydrolyses of sitostanyl oleate (77 nmol) were performed in the presence of 48 nmol sitosterol (hydrolysis product of sitosteryl oleate) and 48 nmol cholestanol (hydrolysis product of cholestanyl oleate), respectively.

Hydrolyses of Cholesteryl Oleate in the Presence/Absence of Sitosteryl 9,10-dihydroxystearate

Additional hydrolyses of cholesteryl oleate (77 nmol) in absence or presence of sitosteryl 9,10-dihydroxystearate (105 nmol) were performed according to the standard procedure, except for the following modifications: (i) use of 19-hydroxycholesterol **IS₉** as internal standard and use of sodium desoxycholate; (ii) use of 19-hydroxycholesterol **IS₉** as internal standard and use of the bile salt mixture; (iii) use of 5 α -cholestane **IS₈** as internal standard and use of sodium desoxycholate; (iv) use of 5 α -cholestane **IS₈** as internal standard and use of the bile salt mixture.

For the determinations using 19-hydroxycholesterol **IS₉** as internal standard, respective relative response factors (2.1 for cholesterol and cholestanol, 2.5 for sitosterol and sitostanol) were taken into account.

3.2.2.2 Determination of Conversion Rates with GC-FID

The quantitation was based on a comparison of the areas of sterol/stanol and that of the internal standard (5 α -cholestane **IS₈** or 19-hydroxycholesterol **IS₉**) to calculate the amount of free sterol/stanol liberated due to hydrolysis. The conversion rate was as ratio of molar amount of released sterol/stanol to the initial molar amount of ester.

$$m_{sterol/stanol} = \frac{A_{sterol/stanol} \cdot m_{IS} \cdot P_{IS} \cdot RRF}{A_{IS}}$$

$$n_{sterol/stanol} = \frac{m_{sterol/stanol}}{M_{sterol/stanol}}$$

$$n_{ester} = \frac{m_{ester} \cdot P_{ester}}{M_{ester}}$$

$$\text{molar hydrolysis rate (\%)} = \frac{n_{sterol/stanol}}{n_{ester}}$$

A: area, ester: steryl/stanyl ester, IS: internal standard, m: mass, M: molecular weight, n: amount of substance, P: purity, RRF: relative response factor

Relative response factors were determined for sitosterol, sitostanol, cholesterol and cholestanol to 5 α -cholestane **IS₈** and 19-hydroxychoelsterol **IS₉**, respectively, in triplicate and calculated as follows:

$$RRF_{sterol\ to\ IS} = \frac{m_{sterol,theoretic}}{m_{sterol,determined}} = \frac{m_{sterol,weighed} \cdot P_{sterol}}{\frac{A_{sterol} \cdot m_{IS,weight} \cdot P_{IS}}{A_{IS}}}$$

A: area, RRF: relative response factor, m: mass, P: purity, IS: internal standard

3.2.3 GC Analysis

3.2.3.1 GC-FID

Analysis of the samples was performed using a 6890N GC equipped with an FID (Agilent Technologies, Böblingen, Germany). The temperature of the injector was 280°C, the temperature of the detector was 340°C (makeup gas: nitrogen, 25 mL/min.). The injection volume was 0.1 µL. A 30m x 0.25mm i.d., 0.1µm film, RTX-200MS fused silica capillary column (Restek, Bad Homburg, Germany) was used for separation with hydrogen as carrier gas at a constant flow rate of 1.5 mL/min. The split ratio was 1:7.5 (split flow: 11 mL/min.). Data acquisition was performed by MSD ChemStation software.

Temperature program for determinations of the purities of synthesized substances (steryl/stanyl esters, oxidized fatty acids) and quantitations of sterols/stanols in in-vitro hydrolyses

Temperature program: starting temperature 100°C (0.1 min. hold); then increases by 15°C/min. to 310°C (2 min. hold) and 1.5°C/min. to 340°C (3 min. hold) (Barnsteiner *et al.*, 2011).

Temperature program for identifications and quantitations of long-chain ACOPs

Temperature program: starting temperature 70°C (5 min. hold); then increases by 15°C/min. to 170°C (4 min. hold), 10°C/min. to 220°C (3 min. hold) and 35°C/min. to 340°C (3 min. hold).

3.2.3.2 GC-MS

Analysis was performed using a 7890A GC equipped with an 5975C inert MSD mass spectrometer (Agilent Technologies, Böblingen, Germany). A 30m x 0.25mm i.d., 0.1µm film, RTX-200MS fused silica capillary column (Restek, Bad Homburg, Germany) was used for separation with helium as carrier gas with a constant flow rate of 1.5 mL/min. The injector was heated to 50°C for manual injection (volume 0.2 µL)

and after 0.5 minutes with 900°C/min. heated to 340°C. The auxiliary line was heated to 280°C. Mass spectra were obtained by positive electron impact ionization in the scan mode at unit resolution from 40 to 700 Da. The quadrupole was heated to 150°C and the ion source to 230°C. Data acquisition was performed by MSD ChemStation software.

Temperature program for identification of long-chain ACOPs

Temperature program: starting temperature 40°C (2 min. hold); then increases by 100°C/min. to 70°C (5 min. hold), 15°C/min. to 170°C (4 min. hold), 10°C/min. to 220°C (3 min. hold) and 35°C/min. to 340°C (3 min. hold).

3.2.4 Further Analysis

3.2.4.1 NMR Spectroscopy

¹H-NMR and ¹³C-NMR spectra of the esters dissolved in deuterated chloroform (400 μL) were acquired at 500 and 126 MHz, respectively with Avance-HD 500 spectrometers operating at 27°C. For ¹H-detected experiments, including two-dimensional COSY, HSQC, and HMBC, an inverse ¹H/¹³C probe head and for direct ¹³C measurements a QNP ¹³C/³¹P/²⁹Si/¹⁹F/¹H cryoprobe were used. All experiments were performed in full automation with the standard parameter sets of the TOPSPIN 3.2 software package (Bruker, Billerica, MA, USA). Proton-decoupled mode was used for ¹³C-NMR spectra. The data were processed using MestreNova software.

3.2.4.2 HPLC-ELSD Analysis

Analysis was performed using an HPLC consisting of a Jasco AS 2055 Plus auto sampler, 2 Jasco PU-2087 pumps, equipped with an analytical TP Cell 1.0 mm, a Jasco DAD MD-2010 (all devices from Jasco, Groß-Umstadt, Germany) and a SEDEX 90 LT-ELSD (Sedere, Alfortville Cedex, France). Separations were performed on a Nucleosil RP-8 column, 4.6 x 250 mm, 5 μm particle size, flow rate of 0.8 mL/min.; injection volumes: 10 μl of solutions (0.1 mg/ml) in ethyl acetate. In the mobile phase (90% methanol and 10% water) the percentage of methanol was increased to 100% within 25 minutes. Data acquisition was performed using ChromPass 1.9 software (Jasco, Groß-Umstadt, Germany).

4. RESULTS AND DISCUSSION

4.1 Syntheses of ACOPs Used as Internal Standards and Reference Compounds for UHPLC-MS/MS-Based Analysis

4.1.1 Introduction

This part of the thesis was embedded in a project aiming at the development of strategies for UHPLC-MS/MS-based analysis of different classes of ACOPs resulting from thermo-oxidation of sitostanyl oleate. The approach developed (Scholz *et al.*, 2019) is outlined in Figure 14.

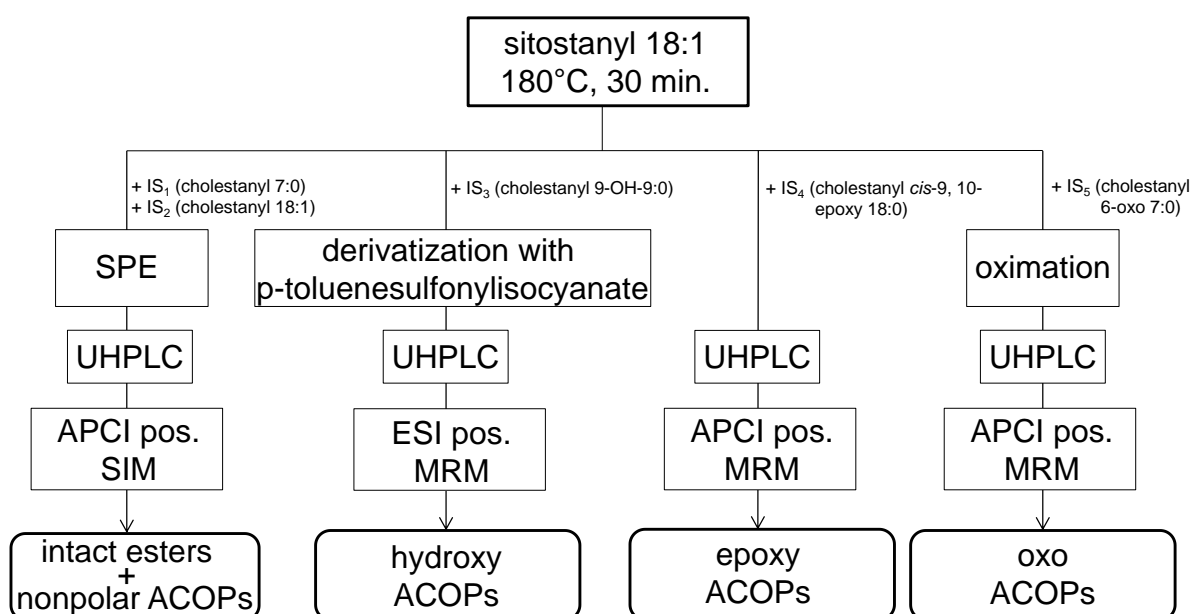


Figure 14: UHPLC-MS/MS-based approach for the analysis of ACOPs of sitostanyl oleate (Scholz *et al.*, 2019).

The UHPLC-MS/MS-based approach summarized in Figure 14 comprises the following key elements:

- (i) partitioning of the heat-treated sitostanyl oleate in four aliquots and application of different routes allowing specific analyses of members of the four major classes of ACOPs to be expected, i.e. non-polar, hydroxy-, oxo- and epoxy-ACOPs;
- (ii) addition of internal standards to the aliquots representing the respective class of ACOPs;

- (iii) application of SPE-based pre-separation (for intact ester and non-polar ACOPs) and selective derivatizations, i.e. reaction with *p*-toluenesulfonylisocyanate (for hydroxy-ACOPs) and oximation (for oxo-ACOPs);
- (iv) use of atmospheric pressure chemical ionization and electrospray ionization techniques and establishment of selective multireaction monitoring transitions.

The tasks performed as part of this thesis were

- (i) syntheses of the internal standards to be used as representatives of the classes of ACOPs;
- (ii) syntheses of authentic reference compounds to be used for the identification of individual ACOPs from the different chemical classes.

4.1.2 Syntheses of Internal Standards

As shown in Figure 14, in the developed UHPLC-MS/MS-based approach aliquots of the oxidized mixture were subjected to different analytical routes involving additional SPE-based pre-separation or selected derivatisation steps prior to UHPLC-separation and mass spectrometric analysis. This enabled the targeted investigations of remaining intact ester and non-polar ACOPs, hydroxy-ACOPs, epoxy-ACOPs and oxo-ACOPs (Scholz *et al.*, 2019). For each of these ACOP-classes, a representative internal standard was required. The structures of the selected candidates are shown in Figure 15. The syntheses of these internal standards were performed according to the principles described below. Their identities were confirmed by NMR analyses.

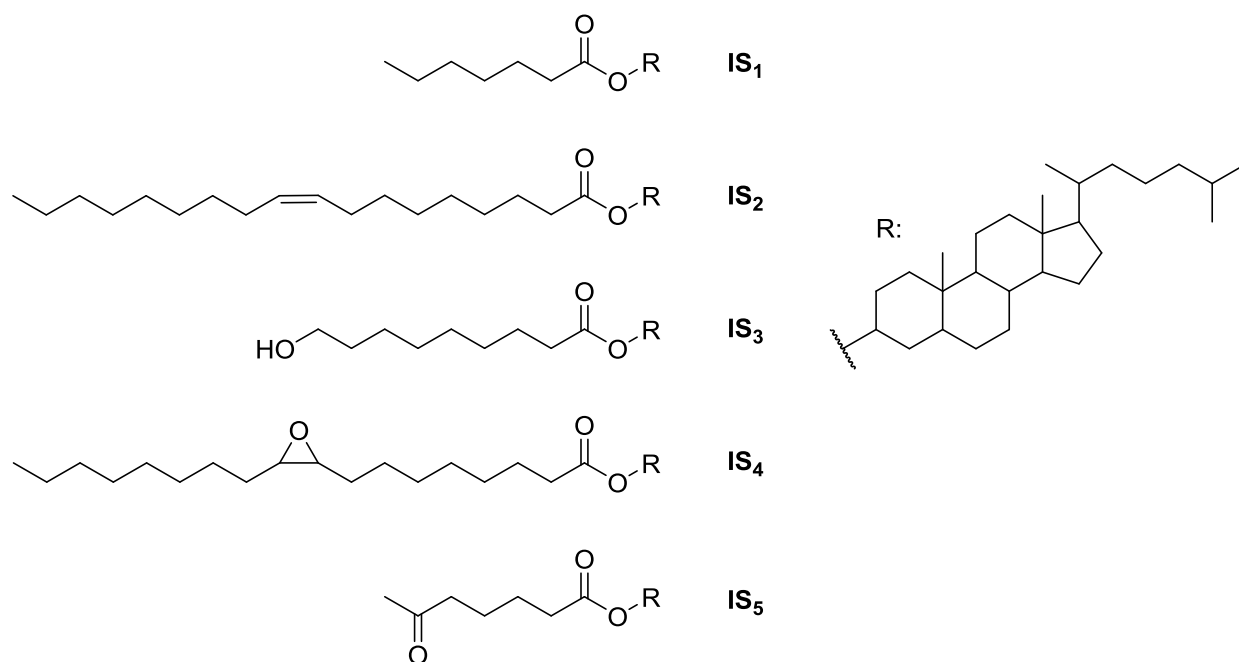


Figure 15: Structures of the synthesized internal standards used for UHPLC-MS/MS-based analysis: cholestanyl heptanoate **IS₁**, cholestanyl oleate **IS₂**, cholestanyl 9-hydroxynonanoate **IS₃**, cholestanyl *cis*-9,10-epoxystearate **IS₄**, and cholestanyl 6-oxoheptanoate **IS₅**.

Cholestanyl heptanoate **IS₁**

Cholestanyl heptanoate **IS₁** was obtained via Steglich esterification of cholestanol and heptanoic acid, using dicyclohexylcarbodiimide (DCC) as coupling reagent and 4-dimethylaminopyridine (DMAP) as catalyst (Figure 16).

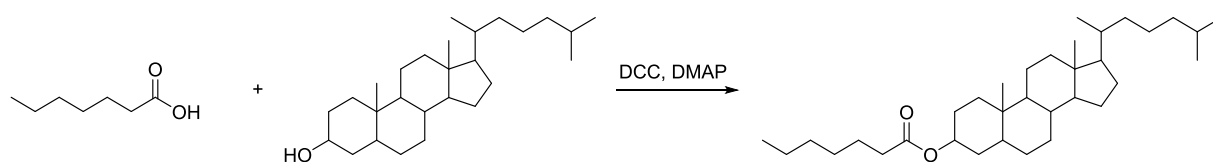


Figure 16: Synthesis of cholestanyl heptanoate **IS₁** via Steglich esterification of heptanoic acid and cholestanol.

NMR-data of cholestanyl heptanoate **IS₁**:

¹H-NMR (500 MHz, CDCl₃): δ = 4.69 (1H, tt, J = 11.2 Hz, 4.9 Hz, St-3), 2.25 (2H, t, J = 7.5 Hz, FA-2), 1.95 (1H, dt, J = 12.5 Hz, 3.3 Hz, St-17), 1.86 - 1.76 (2H, m), 1.72 (1H, dt, J = 13.3 Hz, 3.6 Hz, St-9), 1.64 (1H, dq, J = 13.0 Hz, 3.4 Hz, St-20), 1.62 - 1.43 (8H, m), 1.39 - 0.93 (26H, m), 0.89 (3H, d, J = 6.5 Hz, St-21), 0.88 (3H, d, J = 4.8

Hz, FA-7), 0.86 (3H, d, $J = 2.3$ Hz, St-26/27), 0.85 (3H, d, $J = 2.4$ Hz, St-26/27), 0.81 (3H, s, St-19), 0.64 (3H, s, St-18);

^{13}C -NMR (125 MHz, CDCl_3): $\delta = 173.62$ (FA-1), 73.58 (St-3), 56.55, 56.39, 54.35, 44.79, 42.72, 40.11, 39.65, 36.90, 36.30, 35.95, 35.60, 34.93, 34.21, 32.13, 31.61, 28.94, 28.76, 28.39, 28.16, 27.66, 25.20, 24.35, 23.98, 22.97, 22.71, 22.63, 21.34, 18.81 (St-21), 14.19 (FA-7), 12.37 (St-18/19), 12.21 (St-18/19).

Cholestanyl oleate **IS**₂

According to a procedure described by Barnsteiner *et al.* (2011), the synthesis of cholestanyl oleate **IS**₂ was performed by heating cholestanol and oleic acid in a nitrogen-flooded reaction vessel (Figure 17). Subsequent purification steps comprised alkaline treatment to remove the excess of acid and solid-phase extraction on a silica column.

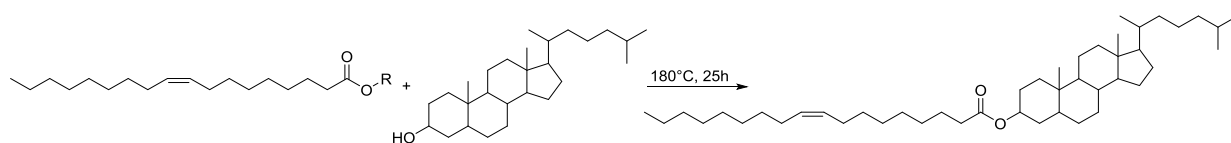


Figure 17: Synthesis of cholestanyl oleate **IS**₂ from oleic acid and cholestanol.

NMR-data of cholestanyl oleate **IS**₂:

^1H -NMR (500 MHz, CDCl_3): $\delta = 5.42$ -5.28 (2H, m, FA-9, FA-10), 4.69 (1H, tt, $J = 11.2$ Hz, 4.8 Hz, St-3), 2.25 (2H, t, $J = 7.6$ Hz, FA-2), 2.06-1.92 (5H, m), 1.85-1.76 (2H, m), 1.72 (1H, dt, $J = 13.3$ Hz, 3.7 Hz, St-17), 1.68-1.43 (9H, m), 1.41-0.94 (40H, m), 0.91-0.84 (12H, m, FA-18, St-21, St-26, St-27), 0.81 (3H, s, St-19), 0.64 (3H, s, St-18);

^{13}C -NMR (125 MHz, CDCl_3): $\delta = 173.61$ (FA-1), 130.12 (FA-9/10), 129.91 (FA-9/10), 73.60 (St-3), 56.55, 56.38, 54.35, 44.79, 42.72, 40.11, 39.65, 36.90, 36.30, 35.95, 35.60, 34.91, 34.21, 32.13, 32.06, 29.92, 29.83, 29.68, 29.48, 29.31, 29.25, 29.24, 28.76, 28.39, 28.16, 27.66, 27.37, 27.31, 25.23, 24.35, 23.98, 22.98, 22.85, 22.72, 21.34, 18.81 (St-21), 14.29 (FA-18), 12.38 (St-18/19), 12.21 (St-18/19).

Cholestanyl 9-hydroxynonanoate IS₃

Cholestanyl 9-hydroxynonanoate **IS₃** was synthesized in three steps as depicted in Figure 18:

- (i) Diol cleavage of aleuritic acid (9,10,16-trihydroxypalmitic acid) resulting in 9-oxononanoic acid.
- (ii) Steglich esterification of 9-oxononanoic acid with cholestanol.
- (iii) Reduction of the formed cholestanyl 9-oxononanoate with sodium borohydride.

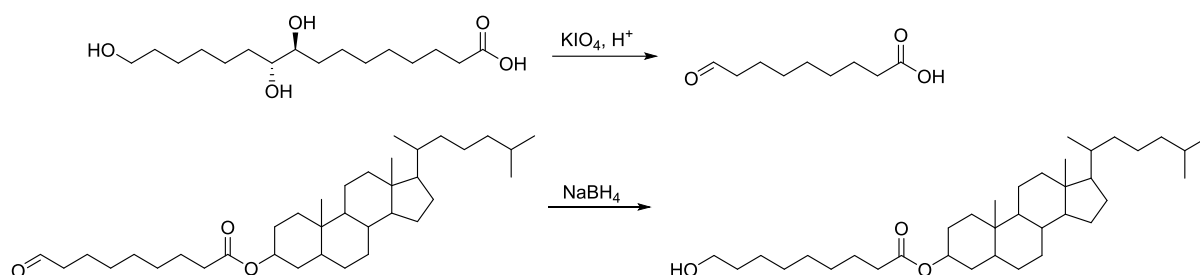


Figure 18: Procedure applied to synthesize cholestanyl 9-hydroxynonanoate **IS₃**.

NMR-data of cholestanyl 9-hydroxynonanoate **IS₃**:

$^1\text{H-NMR}$ (500 MHz, CDCl_3): $\delta = 4.73\text{-}4.64$ (1H, m, St-3), 3.63 (2H, t, $J = 6.6$ Hz, FA-9), 2.24 (2H, t, $J = 7.5$ Hz, FA-2), 1.95 (1H, dt, $J = 12.6$ Hz, 3.4 Hz, St-17), 1.85-1.75 (2H, m), 1.71 (1H, dt, $J = 13.4$ Hz, 3.7 Hz, St-9), 1.64 (2H, dq, $J = 13.5$ Hz, 3.6 Hz, St-20), 1.61-1.42 (9H, m), 1.39-0.92 (30H, m), 0.89 (3H, d, $J = 6.6$ Hz, St-21), 0.86 (3H, d, $J = 2.4$ Hz, St-26/27), 0.85 (3H, d, $J = 2.4$ Hz, St-26/27), 0.81 (3H, s, St-19), 0.64 (3H, s, St-18);

$^{13}\text{C-NMR}$ (125 MHz, CDCl_3): $\delta = 173.59$ (FA-1), 73.62 (St-3), 63.14 (FA-9), 56.53, 56.37, 54.33, 52.72, 44.77, 42.71, 40.10, 39.64, 36.88, 36.29, 35.93, 35.59, 34.87, 34.20, 32.88, 32.12, 29.33, 29.14, 28.74, 28.38, 28.15, 27.65, 25.78, 25.17, 24.34, 23.96, 22.96, 22.70, 21.33, 18.80 (St-21), 12.37 (St-18/19), 12.20 (St-18/19).

Cholestanyl *cis*-9,10-epoxystearate IS₄

In accordance with the procedure described for methyl oleate (Aerts and Jacobs, 2004), synthesized cholestanyl oleate **IS₂** was epoxidized with 3-chloroperoxybenzoic acid (*m*-CPBA) (Figure 19).

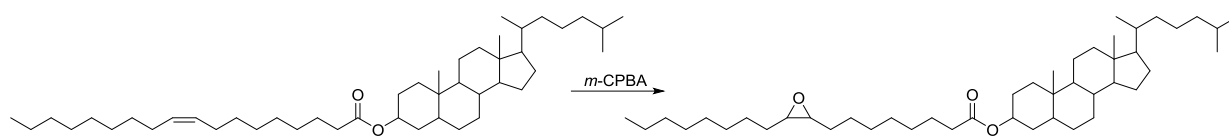


Figure 19: Synthesis of cholestanyl *cis*-9,10-epoxystearate **IS₄** via epoxidation of cholestanyl oleate **IS₂**.

NMR-data of cholestanyl *cis*-9,10-epoxystearate **IS₄**:

¹H-NMR (500 MHz, CDCl₃): δ = 4.75-4.64 (1H, m, St-3), 2.95-2.90 (2H, m, FA-9/10), 2.26 (2H, t, J = 7.5 Hz, FA-2), 1.95 (1H, dt, J = 12.6 Hz, 3.4 Hz, St-17), 1.85-1.76 (2H, m), 1.71 (1H, dt, J = 13.3 Hz, 3.7 Hz, St-9), 1.67-0.93 (53H, m), 0.89 (3H, d, J = 6.5 Hz, St-21), 0.88 (3H, d, J = 6.7 Hz, FA-18), 0.86 (3H, d, J = 2.2 Hz, St-26/27), 0.85 (3H, d, J = 2.3 Hz, St-26/27), 0.81 (3H, s, St-19), 0.64 (3H, s, St-18)

¹³C-NMR (125 MHz, CDCl₃): δ = 173.78 (FA-1), 73.74 (St-3), 57.65 (FA-9/10), 57.60 (FA-9/10), 56.51, 56.36, 54.31, 44.75, 42.69, 40.08, 39.63, 36.86, 36.28, 35.93, 35.57, 34.87, 34.17, 32.10, 31.99, 29.68, 29.67, 29.47, 29.36, 29.31, 29.13, 28.73, 28.37, 28.14, 27.89, 27.85, 27.63, 26.71, 26.66, 25.16, 24.33, 23.96, 22.96, 22.81, 22.70, 21.31, 18.78 (St-21), 14.26 (FA-18), 12.35 (St-18/19), 12.18 (St-18/19).

Cholestanyl 6-oxoheptanoate **IS₅**

Cholestanyl 6-oxoheptanoate **IS₅** was synthesized by Steglich esterification of cholestanol and commercially available 6-oxoheptanoic acid (Figure 20).

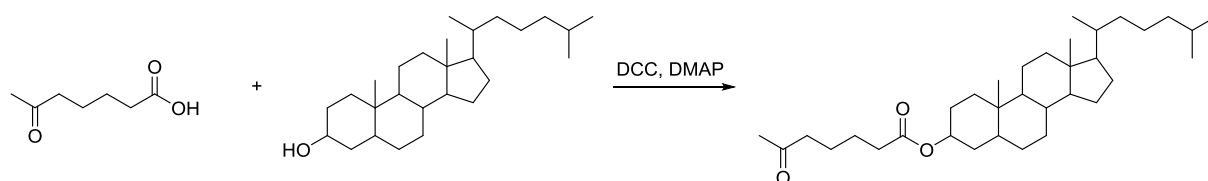


Figure 20: Synthesis of cholestanyl 6-oxoheptanoate **IS₅** via Steglich esterification of 6-oxoheptanoic acid and cholestanol.

NMR-data of cholestanyl 6-oxoheptanoate **IS₅**:

¹H-NMR (500 MHz, CDCl₃): δ = 4.72-4.64 (1H, m, St-3), 2.46-2.41 (2H, m, FA-5), 2.29-2.24 (2H, m, FA-2), 2.13 (3H, s, FA-7), 1.95 (1H, dt, J = 12.6 Hz, 3.3 Hz, St-17), 1.84-

1.75 (2H, m), 1.72 (1H, dt, $J = 13.4$ Hz, 3.7 Hz, St-9), 1.64 (1H, dq, $J = 12.5$ Hz, 3.2 Hz, St-20), 1.61 (1H, s), 1.60 (4H, t, $J = 3.7$ Hz, FA-3/4), 1.57-1.43 (5H, m), 1.38-0.93 (20H, m), 0.89 (3H, d, $J = 6.6$ Hz, St-21), 0.86 (3H, d, $J = 2.4$ Hz, St-26/27), 0.85 (3H, d, $J = 2.4$ Hz, St-26/27), 0.81 (3H, s, St-19), 0.64 (3H, s, St-18);

^{13}C -NMR (125 MHz, CDCl_3): $\delta = 208.75$ (FA-6), 173.09 (FA-1), 73.79 (St-3), 56.53, 56.37, 54.33, 44.77, 43.43 (FA-5), 42.71, 40.10, 39.64, 36.87, 36.29, 35.93, 35.58, 34.57, 34.18, 32.11, 30.04 (FA-7), 28.74, 28.38, 28.14, 27.63, 24.63, 24.33, 23.96, 23.30, 22.96, 22.70, 21.32, 18.80 (St-21), 12.36 (St-18/19), 12.20 (St-18/19).

4.1.3 Syntheses of Reference Substances

Taking into account (i) the knowledge available regarding the oxidation of cholesteryl esters (Kamido *et al.*, 1992; 1993; 1995; Leitinger, 2003; Miyoshi *et al.*, 2013), (ii) the reaction products reported to result from thermo-oxidation and frying of fats, oils and unsaturated fatty acid methyl esters (Velasco *et al.*, 2004b; Dobarganes and Márquez-Ruiz, 2007; Berdeaux *et al.*, 2012) and (iii) the ACOPs identified by GC-MS upon thermal treatment of a mixture of phytosteryl/-stanyl linoleates (Wocheslander *et al.*, 2016), non-polar short-chain ACOPs as well as polar hydroxy-, epoxy- and oxo-ACOPs were anticipated upon thermo-oxidation of sitostanyl oleate. Accordingly, representatives of these four types of ACOPs were synthesized as reference compounds for the UHPLC-MS/MS-based analysis.

The principles of the performed syntheses are described below. If available, NMR data of the synthesized products are provided.

Non-polar ACOPs

In addition to the remaining unaltered sitostanyl oleate **3**, the non-polar short-chain ACOPs sitostanyl heptanoate **1** and sitostanyl octanoate **2** are expected in the first fraction resulting from the scheme depicted in Figure 14. Their structures are shown in Figure 21.

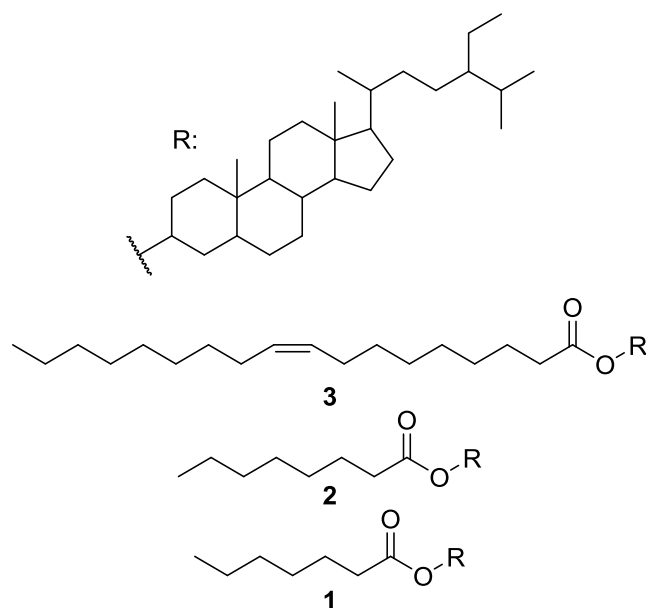


Figure 21: Structures of the remaining unaltered sitostanyl oleate **3** and of the short-chain non-polar ACOPs sitostanyl heptanoate **1** and sitostanyl octanoate **2**.

In accordance with the procedure described for syntheses of acylsterols by Carvalho *et al.* (2011), sitostanyl heptanoate **1** and sitostanyl octanoate **2** were synthesized via Einhorn-acylation from the respective fatty acid chloride and sitostanol, using pyridine as base. As example, the reaction scheme is shown for sitostanyl heptanoate **1** in Figure 22.

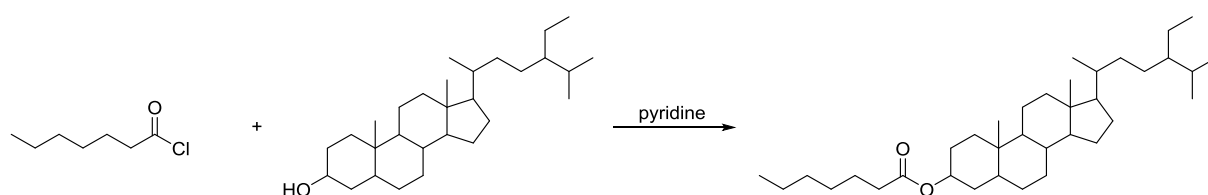


Figure 22: Synthesis of sitostanyl heptanoate **1** via Einhorn-acylation.

Hydroxy-ACOPs

The synthesized ACOPs containing either a terminal hydroxy group, an allylic hydroxy group or vicinal hydroxy groups in the fatty acid moiety are shown in Figure 23.

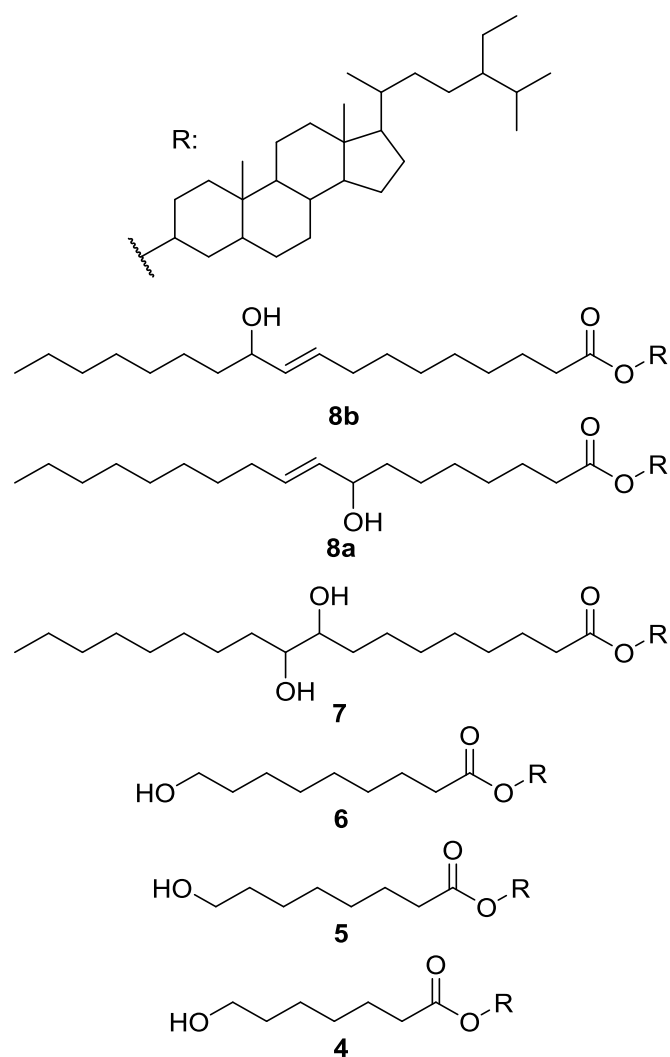


Figure 23: Structures of ACOPs of sitostanyl oleate containing one or two hydroxy groups in the fatty acid moiety: sitostanyl 7-hydroxyheptanoate **4**, sitostanyl 8-hydroxyoctanoate **5**, sitostanyl 9-hydroxynonanoate **6**, sitostanyl 9,10-dihydroxystearate **7**, and sitostanyl 8/11-hydroxyoctadecen-(9E)-oate **8a,b**.

In analogy to the procedure described for cholestanyl 9-hydroxynonanoate **IS₃**, the syntheses of the ACOPs carrying a terminal hydroxy group in the fatty acid moiety, i.e. sitostanyl 7-hydroxyheptanoate **4**, sitostanyl 8-hydroxyoctanoate **5** and sitostanyl 9-hydroxynonanoate **6**, were performed via a two step-procedure, i.e. (i) Steglich esterification of the respective oxo-acid, i.e. 7-oxoheptanoic acid, 8-oxooctanoic acid and 9-oxononanoic acid, with sitostanol, and (ii) reduction of the intermediate oxo-acid sitostanyl ester using sodium borohydride. As example, the reaction scheme is shown for sitostanyl 7-hydroxyheptanoate **4** in Figure 24.

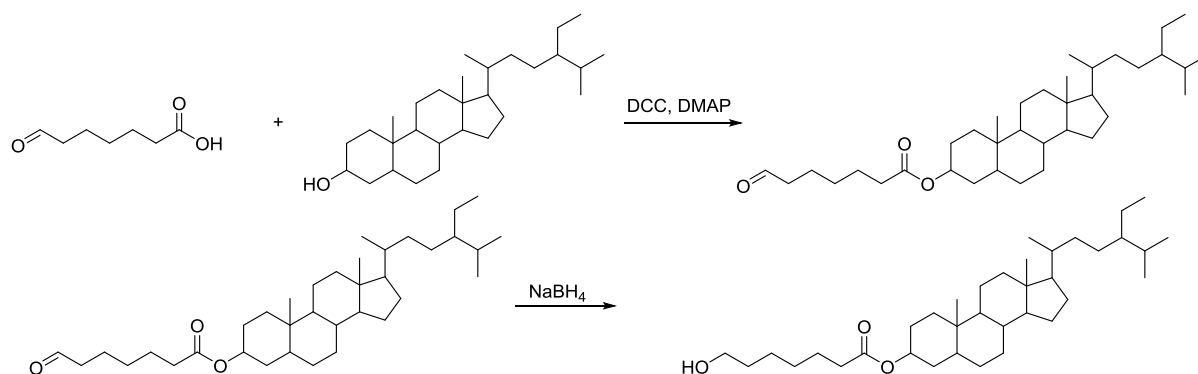


Figure 24: Synthesis of sitostanyl 7-hydroxyheptanoate **4**.

In accordance with the approach described for oleic acid (Knothe *et al.*, 1993) and other monounsaturated fatty acids (Yokoi *et al.*, 2010), 8- and 11-hydroxyoctadecen-(9*E*)-oic acid was synthesized by hydroxylation of oleic acid with the selenium dioxide / *tert*-butylhydroperoxide system (Figure 25).

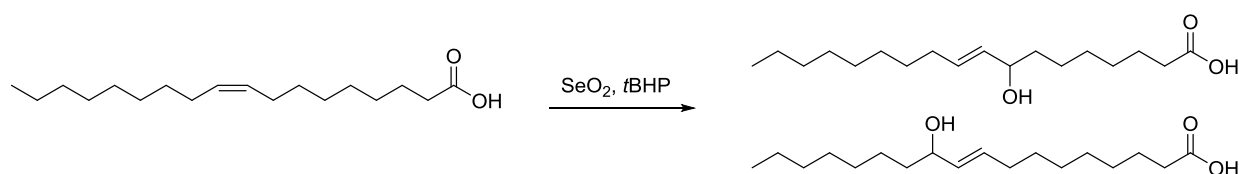


Figure 25: Synthesis of 8/11-hydroxyoctadecen-(9*E*)-oic acid via allylic hydroxylation of oleic acid.

The two ACOPs carrying the hydroxy group in the allylic positions of the 9,10-double bond, i.e. sitostanyl 8/11-hydroxyoctadecen-(9*E*)-oate **8a,b** were obtained by subsequent Steglich esterification of the hydroxylated acids with sitostanol.

In accordance with the method described for methyl 9,10-dihydroxystearate (Ahn *et al.*, 2011), sitostanyl 9,10-dihydroxystearate **7** was synthesized via ring opening of the epoxide of sitostanyl *cis*-9,10-epoxystearate **10a**, using perchloric acid (Figure 26).

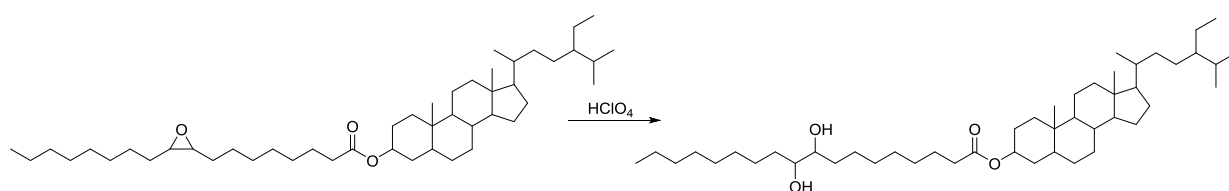


Figure 26: Synthesis of sitostanyl 9,10-dihydroxystearate **7**.

NMR-data of sitostanyl 9,10-dihydroxystearate **7**:

$^1\text{H-NMR}$ (500 MHz, CDCl_3): δ = 4.69 (1H, tt, J = 10.9 Hz, 4.9 Hz, St-3), 3.42-3.36 (2H, m, FA-9/10), 2.25 (2H, t, J = 7.5 Hz, FA-2), 2.09-0.96 (58H, m), 0.91-0.79 (18H, m, FA-18, St-19, St-21, St-24², St-26, St-27), 0.64 (3H, s, St-18)

$^{13}\text{C-NMR}$ (125 MHz, CDCl_3): δ = 173.62 (FA-1), 74.66, 74.61, 73.64 (St-3), 56.52, 56.26, 54.32 (St-18), 45.92, 44.76, 42.70, 40.08, 36.87, 36.30, 35.58, 34.85, 34.19, 34.01, 33.75, 33.69, 32.11, 32.02, 29.83, 29.71, 29.56, 29.43, 29.29, 29.22, 29.13, 28.74, 28.40, 27.64, 26.14, 25.82, 25.69, 25.14, 24.34, 23.16, 22.82, 21.32, 19.96, 19.15, 18.85 (St-21), 14.27 (FA-18), 12.36 (St-18/19/24²), 12.19 (St-18/19/24²), 12.11 (St-18/19/24²).

Epoxy-ACOPs

The structures of the synthesized ACOPs possessing an epoxy-group in the fatty acid side chain are shown in Figure 27.

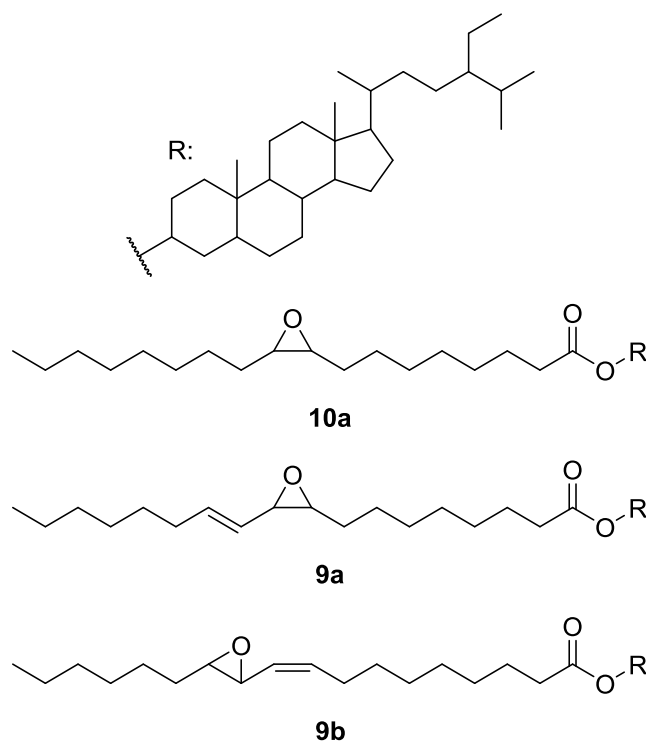


Figure 27: Structures of sitostanyl *cis*-9,10-epoxystearate **10a**, sitostanyl *cis*-9,10-epoxyoctadecen-(11*E*)-oate **9a**, and sitostanyl *trans*-11,12-epoxyoctadecen-(9*Z*)-oate **9b**.

The synthesis of sitostanyl *cis*-9,10-epoxystearate **10a** was performed in analogy to the procedure described for cholestanyl *cis*-9,10-epoxystearate **IS₄** via epoxidation of sitostanyl oleate with *m*-CPBA according to Aerts and Jacobs (2004).

NMR-data of sitostanyl *cis*-9,10-epoxystearate **10a**:

¹H-NMR (500 MHz, CDCl₃): δ = 4.69 (1H, tt, J = 10.9 Hz, 4.9 Hz, St-3), 2.92-2.86 (2H, m, FA-9/10), 2.25 (2H, t, J = 7.5 Hz, FA-2), 1.95 (1H, dt, J = 12.6 Hz, 3.4 Hz, St-17), 1.86-1.75 (2H, m), 1.72 (1H, dt, J = 13.4 Hz, 3.7 Hz, St-9), 1.68-1.53 (7H, m), 1.52-1.45 (7H, m), 1.44-1.38 (2H, m), 1.38-1.29 (14H, m), 1.29-1.23 (12H, m), 1.22-0.92 (12H, m), 0.91-0.79 (18H, m, FA-18, St-19, St-21, FA-18, St-24², St-26, St-27), 0.64 (3H, s, St-18)

¹³C-NMR (125 MHz, CDCl₃): δ = 173.54 (FA-1), 73.61 (St-3), 57.39 (FA-9/10), 57.35 (FA-9/10), 56.53, 56.26, 54.32, 45.92, 44.77, 42.70, 40.08, 36.88, 36.30, 35.59, 34.86, 34.20, 34.02, 32.12, 32.00, 29.70, 29.68, 29.49, 29.49, 29.33, 29.22, 29.14, 28.74, 28.40, 27.97, 27.93, 27.65, 26.75, 26.70, 26.14, 25.17, 24.35, 23.16, 22.82, 21.32, 19.96, 19.15, 18.86 (St-21), 14.27 (FA-18), 12.37 (St-18/19/24²), 12.19 (St-18/19/24²), 12.11 (St-18/19/24²).

Preliminary mass spectrometric data from the UHPLC-MS/MS analyses had indicated that in addition to the ACOP with the epoxy-group in position of the double bond also unsaturated ACOPs with an epoxy-group in allylic positions to the double bond might be present. Therefore, mono-epoxides of conjugated linoleic acid (CLA) were synthesized by reaction with *m*-CPBA, in analogy to the mono-epoxidation described for methyl linoleate (Toschi *et al.*, 1997). As reported by Jie *et al.* (2003), the molar ratio of conjugated linoleic acid to *m*-CPBA determines the ratio of formed mono-epoxides to di-epoxide. For the synthesis performed in this thesis, a molar ratio of approximately 1/0.8 (CLA/*m*-CPBA) was used, which favours the formation of equal amounts of the two possible mono-epoxides and a low amount of di-epoxide. Subsequent Steglich esterification of the mixture of epoxy-acids with sitostanol resulted in **9a,b**.

Oxo-ACOPs

The group of oxo-ACOPs can be divided into two subgroups: ACOPs with keto-functions in the fatty acid side chain and ACOPs with aldehyde-functions.

The structures of the synthesized ACOPs containing keto-groups in the acyl chain are shown in Figure 28.

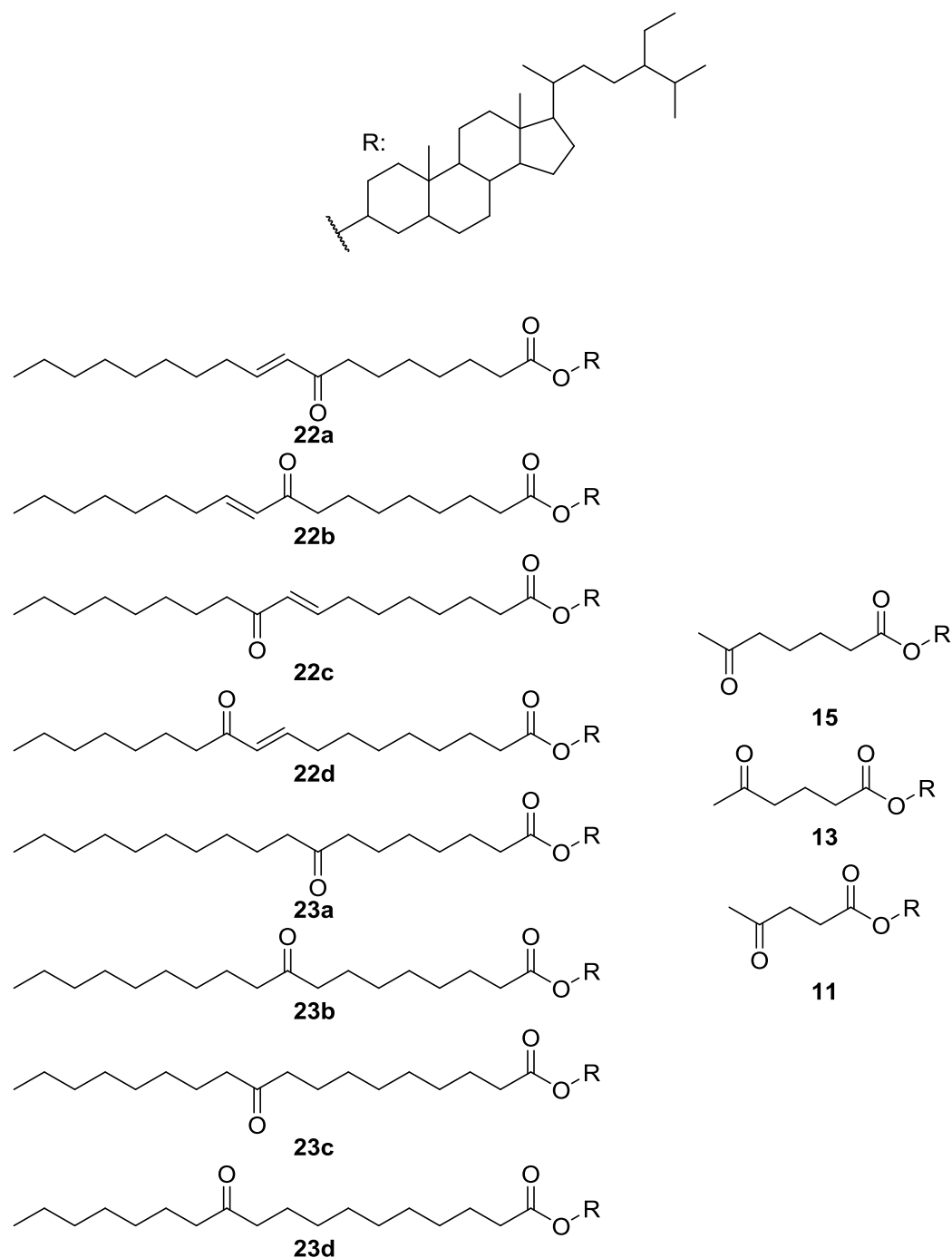


Figure 28: Structures of synthesized ACOPs carrying a keto-group in the fatty acid chain: positional isomers of sitostanyl oxo octadecenoate **22a-d**, positional isomers of sitostanyl oxo octadecanoate **23a-d**, sitostanyl 6-oxoheptanoate **15**, sitostanyl 5-oxohexanoate **13**, and sitostanyl 4-oxopentanoate **11**.

The four positional isomers of sitostanyl oxooctadecenoate **22a-d** were obtained by using manganese(III) acetate and *tert*-butylhydroperoxide (*t*BHP) which have been described as catalyst and cooxidant, respectively, enabling mild allylic oxidations of alkenes (Shing *et al.*, 2006). The synthesis was performed in accordance with the protocol described for the reaction of methyl oleate with manganese(III) acetate / *tert*-butylhydroperoxide (*t*BHP) by Dang *et al.* (2008); they demonstrated the formation of nearly equal amounts of the four *trans*-configured enone-stereoisomers shown in Figure 29.

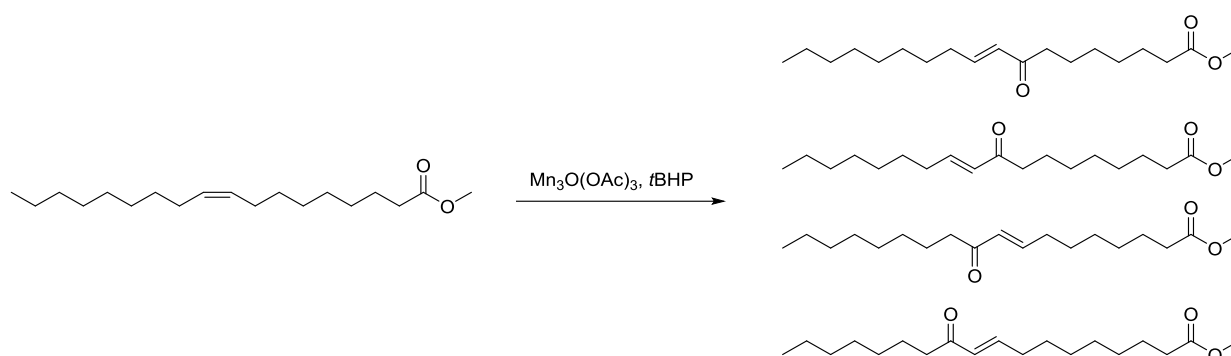


Figure 29: Oxidation of methyl oleate with *t*BHP to positional isomers of methyl oxooctadecenoates.

In the next step the obtained oxo-acid methyl esters were demethylated with barium hydroxide, as described by Julien-David *et al.* (2008). As example, the reaction step is shown for methyl 8-oxooctadecen-(9*E*)-oate in Figure 30.

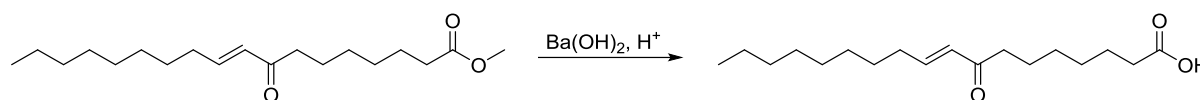


Figure 30: Demethylation of methyl 8-oxooctadecen-(9*E*)-oate with barium hydroxide.

Steglich esterification of the mixture of free oxo-fatty acids with sitostanol resulted in the formation of the four positional isomers of sitostanyl oxooctadecenoate **22a-d** depicted in Figure 28.

In accordance with Dang *et al.* (2008) the respective saturated oxo-ACOPs **23a-d** were obtained by hydrogenation of the mixture of methyl oxooctadecenoate isomers obtained via allylic oxidation of methyl oleate with manganese(III) acetate / *tert*-butylhydroperoxide (*t*BHP), using palladium-charcoal (10% Pd-C). As example, the reaction is shown for methyl 8-oxooctadecen-(9*E*)-oate in Figure 31.

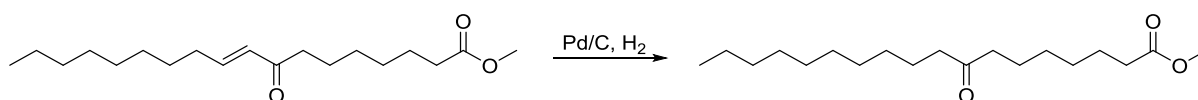


Figure 31: Hydrogenation of methyl oxooctadecenoate.

This step was followed by demethylation of the methyl oxooctadecanoate isomers and Steglich esterification of the resulting oxodecanoic acid isomers with sitostanol.

For other keto-ACOPs, free fatty acids were commercially available. The syntheses of sitostanyl 6-oxo heptanoate **15**, sitostanyl 5-oxo hexanoate **13**, and sitostanyl 4-oxo pentanoate **11** were performed by Steglich esterification as described for aldehyde-containing fatty acids (Wocheslander *et al.*, 2016).

The structures of the synthesized ACOPs containing aldehyde functions in the acyl chain are shown in Figure 32.

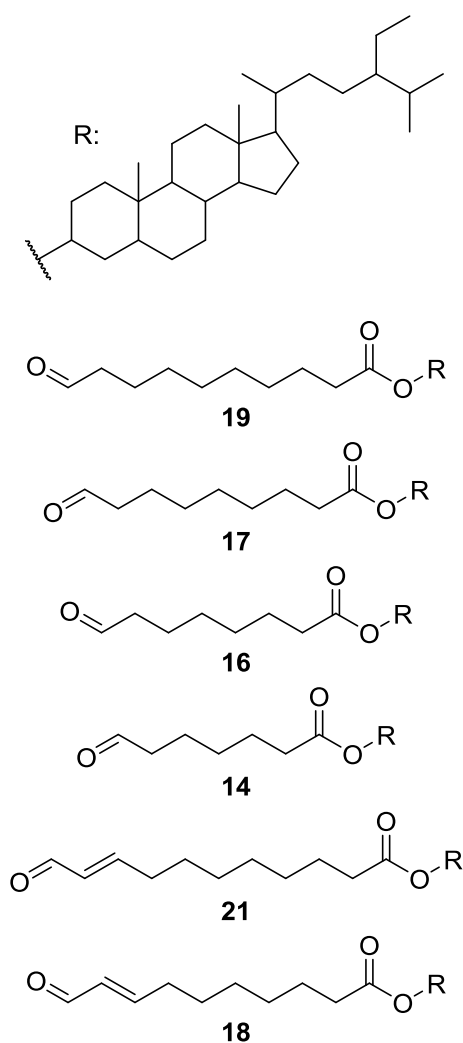


Figure 32: ACOPs containing an aldehyde group: sitostanyl 10-oxodecanoate **19**, sitostanyl 9-oxononanoate **17**, sitostanyl 8-oxooctanoate **16**, sitostanyl 7-oxoheptanoate **14**, sitostanyl 11-oxoundec-9E-anoate **21**, and sitostanyl 10-oxodece-8E-anoate **18**.

Two methyl esters, methyl 10-oxodecanoate and methyl 6-oxohexanoate, were commercially available. Sitostanyl 10-oxodecanoate **19** could be synthesized via Steglich esterification with the demethylated acid (Figure 33).

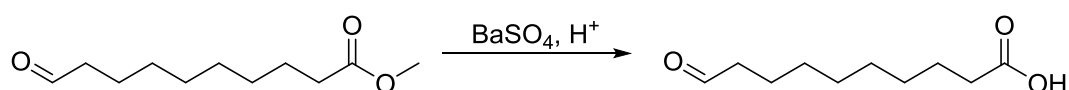


Figure 33: Demethylation of methyl 10-oxodecanoate.

This approach of demethylation and subsequent esterification could not be successfully applied for methyl 6-oxohexanoate, probably due to its greater volatility.

Therefore, sitostanyl 6-oxohexanoate **12** was only assigned tentatively (Scholz *et al.*, 2019).

The syntheses of the fatty acids for the further three saturated aldehyde compounds, sitostanyl 9-oxononanoate **17**, sitostanyl 8-oxooctanoate **16**, and sitostanyl 7-oxoheptanoate **14** (Figure 34) were performed as previously published (Wocheslander *et al.*, 2016).

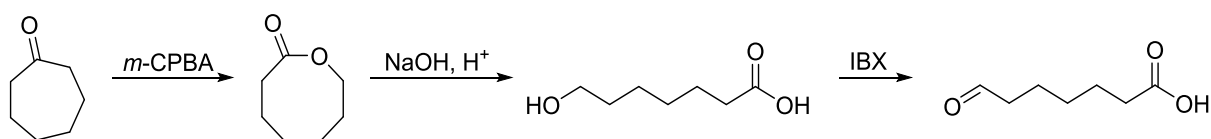


Figure 34: Synthesis of 7-oxoheptanoic acid from heptanone via Baeyer-Villiger-reaction, lactone opening and oxidation with IBX.

The synthesis for the unsaturated fatty acids containing an aldehyde group was adapted from Lin *et al.* (2007). They performed a Wittig-type reaction of methyl 9-oxononanoate with (triphenylphosphoranylidene)acetaldehyde, which results in an α,β -unsaturated aldehyde with the double bond in *trans*-configuration. In analogy, in this thesis sitostanyl 9-oxononanoate **17** was used as substrate to prepare sitostanyl 11-oxo-undec-9(*E*)-noate **21** (Figure 35).

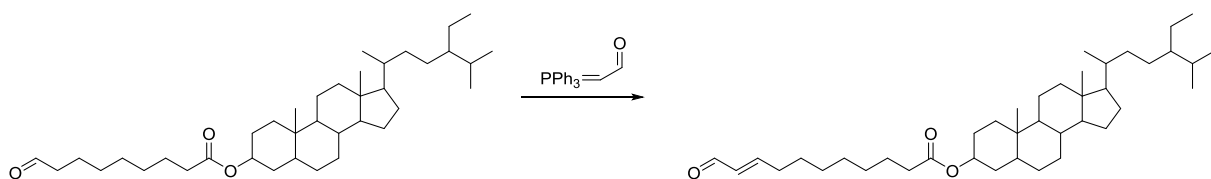


Figure 35: Wittig-type reaction for synthesis of sitostanyl 11-oxo-undec-9(*E*)-noate **21**.

NMR-data of sitostanyl 11-oxo-undec-9(*E*)-enoate **21**:

$^1\text{H-NMR}$ (500 MHz, CDCl_3): δ = 9.49 (1H, d, J = 7.9 Hz, FA-11), 6.84 (1H, dt, J = 15.6 Hz, 6.8 Hz, FA-9), 6.11 (1H, dtt, J = 15.6 Hz, 7.9 Hz, 1.5 Hz, FA-10), 4.69 (1H, tt, J = 11.3 Hz, 5.1 Hz, St-3), 2.32 (2H, dq, J = 7.2 Hz, 1.3 Hz, FA-8), 2.25 (2H, d, J = 7.5 Hz, FA-2), 1.95 (1H, dt, J = 12.6 Hz, 3.4 Hz, St-17), 1.86-1.75 (2H, m), 1.71 (1H, dt, J = 13.3 Hz, 3.6 Hz, St-9), 1.68-1.42 (11H, m), 1.38-0.91 (27H, m), 0.90-0.77 (15H, m, St-19, St-21, St-24², St-26, St-27), 0.64 (3H, s, St-18)

^{13}C -NMR (125 MHz, CDCl_3): δ = 194.28 (FA-11), 173.47 (FA-1), 159.05 (FA-9), 133.11 (FA-10), 73.64 (St-3), 56.53, 56.27, 54.32, 45.93, 44.77, 42.70, 40.08, 36.87, 36.29, 35.59, 34.80, 34.20, 34.02, 32.83, 32.11, 29.23, 29.10, 29.06, 26.06, 28.75, 28.40, 27.88, 27.65, 26.16, 25.10, 24.34, 23.17, 21.32, 19.96, 19.16, 18.86 (St-21), 12.36 (St-18/19/24²), 12.19 (St-18/19/24²), 12.11 (St-18/19/24²)

In analogy, sitostanyl 8-oxooctanoate **16** was used to synthesize sitostanyl 10-oxo-dece-(8*E*)-noate **18**.

NMR-data of sitostanyl 10-oxo-dec-8(*E*)-enoate **18**:

^1H -NMR (500 MHz, CDCl_3): δ = 9.50 (1H, d, J = 7.93 Hz, FA-10), 6.84 (1H, dt, J = 15.6 Hz, 6.8 Hz, FA-8), 6.11 (1H, ddt, J = 15.6 Hz, 7.9 Hz, 1.5 Hz, FA-9), 4.69 (1H, tt, J = 11.4 Hz, 4.9 Hz, St-3), 2.37-2.28 (2H, m, FA-7), 2.25 (2H, t, J = 7.5 Hz, FA-2), 1.95 (1H, dt, J = 12.6 Hz, 3.4 Hz, St-17), 1.85-1.75 (2H, m), 1.72 (1H, dt, J = 13.3 Hz, 3.6 Hz, St-9), 1.69-1.41 (14H, m, FA-3, FS-6), 1.39-0.92 (22H, m), 0.91-0.78 (15H, m, (St-19, St-21, St-24², St-26, St-27), 0.64 (3H, s, St-18)

^{13}C -NMR (125 MHz, CDCl_3): δ = 194.28 (FA-10), 173.39 (FA-1), 158.93 (FA-8), 133.15 (FA-9), 73.70 (St-3), 56.53, 56.27, 54.32, 45.93, 44.77, 42.71, 40.09, 36.87, 36.30, 35.59, 34.75, 34.20, 34.02, 32.12, 29.24, 28.91, 28.75, 28.40, 27.76, 27.65, 26.16, 25.00, 24.34, 23.17, 21.32, 19.96, 19.16, 18.86 (St-21), 12.37 (St-18/19/24²), 12.20 (St-18/19/24²), 12.11 (St-18/19/24²)

4.1.4 ACOPs Formed upon Thermo-oxidation of Sitostanyl Oleate

The internal standards described in chapter 4.1.2 and the reference compounds described in chapter 4.1.3 were used by Scholz *et al.* (2019) for the UHPLC-MS/MS-based identification and quantitation of ACOPs formed by thermo-oxidation of sitostanyl oleate. Aliquots of heated (180°C, 30 min.) sitostanyl oleate were analyzed via different routes comprising SPE or selective derivatisation steps (Figure 14). The peaks detected upon UHPLC-separation were analyzed by MS/MS. For structural assignments, UHPLC and mass spectral data were compared to those of the synthesized references. Semi-quantitations were performed by comparing the peak areas of the analytes to those of the synthesized internal standards. The cholestanyl analogues were also used to establish optimum multiple reaction monitoring (MRM)

transitions and source parameters for the MS/MS-analyses. The data reported by Scholz *et al.* (2019) are compiled in Table 5.

Table 5: ACOPs formed upon heating (180°C, 30 min.) of sitostanyl oleate determined by Scholz *et al.* (2019) via UHPLC-MS/MS-analysis, using the synthesized internal standards and reference substances described in sections 4.1.2 and 4.1.3.

ACOP [$\mu\text{g}/\text{mg}$ ester]		control	180 °C, 30 min
<i>(A) non-polar ACOPs</i>			
1	sitostanyl heptanoate	0.23 \pm 0.02	1.48 \pm 0.1
2	sitostanyl octanoate	0.53 \pm 0.07	1.86 \pm 0.2
<i>(B) hydroxy-ACOPs</i>			
4	sitostanyl 7-hydroxyheptanoate	0.01 \pm 0.001	0.50 \pm 0.05
5	sitostanyl 8-hydroxyoctanoate	0.14 \pm 0.01	1.41 \pm 0.07
6	sitostanyl 9-hydroxynonanoate	0.01 \pm 0.001	0.02 \pm 0.004
7	sitostanyl 9,10-dihydroxystearate	0.09 \pm 0.02	2.43 ^a \pm 0.3
8a,b	sitostanyl 8/11-hydroxyoctadec-9(<i>E</i>)-enoate	0.25 \pm 0.02	11.40 ^b \pm 0.6
<i>(C) epoxy-ACOPs</i>			
9a,b	sitostanyl epoxyoctadecenoate	0.01 \pm 0.001	3.71 ^c \pm 0.4
10a,b	sitostanyl 9,10-epoxystearate	43.55 \pm 9.7	139.66 ^d \pm 14.7
<i>(D) oxo-ACOPs</i>			
11	sitostanyl 4-oxopentanoate	0.01 \pm 0.001	0.01 \pm 0.002
12,13	sitostanyl 6-oxohexanoate / 5-oxohexanoate	0.01 \pm 0.001	0.21 \pm 0.01
14,15	sitostanyl 7-oxoheptanoate / 6-oxoheptanoate	0.02 \pm 0.001	0.62 \pm 0.02
16	sitostanyl 8-oxooctanoate	0.13 \pm 0.005	1.11 \pm 0.03
17	sitostanyl 9-oxononanoate	0.48 \pm 0.02	1.53 \pm 0.06
18	sitostanyl 10-oxodec-8-enoate	0.15 \pm 0.01	1.70 \pm 0.09
19,20	sitostanyl 10-oxodecanoate / 9-oxodecanoate	0.04 \pm 0.001	0.08 \pm 0.003
21	sitostanyl 11-oxoundec-9-enoate	0.15 \pm 0.01	1.53 \pm 0.08
22a-d	sitostanyl 8/9/10/11-oxooctadecenoate	0.22 \pm 0.03	14.76 \pm 1.2
23a-d	sitostanyl 8/9/10/11-oxostearate	n.d. ^e	0.39 \pm 0.05

^a includes a smaller peak with an MS indicating two hydroxy groups; their positions could not be assigned; ^b includes smaller peaks with full scan and product ion spectra in agreement with those of synthesized **8a,b**; ^c includes synthesized **9a,b** and peaks assigned as epoxyoctadecenoates varying in position and configuration of the epoxy group; ^d includes synthesized *cis*-epoxide **10a** and the tentatively assigned *trans*-epoxide **10b**; ^e < signal-to-noise ratio of 10.

4.1.5 Summary

The purpose of this part of the thesis was to provide a spectrum of authentic compounds covering a broad array of oxidation products of sitostanyl oleate with different functional groups in the acyl chain moiety which could be used as reference compounds in the course of a UHPLC-MS/MS-based analysis of ACOPs formed upon thermo-oxidation of sitostanyl oleate.

In total, twenty commercially not available reference compounds of acyl chain oxidation products expected to be formed upon thermo-oxidation of sitostanyl oleate were synthesized. Taking into account the existing information on products known to be formed via oxidation of unsaturated fatty acid moieties in fats and oils, the spectrum of candidates comprised keto-, aldehyde-, hydroxy- and epoxy-ACOPs. Synthesized short- and medium-chain ACOPs (chain lengths from C5 to C11), resulting from oxidative fragmentations of the oleic acid moiety in sitostanyl oleate, included non-polar ACOPs as well as oxidation products possessing aldehyde-, keto- or hydroxy-groups in the remaining acid chains. In addition, long-chain sitostanyl ACOPs exhibiting keto-, hydroxy-, dihydroxy- and epoxy-groups in the unfragmented C18-acyl moiety were synthesized. The ACOPs were either obtained by synthesis of the respective oxidized fatty acid and subsequent esterification with sitostanol or by direct oxidative modifications of sitostanyl esters. For some of the candidates, e.g. sitostanyl oxooctadecenoate, only a mixture of positional isomers could be obtained by the employed synthesis. For most of the substances, GC-purities higher than 94% were achieved.

In addition to these sitostanyl ACOPs, four analogous cholestanyl esters representing the different classes of oxo-, hydroxy- and epoxy-ACOPs were synthesized, purified and characterized by NMR. Together with cholestanyl oleate, reflecting the oxidatively unaltered ester, they should serve as internal standards supporting the quantitation of ACOPs in the course of the UHPLC-MS/MS-based analysis of ACOPs formed upon thermo-oxidation of sitostanyl oleate.

4.2 GC-Based Investigations of Long-Chain ACOPs Formed Upon Thermo-oxidation of Sitostanyl Oleate

4.2.1 Introduction

The investigation via UHPLC-MS/MS (Scholz *et al.*, 2019) demonstrated that sitostanyl *trans*- and *cis*-9,10-epoxystearate **10a,b**, sitostanyl 8- and 11-hydroxyoctadec-9-enoate **8a,b** and sitostanyl 9,10-dihydroxystearate **7** constituted the majority (approximately 83%) of the ACOPs determined in sitostanyl oleate subjected to heating at 180°C for 30 min. (Table 5).

The objective of this part of the thesis was to set up a methodology that allows the quantification of these major long-chain ACOPs formed during the thermo-oxidation of sitostanyl oleate via a GC-based approach. The developed procedure should be suitable to follow the formation of these long-chain ACOPs under various time/temperature conditions to get a first understanding of the amounts to be expected under household-type cooking and baking conditions.

Previous studies had shown that GC is applicable for direct analysis of ACOPs resulting from thermal treatment of a mixture of phytosteryl/-stanyl oleates and linoleates (Wocheslander *et al.*, 2016; Wocheslander *et al.*, 2017). However, the spectrum of ACOPs covered by this approach was limited; the amounts of ACOPs quantified by this methodology amounted to only 8.7% and 9.6% of the total losses of phytostanyl oleates and linoleates, respectively. Long-chain ACOPs with epoxy or hydroxy groups in the acyl chain were not amenable to analysis via this approach. Therefore, in the present study transesterification of the sitostanyl ACOPs and subsequent GC-analysis of the formed methyl esters was applied.

4.2.2 Methodology

The employed analytical procedure involved the key steps outlined in Figure 36.

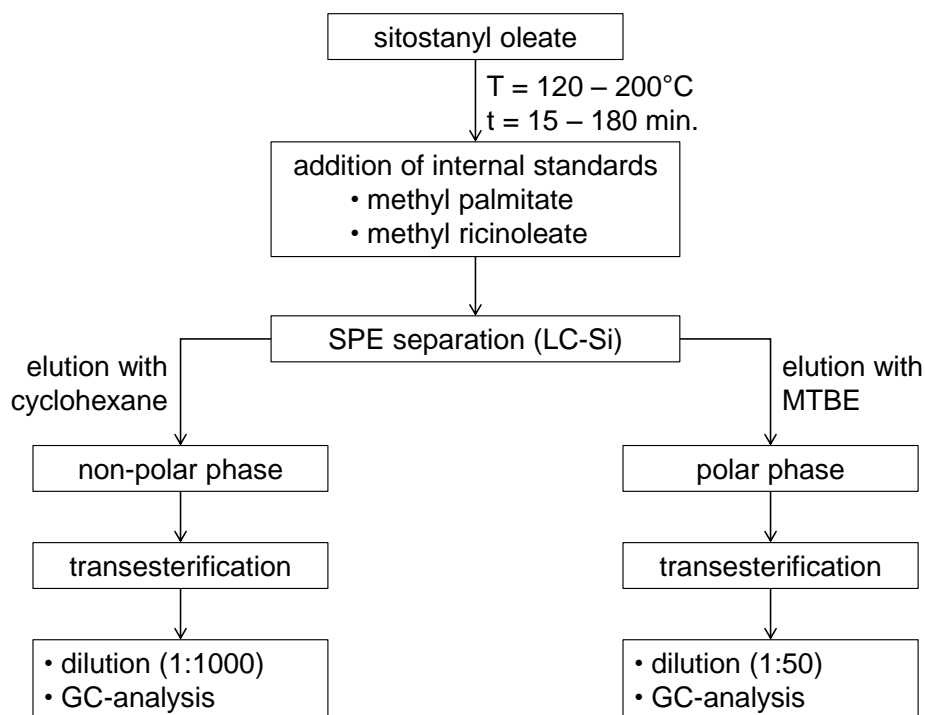


Figure 36: Procedure applied for the GC-based analysis of long-chain ACOPs formed upon heating of sitostanyl oleate.

Fractionation via solid phase extraction (SPE)

A first key step in the employed methodology was the separation of the remaining non-oxidized sitostanyl oleate from the formed polar ACOPs. In accordance with the procedure applied by Wocheslander *et al.* (2017), this was achieved by solid phase extraction (SPE) of the thermo-oxidized mixture on silica gel. Sitostanyl oleate and formed non-polar ACOPs were eluted using cyclohexane and the polar ACOPs using MTBE. Preliminary tests showed that the elution volume of cyclohexane had to be increased (from 21 ml to 50 ml) compared to the protocol described by Wocheslander *et al.* (2017), in order to achieve a sufficient separation of the non-polar and the polar fractions. Prior to the fractionation of the heated sample, two internal standards were added to allow for quantitations of the formed ACOPs; methyl palmitate **IS₆** was used in the non-polar fraction and methyl ricinoleate **IS₇** in the polar fraction (Figure 37).

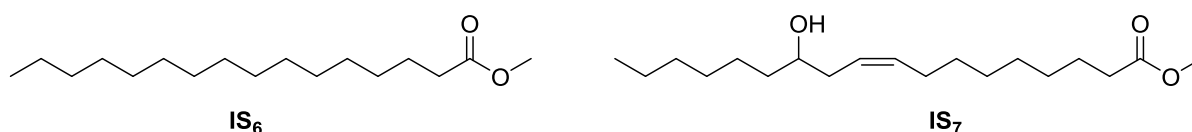


Figure 37: Structures of internal standards used for the GC-based quantitation of long-chain ACOPs: methyl palmitate **IS₆** and methyl ricinoleate **IS₇**.

Transesterification

Biedermann *et al.* (1993) described transesterification as a method for determining free and esterified sterols in fats and oils. Schmarr *et al.* (1996) used the method, which was based on sodium methylate and MTBE, to determine (esterified) cholesterol oxidation products. Transesterification was as well used to investigate POPs in oils (Johnsson and Dutta, 2006). Berdeaux *et al.* (1999b) tested different transesterification procedures and found that using KOH in methanol or sodium methylate in MTBE were the most suitable for transesterification of oxidized short-chain compounds from triglycerides. These methods have also already been established for long-chain oxidation products resulting from triglycerides (Berdeaux *et al.*, 1999a).

A preliminary test with 18 mg sitostanyl oleate **3** showed that the use of 30 μ L 30% sodium methylate and a total reaction time of 3 min. (1 min. shaking and 2 min. standing) at room temperature were sufficient to achieve a complete transesterification.

From the results of UHPLC-MS/MS analysis (Scholz *et al.*, 2019) sitostanyl *cis*-9,10-epoxystearate **10a** was expected as a major ACOP (chapter 4.1). Therefore, the same molar amount of sitostanyl *cis*-9,10-epoxystearate **10a** as of 18 mg sitostanyl oleate **3** was used to determine the efficacy of the transesterification step for this representative of polar ACOPs. Based on the results of this test, for the fraction containing the polar ACOPs the reaction time of the transesterification was slightly extended (3 min. shaking and 2 min. standing at room temperature).

GC-analysis

For the GC-separation, Rtx®-200MS, a fused silica capillary column coated with Crossbond® trifluoropropylmethyl polysiloxane was used. This mid-polarity stationary phase has previously been used for the analysis of phytosteryl/-stanyl esters, sterols/stanols, and their oxidation products such as short-chain ACOPs from phytosteryl/-stanyl oleate or linoleate, as well as phytosteryl oxidation products (POPs) (Barnsteiner *et al.*, 2012; Scholz *et al.*, 2015b; Gleize *et al.*, 2016; Wocheslander *et al.*, 2017). It exhibits high thermal stability, low bleed and inertness. In addition, it offers the possibility to perform GC separations of underivatized as well as derivatized (trimethylsilylated) ACOPs.

4.2.3 Syntheses of Methyl Esters of Long-Chain ACOPs to be Used as Reference Compounds

Methyl *trans*- and *cis*-9,10-epoxystearate **33,34**

The main ACOPs observed in the UHPLC-based analysis of thermally treated sitostanyl oleate (Scholz *et al.*, 2019) were sitostanyl 9,10-epoxystearates **10a,b** (Table 5).

The respective methyl *trans*-9,10-epoxystearate **33** was commercially available. Mass spectral data are shown in Table 6.

Table 6: Mass spectral data of methyl *trans*- and *cis*-9,10-epoxystearate **33,34**.

no.	compound	ions, m/z (relative intensity)	
		molecular ion	fragment ions ^a
33	methyl <i>trans</i> -9,10-epoxystearate	312 (n.d.)	55 (100), 74 (69), 69 (63), 155 (62), 57 (54), 83 (42), 87 (38), 97 (37), 109 (18), 127 (16), 139 (10), 171 (8), 199 (6), 187 (3), 294 (<1)
34	methyl <i>cis</i> -9,10-epoxystearate	312 (<1)	155 (100), 55 (89), 69 (65), 74 (64), 97 (43), 83 (42), 87 (31), 109 (30), 127 (23), 139 (20), 171 (15), 199 (11), 121 (11), 187 (3), 149 (3)

^a Characteristic or identifier ions are in bold, other most abundant fragments in normal font.

The isomeric methyl *cis*-9,10-epoxystearate **34** was synthesized by epoxidation of methyl oleate with *m*-CPBA (Figure 38).

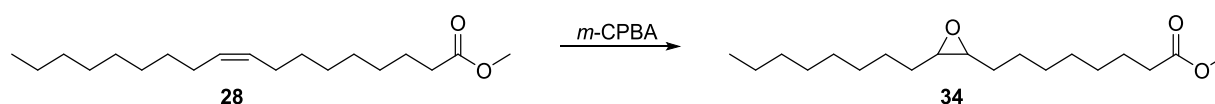


Figure 38: Synthesis of *cis*-9,10-epoxystearate **34** via epoxidation of methyl oleate.

The mass spectrum of **34** (Table 6) was in agreement with available data (Kleiman and Spencer, 1973; Frankel *et al.*, 1977; Gardner *et al.*, 1992; Mubiru *et al.*, 2013; Xia and Budge, 2018).

Methyl 9,10-dihydroxystearate 36

Methyl 9,10-dihydroxystearate **36** was synthesized by ring opening of the epoxide of methyl *cis*-9,10-epoxystearate **34** (Figure 39).

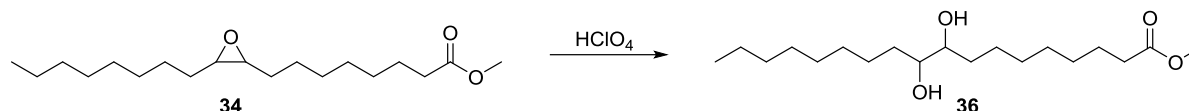


Figure 39: Synthesis of methyl 9,10-dihydroxystearate **36** via ring opening of the epoxide.

Mass spectral data of the synthesized reference compound are shown in Table 7. The molecular ion and the fragment ions resulting from chain-cleavage between the two hydroxy groups are characteristic (Frankel *et al.*, 1977; Xia and Budge, 2017).

Table 7: GC-MS data of methyl 9,10-dihydroxystearate **36**.

no.	compound	ions, m/z (relative intensity)	
		molecular ion	fragment ions ^a
36	methyl 9,10-dihydroxystearate	330 (<1)	155 (100), 187 (36), 138 (30), 74 (30), 55 (29), 87 (27), 69 (24), 109 (22), 67 (18), 83 (16), 96 (14), 127 (5), 170 (3), 281 (1), 143 (1)

^a Characteristic or identifier ions are in bold, other most abundant fragments are in normal font.

Methyl 8/11-hydroxyoctadec-9-enoate 31,32

In analogy to the procedure described for the hydroxylation of oleic acid (Knothe *et al.*, 1993), the anticipated hydroxyocatadecenoates were synthesized by hydroxylation of methyl oleate with selenium dioxide / tBHP, resulting in hydroxylations in allylic positions. The products obtained by this approach are depicted in Figure 40.

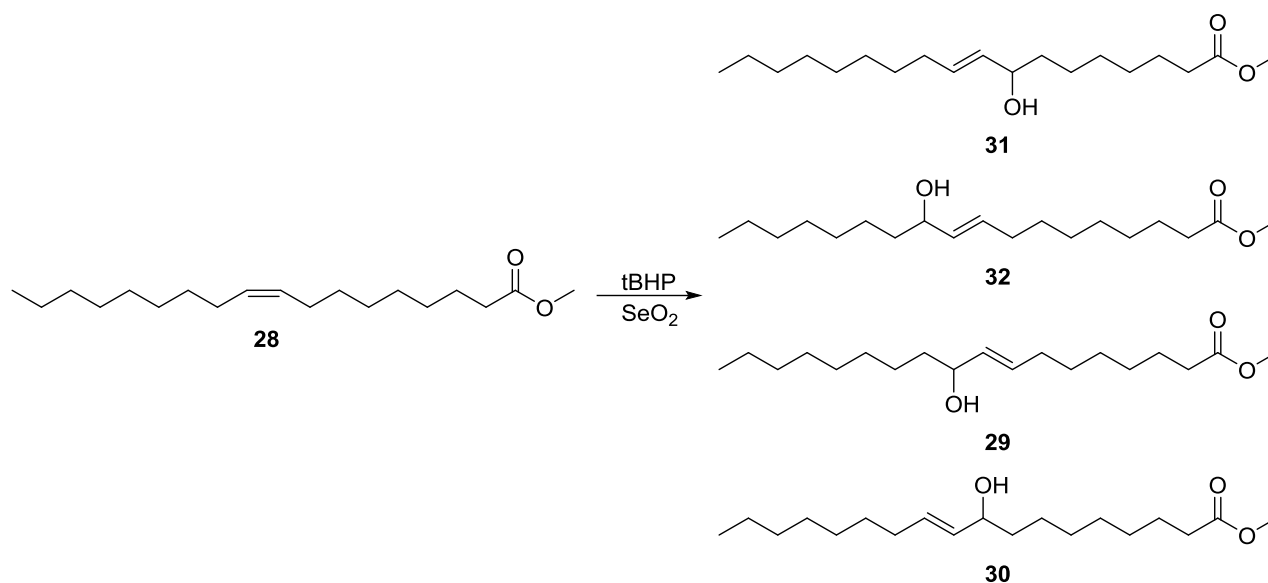


Figure 40: Products obtained by hydroxylation of methyl oleate with selenium dioxide / tBHP.

Capillary gas chromatographic analysis revealed the presence of a major peak accompanied by a small peak at earlier retention time (Figure 41 A). Upon silylation, the GC-chromatogram showed two pairs of peaks shifted to earlier retention times compared to the unsilylated sample (Figure 41 B).

GC-MS-analysis of the non-silylated sample showed that the mass spectrum of the larger peak contained the fragments m/z 213, 199, 169 and 155. These may be assigned to alpha cleavage next to the double bond or to the hydroxy group of methyl 8-hydroxyoctadec-9-enoate **31** and methyl 11-hydroxyoctadec-9-enoate **32**, respectively (Figure 42 A). These characteristic fragments have also been reported by Marmesat *et al.* (2008) in their study on the formation of hydroxylated fatty acids in fats and oils under deep-frying conditions. In addition, m/z 294, which corresponds to the loss of water of methyl hydroxyoctadecenoates, was detected as diagnostic fragment. Screening of the mass spectrum over the entire peak showed that in the rear part the fragments m/z 155 and m/z 213 clearly stood out, whereas in the front part fragment m/z 169 was prominent. This indicated that the larger peak corresponded to a mixture of the anticipated products methyl 8-hydroxyoctadec-9-enoate **31** and methyl 11-hydroxy octadec-9-enoate **32**, with **31** eluting before **32**.

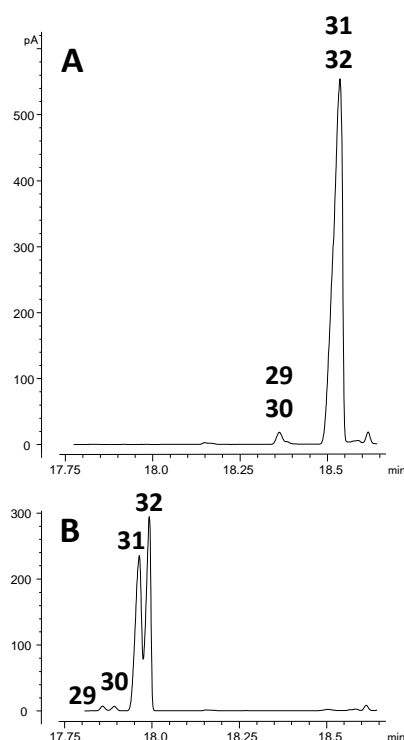


Figure 41: GC-separation of the products obtained by hydroxylation of methyl oleate with selenium dioxide / *t*BHP. A: non-silylated, B: after silylation.

The mass spectrum of the minor peak also showed the fragments m/z 213, 199, 169 and 155. They may be assigned to alpha-cleavage next to the double bond or to the hydroxy group of the positional isomers of the main reaction products, i. e. methyl 10-hydroxyoctadec-8-enoate **29** and methyl 9-hydroxydec-10-enoate **30**, respectively (Figure 42 A). Fragments m/z 169 and m/z 199 were predominant in the mass spectrum recorded in the front part of the peak, whereas the fragments m/z 213 and 155 stood out in the rear part. This indicated an order of elution of methyl 10-hydroxyoctadec-8-enoate **29** before methyl 9-hydroxyoctadec-10-enoate **30**.

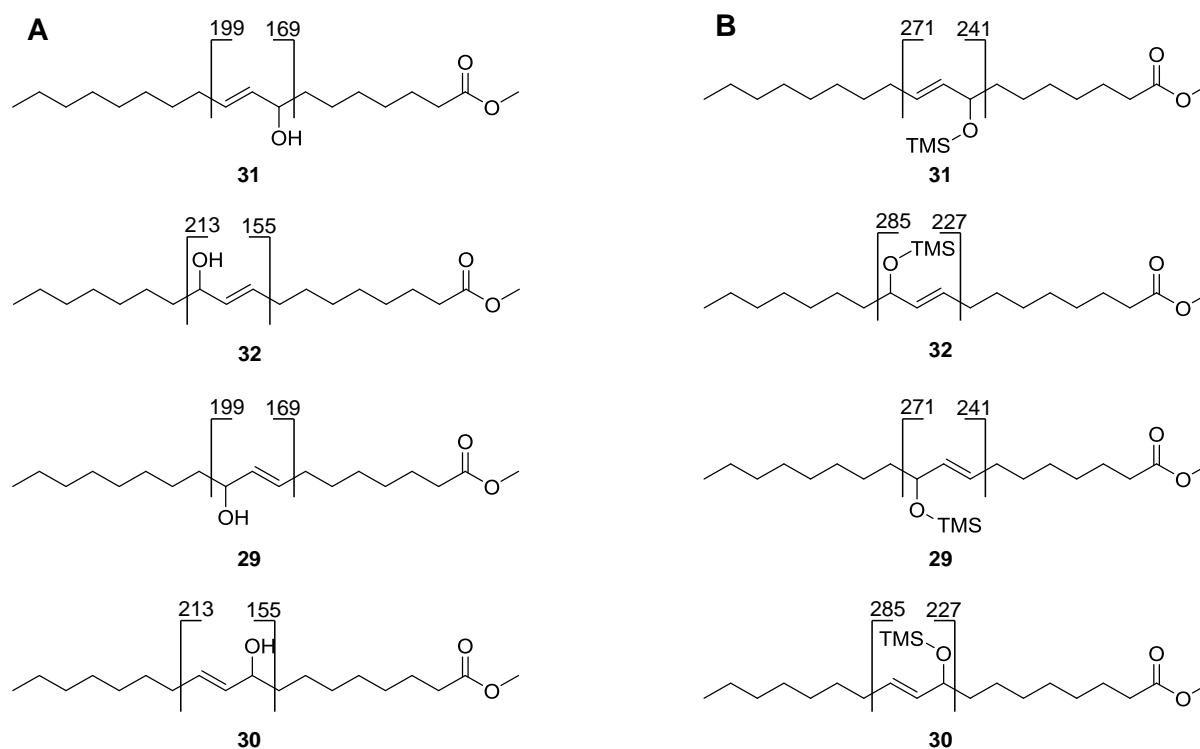


Figure 42: Characteristic mass fragments of methyl hydroxyoctadecenoates (**29-31**) obtained by hydroxylation of methyl oleate with selenium dioxide / *t*BHP in their (A) non-silylated or (B) silylated form.

The identities of the reaction products could be confirmed by GC-MS-analysis of the four peaks detected in the chromatogram of the silylated sample (Figure 42 B, Table 8).

The two major peaks in the chromatogram of the silylated sample (Figure 41 B) were identified as the silylated derivatives of methyl 8-hydroxyoctadec-9-enoate **31** and methyl 11-hydroxyoctadec-9-enoate **32**. Both spectra showed the fragments m/z 73 and 129, which correspond to the trimethylsilyl group and the fragment consisting of the double bond and the silylated hydroxy group in allylic position, respectively. Both also showed m/z 369, corresponding to the cleavage of a methyl group, as diagnostic fragment. The differentiation of the peaks was possible based on the characteristic fragments resulting from alpha cleavage next to the double bond (m/z 271 for **31** and m/z 227 for **32**) and next to the silylated hydroxy group (m/z 241 for **31** and m/z 285 for **32**) (Figure 42 B).

Table 8: GC-MS-data of the silylated products obtained by hydroxylation of methyl oleate with selenium dioxide / tBHP.

no.	compound	ions, m/z (relative intensity)	
		molecular ion	fragment ions ^a
31	methyl 8-hydroxy-octadec-9-enoate	384 (<1)	241 (100), 73 (71), 129 (40), 55 (18), 95 (15), 271 (7), 143 (7), 109 (5), 121 (3), 285 (2), 155 (2), 337 (1), 227 (1), 169 (1), 369 (<1)
32	methyl 11-hydroxy-octadec-9-enoate	384 (<1)	285 (100), 73 (72), 129 (24), 227 (17), 55 (17), 95 (11), 121 (6), 109 (6), 337 (2), 241 (2), 294 (1), 263 (1), 369 (<1), 214 (1)
29	methyl 10-hydroxy-octadec-8-enoate	384 (n.d.)	241 (100), 73 (84), 129 (65), 75 (44), 55 (23), 67 (21), 95 (20), 81 (18), 69 (12), 271 (11), 59 (11), 109 (6), 143 (2), 87 (2), 121 (1)
30	methyl 9-hydroxy-octadec-10-enoate	384 (n.d.)	73 (100), 285 (88), 75 (59), 129 (49), 227 (40), 55 (29), 67 (26), 81 (22), 95 (17), 59 (15), 69 (11), 83 (8), 121 (4), 109 (4), 143 (3)

^a Characteristic or identifier ions are in bold, other most abundant fragments are in normal font.

The GC-MS data of the two minor peaks **29** and **30** revealed their identities as methyl 10-hydroxyoctadec-8-enoate **29** and methyl 9-hydroxyoctadec-10-enoate **30**, respectively (Table 8). Again, the mass spectra of both peaks showed the fragments m/z 73 and 129. Their differentiation was based on the characteristic fragments resulting from alpha cleavage next to the double bond (m/z 241 for **29** and 285 for **30**) and next to the silylated hydroxy group (m/z 271 for **29** and 227 for **30**) (Figure 43 B).

The fragments of the silylated sample were in agreement with those previously reported (Frankel *et al.*, 1977; Xia and Budge, 2017; Xia and Budge, 2018).

Methyl 8/9/10/11-oxooctadecenoate **35**

As depicted in Figure 29 (chapter 4.1.3), methyl 8/9/10/11-oxooctadecenoate **35** was synthesized by reaction of methyl oleate with manganese(III) acetate / *tert*-butylhydroperoxide (tBHP) according to the procedure described by Dang *et al.* (2008).

The formed *trans*-configured enone-stereoisomers could not be separated by GC and eluted under the employed conditions as broad peak. The mass spectrum obtained for the mixture is given in Table 9.

Table 9: Mass spectral data of methyl 8/9/10/11-oxooctadecenoate **35**.

no.	compound	ions, m/z (relative intensity)	
		molecular ion	fragment ions ^a
35	methyl oxooctadecenoate	310 (<1)	279 (3), 226 (2), 211 (12), 197 (4), 183 (5), 167 (22), 153 (59), 137 (15), 123 (7), 109 (24), 97 (38), 83 (34), 69 (41), 55 (100)

^a Characteristic or identifier ions are in bold, other most abundant fragments are in normal font.

4.2.4 Identification of ACOPs

Sitostanyl oleate **3** (18mg) was heated at 180°C for 60 min. and subjected to the analytical procedure depicted in Figure 36. The obtained non-polar and polar fractions were transesterified and subsequently investigated via GC. The chromatograms obtained for the two fractions are shown in Figure 43.

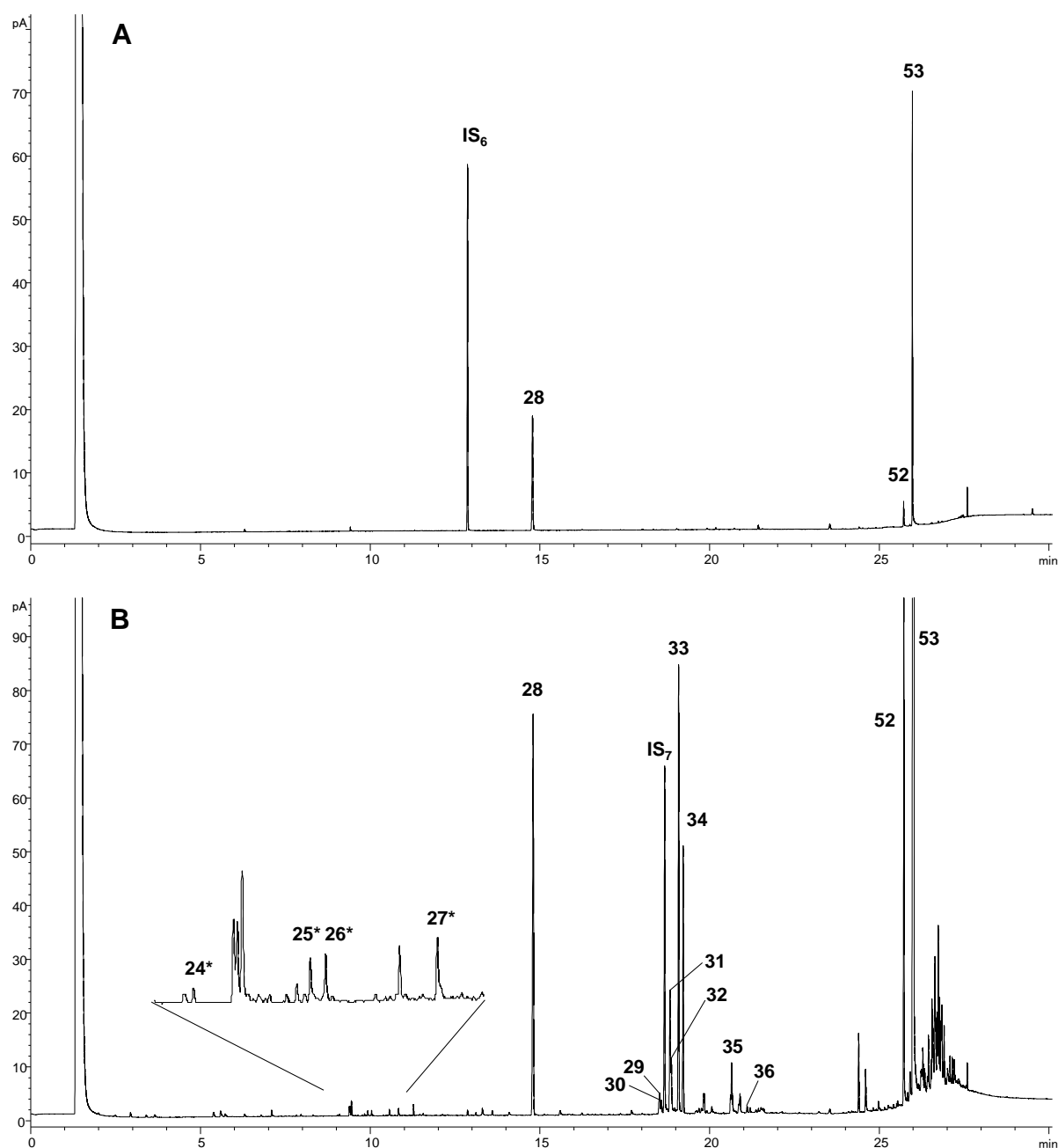


Figure 43: GC-chromatograms of the transesterified non-polar (A) and polar fraction (B) obtained after heating of sitostanyl oleate (180°C, 60 min.). methyl palmitate IS_6 , methyl ricinoleate IS_7 , methyl oleate 28, methyl 10-hydroxyoctadec-8-enoate 29, methyl 9-hydroxyoctadec-10-enoate 30, methyl 8-hydroxyoctadec-9-enoate 31, methyl 11-hydroxyoctadec-9-enoate 32, methyl *trans*-9,10-epoxystearate 33, methyl *cis*-9,10-epoxystearate 34, methyl 8/9/10/11-oxooctadecenoate 35, methyl 9,10-dihydroxystearate 36, campestanol 52, sitostanol 53. Marked (*) compounds were tentatively assigned based on their GC-FID retention times.

The non-polar fraction contained the internal standard methyl palmitate **IS**₆. In addition, methyl oleate **28** formed via transesterification of the remaining non-oxidized sitostanol oleate as well as sitostanol **53** and campestanol **52**, liberated as result of the transesterification step, were detected.

In addition to different ACOPs, the internal standard methyl ricinoleate **IS**₇, methyl oleate **28**, campestanol **52** and sitostanol **53** were identified in the polar fraction (Figure 43 B). The structures of the long-chain ACOPs identified as methyl esters via GC-MS-analysis of the transesterified polar fraction are shown in Figure 44.

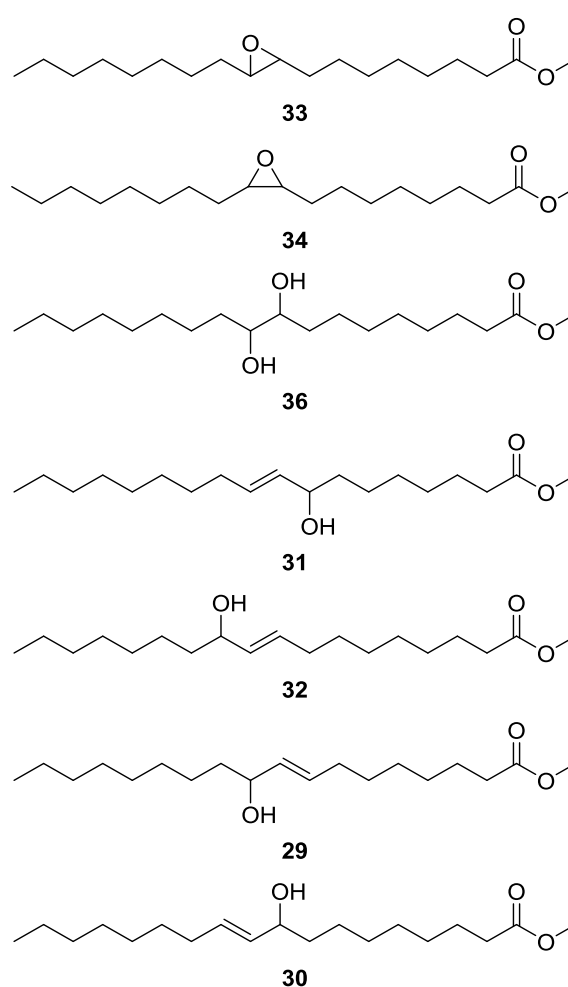


Figure 44: Structures of compounds identified in the transesterified polar fraction of heated (180°C, 60 min.) sitostanyl oleate **3**. Methyl *trans*-9,10-epoxystearate **33**, methyl *cis*-9,10-epoxystearate **34**, methyl 9,10-dihydroxystearate **36**, methyl 8-hydroxyoctadec-(9*E*)-enoate **31**, methyl 11-hydroxyoctadec-(9*E*)-enoate **32**, methyl 10-hydroxyoctadec-8-enoate **29**, and methyl 9-hydroxyoctadec-10-enoate **30**.

The identifications of ACOPs in the polar fraction were based on the comparison of their chromatographic and mass spectral data to those of the synthesized reference compounds.

The quantitatively predominating ACOP methyl *trans*-9,10-epoxystearate **3** was identified by using a commercially available reference compound. The identification of the isomeric methyl *cis*-9,10-epoxystearate **34** was based on a comparison with the respective synthesized reference compound.

Methyl 9,10-dihydroxystearate **36** was also assigned based on the comparison of retention time and mass spectrum to those of the synthesized reference compound.

The identification of the methyl hydroxydecanoates **29**, **30**, **31** and **32** was based on chromatographic and mass spectral data obtained upon silylation of the transesterified polar fraction. Respective segments of the chromatograms obtained before and after silylation of the transesterified polar fraction are shown in Figure 45.

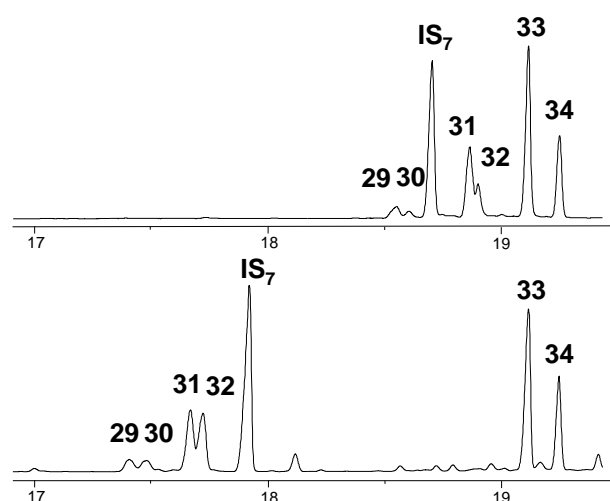


Figure 45: Segments of GC-FID chromatograms of the transesterified polar fraction of heated (180°C, 60 min.) sitostanyl oleate. The upper chromatogram corresponds to the non-silylated, the lower to the silylated sample.

Upon silylation, the positions of peaks **33** and **34**, i.e. *trans*- and *cis*-9,10-epoxystearate, did not change. In contrast, the retention times not only of the internal standard methyl ricinolate **IS₇** but also of the peaks **29** - **32** shifted. This is in agreement with the increased volatilities and thus the decreased retention times expected to result

from silylation of the hydroxy groups of methyl ricinolate **IS₇** and the methyl hydroxyoctadecenoates **29 - 32**.

Comparisons of the data obtained by GC-MS-analysis of the silylated polar fraction isolated from the heated sample of sitostanyl oleate to the mass spectral of the silylated reference compounds (Table 8) confirmed the identities of methyl 8-hydroxyoctadec-9-enoate **31** and methyl 11-hydroxyoctadec-9-enoate **32** and of the minor positional isomers methyl 10-hydroxyoctadec-8-enoate **29** and methyl 9-hydroxyoctadec-10-enoate **30**.

These identifications via the analysis of the silylated polar fraction were complemented by mass spectral data obtained from the non-silylated, heated sample. The mass spectra generated from the front and the rear parts, respectively, of the double peaks **31, 32** and **29, 30** are compiled in Table 10.

Methyl 8-hydroxyoctadec-9-enoate **31** and methyl 11-hydroxyoctadec-9-enoate **32** showed the characteristic fragments corresponding to alpha cleavage (Figure 42 A). Peak **31** showed the fragments m/z 169 and 199, which are characteristic for the alpha-cleavage of methyl 8-hydroxyoctadec-9-enoate. In contrast, peak **32** is dominated by the fragments m/z 155 and 213 and therefore corresponds to methyl 11-hydroxyoctadec-9-enoate.

For the smaller double peak **29/30**, the fragments characteristic for alpha cleavages in methyl 9-hydroxyoctadec-10-enoate **30**, i.e. m/z 155 and 213, were recorded in the rear part of the double peak. In the front part, the intensity of m/z 199, a fragment that could be assigned to alpha cleavage next to the hydroxy group of methyl 10-hydroxyoctadec-8-enoate **29**, was only rather weak. For both peaks, the mass spectral data, e.g. m/z 340, indicated the overlap with other unknown compounds.

Peak **35** was assigned as methyl oxooctadecenoate (Figure 46) based on comparison of retention time and mass spectral data to those of the synthesized reference mixture (Table 9). The reference included four isomers that could not be separated under the employed chromatographic conditions.

Table 10: GC-MS-data of methyl hydroxyoctadecenoates identified in the transesterified polar fraction of heated (180°C, 60 min.) sitostanyl oleate. The compound numbers correspond to those in Figure 43.

no.	compound	ions, m/z (relative intensity)	
		molecular ion	fragment ions
31	methyl 8-hydroxy-octadec-9-enoate	312 (n.d.)	55(100), 57 (91), 67 (70), 81 (63), 95 (58), 167 (42), 121 (30), 139 (21), 169 (15), 199 (14), 109 (14), 181 (12), 144 (10), 213 (5), 155 (5), 294 (3)
32	methyl 11-hydroxy-octadec-9-enoate	312 (n.d.)	55(100), 81 (75), 67 (68), 95 (60), 87 (50), 155 (32), 109 (18), 181 (17), 135 (12), 124 (10), 121 (9), 213 (6), 167 (5), 294 (3), 195 (2)
29	methyl 10-hydroxy-octadec-8-enoate	312 (n.d.)	177 (100), 161 (66), 149 (40), 121 (31), 340 (30), 57 (26), 91 (16), 155 (14), 141 (11), 77 (8), 137 (5), 67 (5), 284 (3), 199 (1), 269 (1), 228 (1), 215 (1)
30	methyl 9-hydroxy-octadec-10-enoate	312 (n.d.)	57 (100), 55 (94), 67 (71), 95 (67), 81 (61), 177 (47), 161 (40), 121 (39), 149 (36), 181 (26), 109 (21), 155 (10), 340 (10), 213 (9), 199 (4), 169 (2)

n.d. = not detected

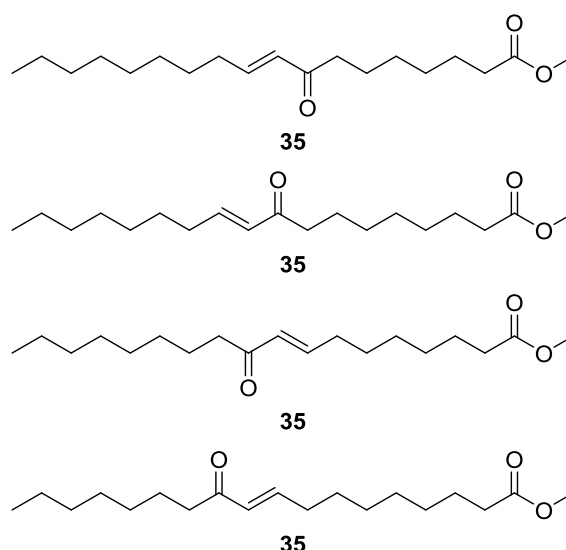


Figure 46: Structures of methyl oxooctadecenoates, which could not be separated under the applied conditions.

Besides long-chain ACOPs, heating sitostanyl oleate **3** also produces short-chain ACOPs (Wocheslander *et al.*, 2016). Short-chain ACPOs were synthesized by transesterification of the corresponding sitostanyl esters. For example, methyl 5-oxohexanoate **24** was prepared by transesterification of sitostanyl 5-oxohexanoate **13** with sodium methylate. Following esters were used for transesterification: sitostanyl 7-oxoheptanoate **14**, 8-oxooctanoate **16**, 9-oxononanoate **17**, 4-oxopentanoate **11**, 5-oxohexanoate **13**, 6-oxoheptanoate **15**, 7-hydroxyheptanoate **4**, 8-hydroxyoctanoate **5**, 9-hydroxynonanoate **6**, heptanoate **1**, and octanoate **2**. Four short-chain oxidation products could tentatively be assigned in the polar fraction of GC-FID chromatogram by comparing their retention times to those of the synthesized references: methyl 5-oxohexanoate **24**, methyl 8-hydroxyoctanoate **25**, methyl 7-oxoheptanoate **26** and 8-oxooctanoate **27** (Figure 47). In the non-polar phase no short-chain oxidation product was identified.



Figure 47: Structures of tentatively assigned short-chain oxidation products in the transesterified polar fraction of heated (180°C, 60 min.) sitostanyl oleate **3**. Methyl 5-oxohexanoate **24**, methyl 8-hydroxyoctanoate **25**, methyl 7-oxoheptanoate **26**, and methyl 8-oxooctanoate **27**.

4.2.5 Quantitation of Long-Chain ACOPs

4.2.5.1 Approach

Quantifications of the long-chain ACOPs methyl 10-hydroxyoctadec-8-enoate **29**, methyl 9-hydroxyoctadec-10-enoate **30**, methyl 8-hydroxyoctadec-9-enoate **31**, methyl 11-hydroxyoctadec-9-enoate **32**, methyl *trans*-9,10-epoxystearate **33**, methyl *cis*-9,10-epoxystearate **34**, methyl oxooctadecenoate **35**, and methyl 9,10-dihydroxystearate **36** were based on comparisons of the determined GC-peak areas to that of the internal standard methyl ricinoleate **IS₇**.

Owing to the insufficient GC-resolutions, methyl 8-hydroxyoctadec-9-enoate **31** / methyl 11-hydroxyoctadec-9-enoate **32** and methyl 10-hydroxyoctadec-8-enoate **29** / methyl 9-hydroxyoctadec-10-enoate **30** were quantified as pairs rather than as individual compounds.

GC-response factors relative to the internal standard were determined (Table 11) and taken into account for the quantifications. Limits of detection (LOD) and limits of quantification (LOQ) were determined according to Vogelgesang and Hädrich (1998) (Table 11).

Table 11: Limits of detection (LOD), limits of quantitation (LOQ) and relative response factors (RRF) of various methyl esters.

no.	compound	LOD ($\mu\text{g/mL}$)	LOQ ($\mu\text{g/mL}$)	RRF
33	methyl <i>trans</i> -9,10-epoxystearate	0.21	0.68	0.64 ^a
34	methyl <i>cis</i> -9,10-epoxystearate	0.15	0.52	0.88 ^a
36	methyl 9,10-dihydroxystearate	0.37	1.4	1.28 ^a
29-32	methyl hydroxyoctadecenoate	0.23	0.76	0.93 ^a
28	methyl oleate	0.29	0.94	0.84 ^a , 1.01 ^b

^a relative to methyl ricinoleate, ^b relative to methyl palmitate

The determination of a RRF for methyl oxooctadecenoate **35** was not possible as the reference compound could not be sufficiently purified. For its quantitation, a RRF of 1 was used.

Recovery rates were determined for the remaining unaltered sitostanyl oleate **3**, for sitostanyl *cis*-9,10-epoxystearate **10a** as representative of the major class of epoxy-ACOPs and for sitostanyl 9,10-dihydroxystearate **7** as example of an hydroxy-ACOP (Table 12).

Table 12: Recovery rates of sitostanyl oleate **3**, sitostanyl *cis* 9,10-epoxystearate **10a**, and sitostanyl 9,10-dihydroxystearate **7**. Values represent means of triplicate experiments and respective standard deviations.

no.	compound	recovery rate (%)
3	sitostanyl oleate	112 ± 12
10a	sitostanyl <i>cis</i> -9,10-epoxystearate	91 ± 3
7	sitostanyl 9,10-dihydroxystearate	88 ± 1

4.2.5.2 Temperature Dependence of the Formation of Long-Chain ACOPs

Sitostanyl oleate **3** (18 mg) was heated for 30 minutes at temperatures ranging from 120°C to 200°C. The formed amounts of ACOPs, expressed as µg/mg sitostanyl oleate, are depicted in Figure 48.

At the lowest applied temperature (120°C), no long-chain ACOPs were detectable. Upon heating at 150°C for 30 minutes, only the pair 8/11-hydroxyoctadec-9-enoate **31/32** was detected.

Starting from 160°C, methyl *trans*-9,10-epoxystearate **33** was consistently the main oxidation product. Additionally, methyl *cis*-9,10-epoxystearate **34** and the pair 8/11-hydroxyoctadec-9-enoate **31/32** were detected in larger proportions at all temperatures, while the other pair methyl 10-hydroxyoctadec-8-enoate / 9-hydroxyoctadec-10-enoate **29/30** as well as methyl oxooctadecenoate **35** were present in significantly lower amounts. Methyl 9,10-dihydroxystearate **36** was only detected at low concentrations starting from 180°C.

Only the amount of methyl *trans*-9,10-epoxystearate **33** exhibited a consistent increase with increasing temperature; all other ACOPs initially showed an increase, but then levelled off with increasing temperature. For the pair 8/11-hydroxy octadec-9-enoate **31/32**, the amount even dropped significantly at 200°C compared to that at 180°C.

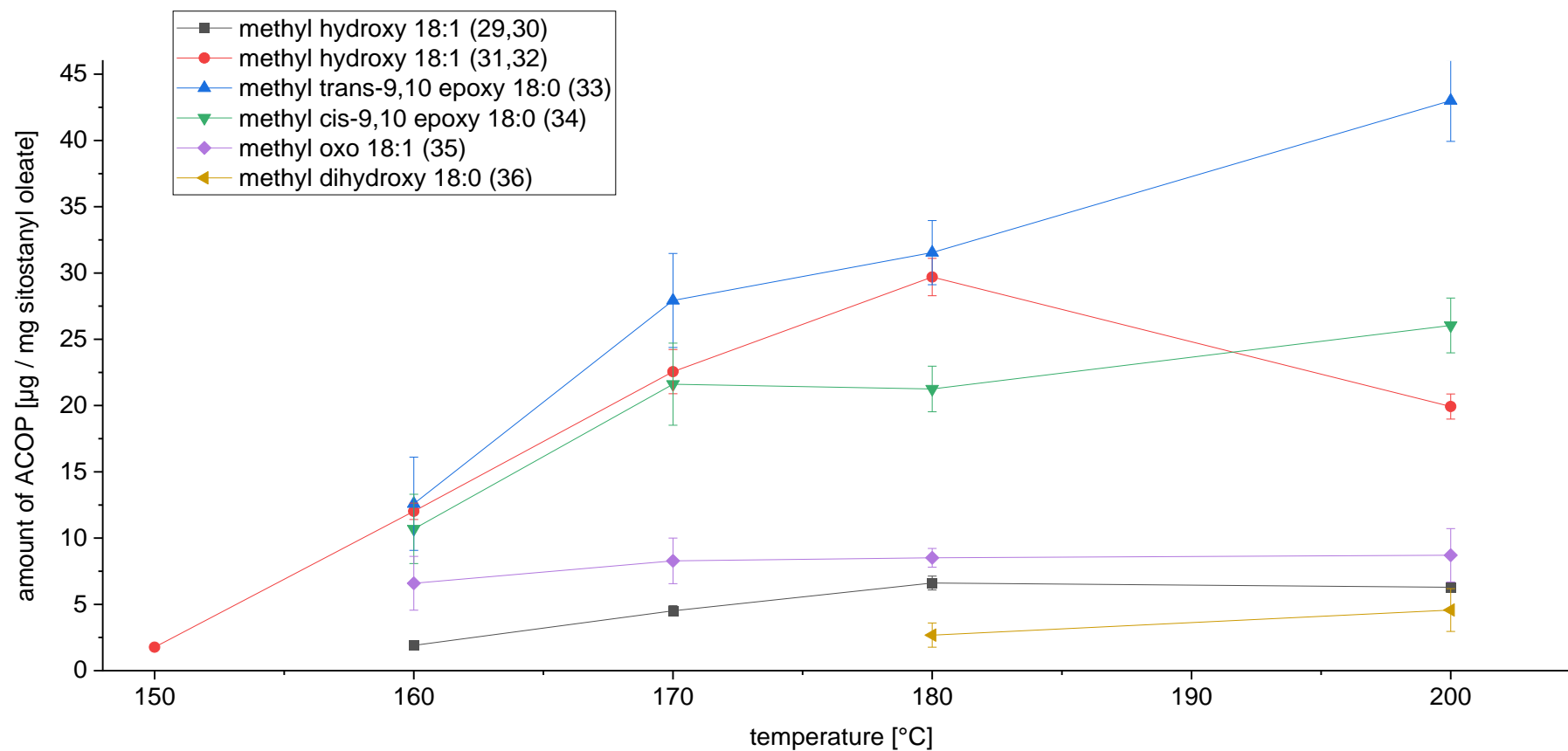


Figure 48: Amounts of long-chain ACOPs formed upon heating of sitostanyl oleate for 30 minutes at different temperatures. Values represent means of triplicate experiments and respective standard deviations.

Table 13: Amounts (mol%) of long-chain ACOPs formed upon heating of sitostanyl oleate for 30 minutes at different temperatures. Values represent means of triplicate experiments and respective standard deviations.

no.	proportion of starting molar amount of sitostanyl oleate [mol%]				
	150°C	160°C	170°C	180°C	200°C
ACOPs					
29,30		0.19 ± 0.02	0.44 ± 0.04	0.65 ± 0.05	0.61 ± 0.03
31,32	0.17 ± 0.01	1.17 ± 0.06	2.20 ± 0.16	2.90 ± 0.14	1.95 ± 0.09
33		1.23 ± 0.34	2.73 ± 0.35	3.08 ± 0.24	4.20 ± 0.30
34		1.04 ± 0.26	2.11 ± 0.30	2.08 ± 0.17	2.54 ± 0.20
35		0.65 ± 0.20	0.81 ± 0.17	0.83 ± 0.07	0.85 ± 0.20
36				0.26 ± 0.09	0.44 ± 0.15
total	0.17 ± 0.01	4.35 ± 0.67	8.52 ± 0.61	9.80 ± 0.51	10.60 ± 0.04

The proportions of formed ACOPs expressed on a molar basis related to the starting amount of sitostanyl oleate are listed in Table 13.

The total amounts of ACOPs increased with the increase in heating temperature. The most pronounced increase was observed when changing the heating temperature from 150°C to 170°C. Upon further increase of the temperature up to 200°C, the increase diminished, resulting in a plateau of the total amounts of ACOPs.

4.2.5.3 Time Dependence of the Formation of Long-Chain ACOP at 180°C and 200°C

The time dependence of the formation of long-chain ACOPs was determined for two temperatures (180°C and 200°C) at heating times ranging from 15 minutes to 180 minutes. The temperature and time conditions were selected to reflect conditions typically used for cooking and baking.

The amounts of remaining sitostanyl oleate, in which the acyl chain had not been oxidized, are depicted in Figure 49; they were determined based on the amounts of methyl oleate formed upon transesterification. After heating at 180°C for 15 minutes, 85 mol% sitostanyl oleate was remaining. With longer heating time, the amount of non-oxidized material decreased to 9 mol% after 180 minutes. The decline was most pronounced up to 60 minutes and then slowed down.

At the higher oxidation temperature of 200°C and a heating time of 15 minutes, 68 mol% sitostanyl oleate remained. This amount is clearly lower than that observed for 180°C after the same time. Up to a heating time of 120 minutes, there was a parallel shift of the curves obtained for 180°C and 200°C. For each investigated heating time, 15 mol% less remained at the heating temperature of 200°C compared to 180°C. After 180 minutes, for both heating temperatures the amounts of remaining sitostanyl oleate were nearly the same.

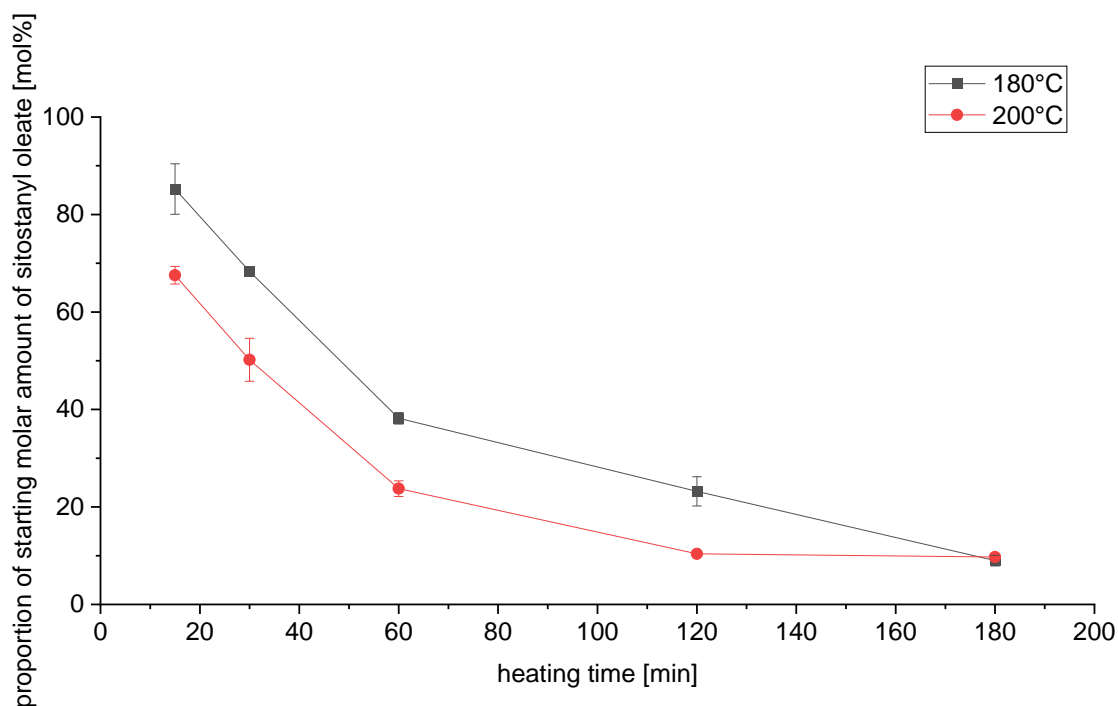


Figure 49: Amounts of remaining sitostanyl oleate, in which the acyl chain has not been oxidized, after heating for different periods at 180°C and 200°C, respectively. Values represent means of triplicate experiments and respective standard deviations.

The amounts of long-chain ACOPs observed after heating sitostanyl oleate for different durations at 180°C and 200°C, respectively, are depicted in Figure 50 A and B; the amounts are expressed as $\mu\text{g}/\text{mg}$ sitostanyl oleate **3**.

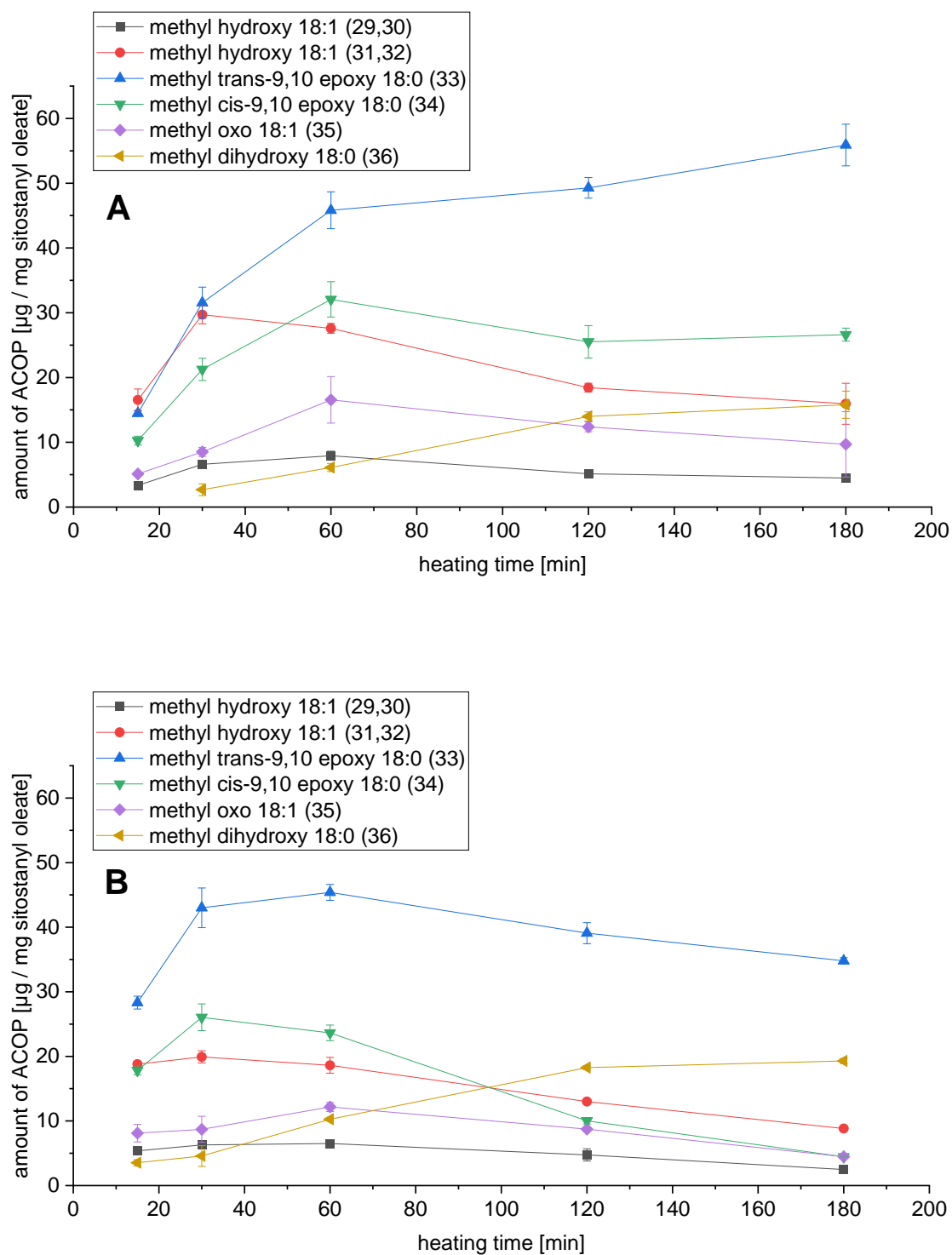


Figure 50: Amounts of ACOPs formed upon heating of sitostanyl oleate for different times from 15 min. to 180 min. **A:** 180°C, **B:** 200°C. Values represent means of triplicate experiments and respective standard deviations.

Upon heating at 180°C, *trans*-9,10-epoxystearate **33** was identified as the main oxidation product in all cases except for the shortest oxidation time (15 min.). Its amount showed a steady increase up to a heating duration of 60 minutes; then the curve levelled off. The only other ACOP showing a steady increase was 9,10-dihydroxystearate **36**, which however was only detectable after a heating time of at least 30 minutes. For the amounts of all other ACOPs, maxima after 30 or 60 minutes of heating were observed. Similar to the observations made with different heating temperatures, *trans*-9,10-epoxystearate **33**, *cis*-9,10-epoxystearate **34**, and 8/11-hydroxyoctadecenoate **31/32** were found to be the most strongly represented ACOPs for short heating times. The oxooctadecenoates **35**, 9/10-hydroxyoctadecenoate **29/30**, and 9,10-dihydroxystearate **36** showed lower proportions. The longer the exposure to heat, the more *trans*-9,10-epoxystearate **33** stood out as the main oxidation product, and all others were detected at significantly lower levels.

At 200°C, *trans*-9,10-epoxystearate **33** was clearly the main oxidation product for all heating times. While a continuous increase in *trans*-9,10 epoxy stearate **33** was visible at 180°C, the amount detected at 200°C initially increased with heating time and decreased after 60 minutes. This phenomenon was also observable for all other ACOPs at this temperature. However, the decrease in quantity at longer heating times was more evident than at 180°C. One ACOP did not show the same trend as the others; 9,10-dihydroxystearate **36** exhibited a steady increase in quantity with increasing heating time.

The proportions of formed ACOPs related to the starting amount of sitostanyl oleate expressed on a molar basis are listed in Table 14 (for heating at 180°C) and Table 15 (for heating at 200°C).

Upon heating at 180°C, there was a significant increase in the total amount of formed ACOPs up to a heating time of 60 minutes. For longer durations of heating, no further increase in the total amount of ACOPs was observed (Table 14).

Upon heating at 200°C, the total amount ACOPs increased up to a heating time of 60 minutes. After longer durations of heating, the total amounts of formed ACOPs even decreased (Table 15).

Table 14: Amounts (mol%) of remaining unaltered ester and of long-chain oxidation products formed upon heating of sitostanyl oleate **3** at 180°C for different time periods. Values represent means of triplicate experiments and respective standard deviations.

		proportion of starting molar amount of sitostanyl oleate [mol%]				
		15 min	30 min	60 min	120 min	180 min
Unaltered ester						
28	methyl oleate	85.23 ± 5.16	68.33 ± 0.75	38.19 ± 1.18	23.21 ± 3.00	8.99 ± 1.09
ACOPs						
29,30	methyl 9/10 hydroxy 18:1	0.33 ± 0.03	0.65 ± 0.05	0.78 ± 0.07	0.50 ± 0.02	0.44 ± 0.04
31,32	methyl 8/11 hydroxy 18:1	1.62 ± 0.16	2.90 ± 0.14	2.70 ± 0.07	1.80 ± 0.07	1.56 ± 0.31
33	methyl <i>trans</i> -9,10-epoxy 18:0	1.41 ± 0.04	3.08 ± 0.24	4.48 ± 0.28	4.81 ± 0.16	5.46 ± 0.31
34	methyl <i>cis</i> -9,10-epoxy 18:0	1.00 ± 0.07	2.08 ± 0.17	3.13 ± 0.27	2.49 ± 0.24	2.60 ± 0.10
35	methyl oxo 18:1	0.50 ± 0.02	0.83 ± 0.07	1.62 ± 0.35	1.21 ± 0.08	0.95 ± 0.50
36	methyl 9,10-dihydroxy 18:0		0.26 ± 0.09	0.58 ± 0.06	1.33 ± 0.07	1.50 ± 0.20
	total	4.96 ± 0.25	9.80 ± 0.51	13.29 ± 0.21	12.16 ± 0.60	12.51 ± 0.99

Table 15: Amounts (mol%) of remaining unaltered ester and of long-chain oxidation products formed upon heating of sitostanyl oleate **3** at 200°C for different time periods. Values represent means of triplicate experiments and respective standard deviations.

		proportion of starting molar amount of sitostanyl oleate [mol%]				
		15 min	30 min	60 min	120 min	180 min
Unaltered ester						
28	methyl oleate	67.55 ± 1.82	50.20 ± 4.41	23.76 ± 1.59	10.38 ± 0.45	9.72 ± 0.71
ACOPs						
29,30	methyl 9/10-hydroxy 18:1	0.52 ± 0.02	0.61 ± 0.03	0.64 ± 0.04	0.46 ± 0.09	0.24 ± 0.01
31,32	methyl 8/11-hydroxy 18:1	1.84 ± 0.04	1.95 ± 0.09	1.82 ± 0.12	1.27 ± 0.03	0.86 ± 0.00
33	methyl <i>trans</i> -9,10-epoxy 18:0	2.77 ± 0.10	4.20 ± 0.30	4.44 ± 0.12	3.82 ± 0.16	3.40 ± 0.05
34	methyl <i>cis</i> -9,10-epoxy 18:0	1.74 ± 0.07	2.54 ± 0.20	2.31 ± 0.12	0.98 ± 0.05	0.44 ± 0.01
35	methyl oxo 18:1	0.80 ± 0.13	0.85 ± 0.20	1.19 ± 0.07	0.86 ± 0.02	0.44 ± 0.01
36	methyl 9,10-dihydroxy 18:0	0.34 ± 0.05	0.44 ± 0.15	0.98 ± 0.03	1.74 ± 0.03	1.84 ± 0.04
	total	8.00 ± 0.33	10.60 ± 0.04	11.37 ± 0.40	9.13 ± 0.21	7.22 ± 0.08

4.2.5.4 Formation of Long-Chain ACOPs Upon Heating of Other Oleates

In order to assess the impact of the sitostanol moiety on the formation of long-chain ACOPs upon thermo-oxidation of sitostanyl oleate, oleates containing other esterified alcohol moieties were also investigated. Heating experiments were performed with (i) sitosteryl oleate containing the respective unsaturated phytosterol as esterified moiety, (ii) the most simple ester representative methyl oleate, (iii) the monoglyceride monoolein and (iv) the oil-like triglyceride triolein.

Initial experiments demonstrated that for sitosteryl oleate as well as for monoolein and triolein the SPE-separation as performed for thermo-oxidized sitostanyl oleate was not applicable, owing to the insufficient separation of the formed ACOPs from material that remained unaltered in the fatty acid chain. For example, 6,7-epoxysitosteryl oleate resulting from oxidation of the unsaturated sterol ring, was eluted in the polar fraction, although the fatty acid residue was not oxidized. Therefore, the transesterification was performed as first step and the resulting methyl esters were subsequently subjected to SPE separation. The elution volumes were adjusted based on monitoring using thin layer chromatography. No further validations of the SPE procedure, e.g. regarding recoveries, were performed. The relative GC-response factors listed in Table 11 were applied for quantitations.

The proportions (mol%) of the starting amounts of the different oleates remaining after subjecting them to heating at 180°C for 30 minutes are shown in Figure 51.

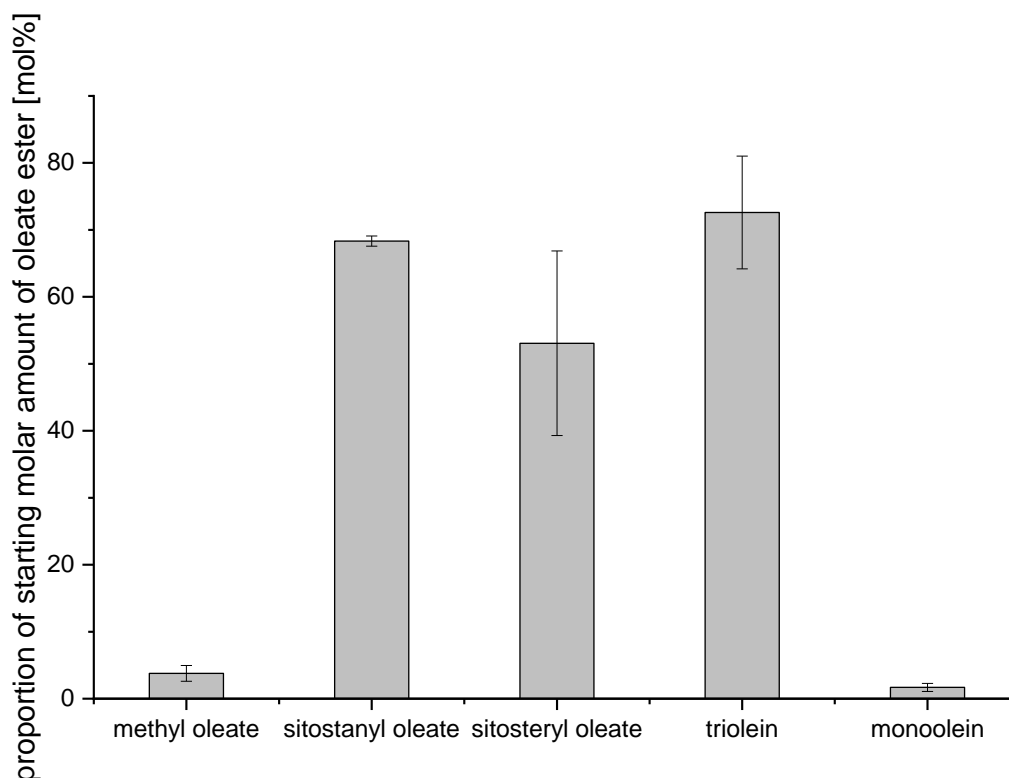


Figure 51: Amounts of remaining oleate after heating to 180°C for 30 minutes. The data are based on the quantitation of methyl oleate resulting from transesterification; for the calculation of the value for triolein, the presence of three oleic acid moieties was taken into account. Values represent means of triplicate experiments and respective standard deviations.

The proportion of remaining sitosteryl oleate in which no oxidation of the acyl chain had occurred owing to the thermal treatment was in the same order of magnitude as the remaining proportion of unaltered sitostanyl oleate. A similar amount of unaltered oleate remained when subjecting triolein to the thermo-oxidation. In contrast, the remaining proportions of unaltered methyl oleate and monoolein were significantly lower.

It should be noted that in the case of sitosteryl oleate and triolein, the quantified amount of methyl oleate does not correlate with the amount of unaltered starting material. For sitosteryl oleate, the analysis does not consider oxidations in the sterol moiety. For triolein, the analysis considers the change in the individual oleates, but not whether they originate from a triolein molecule with three unaltered oleate moieties or with up to two oxidized moieties.

The amounts of formed ACOPs, expressed as proportions (mol%) of the starting amount of the respective oleate, are shown in Figure 52.

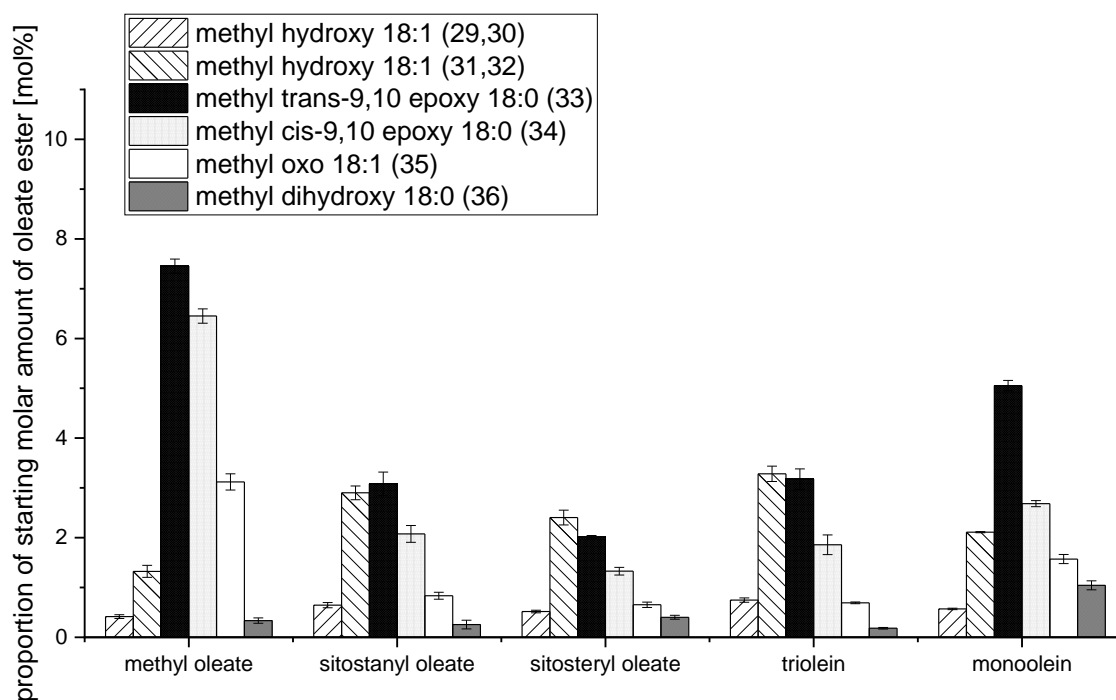


Figure 52: Long-chain ACOPs determined after heating different oleates for 30 minutes at 180°C. The data are based on the quantitation of methyl esters resulting from transesterification; for the calculation of the value for triolein, the presence of three oleic acid moieties was taken into account. Values represent means of triplicate experiments and respective standard deviations.

The distributions of the long-chain ACOPs determined upon heating of the phytosteryl ester sitosteryl oleate and of the triglyceride trioleine were very similar to that observed for sitostanyl oleate: The two epoxy-ACOPs *trans*-9,10-epoxystearate **33** and *cis*-9,10-epoxystearate **34** and the pair of the hydroxy-ACOPs 8/11-hydroxyoctadecenoate **31/32** were preferentially formed, followed by oxooctadecenoate **35**, the pair 9/10-hydroxyoctadecenoate **29/30** and finally 9,10-dihydroxystearate **36**. For these three starting materials subjected to heating, not only the profiles of the formed ACOPs but also their total amounts were quite similar.

In contrast, for methyl oleate, the total amount of ACOPs was clearly higher than for sitostanyl oleate, sitosteryl oleate and triolein. The epoxy-ACOPs **33** and **34** were

predominating and the relative proportion of the pair 8/11-hydroxyoctadecenoate **31/32** was diminished.

For monoolein, *trans*-9,10-epoxystearate **33** stood out as representative of the epoxy-ACOPs and the proportion of 9,10-dihydroxystearate **36** was higher than for the other heated substrates.

4.2.5.5 Discussion

Methodology

The analysis of long-chain ACOPs involved several steps: (i) separation using solid-phase extraction (SPE), (ii) transesterification, and (iii) GC-analysis.

In accordance with the approach employed by Wocheslander *et al.* (2016) for the GC-investigation of short-chain ACOPs formed upon heat-treatment of phytosteryl-/stanyl oleates and linoleates, the formed ACOPs were separated from the remaining unaltered starting material via SPE of the respective sitostanyl esters; the transesterification was carried out as a second step.

This sequence differs from other approaches described in the literature in the context of GC-based investigations of ACOPs formed upon thermooxidation of fats and oils (Berdeaux *et al.*, 1999a; Velasco *et al.*, 2002; Velasco *et al.*, 2004b). In these studies, remaining non-oxidized material and formed oxidation products have been separated on the level of the fatty acid methyl esters (FAMES), i.e. the oxidized mixture was not directly subjected to SPE but the thermooxidized mixture was first converted into the respective methyl esters via transesterification. The non-polar fraction containing the unaltered FAMES has subsequently been eluted with hexane/diethylether (95:5, v/v) and the polar fraction with diethyl ether (Velasco *et al.*, 2002; Velasco *et al.*, 2004b). This approach has been further refined by applying a three steps fractionation of the transesterified sample: Non-altered FAMES have been eluted with hexane-diethyl ether (98:2, v/v); upon elution with hexane-diethylether (90:10, v/v) a polar fraction containing epoxy compounds has been obtained, and hexane/diethyl ether (70:30, v/v) or pure diethyl ether have been used to obtain a second polar fraction containing hydroxy fatty acids (Mubiru *et al.*, 2013; Xia and Budge, 2017). In particular, when using a matrix containing derivatives of acids that are more unsaturated than oleic acid,

a broader spectrum of oxidation products is to be expected which could be separated in this way (Mubiru *et al.*, 2013; Xia and Budge, 2017).

The approach based on transesterification followed by SPE separation of the resulting methyl esters was applied as work-up procedure for the GC analysis of ACOPs formed upon heating of sitosteryl oleate, monolein and triolein. This approach would also be required when extending the investigations of the formation of ACOPs from a simple model substance such as sitostanyl oleate to thermooxidized fats and oils enriched with phytosteryl/-stanyl fatty acid esters.

In this study, GC-separations were performed using a medium polar stationary phase. The investigated esters could not be fully separated. Improved GC-separations of the long-chain ACOPs might be achievable by employing other stationary phases. Previous studies have successfully separated FAMEs by utilizing strongly polar stationary phases such as CPSil 88 or DB-23 (cyanopropyl phase) (Mubiru *et al.*, 2013; Xia and Budge, 2017; Xia and Budge, 2018). A comparable polar phase (biscyanopropyl-cyanopropylphenyl polysiloxane; Rtx 2330) has been shown to be effective in separating *cis/trans* FAMEs, as demonstrated by Lercker *et al.* (2002); Xia and Budge (2017) and Xia and Budge (2018). Several studies have utilized polar polyethylene glycol (e.g. HP Innowax or DB-WAX) as stationary phase for analysis of FAMEs (Gardner *et al.*, 1992; Berdeaux *et al.*, 1999a; Berdeaux *et al.*, 1999b; Velasco *et al.*, 2002; Velasco *et al.*, 2004a; Velasco *et al.*, 2004b; Dobarganes and Márquez-Ruiz, 2007; Marmesat *et al.*, 2008; Berdeaux *et al.*, 2012; Raczyk *et al.*, 2017). Oxidized FAMEs could also be detected using non-polar phases such as (5% phenyl)methylpolysiloxanes (DB-5, ZB-5) (Gardner *et al.*, 1992; Marmesat *et al.*, 2008) or dimethylpolysiloxanes (DB-1ms) (Xia and Budge, 2017). The analysis of hydroxy FAME has been conducted using 35% phenyl / 65% dimethylpolysiloxane phase (ZB-35HT) with medium polarity (Xia and Budge, 2017).

For instance, Xia and Budge (2017) successfully separated *cis*- and *trans*-isomers of hydroxyoctadecenoates. However, even with the polar DB-23 column used in that study, it was only possible to separate *cis*- and *trans*-isomers of methyl 8-hydroxyoctadecenoate and methyl 11-hydroxyoctadecenoate, but not those of methyl 9-hydroxyoctadecenoate and 10-hydroxyoctadecenoate. It was also observed that use of other polar columns, such as RTX-2330, resulted in less effective separations, making it impossible to separate monounsaturated 9- or 10-hydroxyoctadecenoates

from the corresponding saturated compounds. Even poorer separations were achieved on DB-1 (non-polar) and ZB-HT35 (medium polar) columns. It is important to note that all analyses described by Xia and Budge (2017) were conducted using silylated compounds. The silylation of the compounds was also shown to be necessary for their elution on polar phases such as CPSil88 (Mubiru *et al.*, 2013). It should be noted that in this thesis, the separations were possible on the basis of non-silylated compounds.

Quantitations were based on the use of internal standards for each fraction generated by SPE. Relative response factors, LOD and LOQ were determined. These determinations were not possible for methyl oxooctadecenoate **35**, because this reference could not be sufficiently purified. For methyl hydroxyoctadecenoates **29-32**, as mentioned above, separation was only partially possible. The RRF, LOD and LOQ were determined for these compounds in total. The quantitations of methyl oxooctadecenoate **35** or methyl hydroxyoctadecenoate **29-32** might therefore be improved by generating a purer reference or by enhancing the separation of the compounds.

Recovery rates of sitostanyl esters over the total analytical approach were determined for three compounds (sitostanyl oleate **3**, sitostanyl *cis*-9,10-epoxystearate **10a**, sitostanyl 9,10-dihydroxystearate **7**). A further improvement of the method would be the determination of recovery rates for all compounds investigated.

Previous studies on the quantitation of methyl epoxystearates were also based on the use of an internal standard and the determination of RRF (Berdeaux *et al.*, 1999a) or included recoveries related to the SPE separation (Velasco *et al.*, 2002). Marmesat *et al.* (2008) utilized an internal standard to establish the RRFs for three types of compounds: hydroxyFAMEs, epoxyFAMEs, and ketoFAMEs, determined by a representative compound for each class. The limits of quantitation were determined to be 1.6, 1.8, and 2.1 µg/ml for methyl *trans*-9,10-epoxystearate, methyl 12-oxostearate, and methyl 12-hydroxystearate, respectively. These limits are similar to those determined in this thesis (Table 11), which range from 0.5 to 1.4 µg/ml. Additionally, in both studies the LOQ of epoxy-ACOPs was found to be lower than that of hydroxy-ACOPs.

Comparison of GC-based and UHPLC-MS/MS-based data on long-chain ACOPs formed by thermo-oxidation of sitostanyl oleate

The established GC-based methodology enabled to determine representatives of long-chain epoxy-, hydroxy-, dihydroxy- and oxo-ACOPs, i.e. those classes of ACOPs that constituted the majority of the ACOPs covered by UHPLC-MS/MS analysis (Scholz *et al.*, 2019). A comparison of the amounts of these classes of ACOPs determined by the two approaches is shown in Figure 53.

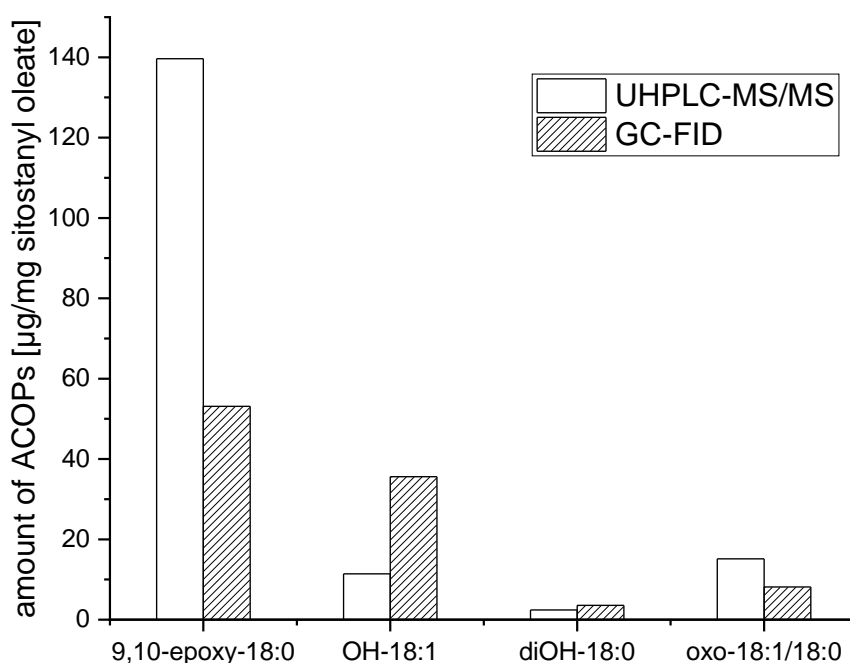


Figure 53: Amounts of different classes of long-chain ACOPs in heated (180°C, 30 min.) sitostanyl oleate determined by UHPLC/MS-MS analysis (Scholz *et al.*, 2019) and by GC, respectively.

The total amount of ACOPs from these classes determined by UHPLC-MS/MS analysis (169 µg/mg sitostanyl oleate) was higher than that determined via GC (100 µg/mg sitostanyl oleate). According to UHPLC-MS/MS analysis, epoxy-ACOPs constituted the vast majority (83%) of these ACOPs. They were also the quantitatively predominating class of ACOPs determined by GC; however, their proportion dropped to 53%. On the other hand, according to GC-analysis hydroxy-ACOPs constituted the

second most important class of ACOPs (35%), whereas, according to UHPLC-MS/MS analysis, they made up only 7%. The amounts of oxo- and dihydroxy-ACOPs determined by the two approaches also slightly differed, but according to both analyses they constitute only minor groups of ACOPs.

Various aspects need to be taken into account when comparing the absolute amounts of long-chain ACOPs determined by the two approaches. For example, owing to the better resolution of methyl *cis*- and *trans*-9,10-epoxystearates via GC compared to the UHPLC separation of the respective sitostanyl esters, the quantitation of these two major ACOPs was improved. In the UHPLC-MS/MS analysis, the hydroxyoctadecenoates were determined in total; the GC method resulted in a partial separation of these compounds, allowing at least determinations of two pairs **29/30** and **31/32**. The semiquantitative assessment performed in the UHPLC-MS/MS analysis used representative internal standards for the various classes of ACOPs separated via SPE; however, no individual response factors were determined. On the other hand, for the GC-approach, relative response factors could not be determined for methyl oxooctadecenoate **35** and were only available for the mixture of methyl hydroxyoctadecenoates **29-32**. In the course of the UHPLC-MS/MS analysis, all ACOPs were also quantitated in triplicate experiments in the untreated starting material (control); for the GC-based analysis, a single preliminary test was performed demonstrating that none of the investigated ACOPs was present at amounts above the limits of quantification.

Comparison with long-chain ACOPs reported for thermo-oxidations of fats and oils

The formation of long-chain ACOPs upon thermal treatment of lipids containing unsaturated fatty acid moieties has been extensively studied in the past. The investigations ranged from model substances such as fatty acid methyl esters and monoacid triglycerides (Berdeaux *et al.*, 1999a) to experiments involving heating and frying of fats and oils (Gardner *et al.*, 1992; Berdeaux *et al.*, 1999a; Velasco *et al.*, 2002; Berdeaux *et al.*, 2008; Marmesat *et al.*, 2008). Recent studies on deep-frying of high-oleic sunflower oil reflect the continuous interest in this topic (Koch *et al.*, 2023) which is also being tackled via bioassays in order to assess the potential genotoxicity of these lipid oxidation products (Morlock and Meyer, 2023). Therefore, the data

elaborated in this study for sitostanyl oleate were compared to the existing body of knowledge on long-chain ACOPs formed from other lipids containing oleic acid as acyl moiety.

Trans- and *cis*-epoxystearates were among the quantitatively predominating ACOPs determined in this study after thermo-oxidation of sitostanyl oleate. This is in agreement with various studies describing epoxystearates as main oxidation products from heating of methyl oleate and triolein (Berdeaux *et al.*, 1999a) or fats and oils (Gardner *et al.*, 1992; Berdeaux *et al.*, 1999a; Velasco *et al.*, 2002; Berdeaux *et al.*, 2008; Marmesat *et al.*, 2008). In addition, it has been reported that the amount of *trans*-9,10-epoxystearate was higher than *cis*-9,10-epoxystearate (Velasco *et al.*, 2004b; Marmesat *et al.*, 2008; Brühl, 2014), which is also reflected in the data of this thesis. Koch *et al.* (2023) proposed the ratio of *cis/trans*-epoxystearate as marker to characterize the status of frying oils, with a ratio > 1 describing fresh oil and a ratio of < 1 for oil used several times. In the studies performed with sitostanyl oleate, except for the heating temperature of 150°C, at which after treatment for 30 minutes no epoxystearates were detected, under all other tested time/temperature conditions the ratio of *cis/trans*-epoxystearate was < 1. This indicates an advanced oxidation status and is in agreement with the observed decreases of the intact starting ester. As shown in Table 13, the treatment of sitostanyl oleate for 30 minutes at increasing heating temperatures resulted in a continuous decrease of the ratio of *cis/trans*-epoxystearate from 0.85 (at 160°C) to 0.60 (at 200°C). Table 14 shows that at a heating temperature of 180°C the prolongation of the heating duration resulted in a decrease of the ratio of *cis/trans*-epoxystearate from 0.71 (after 15 min.) to 0.48 (after 3h). At a heating temperature of 200°C, this effect was even more pronounced; the ratio of *cis/trans*-epoxystearate decreased from 0.63 (after 15 min.) to only 0.13 (after 3h). Again, these decreases are in agreement with the observed increases in ester loss upon elongation of the duration of heat treatment. The data indicate that the ratio of *cis*- and *trans*-9,10-epoxystearate is also a useful parameter to reflect the oxidation status of sitostanyl oleate.

Considering that epoxy-ACOPs can be hydrolyzed to the respective vicinal diols, Koch *et al.* (2023) also proposed the epoxy/diol ratio as potential marker for the oxidation status. As shown in Table 13, thermo-oxidation of sitostanyl oleate for 30 minutes resulted in the formation of 9,10-dihydroxystearate at heating temperatures of 180°C and 200°C. At both temperatures, prolongation of the heating duration resulted in

significant decreases of the ratio of *cis*- and *trans*-9,10-epoxystearate/9,10-dihydroxystearate (Table 14 and Table 15), indicating advanced oxidation. The beginning of oxidation would be characterized by increasing or constant ratios, according to Koch *et al.* (2023).

The ratio of *erythro*- and *threo*-9,10-dihydroxystearate, resulting from the hydrolysis of *cis*- and *trans*-9,10-epoxystearate, respectively, has also been proposed as parameter to assess the oxidation status (Koch *et al.*, 2023). The capillary gas chromatographic conditions applied in this study did not allow a differentiation of *erythro*- and *threo*-9,10-dihydroxystearate; therefore, the suitability of this marker for the thermo-oxidation of sitostanyl oleate could not be assessed.

There is less information available on the other long-chain ACOPs. Long-chain keto- and hydroxy-fatty acids have been described as other major classes of oxidation products that are formed upon heating and frying of oils and fats in addition to the epoxy-fatty acids (Gardner *et al.*, 1992). Schwartz *et al.* (1994) and Marmesat *et al.* (2008) reported quantitative data for the total hydroxy- and ketofatty acids formed in thermo-oxidized oils. Xia and Budge (2018) provided chromatographic and mass spectral data for the TMS-derivatives of the individual representatives methyl 10-hydroxyoctadec-8-enoate **29**, methyl 9-hydroxyoctadec-10-enoate **30**, methyl 8-hydroxyoctadec-9-enoate **31**, methyl 11-hydroxyoctadec-9-enoate **32** and quantitated **29** and **30** in sunflower and canola oil stored for 40 days at 40°C.

Studies on the temperature dependence of the formation of ACOPs are rare. In one study volatile oxidation products of olive oil (containing 80% oleic acid as acyl moiety) were investigated, and it was found that their proportion increased with increasing temperature from 100°C to 200°C (Zhuang *et al.*, 2022). For several model substances, including oleic acid, triolein, and monoolein, the temperature dependence of the formation of hydroperoxides has been studied (Zhou *et al.*, 2022). Hardly any hydroperoxides were formed at low temperature (80°C). Their content increased with rising temperature; however, at higher temperatures (140-170°C) the degradation of hydroperoxides increased and thus their content decreased. This observed increase in oxidation product content with temperature and a subsequent decrease or stagnation is in accordance with the results obtained in this study for sitoastanyl oleate; at a heating temperature of 120°C no ACOPs were detected and only starting from

150°C ACOPs could be determined in increasing amounts with increasing temperature.

Correlation between formed amounts of ACOPs and decrease of sitostanyl oleate

In the first GC-based study on the ACOPs formed upon thermo-oxidation of phytosteryl/-stanyl oleates and linoleates, the oxidation products determined after heating of phytostanyl oleates at 180°C for 40 minutes accounted for 8.7% of the observed loss of starting ester (Wocheslander *et al.*, 2017). In the subsequent UHPLC-MS/MS-based study, the spectrum of analytes could be extended from short- and medium-chain ACOPs resulting from the degradation of the fatty acid chain to the quantitatively predominating long-chain ACOPs (Scholz *et al.*, 2019). Consequentially, the proportion of the loss of sitostanyl oleate heated at 180°C for 30 minutes that could be explained by the covered ACOPs increased to 48.7%. In the present GC-based study, the proportion of loss of sitostanyl oleate after heating at 180°C for 30 minutes that is attributable to the determined ACOPs amounted to 32% (Table 14). Taking into account that (i) the short- and medium-chain ACOPs have not been included in the applied methodology and (ii) that the quantitated long-chain ACOPs covered only approximately 91% of the ACOPs determined by the UHPC-MS/MS-approach, the proportions of loss of sitostanyl oleate that can be explained by the results obtained by the two methodologies can be considered as comparable.

However, the data obtained for the time dependence of the formation of ACOPs demonstrated that the contributions of the formed long-chain ACOPs decrease with the decreases of sitostanyl oleate observed under the different time/temperature (Figure 54). As depicted in Figure 54 A, there was a decrease of sitostanyl oleate up to a maximum of about 900 µg/mg sitostanyl oleate upon heating at 180°C for 180 minutes. The total amount of formed ACOPs showed a maximum after heating for 60 minutes. For longer heating times, the total amount of ACOPs was similar to that at 60 minutes. As a result, the proportion of ester loss that can be explained by the investigated ACOPs decreased continuously. After heating for 15 minutes at 180°C, 34% of the ester loss could be explained by the determined long-chain ACOPs, whereas after 180 minutes only 14% of the ester loss was attributable to the investigated ACOPs.

The decrease of sitostanyl oleate upon heating at 200°C (Figure 54 B) was higher than at 180°C and reached a plateau already after a heating period of 120 minutes. Comparable to the heating temperature of 180°C, the total amount of ACOPs increased with heating time up to 60 minutes. After that, the total amount of quantified ACOPs decreased. After 15 minutes at 200°C, 25% of the ester loss could be explained by the long-chain ACOPs. This is less than the proportion that could be explained at 180°C, although the total amount at 200°C after 15 minutes was higher than at 180°C. With longer heating times at 200°C, the amount of ester loss that could be explained decreased. Only 8% of the ester loss after 180 minutes could be explained by the determined long-chain ACOPs.

This phenomenon is assumed to be due to the formation of further oxidation products and chain breaking during oxidation and therefore formation of short chain oxidation products or formation of dimers, oligomers, polymers and volatile or cyclized oxidation products where oxygen groups can be involved into dimer linkage (Dobarganes and Márquez-Ruiz, 2007)

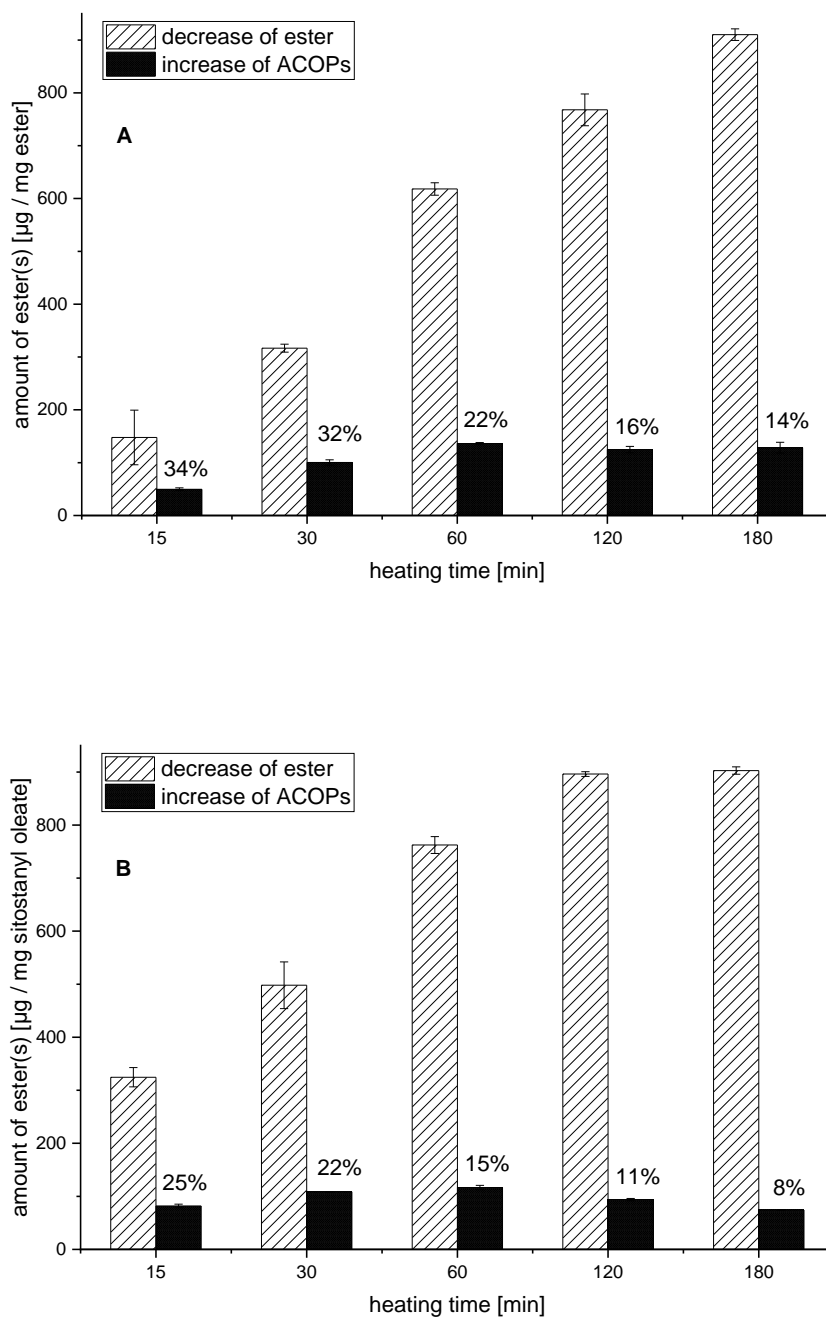


Figure 54: Comparison of the decrease of sitostanyl oleate and the increase of sitostanyl long-chain ACOPs upon thermal treatment of sitostanyl oleate at 180°C (**A**) or 200°C (**B**) for different durations. Values represent means of triplicate experiments and respective standard deviations.

Comparison of the formation of long-chain ACOPs from different oleates

A comparative assessment of the oxidative fate of sitostanyl oleate and sitosteryl oleate based on the results obtained by GC-analysis is hampered by the fact that the employed approach does not allow a differentiation of ACOPs with intact or oxidized sterol ring. Notwithstanding this disadvantage, the obtained data show that the amounts of the long-chain ACOPs covered by the applied methodology and determined for sitosteryl oleate were comparable to those determined for sitostanyl oleate. Similar amounts of ACOPs were also determined upon thermo-oxidation of triolein. In contrast, for methyl oleate and monoolein the amounts of ACOPs as well as the proportions of remaining intact ester clearly differed. The data suggest a protecting effect of the steryl and stanyl moieties regarding oxidations of the fatty acid chain.

The gap between the observed decreases of oleate and the amounts of oxidation products determined in this study may be explained by the formation of other oxidation products, such as short-chain oxidation products, dimers, polymers and volatile or cyclized oxidation products (Dobarganes and Márquez-Ruiz, 2007).

Differences in the amounts of oxidation products depending on the type of oleic acid ester have been shown for methyl oleate and triolein (Berdeaux *et al.*, 1999a). The proportion of *cis*-9,10-epoxystearate in total epoxystearates was higher when methyl oleate was heated compared to triolein. Zhou *et al.* (2022) investigated the loss of oleate using different esterified moieties. They investigated oleic acid, triolein, and monoolein heated for 40 min. at 170°C. The amount of oleic acid decreased under these conditions from 1 mg/mg to about 0.5 mg/mg, monoolein decreased to about 0.3 mg/mg and triolein even decreased to < 0.05 mg/mg.

4.2.5.6 Summary

An approach for the GC-based analysis of long-chain ACOPs formed upon heat-treatment of sitostanyl oleate was established. The applied methodology comprised (i) SPE to separate the polar long-chain ACOPs from unaltered sitostanyl oleate, (ii) transesterification of the ACOPs, and (iii) GC-analysis of the resulting methyl esters. GC-separations were performed for the non-silylated compounds using a medium polar stationary phase. Assignments were based on comparisons of retention times and mass spectral data to those of synthesized reference compounds. For

quantitations, methyl ricinoleate was used as internal standard and relative response factors were taken into account.

In a sample of heat-treated (180°C, 60 min.) sitostanyl oleate, methyl *trans*- and *cis*-9,10-epoxystearates **33**, **34** were the main oxidation products, followed by the pair methyl 8/11-hydroxyoctadec-9-enoate **31/32** and methyl oxooctadecenoate **35**. The pair methyl 10-hydroxyoctadec-8-enoate/9-hydroxyoctadec-10-enoate **29/30** and methyl 9,10-dihydroxystearate **36** were present in significantly lower amounts.

The method was applied to follow the formation of these long-chain ACOPs under different time/temperature conditions. Studies on the temperature dependence (120°C - 200°C, 30 min.) demonstrated that methyl *trans*-9,10-epoxystearate **33** was the quantitatively dominating ACOP starting from 160°C; only this oxidation product showed a consistent increase with increasing temperature. The formed amounts of the other ACOPs showed notable increases up to 170°C/180°C but then levelled off or declined.

Studies on the dependence of the formation of ACOPs on the heating duration (15 min. - 180 min.) at two temperatures (180°C, 200°C) confirmed the outstanding role of methyl *trans*-9,10-epoxystearate **33** as oxidation product. This ACOP showed a consistent increase of the formed amount upon prolonged duration of heating at 180°C; at 200°C, a maximum after 30-60 min. followed by a slight decrease was observed. Except for methyl 9,10-dihydroxystearate **36**, all other investigated ACOPs exhibited concentration maxima at both temperatures after 30 or 60 min. of heat treatment. The continuous decrease of sitostanyl oleate **3** and the maxima of the amounts of total ACOPs observed after 60 min. demonstrated that with increasing heating duration the proportion of ester loss that can be explained by the amounts of the quantitated ACOPs decreased. This effect was even more pronounced at 200°C. Experiments with oleates esterified to different moieties showed that the esterified moiety has a significant influence on the formation of ACOPs, affecting both the total amounts and the proportions of individual oxidation products. The oxidations of methyl oleate and monoolein were more pronounced than those of sitostanyl oleate, sitosteryl oleate and triolein.

4.3 *In-Vitro* Hydrolyses of Steryl/Stanyl Oleates and Respective ACOPs

4.3.1 Introduction

One of the mechanisms acknowledged to contribute to the cholesterol-lowering properties of phytosterols/-stanols is their competition with cholesterol for incorporation into mixed micelles (Trautwein *et al.*, 2003; Mel'nikov *et al.*, 2004). Consequentially, if phytosteryl/-stanyl fatty acid esters are employed to enrich foods, liberation of the free sterols/stanols via hydrolysis in the gastrointestinal tract is a key prerequisite to achieve the intended cholesterol-lowering effect of the functional ingredients. Pancreatic cholesteryl esterase (PCE) is one of the main enzymes involved in this hydrolytic step (Moreau and Hicks, 2004; Boyd *et al.*, 2022b).

The investigation of the potential impact of oxidative modifications of the fatty acid chains of phytosteryl/-stanyl fatty acid esters on their PCE-catalyzed hydrolysis and thus on the cholesterol-lowering properties of the ACOPs compared to the non-altered fatty acid esters was the topic of this final part of the thesis.

Indications for possible interference of ACOPs with the cholesterol-lowering effect of phytosteryl/-stanyl fatty acid esters come from the lowered inhibition of cholesterol micellarization observed for thermooxidized phytosteryl/-stanyl fatty acid mixtures (Scholz *et al.*, 2017). In addition, sitosteryl 9,10-dihydroxystearate has been reported as non-competitive inhibitor in PCE-catalyzed *in-vitro* hydrolyses of cholesteryl oleate and sitosteryl oleate (Julien-David *et al.*, 2009).

There are data on hydrolyses of phytosteryl/-stanyl fatty acid esters from *in-vitro* experiments (Brown *et al.*, 2010) and from bioavailability/bioaccessability studies with enriched foods (Gleize *et al.*, 2016; Vaghini *et al.*, 2016). However, apart from the data reported for sitostanyl 9,10-dihydroxysterate (Julien-David *et al.*, 2009), no information on hydrolyses of other ACOPs were available.

Therefore, conversions of synthesized representatives of different classes of ACOPs shown to be formed upon thermoxidation of sitostanyl oleate in the previous chapters should be compared in *in-vitro* PCE-catalyzed hydrolyses to that of sitostanyl oleate. Analogous comparative data should be elaborated for a series of ACOPs derived from sitosteryl oleate. In addition, the potential impact of the presence of cholesteryl oleate on the conversions of ACOPs and the influence of ACOPs on the conversions of cholesteryl oleate should be investigated.

4.3.2 Methodology

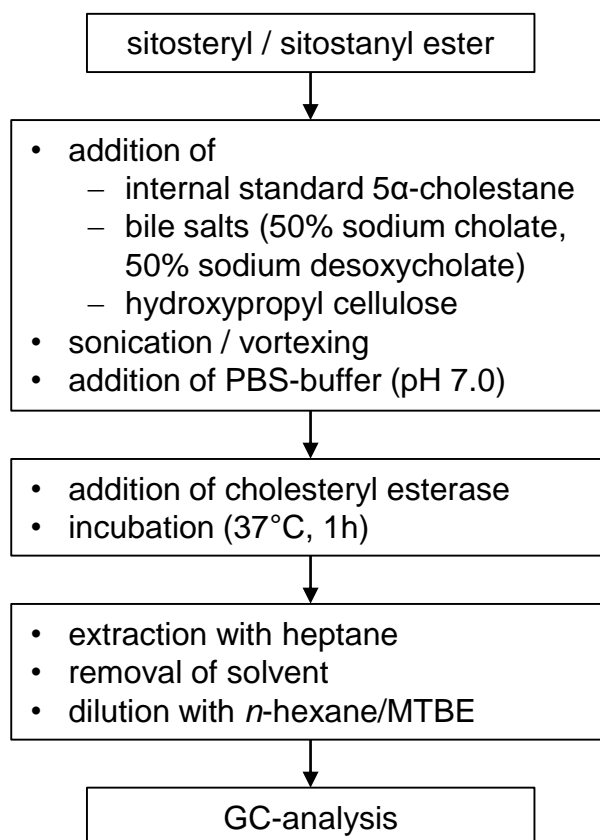


Figure 55: Procedure applied for the *in-vitro* hydrolyses.

The following elements of the employed procedure were adopted from the approach described by Julien-David *et al.* (2009) for the investigation of the extent of *in-vitro* hydrolyses by porcine cholesteryl esterase of 7-oxositosteryl oleate and sitosteryl 9,10-dihydroxystearate, as compared to cholesteryl oleate.

- Hydrolyses were performed in buffer solutions (pH 7). Dissolutions of ester and internal standard were supported by the addition of bile salts and hydroxypropyl cellulose solutions and by the application of vortexing and sonication.
- The same amount of cholesteryl esterase solution (corresponding to 3.2 µg enzyme per reaction) was used.
- Hydrolyses were performed under shaking for 1h at 37°C. Heptane was used for stopping the hydrolysis and for extracting remaining substrate and formed hydrolysis products.
- The conversions were determined by quantitations of the extracted amounts of liberated sterols/stanols via capillary gas chromatography.

The employed procedure differed from the approach described by Julien-David *et al.* (2009) in the following aspects:

- Instead of 19-hydroxycholesterol, in the present study 5 α -cholestane **IS₈** was used as internal standard. For quantification of the liberated stanols/sterols, relative GC-response factors were taken into account (for cholesterol and cholestanol: 1.1, sitosterol: 1.2, sitostanol: 1.3).
- Instead of sodium desoxycholate, a mixture of 50% sodium cholate and 50% desoxycholate was used as bile salts.

Substrates Used for Hydrolysis

In total, 22 representatives of the different classes of ACOPs determined upon thermo-oxidation of phytosteryl and phytostanyl oleates (Wocheslander *et al.*, 2017; Scholz *et al.*, 2019) were subjected to cholesteryl esterase-catalyzed *in-vitro* hydrolyses (Figure 56). In addition, the unaltered esters sitosteryl and sitostanyl oleate **43**, **3** as well as cholesteryl and cholestanyl oleate **37**, **38** were hydrolyzed under the same conditions. Prior to their use as substrates, the synthesized esters were purified via flash chromatography (Table 1).

Repeatability and reproducibility

Conversions were determined for cholesteryl oleate **37** and sitostanyl oleate **3**, and for the selected set of ACOP representatives listed in Table 16 in three independent hydrolysis experiments performed either on the same day or on three different days. Table 16 shows that apart from slightly higher confidence intervals observed for the results determined on three different days, the mean conversions were nearly identical. Considering these results, the triplicate hydrolysis experiments were subsequently performed on one day.

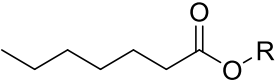
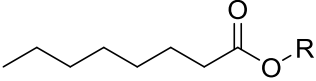
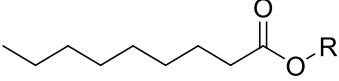
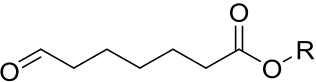
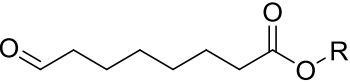
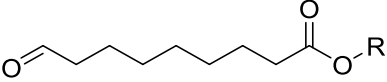
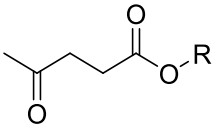
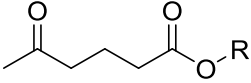
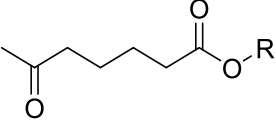
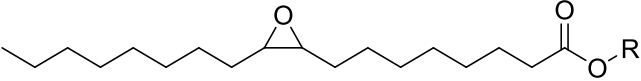
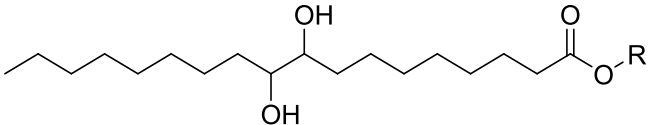
	R	
	sitosteryl	sitostanyl
aliphatic ACOPs		
	40	1
	41	2
	42	39
aldehyde-ACOPs		
	48	14
	50	16
	51	17
keto-ACOPs		
	46	11
	47	13
	49	15
epoxy-ACOP		
	45	10a
dihydroxy-ACOP		
	44	7

Figure 56: Structures of ACOPs subjected to *in-vitro* hydrolyses.

Table 16: Conversions (%) determined in triplicate experiments performed either on one or on three different days. Values represent means and confidence intervals.

no.	compound	conversion [%]	
		one day	three days
37	cholesteryl oleate	70 ± 20	69 ± 29
3	sitostanyl oleate	31 ± 5	32 ± 18
16	sitostanyl 8-oxooctanoate	34 ± 14	32 ± 22
13	sitostanyl 5-oxohexanoate	9 ± 1	8 ± 3
10a	sitostanyl <i>cis</i> -9,10-epoxystearate	3 ± 3	3 ± 3
2	sitostanyl octanoate	7 ± 7	8 ± 6
7a	sitostanyl 9,10-dihydroxystearate	3 ± 1	3 ± 1

Statistical evaluations were performed using several tests. The selection of the appropriate statistical test was based on the results of the Levene-test, which was used to evaluate variance homogeneity. As the values did not show variance homogeneity, Welch-ANOVA with Games-Howell post-hoc test was chosen for statistical evaluation of more than two values; the comparison of two values was conducted using the Welch-Test.

4.3.3 Hydrolysis of Unaltered Steryl/Stanyl Oleates

In the first step, the conversions (%) of various steryl/stanyl oleates with pancreatic cholesteryl esterase were investigated to assess the overall hydrolysis performance under the employed *in-vitro* hydrolysis conditions. For the hydrolysis of 50 µg (77 nmol) cholesteryl oleate **37**, the actual substrate for cholesteryl esterase, a mean conversion of 70 % was determined (Figure 57). The conversions determined for the same molar amounts of sitosteryl and cholestanyl oleate showed no statistical differences. Only for sitostanyl oleate **3**, the conversion (31 %) was statistically significantly lower than those determined for the other investigated esters.

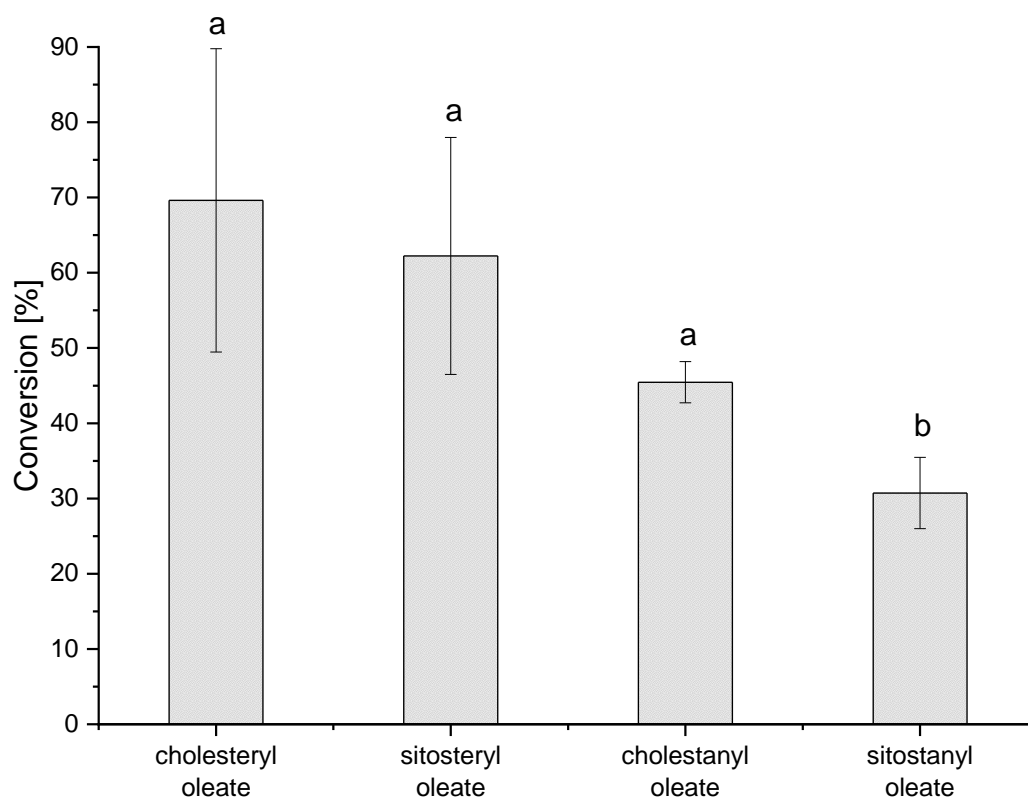


Figure 57: Conversions determined in PCE-catalyzed hydrolyses of different steryl and stanyl oleates (77 nmol). Values represent means of triplicate experiments and confidence intervals. Different letters indicate statistically significant differences (Games-Howell $p < 0.05$).

4.3.4 Hydrolysis of ACOPs Derived from Sitostanyl and Sitosteryl Oleate

A comparison of the conversions determined for the PCE-catalyzed *in-vitro* hydrolyses of sitostanyl oleate **3** and for the respective ACOPs is shown in Figure 58. The analogous data set, i.e. the comparison of the conversions determined for sitosteryl oleate **43** and the respective ACOPs is presented in Figure 59.

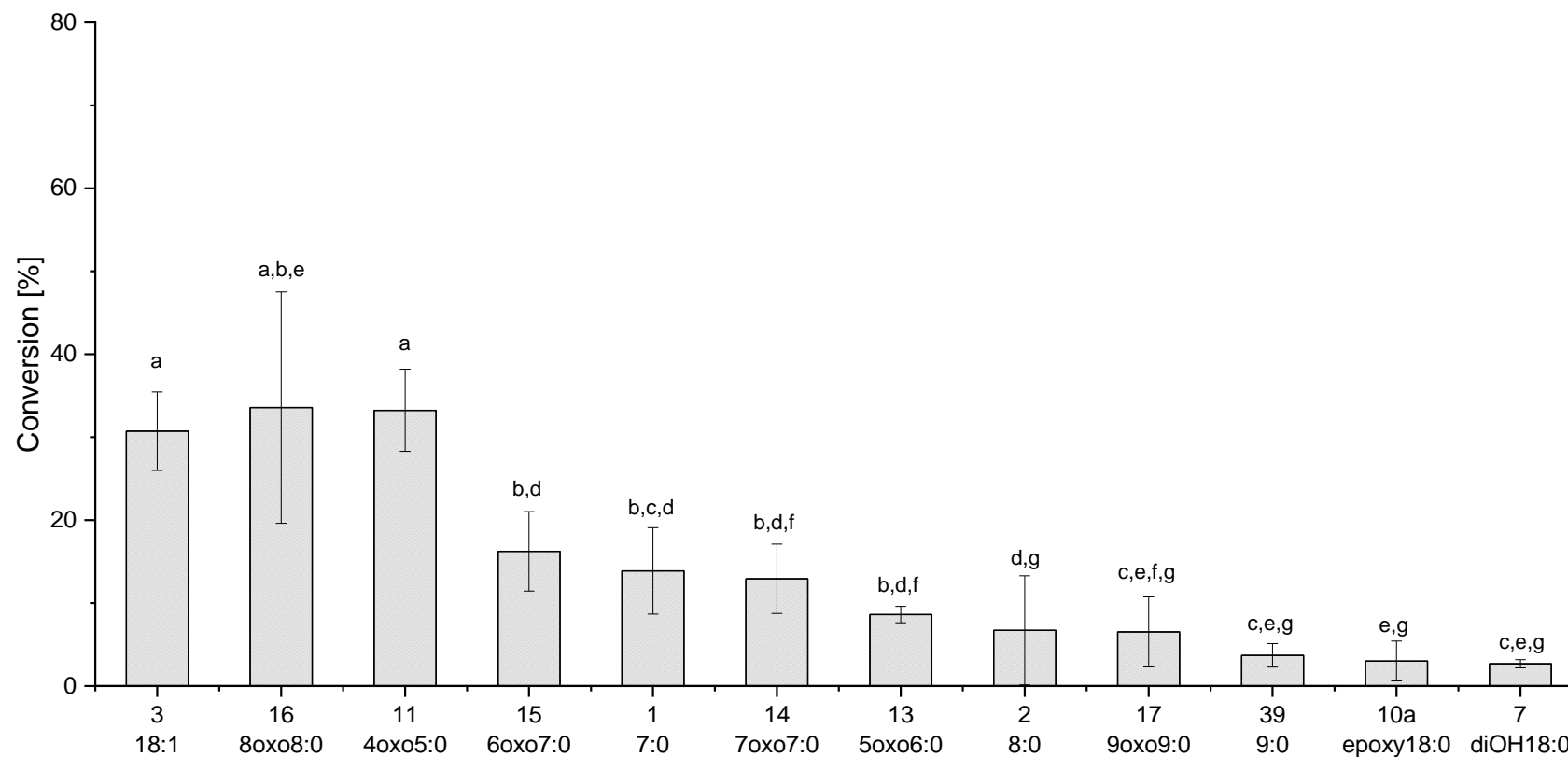


Figure 58: Conversions (%) of sitostanyl oleate **3** and respective ACOPs (77 nmol each) upon *in-vitro* PCE-catalyzed hydrolysis (1h). The substrate numbers and the abbreviations correspond to those in Table 17. The data were assessed by one-way ANOVA; different letters indicate statistically significant differences (Games-Howell test at $p < 0.05$). Values represent means of triplicate experiments and respective confidence intervals.

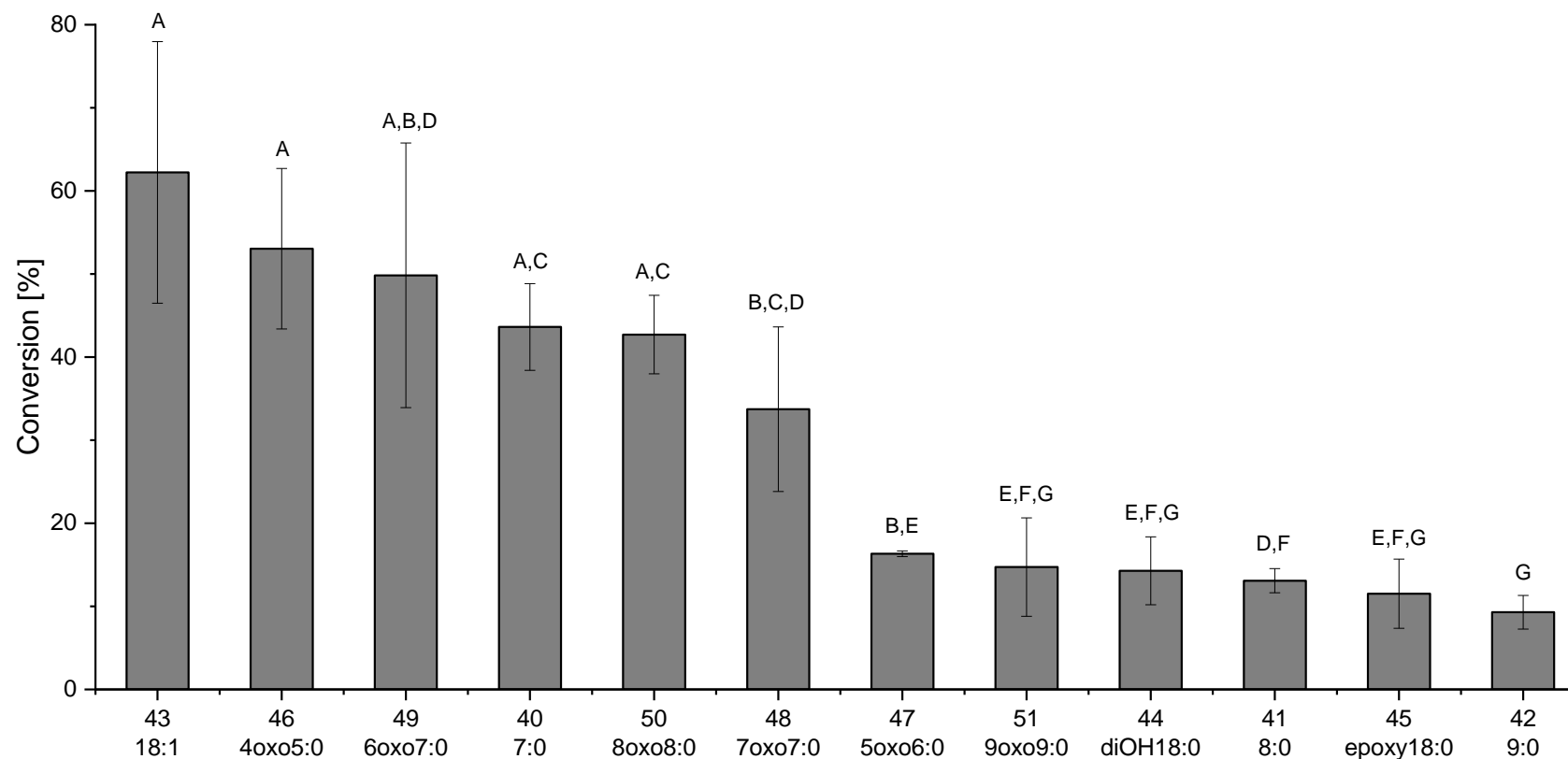


Figure 59: Conversions (%) of sitosteryl oleate **43** and respective ACOPs (77 nmol each) upon *in-vitro* PCE-catalyzed hydrolysis (1h). The substrate numbers and the abbreviations correspond to those in Table 17. The data were assessed by one-way ANOVA; different letters indicate statistically significant differences (Games-Howell test at $p < 0.05$). Values represent means of triplicate experiments and respective confidence intervals.

As shown in Figure 58, under the employed *in-vitro* hydrolysis conditions, only for two of the investigated ACOPs, i.e. sitostanyl 8-oxooctanoate **16** and sitostanyl 4-oxopentanoate **11**, no statistically significant differences in the conversions compared to the unaltered ester sitostanyl oleate **3** were observed. All other investigated ACOPs showed conversions that were significantly lower. Six of the ACOPs, i.e. sitostanyl 5-oxohexanoate **13**, octanoate **2**, 9-oxononanoate **17**, nonanoate **39**, *cis*-9,10-epoxystearate **10a**, and 9,10-dihydroxystearate **7**, exhibited particularly low conversions ranging only from 10 to 29% of the conversion determined for the unaltered ester. For three ACOPs, i.e. sitostanyl 6-oxoheptanoate **15**, heptanoate **1**, and 7-oxoheptanoate **14**, moderately lowered conversions ranging from 42% to 52% compared to sitostanyl oleate were observed. It is noteworthy that the long-chain ACOP sitostanyl *cis*-9,10-epoxystearate **10a** which is the quantitatively dominating ACOP formed upon heating of sitostanyl oleate exhibited a conversion of only 3%, corresponding to 10% of that of sitostanyl oleate. A similarly low conversion of 3% was determined for sitostanyl 9,10-dihydroxystearate **7a**.

A similar picture was observed regarding the conversions of sitosteryl oleate **43** and its respective ACOPs under the employed *in-vitro* hydrolysis conditions (Figure 59). Again, the analogous six ACOPs, i.e. sitosteryl 5-oxohexanoate **47**, 9-oxononanoate **51**, 9,10-dihydroxystearate **44**, octanoate **41**, *cis*-9,10-epoxystearate **45**, and nonanoate **42**, showed the lowest conversions corresponding to only 15 to 26% of the conversion of the unaltered sitosteryl oleate **43**. For sitosteryl 4-oxopentanoate **46** and sitosteryl 8-oxooctanoate **50**, the determined conversions were also not statistically significantly different to that of sitosteryl oleate **43**. In contrast to the data obtained for the sitostanyl ACOPs, the conversion of two further ACOPs, i.e. sitosteryl 6-oxoheptanoate **49** and heptanoate **40**, did not show statistically significant differences to that of sitosteryl oleate **43**. The remaining sitosteryl 7-oxoheptanoate **48** showed a moderately lowered conversion compared to sitosteryl oleate **43**. Again, it is noteworthy that sitosteryl *cis*-9,10-epoxystearate **45**, the long-chain epoxy-ACOP corresponding to the quantitatively dominating sitostanyl *cis*-9,10-epoxystearate **10a** formed upon thermooxidation from sitostanyl oleate **3**, showed one of the lowest conversions corresponding to only 19% of that of sitosteryl oleate **43**.

Table 17 provides a comparison of the observed conversions sorted according to the functional groups of the investigated ACOPs.

Table 17: Conversions (%) of sitostanyl oleate **3** and sitosteryl oleate **43** and their ACOPs (77 nmol each) upon PCE-catalyzed *in-vitro* hydrolysis. Values represent means of triplicate experiments and respective confidence intervals.

	no.	sitostanyl	conversion (%)			
			stat. ^a	no.	sitosteryl	stat. ^b
Intact ester						
oleate	3	31 ± 5	a	43	62 ± 16	A
Aliphatic ACOPs						
heptanoate	1	14 ± 5	b,c,d	40	44 ± 5	A,C
octanoate	2	7 ± 7	d,g	41	13 ± 1	D,F
nonanoate	39	4 ± 1	c,e,g	42	9 ± 2	G
Aldehyde-ACOPs						
7-oxoheptanoate	14	13 ± 4	b,d,f	48	34 ± 10	B,C,D
8-oxooctanoate	16	34 ± 14	a,b,e	50	43 ± 5	A,C
9-oxononanoate	17	7 ± 4	c,e,f,g	51	15 ± 6	E,F,G
Keto-ACOPs						
4-oxopentanoate	11	33 ± 5	a	46	53 ± 10	A
5-oxohexanoate	13	9 ± 1	b,d,f	47	16 ± 0.4	B,E
6-oxoheptanoate	15	16 ± 5	b,d	49	50 ± 16	A,B,D
Epoxy-ACOP						
<i>cis</i> -9,10-epoxystearate	10a	3 ± 2	e,g	45	12 ± 4	E,F,G
Dihydroxy-ACOP						
9,10-dihydroxystearate	7a	3 ± 1	c,e,g	44	14 ± 4	E,F,G

^a different letters indicate significant differences (Games-Howell test at $p < 0.05$) in the conversions within sitostanyl esters

^b different letters indicate significant differences (Games-Howell test at $p < 0.05$) in the conversions within sitosteryl esters

The conversions of the sitosteryl ACOPs were consistently higher than those determined for the corresponding sitostanyl ACOPs. This was in agreement with the higher conversion determined for sitosteryl oleate **43** compared to sitostanyl oleate **3**.

The conversions of the aliphatic ACOPs sitosteryl heptanoate **40**, octanoate **41** and nonanoate **42** were dependent on the chain lengths; the conversions significantly decreased from chain length C7 to C9. For the respective sitostanyl ACOPs **1**, **2** and **39** there was a similar trend; however, the differences were not statistically significant. Among the investigated aldehyde-ACOPs (chain lengths C7 to C9), the mid-chain representatives sitostanyl 8-oxooctanoate **16** and sitosteryl 8-oxooctanoate **50**, respectively, showed the highest conversions. The difference to other chain lengths was in most cases not significant.

Among the investigated keto-ACOPs (chain lengths C5 to C7), the mid-chain representatives sitostanyl 5-oxohexanoate **13** and sitosteryl 5-oxohexanoate **47**, respectively, showed the lowest conversions. However, differences in conversion within this groups were only significant for the short-chain representative sitostanyl 4-oxopentanoate **46**.

There was no significant difference observed between the conversions of the respective heptanoate, 7-oxoheptanoate, and 6-oxoheptanoate, despite having the same chain length but different functional groups.

The investigated polar, non-fragmented long-chain ACOPs, i.e. the *cis*-9,10-epoxystearates **10a**, **45** and the 9,10-dihydroxystearates **7a**, **44** all belonged to the least hydrolyzed ACOPs.

4.3.5 Influence of Cholesteryl Oleate on the Conversions of ACOPs

In food matrices it is likely that cholesteryl esters are present together with sitostanyl/sitosteryl esters. In order to investigate a potential impact of cholesteryl oleate **37** on the hydrolysis of ACOPs derived from sitostanyl or sitosteryl oleate, *in-vitro* hydrolysis experiments of sitostanyl/sitosteryl ACOPs were performed in the presence of an equimolar amount (77nmol) of cholesteryl oleate **37**.

4.3.5.1 *In-vitro* Hydrolyses of Stanyl ACOPs in the Presence of Cholesteryl Oleate

A comparison of the conversions determined for the PCE-catalyzed *in-vitro* hydrolyses of sitostanyl oleate **3** and for the respective ACOPs in the absence and in the presence of an equimolar amount of cholesteryl oleate **37** is shown in Figure 60.

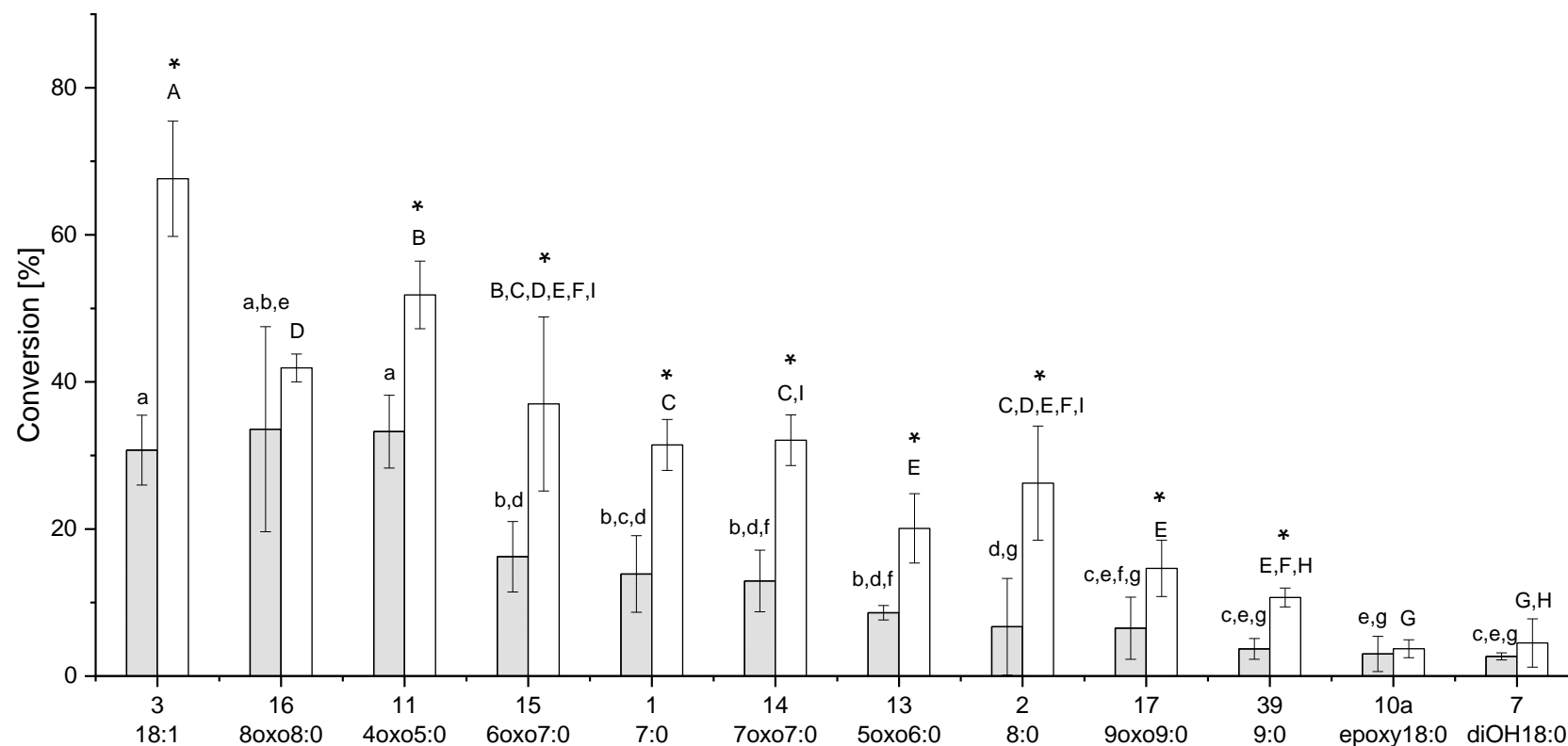


Figure 60: Conversions (%) of sitostanyl oleate **3** and its ACOPs (each 77nmol) upon PCE-catalyzed *in-vitro* hydrolysis. The grey bars represent sitostanyl esters in the absence of cholesteryl oleate **37**, the white bars represent sitostanyl esters in the presence of an equimolar amount of cholesteryl oleate **37**. The data were assessed by one-way ANOVA; different letters indicate significant differences (Games-Howell test at $p < 0.05$) in the conversions for the series of stanyl esters with and without addition of cholesteryl oleate **37**, respectively. The * indicate a significant difference (Welch-test at $p < 0.05$) at pairwise comparison of the conversions of the respective ACOP without/with added cholesteryl oleate. The peak numbers and the abbreviations correspond to those of Table 17. Values represent means of triplicate experiments and respective confidence intervals.

As shown in Figure 60, the addition of an equimolar amount of cholesteryl oleate (77nmol) resulted in a significant increase (factor 2.2) of the conversion of sitostanyl oleate **3** under the employed *in-vitro* hydrolysis conditions. Pairwise comparisons also showed statistically significantly increased conversions (on average factor 2.5) for eight of the eleven investigated ACOPs (indicated by asterices in Figure 60), in the presence of cholesteryl oleate. Upon addition of cholesteryl oleate, the conversions of all investigated ACOPs were statistically significantly lower than that of the unaltered sitostanyl oleate **3**. The addition of cholesteryl oleate had only a minor influence on the ranking of the ACOPs in terms of lowered conversion compared to sitostanyl oleate **3**. Sitostanyl *cis*-9,10-epoxystearate **10a** belonged to those ACOPs for which the addition of cholesteryl oleate did not result in a statistically significantly increased conversion compared to the experiment without added cholesteryl oleate. Consequentially, also upon addition of cholesteryl oleate, the conversion of this quantitatively dominating ACOP amounted to only 6% of that determined for sitostanyl oleate **3**.

Table 18 provides a comparison of the observed conversions in the absence or presence of cholesteryl oleate **37**, sorted according to the functional groups of the investigated ACOPs. Despite the statistically significant increases of the conversions observed for most of the ACOPs as a result of the addition of cholesteryl oleate to the hydrolysis mixture, there were no major changes in terms of differences and ranking of the conversions within the structurally related subgroups of ACOPs compared to the hydrolysis experiments without the presence of cholesteryl oleate.

Table 18: Conversion (%) of sitostanyl oleate **3** and its ACOPs (each 77nmol) upon PCE-catalyzed *in-vitro* hydrolyses with and without addition of an equimolar amount of cholesteryl oleate (CO) **37** to the hydrolysis mixtures. Values represent means of triplicate experiments and respective confidence intervals.

	no.	conversion (%)			
		without CO	stat. ^a	with CO	stat. ^b
Intact ester					
oleate	3	31 ± 5	a	68 ± 8	A
Aliphatic ACOPs					
heptanoate	1	14 ± 5	b,c,d	31 ± 3	C
octanoate	2	7 ± 7	d,g	26 ± 8	C,D,E,F,I
nonanoate	39	4 ± 1	c,e,g	11 ± 1	E,F,H
Aldehyde-ACOPs					
7-oxo heptanoate	14	13 ± 4	b,d,f	32 ± 3	C,I
8-oxo octanoate	16	34 ± 14	a,b,e	42 ± 2	D
9-oxo nonanoate	17	7 ± 4	c,e,f,g	15 ± 4	E
Keto-ACOPs					
4-oxo pentanoate	11	33 ± 5	a	52 ± 5	B
5-oxo hexanoate	13	9 ± 1	b,d,f	20 ± 5	E
6-oxo heptanoate	15	16 ± 5	b,d	37 ± 12	B,C,D,E,F,I
Epoxy-ACOP					
<i>cis</i> -9,10-epoxystearate	10a	3 ± 2	e,g	4 ± 1	G
Dihydroxy ACOP					
9,10-dihydroxystearate	7a	3 ± 1	c,e,g	5 ± 3	G,H

^a different letters indicate significant differences (Games-Howell test at p<0.05) in the conversions within the hydrolyses of sitostanyl esters without cholesteryl oleate

^b different letters indicate significant differences (Games-Howell test at p<0.05) in the conversions within the hydrolyses of sitostanyl esters with cholesteryl oleate

4.3.5.2 *In-vitro* Hydrolyses of Steryl ACOPs in the Absence/Presence of Cholesteryl Oleate

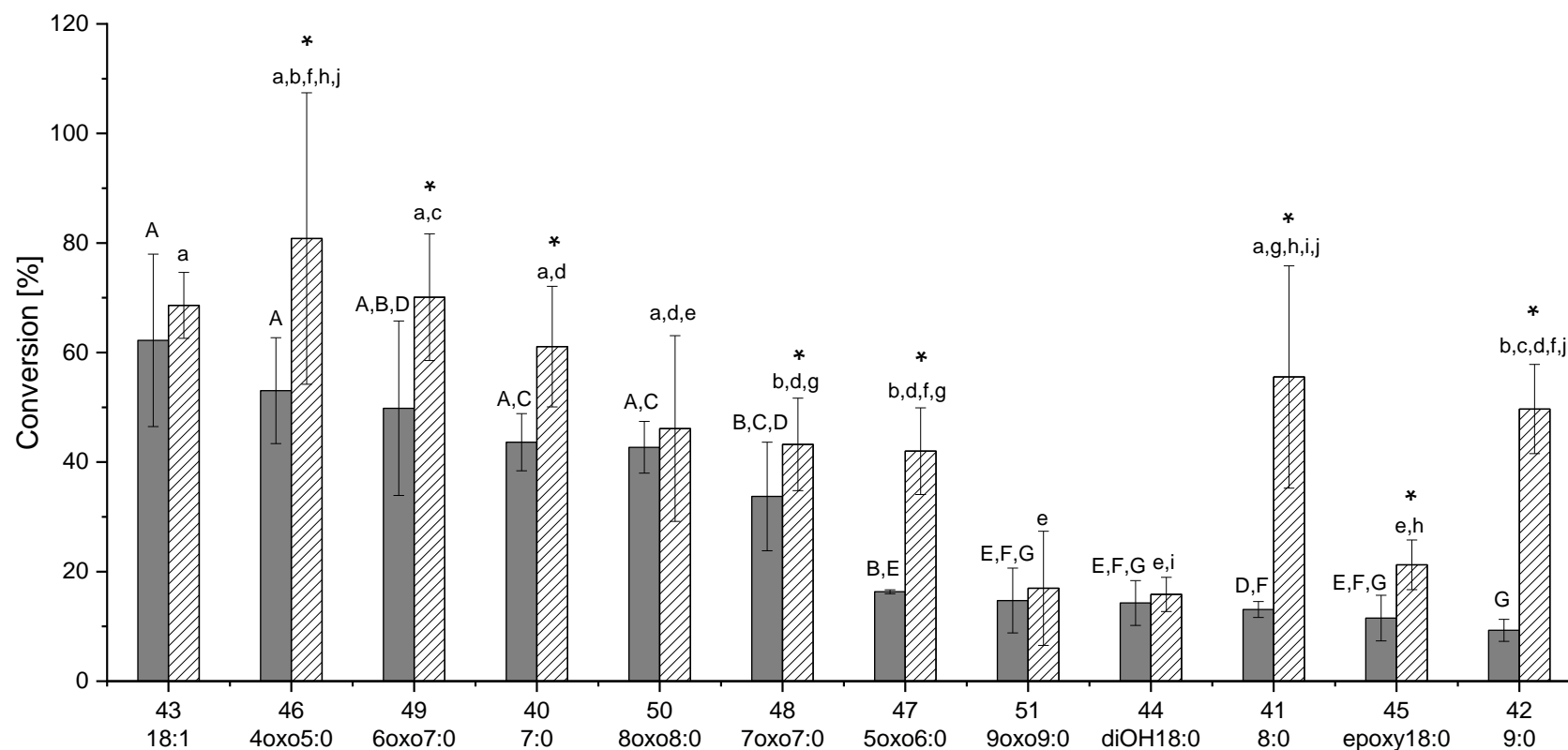


Figure 61: Conversions (%) of sitosteryl oleate **43** and its ACOPs (each 77nmol) upon PCE-catalyzed *in-vitro* hydrolysis. The black bars represent sitosteryl esters in the absence of cholesteryl oleate **37**, the shaded bars represent sitosteryl esters in the presence of an equimolar amount of cholesteryl oleate **37**. The data were assessed by one-way ANOVA; different letters indicate significant differences (Games-Howell test, $p < 0.05$) in the conversions for the series of steryl esters with and without addition of cholesteryl oleate **37**, respectively. The * indicate a significant difference (Welch-Test, $p < 0.05$) at pairwise comparison of conversions of the respective ACOP without/with added cholesteryl oleate. The peak numbers and the abbreviations correspond to those of Table 17. Values represent means of triplicate experiments and respective confidence intervals.

A comparison of the conversions determined for sitosteryl oleate **43** and the respective ACOPs in the absence and in the presence of an equimolar amount of cholesteryl oleate is presented in Figure 61.

In contrast to the results obtained for sitostanyl oleate **3**, there was no statistically significant difference in the conversions of sitosteryl oleate **43** depending on the absence or presence of cholesteryl oleate **37**. However, in agreement with the data obtained for ACOPs formed upon heating of sitostanyl oleate **3**, pairwise comparisons showed that there were statistically significant increases of the conversions upon addition of an equimolar amount of cholesteryl oleate for most of the eleven investigated ACOPs derived from sitosteryl oleate **43**. The pronounced increases of the conversions of sitosteryl octanoate **41** and sitosteryl nonanoate **42** upon addition of cholesteryl oleate to the hydrolysis mixtures resulted in different rankings in terms of conversion. The increases were particularly pronounced for the non-polar ACOPs sitosteryl octanoate **41** (factor 4.3) and sitosteryl nonanoate **42** (factor 5.5); as a result, the number of ACOPs for which the conversions showed no statistical difference to that of sitosteryl oleate **43** increased. The higher conversion in the presence of cholesteryl oleate **37** was not statistically significant for sitosteryl oleate **43**, sitosteryl 8-oxooctanoate **50**, sitosteryl 9-oxononanoate **51**, and sitosteryl 9,10-dihydroxystearate **44** regarding a pairwise comparison of the ester with or without added cholesteryl oleate.

Table 19 provides a comparison of the observed conversions in the absence or presence of cholesteryl oleate **37**, sorted according to the functional groups of the investigated ACOPs. There were no major changes in terms of differences and ranking of the conversions within the different structurally related subgroups of ACOPs compared to the hydrolysis experiments without the presence of cholesteryl oleate.

Table 19: Conversions (%) of sitosteryl oleate **43** and its ACOPs (each 77nmol) upon PCE-catalyzed *in-vitro* hydrolysis with and without addition of an equimolar amount of cholesteryl oleate (CO) **37** to the hydrolysis mixture. Values represent means of triplicate and respective confidence intervals.

	no.	conversion (%)			
		without CO	stat. ^a	with CO	stat. ^b
Intact ester					
oleate	43	62 ± 16	A	69 ± 6	a
Aliphatic ACOPs					
heptanoate	40	44 ± 5	A,C	61 ± 11	a,d
octanoate	41	13 ± 1	D,F	56 ± 20	a,g,h,i,j
nonanoate	42	9 ± 2	G	50 ± 8	b,c,d,f,j
Aldehyde-ACOPs					
7-oxoheptanoate	48	34 ± 10	B,C,D	43 ± 8	b,d,g
8-oxooctanoate	50	43 ± 5	A,C	46 ± 17	a,d,e
9-oxononanoate	51	15 ± 6	E,F,G	17 ± 10	e
Keto-ACOPs					
4-oxopentanoate	46	53 ± 10	A	81 ± 27	a,b,f,h,j
5-oxohexanoate	47	16 ± 1	B,E	42 ± 8	b,d,f,g
6-oxoheptanoate	49	50 ± 16	A,B,D	70 ± 12	a,c
Epoxy-ACOP					
<i>cis</i> -9,10-epoxystearate	45	12 ± 4	E,F,G	21 ± 5	e,h
Dihydroxy-ACOP					
9,10-dihydroxystearate	44	14 ± 4	E,F,G	16 ± 3	e,i

^a different letters indicate significant differences (Games-Howell test at $p < 0.05$) in the conversions within the hydrolyses of sitosteryl esters without cholesteryl oleate

^b different letters indicate significant differences (Games-Howell test at $p < 0.05$) in the conversions within the hydrolyses of sitosteryl esters with cholesteryl oleate

4.3.5.3 Additional Studies on the Influence of Cholesteryl Oleate on the Conversions of Sitostanyl Oleate and Respective ACOPs

In order to gain more information on the increases of the conversions of sitostanyl oleate and of most of the investigated respective ACOPs in the *in-vitro* hydrolyses in

the presence of cholesteryl oleate, additional experiments investigating the importance of the concentration of cholesteryl oleate and the potential role of the hydrolysis products of cholesteryl oleate, i.e. cholesterol and oleic acid, were performed.

Role of the Concentration of Cholesteryl Oleate in the Hydrolysis Mixture

Figure 62 shows the conversions of sitostanyl oleate **3** depending on the amount of cholesteryl oleate **37** added to the hydrolysis mixture. Already small amounts of cholesteryl oleate **37** had an effect on the conversion of sitostanyl oleate **3**. The conversion could only be increased to a maximum level; a plateau was reached after addition of 77 nmol cholesteryl oleate **37**.

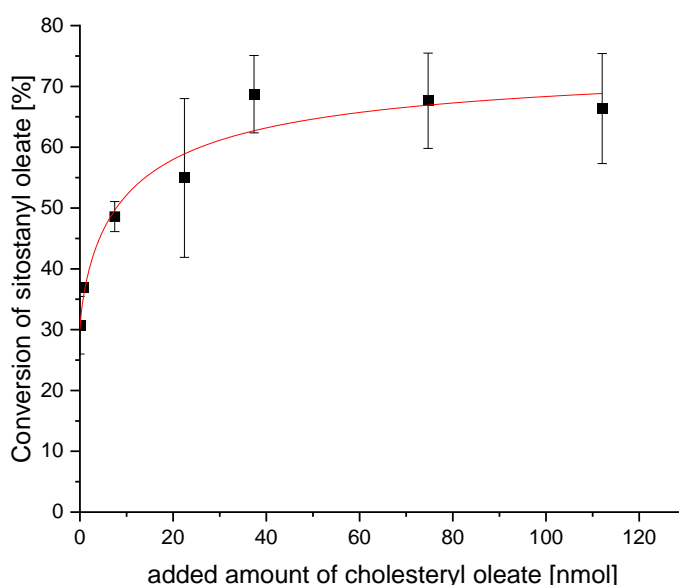


Figure 62: Conversion of sitostanyl oleate **3** depending on the amount of cholesteryl oleate **37** added to the hydrolysis mixture. Values represent means of triplicate experiments and respective confidence intervals.

Role of the Hydrolysis Products Oleic acid and Cholesterol

The data presented in Figure 64 showed that upon addition of cholesteryl oleate **37** to an *in-vitro* system containing sitostanyl oleate **3** as substrate, not only this sitostanyl ester but also the added cholesteryl ester will be hydrolyzed. In order to investigate the potential importance of the formed hydrolysis products oleic and cholesterol on the conversion of sitostanyl oleate **3**, they were added to a respective hydrolysis mixture. The added amounts of oleic acid and cholesterol, respectively, corresponded to the

amounts calculated based on the conversion of cholesteryl oleate **37** observed in the presence of sitostanyl oleate **3** (see section 4.3.6 and Table 4).

As shown in Figure 63, the addition of both oleic acid and cholesterol resulted in statistically significantly increased conversions of sitostanyl oleate **3** compared to the hydrolysis without their addition. The increases were lower than the increase in the conversion of sitostanyl oleate **3** upon addition of cholesteryl oleate **37** to the *in-vitro* system.

Analogous experiments were performed by addition of cholesteryl oleate **37** or its hydrolysis products oleic acid and cholesterol to PCE-catalyzed *in-vitro* hydrolyses of the ACOPs sitostanyl 7-oxoheptanoate **14**, sitostanyl heptanoate **1** and sitostanyl 5-oxohexanoate **15**. The added amounts of oleic acid and cholesterol, respectively, were calculated based on the conversions of cholesteryl oleate **37** observed in the presence of the three sitostanyl ACOPs **14**, **1** and **15** (see section 4.3.6 and Table 4).

As shown in Figure 63, for all three ACOPs the addition of oleic acid to the *in-vitro* hydrolysis did not result in increases of the conversion compared to the experiments without addition. For sitostanyl 7-oxoheptanoate **14** and sitostanyl 5-oxohexanoate **15**, the addition of both cholesterol and cholesteryl oleate **37** resulted in significant increases of the conversions of the ACOPs. For sitostanyl heptanoate **1**, the increase in conversion was also statistically significantly increased for both free cholesterol and cholesteryl oleate **37**, but more pronounced upon addition of the ester.

Another experiment showed that the addition of both sitosteryl oleate **3** and free sitosterol to the *in-vitro* system resulted in increases of the conversion of sitostanyl oleate **3** from 31% to 44% (addition of sitosterol) and 59% (addition of sitosteryl oleate **3**), respectively. Similarly, the addition of both cholestanyl oleate **38** and free cholestanol to the *in-vitro* system resulted in increases of the conversion of sitostanyl oleate **3** from 31% to 43% (for both the addition of cholestanyl oleate **38** and of cholestanol).

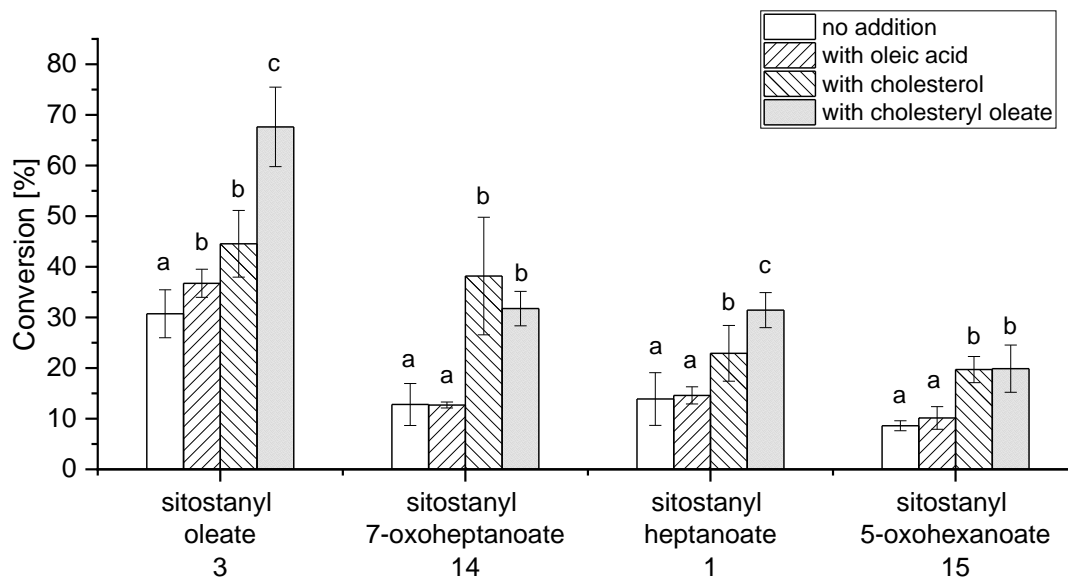


Figure 63: Conversions (%) of sitostanyl oleate **3**, sitostanyl 7-oxoheptanoate **14**, sitostanyl heptanoate **1** and sitostanyl 5-oxohexanoate **15** upon *in-vitro* PCE-catalyzed hydrolysis (1h) in the presence of either cholesteryl oleate or its hydrolysis products oleic acid and cholesterol, respectively. The data were assessed by one-way ANOVA; different letters indicate significant differences (Games-Howell test at $p < 0.05$) in the conversions for the series of different stanyl esters, respectively. Values represent means of triplicate experiments and respective confidence intervals.

4.3.6 Influence of ACOPs on the Conversion of Cholesteryl Oleate

In the previous chapter 4.3.5, the influence of the presence of an equimolar amount of cholesteryl oleate on the PCE-catalyzed *in-vitro* hydrolysis of ACOPs derived from sitostanyl oleate and sitosteryl oleate, respectively, has been investigated. The objective of the studies described in this chapter was to investigate the inverse influence of the presence of equimolar amounts of ACOPs derived from sitostanyl and sitosteryl oleate, respectively, on the conversion of cholesteryl oleate **37**.

A comparison of the conversion determined for the hydrolysis of cholesteryl oleate **37** (77nmol) under the employed *in-vitro* hydrolysis conditions with those determined in the presence of equimolar amounts of (i) intact steryl/stanyl oleates, (ii) sitostanyl ACOPs, and (iii) sitosteryl ACOPs is shown in Figure 64.

Statistical assessment of the data revealed that the addition of equimolar amounts of the investigated intact esters or the investigated ACOPs did not result in a statistically significantly changed conversion of cholesteryl oleate **37**.

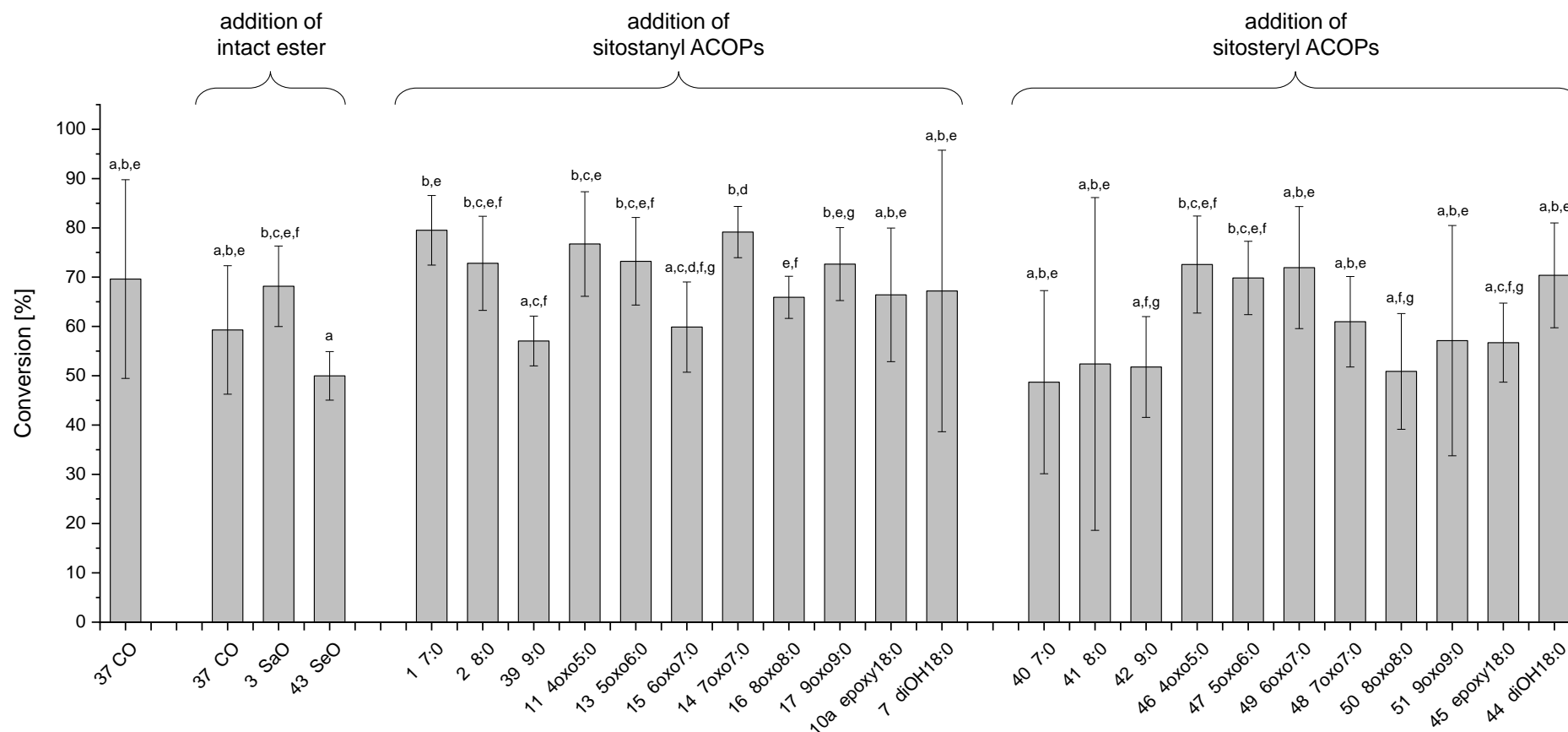


Figure 64: Conversions (%) of cholesteryl oleate **37** upon *in-vitro* PCE-catalyzed hydrolysis (1h) in the presence of equimolar amounts (77 nmol each) of (i) intact stanyl/steryl oleates, (ii) ACOPs derived from sitostanyl oleate, and (iii) ACOPs derived from sitosteryl oleate. The data were assessed by one-way ANOVA; different letters indicate significant differences (Games-Howell test at $p < 0.05$). Values represent means of triplicate experiments and respective confidence intervals.

To investigate whether the observed effect might be due to the increased molar amount of esters in the hydrolysis matrix rather than to the presence of another ester, one hydrolysis experiment was performed with the doubled amount of cholesteryl oleate **37** (154 nmol). The conversion determined for cholesteryl oleate **37** under these conditions was neither significantly different from the conversion of 77 nmol cholesteryl oleate **37** nor from the conversions in the experiments with cholesteryl oleate **37** mixed with any other ACOP.

4.3.6.1 Impact of the *In-vitro* Hydrolysis Conditions on the Conversion of Cholesteryl Oleate in the Absence/Presence of Sitosteryl 9,10-Dihydroxystearate

Sitosteryl 9,10-dihydroxystearate **44** has been reported to act as non-competitive inhibitor of the hydrolysis of cholesteryl oleate **37** (Julien-David *et al.*, 2009). Under the *in-vitro* hydrolysis conditions applied in this thesis, no statistically significant difference between the PCE-catalyzed conversions of cholesteryl oleate in the absence or presence of sitosteryl 9,10-dihydroxystearate was observed (Figure 64). The conditions differed from the experimental setting of Julien-David *et al.* (2009) in the use of another internal standard (5 α -cholestane **IS₈** vs. 19-hydroxycholesterol **IS₉**) and the replacement of sodium desoxycholate by a mixture containing 50% sodium cholate and 50% desoxycholate. In a comparative experiment, the potential impact of these differences on the conversion of cholesteryl oleate in the absence or presence of the sitosteryl ACOP was investigated. The highest amount (105 nmol) of sitosteryl 9,10-dihydroxystearate **44** added by Julien-David *et al.* (2009) was used rather than an amount equimolar to cholesteryl oleate (77 nmol). Four combinations of internal standard and bile salts were investigated; the obtained results are presented in Figure 65.

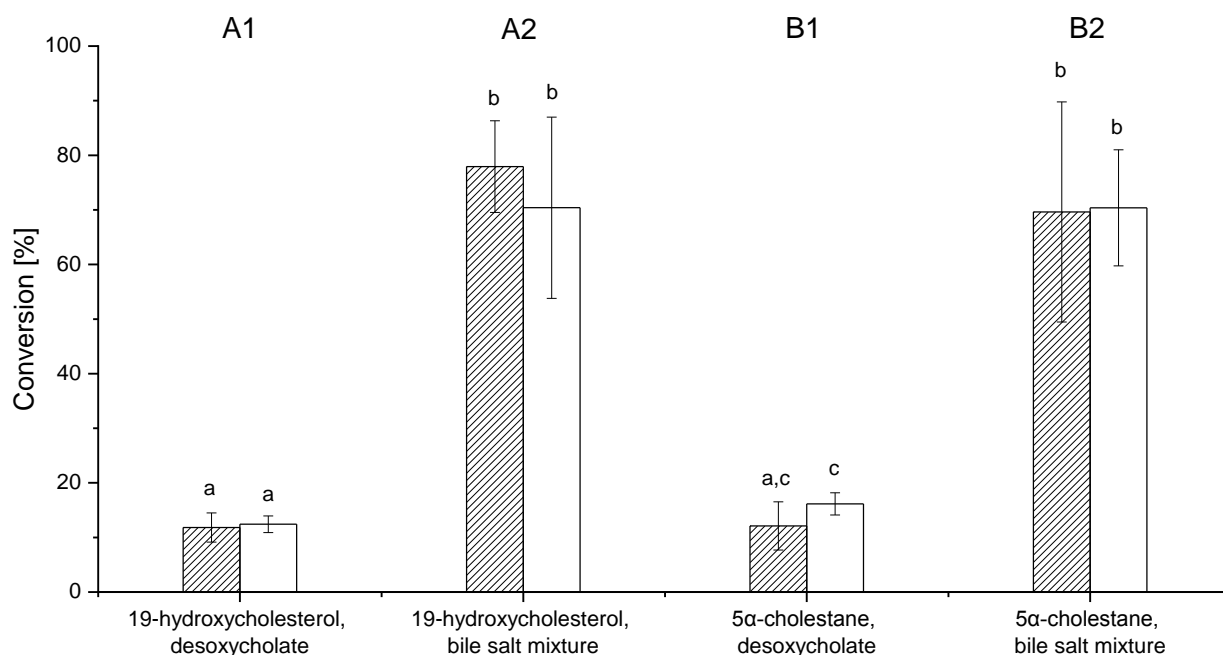


Figure 65: Conversions (%) of 77 nmol cholesteryl oleate **37** without addition of sitosteryl 9,10-dihydroxystearate **44** (shaded bars) or with addition of 105 nmol sitosteryl 9,10-dihydroxystearate **44** (white bars) to the hydrolysis mixture. Experiments were performed using (A) 19-hydroxycholesterol **IS₉** or (B) 5α-cholestane **IS₈** as internal standard, and sodium desoxycholate (A1, B1) or a bile salt mixture (A2, B2). The data were assessed by one-way ANOVA; different letters indicate significant differences (Games-Howell test at $p < 0.05$). Values represent means of triplicate experiments and respective confidence intervals.

The data demonstrated that the difference regarding the internal standard used had only a marginal impact on the quantitations. The amounts of liberated cholesterol determined with the bile salt mixture (A2, B2) were not significantly different depending on the internal standard. With sodium desoxycholate (A1, B1), only upon addition of sitosteryl 9,10-dihydroxystearate **44** a slightly higher amount of cholesterol was quantitated with 5α-cholestane **IS₈** than with 19-hydroxycholesterol **IS₉**.

The results obtained for the different bile salts confirmed their essential roles regarding the activity of pancreatic cholesteryl esterase. Upon use of the bile salt mixture (A2, B2), the amounts of liberated cholesterol increased significantly compared to the use of sodium desoxycholate only (A1, B1). However, the important result regarding the question to be answered in these experiments, was the fact that with the bile salt

mixture (A2, B2) no significant differences in the conversions of cholesteryl oleate **37** in the absence or presence of sitosteryl 9,10-dihydroxystearate **44** were observed and that with sodium desoxycholate (A1, B1) only the quantification with 5 α -cholestane **IS₈** showed a slight increase of the liberated amount of cholesterol in the presence of sitosteryl 9,10-dihydroxystearate **44**.

4.3.7 Discussion

Methodology

As described in section 4.3.2, several elements of the hydrolysis procedure were adopted from the study of Julien-David *et al.* (2009). The experiments were performed with 77 nmol ester which corresponds to the lowest amount employed by Julien-David *et al.* (2009) in their experiments with cholesteryl oleate as substrate. In order to facilitate a molar-based comparison of the results obtained for the spectrum of investigated ACOPs, ranging from short-chain to long-chain representatives, for all substrates equimolar amounts were used.

The experimental set-up was modified by using 5 α -cholestane **IS₈** rather than 19-hydroxycholesterol **IS₉** as internal standard. 5 α -Cholestane **IS₈** has been previously employed in hydrolysis studies of stanyl-/steryl esters (Brown *et al.*, 2010; Gleize *et al.*, 2016) and was considered useful for the quantitation of the liberated non-oxidized sterols/stanols. In addition, sodium desoxycholate was replaced by a bile salt mixture containing sodium cholate and sodium desoxycholate. This mixture was considered more appropriate regarding the *in-vivo* situation, as the main bile salts in humans are sodium cholate and sodium chenodesoxycholate (Carulli *et al.*, 2000; Guzior and Quinn, 2021). The influence of bile acids on cholesteryl esterase activity has been described (Swell *et al.*, 1953; Vahouny *et al.*, 1965; Jacobson *et al.*, 1990). Conjugation of cholate to taurocholate or glycocholate has an influence as well as the number of hydroxy groups in the bile salt. The activity of cholesteryl esterase decreases with decreasing number of hydroxy groups: cholate (three groups) > desoxycholate (two groups) > lithocholate (one group) > dehydrocholate (no hydroxy group). The results of the comparative experiments regarding hydrolyses of cholesteryl oleate **37** in the absence or presence of sitosteryl 9,10-dihydroxystearate **44** performed with different combinations of standards and bile salts (section 4.3.6.1) demonstrated that the choice

of the standard only marginally influenced the quantitated amounts of sterol whereas the replacement of desoxycholate by the bile salt mixture resulted in significant increases of the liberated amounts of sterol. The higher conversion with the bile salt mixture is consistent with the previously reported impact of the number of hydroxy groups in the employed bile salts. This also explains that Julien-David *et al.* (2009) found almost no hydrolysis for sitosteryl 9,10-dihydroxystearate **44**, whereas in this thesis a conversion of 14 % was observed.

Conversions of Unaltered Esters

There is some variation in the results reported for *in-vitro* hydrolyses of cholesteryl oleate **37** and sitosteryl oleate **43** (Swell *et al.*, 1954; Julien-David *et al.*, 2009; Brown *et al.*, 2010). However, it is notable that the conversions observed for these oxidatively unaltered esters under the *in-vitro* conditions applied in this thesis were consistently higher than those previously reported. The lower conversions described by Brown *et al.* (2010) may be explained by the significantly lower duration of hydrolysis (8 min.) compared to 1 h applied in this thesis. The different results obtained by Julien-David *et al.* (2009) are due to the influence of the employed bile salts, as discussed above. In the study of Swell *et al.* (1954) the hydrolysis conditions differed in several aspects to those of this thesis, e.g. the use of hog pancreas homogenate instead of cholesteryl esterase.

Stanyl oleate was less hydrolyzed than steryl oleate under the applied conditions. This is in agreement with the lower conversion reported for cholestanyl butyrate compared to cholesteryl butyrate (Swell *et al.*, 1954). Comparative data reported for hydrolyses of sitosteryl oleate **43** and sitostanyl oleate **3** are inconsistent as to which ester is hydrolyzed more efficiently (Moreau and Hicks, 2004; Brown *et al.*, 2010; Gleize *et al.*, 2016).

Conversions of ACOPs

The fact that all investigated sitosteryl and sitostanyl ACOPs were hydrolyzed, at least to a certain extent, by pancreatic cholesteryl esterase is in agreement with the wide substrate specificity reported for this enzyme (Hui, 1996).

Under the applied hydrolysis conditions, except for sitostanyl 8-oxooctanoate **16** and sitostanyl 4-oxopentanoate **11**, the conversions observed for all other investigated sitostanyl ACOPs were significantly lower than those of the oxidatively unaltered

sitostanyl oleate **3**. Similar results were obtained for the analogous sitosteryl ACOPs. The conversions of sitosteryl ACOPs were higher than those of the respective sitostanyl ACOPs; however, also in this series seven of the eleven investigated sitosteryl ACOPs showed conversions that were significantly lower than that determined for the unaltered sitosteryl oleate.

It was not possible to establish clear correlations between the conversions and the structural characteristics of ACOPs. Studies with short- and long-chain aliphatic cholesteryl esters showed that PCE-catalyzed hydrolysis of cholesteryl oleate **37** resulted in a lower release of cholesterol than hydrolysis of cholesteryl acetate, cholesteryl propionate, and cholesteryl butyrate (Swell and Treadwell, 1955). Sgoutas (1971) determined the amounts of cholesterol liberated by hydrolysis of aliphatic cholesteryl esters with fatty acid chains from C2 to C20 with rat liver homogenate containing cholesterol esterase and did not find a general dependence of released cholesterol on the chain length. For the chain lengths C7, C8, and C9, they reported the highest release of cholesterol for cholesteryl nonanoate followed by octanoate and heptanoate. For the respective sitostanyl and sitosteryl esters investigated in this thesis, this dependence of the conversion on the chain length was reversed. In a study by Gleize *et al.* (2016), a mixture containing medium-chain phytosteryl/stanyl esters (main component: sitosteryl octanoate, 46%) showed a higher hydrolysis rate than a mixture containing long-chain phytosteryl/stanyl esters (main component: sitosteryl oleate, 53%). In the *in-vitro* hydrolyses performed in this thesis, both sitosteryl and sitostanyl octanoate showed significantly lower conversions than sitosteryl and sitostanyl oleate, respectively.

Cholesteryl oleate was added to the hydrolysis mixtures in order to mimick the potential simultaneous intake of phytosteryl/-stanyl fatty acids and cholesteryl esters via the diet. For the majority of the investigated sitostanyl and sitosteryl ACOPs, the addition of an equimolar amount of cholesteryl oleate resulted in significantly increased conversions. The addition of equimolar amounts of sitosteryl and cholestanyl oleate, respectively, also resulted in increased conversions of sitostanyl oleate.

For sitostanyl oleate, the increased conversion was shown to be dependent on the amount of added cholesteryl oleate. Considering that cholesteryl oleate added to the hydrolysis mixture is also subjected to PCE-catalyzed hydrolysis, the impact of the

resulting hydrolysis products cholesterol and oleic acid was investigated. The addition of oleic acid resulted in a slight improvement of the conversion of sitostanyl oleate, whereas no influence on the conversions of ACOPs was observed. The addition of cholesterol resulted in a significantly higher conversion for all investigated substrates. For sitostanyl oleate **3**, additionally an improvement of the conversion was found upon addition of sitosterol or cholestanol. Brown *et al.* (2010) demonstrated that phytosterols had no significant influence on the conversion of cholesteryl oleate **37**. They also found no significant difference by adding moderate amounts of oleic acid and a slight improvement of conversion by adding a very high amount of oleic acid.

The mechanisms underlying the observed increases of the conversions upon addition of cholesteryl oleate to the hydrolysis mixtures were not further investigated. They may be related to better solubility, bile-like properties of sterols/stanols or activation of cholesteryl esterase. The overall conclusion to be drawn from the performed experiments is that the addition of cholesteryl oleate had no major impact on the ranking of the ACOPs regarding the lowered conversion compared to sitostanyl and sitosteryl oleate, respectively.

Impact of ACOPs on the Conversion of Cholesteryl Oleate

Under the applied conditions, the presence of equimolar amounts of sitosteryl and sitostanyl ACOPs, respectively, in the hydrolysis mixtures did not result in statistically significant changes of the conversion of cholesteryl oleate.

For sitosteryl 9,10-dihydroxystearate **44**, this result seemed to be in contradiction to the data reported by Julien-David *et al.* (2009) who identified this ACOP as non-competitive inhibitor of the hydrolysis of cholesteryl oleate and sitosteryl oleate. The hydrolysis conditions applied in this thesis differed from those applied by Julien-David *et al.* (2009) regarding the use of 5 α -cholestane **IS₈** rather than 19-hydroxycholesterol **IS₉** as internal standard and the replacement of sodium desoxycholate by a bile salt mixture containing sodium cholate and sodium desoxycholate. A series of experiments with different combinations of internal standards and bile salts demonstrated that independent of the used combination the conversion of cholesteryl oleate **37** in the presence of an equimolar amount of sitosteryl 9,10-dihydroxystearate **44** was not statistically significantly different from the conversion determined in the absence of this sitosteryl ACOP.

The data also showed that owing to the use of the bile salt mixture the conversions of the substrates in the hydrolyses were significantly higher than those observed by Julien-David *et al.* (2009). That means, the prerequisites for elaboration of kinetic data as performed by Julien-David *et al.* (2009) were not fulfilled. The results obtained under the conditions employed cannot be used to draw conclusions on the potential role of sitosteryl 9,10-dihydroxystearate **44** as competitive inhibitor.

Impact of ACOPs on the Cholesterol-Lowering Effect

Hydrolysis of phytosteryl/-stanyl esters and liberation of the free sterols/stanols is a prerequisite for their competition with cholesterol regarding the incorporation into mixed micelles which is considered as one of the processes contributing to the cholesterol-lowering effect of phytosteryl/-stanyl esters. The UHPLC-MS/MS-based study by Scholz *et al.* (2019) and the GC-based study on long-chain ACOPs described in chapter 4.2 demonstrated that sitostanyl *cis*-9,10-epoxystearate **10a** is the quantitatively dominating ACOP formed upon heating of sitostanyl oleate. For heat-treated sitosteryl oleate, the quantitative preponderance of the analogous sitosteryl *cis*-9,10-epoxystearate **45** may also be anticipated. Both, sitostanyl and sitosteryl *cis*-9,10-epoxystearate **10a**, **45** were among those ACOPs exhibiting the lowest conversions (3% and 12%, respectively) compared to those of sitostanyl and sitosteryl oleate **3**, **43** (31% and 62%, respectively). Thus, the conversions of these main ACOPs and consequentially the amounts of liberated sitostanol and sitosterol available for competition with cholesterol for incorporation into mixed micells constitute only 10% and 19%, respectively, of those of the unaltered sitostanyl and sitosteryl oleate **3**, **43**. It may therefore be hypothesized that the consumption of a food enriched with phytosteryl/-stanyl fatty acid esters which has undergone thermal processing results in a lower cholesterol-lowering effect than the consumption of the unprocessed enriched food. This hypothesis is supported by the studies performed by Scholz *et al.* (2017) on thermooxidized phytosteryl/-stanyl fatty acid esters demonstrating a loss of efficacy to inhibit cholesterol micellarization *in-vitro* due to the thermally induced losses of intact esters.

4.3.8 Summary

Two series of ACOPs derived from sitostanyl and sitosteryl oleate, respectively, were subjected to *in-vitro* hydrolyses by pancreatic cholesterol esterase. For both, sitostanyl and sitosteryl ACOPs, eleven representatives of different classes of oxidation products including (i) short-chain ACOPs with oxo, aldehyde, or aliphatic groups and (ii) long-chain ACOPs with epoxy and hydroxy groups were synthesized and used as substrates.

For nine of the investigated sitostanyl ACOPs and for seven of the sitosteryl ACOPs, the conversions determined under the applied hydrolysis conditions were significantly lower than those of the oxidatively unaltered sitostanyl oleate and sitosteryl oleate, respectively. The sitosteryl esters showed consistently higher conversions than the respective sitostanyl esters. No clear dependencies of the conversions on chain lengths within the different classes of ACOPs were observed. Remarkably, the conversion of sitostanyl *cis*-9,10-epoxystearate **10a**, one of the quantitatively dominating long-chain ACOPs formed upon thermo-oxidation of sitostanyl oleate, exhibited a conversion corresponding to only 10% of that of sitostanyl oleate. Similarly, sitosteryl *cis*-9,10-epoxystearate **45** showed a conversion corresponding to only 19% of that of sitosteryl oleate.

The addition of equimolar amounts of cholesteryl oleate to the hydrolysis mixtures resulted in statistically significant increases of the conversions for sitostanyl oleate and for most of the sitostanyl and sitosteryl ACOPs. For sitostanyl oleate, the impact of cholesteryl oleate on the conversion was shown to be concentration-dependent. The presence of cholesterol, one of the hydrolysis products of cholesteryl oleate, also enhanced the conversions of sitostanyl oleate and sitostanyl ACOPs, whereas oleic acid only had a minor impact.

The presence of equimolar amounts of sitostanyl and sitosteryl ACOPs, respectively, in the hydrolysis mixtures had no statistically significant impact on the conversion of cholesteryl oleate. Experiments performed in the absence and presence of sitosteryl 9,10-dihydroxystearate **44** confirmed the importance of the bile acids used for the conversions observed in *in-vitro* hydrolyses, but also showed that there was no impact of this ACOP on the conversion of cholesteryl oleate **37**.

5. SUMMARY

An increased plasma low-density lipoprotein (LDL)-cholesterol level is a recognized risk factor for the development of cardiovascular diseases. The consumption of phytosterols/-stanols and their fatty acid esters has been implemented as approach to reduce LDL-cholesterol levels. Like other lipophilic constituents, they are expected to be subject to oxidations during processing or storage. There has been extensive research on products resulting from thermo-oxidation of free sterols/stanols or steryl/stanyl moieties in fatty acid esters and on oxidations of unsaturated fatty acid moieties in fats and oils. However, studies on the formation of acyl chain oxidation products (ACOPs) resulting from thermo-oxidation of the unsaturated fatty acid moieties of phytosteryl/-stanyl esters are scarce. The studies underlying this thesis aimed to elaborate data on the identification and the formation of ACOPs derived from sitostanyl oleate and on the conversions of these ACOPs in the course of *in-vitro* enzyme-catalyzed hydrolyses.

In the first part, twenty commercially not available authentic reference compounds of ACOPs anticipated as thermo-oxidation products of sitostanyl oleate were synthesized. Short- and medium-chain ACOPs (C5 to C11), resulting from oxidative fragmentations of the oleic acid moiety, comprised non-polar ACOPs and oxidation products with aldehyde-, keto- or hydroxy-groups in the shortened acid chains. In addition, sitostanyl ACOPs with keto-, hydroxy-, dihydroxy- and epoxy-groups in the unfragmented acid chain were synthesized. Either the respective oxidized fatty acids were synthesized and esterified with sitostanol or sitostanyl esters were directly subjected to oxidative modifications. Together with four synthesized cholestanyl esters, representing the different classes of ACOPs, these substances were provided as references and standards, respectively, for a UHPLC-MS/MS-based analysis of ACOPs formed upon thermo-oxidation of sitostanyl oleate.

In the second part, an approach for the GC-based analysis of long-chain ACOPs formed upon heat-treatment of sitostanyl oleate was established. The methodology comprised (i) solid-phase extraction to separate the polar long-chain ACOPs from unaltered sitostanyl oleate, (ii) transesterification of the ACOPs, and (iii) GC-analysis of the resulting methyl esters. For assignments, GC and mass spectral data were compared to those of synthesized reference compounds. Upon heating of sitostanyl oleate (180°C, 60 min.), methyl *trans*- and *cis*-9,10-epoxystearate were the main oxidation products detected, followed by the pair methyl 8/11-hydroxyoctadec-9-

enoate and methyl oxooctadecenoate. The pair methyl 10-hydroxyoctadec-8-enoate/9-hydroxyoctadec-10-enoate and methyl 9,10-dihydroxystearate were present in lower amounts. The method was applied to follow the formation of these long-chain ACOPs depending on the temperature (120°C - 200°C, 30 min.) and on the heating duration (15 min. - 180 min.; 180°C, 200°C). Only methyl *trans*-9,10-epoxystearate showed a consistent increase with increasing temperature. The amounts of the other ACOPs only increased up to 170°C/180°C; they showed concentration maxima after 30 or 60 min. of heat treatment at 180°C and 200°C, respectively. Heating of sitostanyl oleate, methyl oleate, monoolein and triolein showed the influence of the esterified moiety on total amounts and proportions of individual ACOPs formed from these oleates.

Intestinal hydrolysis and liberation of the free sterols/stanols is an essential step for phytosteryl/-stanyl fatty acid esters to exert their cholesterol-lowering effects. Therefore, in the final part, series of synthesized sitostanyl and sitosteryl ACOPs from different classes were subjected to *in-vitro* hydrolyses catalyzed by porcine cholesteryl esterase. For both, sitostanyl and sitosteryl ACOPs, eleven representatives of (i) short-chain ACOPs with oxo, aldehyde, or aliphatic groups and (ii) long-chain ACOPs with epoxy and hydroxy groups were synthesized and used as substrates. For nine of the sitostanyl ACOPs and for seven of the sitosteryl ACOPs, the determined conversions were significantly lower than those of the oxidatively unaltered sitostanyl oleate and sitosteryl oleate, respectively. In particular, the conversion of sitostanyl *cis*-9,10-epoxystearate, one of the quantitatively dominating ACOPs formed upon thermo-oxidation of sitostanyl oleate, exhibited a conversion corresponding to only 10% of that of sitostanyl oleate. Sitosteryl esters showed consistently higher conversions than the respective sitostanyl esters. However, also within this series of ACOPs, sitosteryl *cis*-9,10 epoxystearate showed one of the lowest conversions corresponding to only 19% of that of sitosteryl oleate. No clear dependencies of the conversions on chain lengths within the different classes of ACOPs were observed. The addition of equimolar amounts of cholesteryl oleate to the hydrolysis mixtures resulted in statistically significant increases of the conversions of sitostanyl oleate and most of the sitostanyl and sitosteryl ACOPs. The presence of cholesterol, one of the hydrolysis products of cholesteryl oleate, also enhanced the conversions of sitostanyl oleate and sitostanyl ACOPs, whereas oleic acid only had a minor impact. The presence of equimolar amounts of sitostanyl and sitosteryl ACOPs, respectively, in the hydrolysis mixtures

had no statistically significant impact on the conversion of cholesteryl oleate. Further experiments confirmed the importance of the bile acids used for the conversions observed in *in-vitro* hydrolyses.

The generated data extend the knowledge particularly on the formation of long-chain ACOPs; however, the analytic studies were limited to the model substance sitostanyl oleate. Future studies should cover the formation of ACOPs from the broader spectrum of phytosteryl/-stanyl fatty acid esters used for addition to foods. Ultimately, the investigations should be extended from the pure substances/mixtures to the enriched food matrices. This will, of course, pose new challenges in terms of reference compounds, sample preparations and analytical approaches. The fact that the quantitatively dominating ACOPs formed upon thermo-oxidation of sitostanyl oleate showed the lowest conversion rates in the employed *in-vitro* hydrolyses emphasizes the need for further research on the potential impact of oxidative changes of phytosteryl/-stanyl fatty acid esters during processing on their cholesterol-lowering properties. Ongoing improvements and standardizations of protocols used for bioavailability/bioaccessibility studies of steryl/-stanyl fatty acid esters might be helpful in that respect.

6. ZUSAMMENFASSUNG

Ein erhöhter LDL (Low-Density-Lipoprotein)-Cholesterolspiegel im Blutplasma ist ein anerkannter Risikofaktor für die Entstehung von Herz-Kreislauf-Erkrankungen. Der Verzehr von Phytosterolen/-stanolen oder deren Fettsäureestern ist eine Möglichkeit den LDL-Cholesterolspiegel zu senken. Wie bei anderen lipophilen Nahrungsbestandteilen ist davon auszugehen, dass sie während der Verarbeitung oder Lagerung oxidiert werden können. Es gibt umfangreiche Forschungsarbeiten zu Oxidationsprodukten, die aus freien Sterolen/Stanolten oder dem Steryl-/Stanyl-Anteil in Fettsäureestern sowie aus ungesättigten Fettsäureresten in Fetten und Ölen entstehen. Es gibt jedoch kaum Studien über die Bildung von Oxidationsprodukten, die aus der Thermooxidation ungesättigter Fettsäurereste von Phytosteryl/-stanylestern resultieren. Die im Rahmen dieser Arbeit durchgeführten Untersuchungen hatten das Ziel, Daten zur Identifizierung und Bildung dieser Oxidationsprodukte, sogenannter ACOPs (Acyl Chain Oxidation Products), aus Sitostanyloleat sowie zu deren Umsätzen im Zuge enzymkatalysierter *in-vitro* Hydrolysen zu erarbeiten.

Im ersten Teil der Arbeit wurden zwanzig nicht kommerziell erhältliche authentische Referenzverbindungen von ACOPs, die als Thermooxidationsprodukte von Sitostanyloleat erwartet wurden, synthetisiert. Die kurz- und mittelkettigen ACOPs (C5 bis C11), die aus oxidativen Fragmentierungen des Ölsäurerests resultieren, umfassten unpolare ACOPs und solche mit Aldehyd-, Keto- oder Hydroxy-Gruppen in den verkürzten Fettsäureketten. Darüber hinaus wurden Sitostanyl-ACOPs mit Keto-, Hydroxy-, Dihydroxy- und Epoxy-Gruppen in der nicht fragmentierten Fettsäurekette synthetisiert. Die jeweiligen Referenzen wurden entweder durch Veresterung der entsprechenden synthetisierten, oxidierten Fettsäure mit Sitostanol generiert, oder es wurden oxidative Modifikationen an Sitostanylestern vorgenommen. Zusammen mit vier synthetisierten Cholestanylestern, die die verschiedenen ACOP-Klassen repräsentieren, dienten diese Substanzen als Referenzen bzw. Standards für eine UHPLC-MS/MS-basierte Analyse von ACOPs, die bei der Thermooxidation von Sitostanyloleat entstehen.

Im zweiten Teil wurde eine Methode für die GC-basierte Analyse langkettiger ACOPs, die bei der Thermooxidation von Sitostanyloleat gebildet werden, entwickelt. Diese umfasste (i) Festphasenextraktion zur Separation der polaren langkettigen ACOPs von nicht oxidiertem Sitostanyloleat, (ii) Umesterung der ACOPs und (iii) GC-Analyse der resultierenden Methylester. Für die Identifizierung der ACOPs wurden die GC-Daten

und Massenspektren mit denen synthetisierter Referenzverbindungen verglichen. Beim Erhitzen von Sitostanyloleat (180°C, 60 Min.) waren Methyl-*trans*- und *cis*-9,10-epoxystearat die Hauptoxidationsprodukte, gefolgt von dem Paar Methyl-8/11-hydroxyoctadec-9-enoat sowie Methyloxooctadecenoat. Das Paar Methyl-10-hydroxyoctadec-8-enoat / 9-hydroxyoctadec-10-enoat und Methyl-9,10-dihydroxystearat lagen in geringeren Mengen vor. Mit der Methode wurde die Bildung dieser langkettigen ACOPs in Abhängigkeit von Temperatur (120°C - 200°C, 30 min.) und Erhitzungsdauer (15 min. - 180 min.; 180°C, 200°C) verfolgt. Nur Methyl-*trans*-9,10-epoxystearat zeigte eine konstante Zunahme mit ansteigender Temperatur. Die Mengen der anderen ACOPs nahmen nur bis 170°C/180°C zu; außerdem zeigten sie Konzentrationsmaxima nach einer Erhitzungsdauer von 30 bzw. 60 Minuten bei 180°C bzw. 200°C. Die Erhitzung von Sitostanyloleat, Methyloleat, Monoolein und Triolein zeigte den Einfluss der veresterten Gruppe auf die Gesamtmenge der ACOPs sowie auf die individuellen Anteile der einzelnen ACOPs.

Die intestinale Hydrolyse und Freisetzung der freien Sterole/Stanole ist ein wesentlicher Schritt, damit Phytosteryl/-stanylfettsäureester ihre cholesterolsenkende Wirkung entfalten können. Daher wurden im letzten Teil dieser Arbeit eine Reihe synthetisierter Sitostanyl- und Sitosteryl-ACOPs aus verschiedenen Klassen einer durch Cholesterolesterase katalysierten *in-vitro* Hydrolyse unterzogen. Sowohl für Sitostanyl- als auch für Sitosteryl-ACOPs wurden elf Vertreter (i) kurzkettiger ACOPs mit Oxo-, Aldehyd- oder aliphatischen Gruppen und (ii) langkettiger ACOPs mit Epoxy- oder Hydroxygruppen synthetisiert und als Substrate verwendet. Für neun der Sitostanyl-ACOPs und für sieben der Sitosteryl-ACOPs waren die ermittelten Umsätze signifikant niedriger als die des nicht oxidierten Sitostanyloleats bzw. Sitosteryloleats. Der Umsatz von Sitostanyl-*cis*-9,10-epoxystearat, einem der quantitativ dominierenden ACOPs bei der Thermooxidation von Sitostanyloleat, entsprach nur 10% des Umsatzes von Sitostanyloleat. Sitosterylester zeigten stets höhere Umsätze als die entsprechenden Sitostanylester. Gleichwohl wies Sitosteryl-*cis*-9,10-epoxystearat innerhalb dieser ACOP-Reihe auch einen der niedrigsten Umsätze auf, der lediglich 19% des Sitosteryloleat-Umsatzes betrug. Es wurden keine eindeutigen Abhängigkeiten der Umsätze von der Kettenlänge innerhalb der verschiedenen ACOP-Klassen festgestellt. Die Zugabe äquimolarer Mengen von Cholesteryloleat zu den Hydrolysegemischen führte zu signifikanten Steigerungen der Umsätze von Sitostanyloleat und den meisten Sitostanyl- und Sitosteryl-ACOPs. Die Anwesenheit

von Cholesterol, einem der Hydrolyseprodukte von Cholesteryloleat, erhöhte ebenfalls die Umsätze von Sitostanyloleat und Sitostanyl-ACOPs, während die Anwesenheit von Ölsäure nur einen geringen Einfluss hatte. Die Zugabe äquimolarer Mengen von Sitostanyl- bzw. Sitosteryl-ACOPs zu den Hydrolysegemischen hatte keine statistisch signifikante Auswirkung auf den Umsatz von Cholesteryloleat. In weiteren Experimenten wurde der Einfluss der verwendeten Gallensäuren auf die Umsätze in den *in-vitro* Hydrolysen bestätigt.

Die gewonnenen Daten erweitern das Wissen vor allem über die Bildung langkettiger ACOPs. Die analytischen Untersuchungen waren jedoch auf die Modellsubstanz Sitostanyloleat beschränkt. Zukünftige Studien sollten die Bildung von ACOPs eines breiteren Spektrums von Phytosteryl/-stanylfettsäureestern, die für den Zusatz zu Lebensmitteln verwendet werden, abdecken. Schließlich sollten die Untersuchungen von den reinen Stoffen/Gemischen auf angereicherte Lebensmittel ausgeweitet werden. Dies wird natürlich neue Herausforderungen in Bezug auf Referenzsubstanzen, Probenvorbereitung und analytische Methoden mit sich bringen. Die Ergebnisse zeigen, dass die quantitativ dominierenden ACOPs, die bei der Thermooxidation von Sitostanyloleat gebildet wurden, die niedrigsten Umsatzraten in den *in-vitro* Hydrolysen aufwiesen. Dies unterstreicht die Notwendigkeit weiterer Untersuchungen zu den potenziellen Auswirkungen oxidativer Veränderungen von Phytosteryl/-stanylfettsäureestern während der Verarbeitung auf ihre cholesterolsenkenden Eigenschaften. Laufende Verbesserungen und Standardisierungen von Protokollen, die für Studien zur Bioverfügbarkeit / Biozugänglichkeit von Steryl/-stanylfettsäureestern verwendet werden, könnten in dieser Hinsicht hilfreich sein.

7. REFERENCES

- Aerts, H. A. J.; Jacobs, P. A., Epoxide Yield Determination of Oils and Fatty Acid Methyl Esters Using ^1H NMR. *Journal of the American Oil Chemists' Society* **2004**, *81*, 841-846.
- Ahn, B.-J. K.; Kraft, S.; Sun, X. S., Chemical Pathways of Epoxidized and Hydroxylated Fatty Acid Methyl Esters and Triglycerides with Phosphoric Acid. *Journal of Materials Chemistry* **2011**, *21*, 9498-9505.
- Barnsteiner, A.; Esche, R.; di Gianvito, A.; Chiavaro, E.; Schmid, W.; Engel, K.-H., Capillary Gas Chromatographic Analysis of Complex Phytosteryl/-stanyl Ester Mixtures in Enriched Skimmed Milk-Drinking Yoghurts. *Food Control* **2012**, *27*, 275-283.
- Barnsteiner, A.; Lubinus, T.; di Gianvito, A.; Schmid, W.; Engel, K. H., GC-Based Analysis of Plant Stanyl Fatty Acid Esters in Enriched Foods. *Journal of Agricultural and Food Chemistry* **2011**, *59*, 5204-5214.
- Barriuso, B.; Astiasaran, I.; Ansorena, D., Unsaturated Lipid Matrices Protect Plant Sterols from Degradation During Heating Treatment. *Food Chemistry* **2016**, *196*, 451-458.
- Belitz, H.-D.; Grosch, W.; Schieberle, P., *Lehrbuch der Lebensmittelchemie*. 6th ed.; Springer-Verlag: Berlin 2008.
- Benveniste, P., Sterol Biosynthesis. *Annual Review of Plant Physiology* **1986**, *37*, 275-308.
- Berdeaux, O.; Dutta, P. C.; Dobarganes, M. C.; Sébédio, J. L., Analytical Methods for Quantification of Modified Fatty Acids and Sterols Formed as a Result of Processing. *Food Analytical Methods* **2008**, *2*, 30-40.
- Berdeaux, O.; Fontagne, S.; Semon, E.; Velasco, J.; Sebedio, J. L.; Dobarganes, C., A Detailed Identification Study on High-Temperature Degradation Products of Oleic and Linoleic Acid Methyl Esters by GC-MS and GC-FTIR. *Chemistry and Physics of Lipids* **2012**, *165*, 338-347.
- Berdeaux, O.; Marquez-Ruiz, G.; Dobarganes, C., Selection of Methylation Procedures for Quantitation of Short-Chain Glycerol-Bound Compounds Formed During Thermo-oxidation. *Journal of Chromatography A* **1999b**, *863*, 171-181.

- Berdeaux, O.; Márquez-Ruiz, G.; Dobarganes, M. C., Characterization, Quantitation and Evolution of Monoepoxy Compounds Formed in Model Systems of Fatty Acid Methyl Esters and Monoacid Triglycerides Heated at High Temperature. *Grasas y Aceites* **1999a**, *50*, 53-59.
- Berdeaux, O.; Velasco, J.; Marquez-Ruiz, G.; Dobarganes, C., Evolution of Short-Chain Glycerol-Bound Compounds During Thermo-oxidation of FAME and Monoacid TAG. *Journal of American Oil Chemistry Society* **2002**, *59*, 279-285.
- Biedermann, M.; Grob, K.; Mariani, C., Transesterification and On-Line LC-GC for Determining the Sum of Free and Esterified Sterols in Edible Oils and Fats. *European Journal of Lipid Science and Technology* **1993**, *95*, 127-133.
- Billheimer, J. T.; Avart, S.; Milani, B., Separation of Steryl Esters by Reversed-Phase Liquid Chromatography. *Journal of Lipid Research* **1983**, *24*, 1646-1651.
- Boyd, A. P.; Acevedo, N. C.; Talbert, J. N., Evaluation of Pure Bile Salts in Place of Bile Extract in the Standardized INFOGEST Digestion Protocol for Quantification of Sterol Bioaccessibility. *Journal of Agricultural and Food Chemistry* **2022a**, *70*, 11554-11559.
- Boyd, A. P.; Talbert, J. N.; Acevedo, N. C., Cholesterol Esterase Substantially Enhances Phytosterol Ester Bioaccessibility in a Modified INFOGEST Digestion Model. *Food Chemistry Advances* **2022b**, *1*, 100105.
- Boyd, A. P.; Talbert, J. N.; Acevedo, N. C., Effect of agitation and added cholesterol esterase on bioaccessibility of phytosterols in a standardized in vitro digestion model. *LWT - Food Science and Technology* **2021**, *150*, 112051.
- Brodkorb, A.; Egger, L.; Alming, M.; Alvito, P.; Assuncao, R.; Ballance, S.; Bohn, T.; Bourlieu-Lacanal, C.; Boutrou, R.; Carriere, F.; Clemente, A.; Corredig, M.; Dupont, D.; Dufour, C.; Edwards, C.; Golding, M.; Karakaya, S.; Kirkhus, B.; Le Feunteun, S.; Lesmes, U.; Macierzanka, A.; Mackie, A. R.; Martins, C.; Marze, S.; McClements, D. J.; Menard, O.; Minekus, M.; Portmann, R.; Santos, C. N.; Souchon, I.; Singh, R. P.; Vegarud, G. E.; Wickham, M. S. J.; Weitschies, W.; Recio, I., INFOGEST Static In Vitro Simulation of Gastrointestinal Food Digestion. *Nature Protocols* **2019**, *14*, 991-1014.
- Brown, A. W.; Hang, J.; Dussault, P. H.; Carr, T. P., Plant Sterol and Stanol Substrate Specificity of Pancreatic Cholesterol Esterase. *Journal of Nutritional Biochemistry* **2010**, *21*, 736-740.

- Brufau, G.; Canela, M. A.; Rafecas, M., Phytosterols: Physiologic and Metabolic Aspects Related to Cholesterol-Lowering Properties. *Nutrition Research* **2008**, *28*, 217-225.
- Brühl, L., Fatty Acid Alterations in Oils and Fats During Heating and Frying. *European Journal of Lipid Science and Technology* **2014**, *116*, 707-715.
- Byrdwell, W. C.; Neff, W. E., Non-Volatile Products of Triolein Produced at Frying Temperatures Characterized Using Liquid Chromatography with Online Mass Spectrometric Detection. *Journal of Chromatography A* **1999**, *852*, 417-432.
- Caboni, M. F.; Iafelice, G.; Pelillo, M.; Marconi, E., Analysis of fatty acid steryl esters in tetraploid and hexaploid wheats: identification and comparison between chromatographic methods. *Journal of Agricultural and Food Chemistry* **2005**, *53*, 7465-7472.
- Calpe-Berdiel, L.; Escola-Gil, J. C.; Blanco-Vaca, F., New Insights Into the Molecular Actions of Plant Sterols and Stanols in Cholesterol Metabolism. *Atherosclerosis* **2009**, *203*, 18-31.
- Carulli, N.; Bertolotti, M.; Carubbi, F.; Concari, M.; Martella, P.; Carulli, L.; Loria, P., Review Article: Effect of Bile Salt Pool Composition on Hepatic and Biliary Functions. *Alimentary Pharmacology & Therapeutics* **2000**, *14 Suppl 2*, 14-18.
- Carvalho, J. F.; Silva, M. M.; Moreira, J. N.; Simoes, S.; Sa, E. M. M. L., Selective Cytotoxicity of Oxysterols Through Structural Modulation on Rings A and B. Synthesis, In Vitro Evaluation, and SAR. *Journal of Medical Chemistry* **2011**, *54*, 6375-6393.
- Cerqueira, N. M.; Oliveira, E. F.; Gesto, D. S.; Santos-Martins, D.; Moreira, C.; Moorthy, H. N.; Ramos, M. J.; Fernandes, P. A., Cholesterol Biosynthesis: A Mechanistic Overview. *Biochemistry* **2016**, *55*, 5483-5506.
- Chawla, R.; S, S.; Goel, N., Phytosterol and Its Esters as Novel Food Ingredients: A Review. *Asian Journal of Dairy and Food Research* **2016**, *35*, 217-226.
- Dang, H. T.; Lee, H. J.; Yoo, E. S.; Shinde, P. B.; Lee, Y. M.; Hong, J.; Kim, D. K.; Jung, J. H., Anti-Inflammatory Constituents of the Red Alga *Gracilaria Verrucosa* and Their Synthetic Analogues. *Journal of Natural Products* **2008**, *71*, 232-240.
- De Smet, E.; Mensink, R. P.; Plat, J., Effects of Plant Sterols and Stanols on Intestinal Cholesterol Metabolism: Suggested Mechanisms from Past to Present. *Molecular Nutrition and Food Research* **2012**, *56*, 1058-1072.

- Deykin, D.; Goodman, D. S., The Hydrolysis of Long-Chain Fatty Acid Esters of Cholesterol with Rat Liver Enzymes. *Journal of Biological Chemistry* **1962**, *237*, 3649-3656.
- Dobarganes, M. C.; Márquez-Ruiz, G., Formation and Analysis of Oxidized Monomeric, Dimeric, and Higher Oligomeric Triglycerides. In *Deep Frying*, 2nd ed.; AOCS Press: 2007; pp 87-110.
- Dutta, P. C., Chemistry, Analysis, and Occurrence of Phytosterol Oxidation Products in Foods. In *Phytosterols as Functional Food Components and Nutraceuticals*, 1st ed.; Dekker: New York, 2004; pp 397-417.
- Dyas, L.; Goad, L. J., Steryl Fatty Acyl Esters in Plants. *Phytochemistry* **1993**, *34*, 17-29.
- EFSA, Consumption of Food and Beverages with Added Plant Sterols. *EFSA Journal* **2008**, *6*, 1-21.
- EFSA, Safety of the Extension of Use of Plant Sterol Esters as a Novel Food Pursuant to Regulation (EU) 2015/2283. *EFSA Journal* **2020**, *18*.
- EFSA, Scientific Opinion on the Substantiation of Health Claims Related to Plant Sterols and Plant Stanols and Maintenance of Normal Blood Cholesterol Concentrations (ID 549, 550, 567, 713, 1234, 1235, 1466, 1634, 1984, 2909, 3140), and Maintenance of Normal Prostate Size and Normal Urination (ID 714, 1467, 1635) Pursuant to Article 13(1) of Regulation (EC) No 1924/20061. *EFSA Journal* **2010**, *8*, 1813.
- Elshourbagy, N. A.; Meyers, H. V.; Abdel-Meguid, S. S., Cholesterol: the Good, the Bad, and the Ugly - Therapeutic Targets for the Treatment of Dyslipidemia. *Medical Principles and Practice* **2014**, *23*, 99-111.
- Esche, R.; Barnsteiner, A.; Scholz, B.; Engel, K. H., Simultaneous Analysis of Free Phytosterols/Phytostanols and Intact Phytosteryl/Phytostanyl Fatty Acid and Phenolic Acid Esters in Cereals. *Journal of Agricultural and Food Chemistry* **2012**, *60*, 5330-5339.
- Esche, R.; Carcelli, A.; Barnsteiner, A.; Sforza, S.; Engel, K.-H., Analysis of Phytosteryl and Phytostanyl Fatty Acid Esters in Enriched Dairy Foods: a Combination of Acid Digestion, Lipid Extraction, and On-Line LC-GC. *European Food Research and Technology* **2013a**, *236*, 999-1007.

- Esche, R.; Scholz, B.; Engel, K. H., Online LC-GC analysis of Free Sterols/Stanoles and Intact Steryl/Stanyl Esters in Cereals. *Journal of Agricultural and Food Chemistry* **2013b**, *61*, 10932-10939.
- Esrey, K. L.; Joseph, L.; Grover, S. A., Relationship Between Dietary Intake and Coronary Heart Disease Mortality: Lipid Research Clinics Prevalence Follow-up Study. *Journal of Clinical Epidemiology* **1996**, *49*, 211-216.
- Evtugin, D. D.; Evtugin, D. V.; Casal, S.; Domingues, M. R., Advances and Challenges in Plant Sterol Research: Fundamentals, Analysis, Applications and Production. *Molecules* **2023**, *28*, 6526.
- Feng, S.; Belwal, T.; Li, L.; Limwachiranon, J.; Liu, X.; Luo, Z., Phytosterols and Their Derivatives: Potential Health-Promoting Uses Against Lipid Metabolism and Associated Diseases, Mechanism, and Safety Issues. *Comprehensive Reviews in Food Science and Food Safety* **2020**, *19*, 1243-1267.
- Frankel, E. N., Hydroperoxide decomposition. In *Lipid Oxidation*, 2nd ed.; Oily Press: Bridgwater, 2005; pp 67-98.
- Frankel, E. N.; Neff, W. E.; Rohwedder, W. K.; Khambay, B. P. S.; Garwood, R. F.; Weedon, B. C. L., Analysis of Autoxidized Fats by Gas Chromatography-Mass Spectrometry: I. Methyl Oleate. *Lipids* **1977**, *12*, 901-907.
- Fujioka, S.; Sakurai, A., Biosynthesis and Metabolism of Brassinosteroids. *Physiologia Plantarum* **1997**, *100*, 710-715.
- García-González, A.; Velasco, J.; Velasco, L.; Ruiz-Méndez, M. V., An Analytical Simplification for Faster Determination of Fatty Acid Composition and Phytosterols in Seed Oils. *Food Analytical Methods* **2017**, *11*, 1234-1242.
- García-Llatas, G.; Rodríguez-Estrada, M. T., Current and New Insights on Phytosterol Oxides in Plant Sterol-Enriched Food. *Chemistry and Physics of Lipids* **2011**, *164*, 607-624.
- Gardner, D. R.; Sanders, R. A.; Henry, D. E.; Tallmadge, D. H.; Wharton, H. W., Characterization of Used Frying Oils. Part 1: Isolation and Identification of Compound Classes. *Journal of American Oil Chemistry Society* **1992**, *69*, 499-508.
- Gleize, B.; Nowicki, M.; Daval, C.; Koutnikova, H.; Borel, P., Form of Phytosterols and Food Matrix in which They are Incorporated Modulate Their Incorporation Into Mixed Micelles and Impact Cholesterol Micellarization. *Molecular Nutrition and Food Research* **2016**, *60*, 749-759.

- Goller, H. J.; Sgoutas, D. S.; Ismail, I. A.; Gunstone, F. D., Dependence of Sterol Ester Hydrolase Activity on the Position of Ethylenic Bond in Cholesteryl Cis-Octadecenoates. *Biochemistry* **1970**, *9*, 3072-3076.
- Guardiola, F.; Bou, R.; Boatella, J.; Codony, R., Analysis of Sterol Oxidation Products in Foods. *Journal of AOAC INTERNATIONAL* **2004**, *87*, 441-466.
- Guzior, D. V.; Quinn, R. A., Review: Microbial Transformations of Human Bile Acids. *Microbiome* **2021**, *9*, 140.
- Hartmann, M., Plant Sterols and the Membrane Environment. *Trends in Plant Science* **1998**, *3*, 170-175.
- Hui, D. Y., Molecular Biology of Enzymes Involved with Cholesterol Ester Hydrolysis in Mammalian Tissues. *Biochimica et Biophysica Acta* **1996**, *1303*, 1-14.
- Hutchins, P. M.; Moore, E. E.; Murphy, R. C., Electrospray MS/MS Reveals Extensive and Nonspecific Oxidation of Cholesterol Esters in Human Peripheral Vascular Lesions. *Journal of Lipid Research* **2011**, *52*, 2070-2083.
- Ichihara, K.; Fukubayashi, Y., Preparation of Fatty Acid Methyl Esters for Gas-Liquid Chromatography. *Journal of Lipid Research* **2010**, *51*, 635-640.
- Jacobson, P. W.; Wiesenfeld, P. W.; Gallo, L. L.; Tate, R. L.; Osborne, J. C., Sodium Cholate-Induced Changes in the Conformation and Activity of Rat Pancreatic Cholesterol Esterase. *Journal of Biological Chemistry* **1990**, *265*, 515-521.
- Jie, M. S. F. L. K.; Lam, C. N. W.; Ho, J. C. M.; Lau, M. M. L., Epoxidation of a Conjugated Linoleic Acid Isomer. *European Journal of Lipid Science and Technology* **2003**, *105*, 391-396.
- Johnsson, L.; Dutta, P. C., Characterization of Side-Chain Oxidation Products of Sitosterol and Campesterol by Chromatographic and Spectroscopic Methods. *Journal of the American Oil Chemists' Society* **2003**, *80*, 767-776.
- Johnsson, L.; Dutta, P. C., Determination of Phytosterol Oxides in some Food Products by Using an Optimized Transesterification Method. *Food Chemistry* **2006**, *97*, 606-613.
- Julien-David, D.; Ennahar, S.; Miesch, M.; Geoffroy, P.; Raul, F.; Aoude-Werner, D.; Lessinger, J. M.; Marchioni, E., Effects of Oxidation on the Hydrolysis by Cholesterol Esterase of Sitosteryl Esters as Compared to a Cholesteryl Ester. *Steroids* **2009**, *74*, 832-836.
- Julien-David, D.; Geoffroy, P.; Marchioni, E.; Raul, F.; Aoude-Werner, D.; Miesch, M., Synthesis of Highly Pure Oxyphytosterols and (Oxy)Phytosterol Esters. Part II.

- (Oxy)-Sitosterol Esters Derived from Oleic Acid and from 9,10-Dihydroxystearic Acid [1]. *Steroids* **2008**, *73*, 1098-1109.
- Julien-David, D.; Zhao, M.; Geoffroy, P.; Miesch, M.; Raul, F.; Aoude-Werner, D.; Ennahar, S.; Marchioni, E., Analysis of Sitosteryl Oleate Esters in Phytosterols Esters Enriched Foods by HPLC-ESI-MS². *Steroids* **2014**, *84*, 84-91.
- Kamido, H.; Kuksis, A.; Marai, L.; Myher, J. J., Identification of Cholesterol-Bound Aldehydes in Copper-Oxidized Low Density Lipoprotein. *FEBS Letters* **1992**, *304*, 269-272.
- Kamido, H.; Kuksis, A.; Marai, L.; Myher, J. J., Identification of Core Aldehydes Among In Vitro Peroxidation Products of Cholesteryl Esters. *Lipids* **1993**, *28*, 331-336.
- Kamido, H.; Kuksis, A.; Marai, L.; Myher, J. J., Lipid Ester-Bound Aldehydes Among Copper-Catalyzed Peroxidation Products of Human Plasma Lipoproteins. *Journal of Lipid Research* **1995**, *36*, 1876-1886.
- Katan, M. B.; Grundy, S. M.; Jones, P.; Law, M.; Miettinen, T.; Paoletti, R.; Stresa Workshop, P., Efficacy and Safety of Plant Stanols and Sterols in the Management of Blood Cholesterol Levels. *Mayo Clinic Proceedings* **2003**, *78*, 965-978.
- Kleiman, R.; Spencer, G. F., Gas Chromatography-Mass Spectrometry of Methyl Esters of Unsaturated Oxygenated Fatty Acids. *Journal of the American Oil Chemists' Society* **1973**, *50*, 31-38.
- Knothe, G.; Weisleder, D.; Bagby, M. O.; Peterson, M. E., Hydroxy Fatty Acids Through Hydroxylation of Oleic Acid with Selenium Dioxide/tert.-Butylhydroperoxide. *Journal of American Oil Chemistry Society* **1993**, *70*, 401-404.
- Koch, E.; Lowen, A.; Nikolay, S.; Willenberg, I.; Schebb, N. H., Trans-Hydroxy, Trans-Epoxy, and Erythro-Dihydroxy Fatty Acids Increase During Deep-Frying. *Journal of Agricultural and Food Chemistry* **2023**, *71*, 7508-7513.
- Kostiainen, R.; Kauppila, T. J., Effect of Eluent on the Ionization Process in Liquid Chromatography-Mass Spectrometry. *Journal of Chromatography A* **2009**, *1216*, 685-699.
- Kuksis, A., Lipidomics in Triacylglycerol and Cholesteryl Ester Oxidation. *Frontiers in Bioscience* **2007**, *12*, 3203-3246.

- Lehtonen, M.; Lampi, A.-M.; Ollilainen, V.; Struijs, K.; Piironen, V., The Role of Acyl Moiety in the Formation and Reactions of Steryl Ester Hydroperoxides. *European Food Research and Technology* **2011**, 233, 51-61.
- Lehtonen, M.; Lampi, A. M.; Riuttamaki, M. A.; Piironen, V., Oxidation Reactions of Steryl Esters in a Saturated Lipid Matrix. *Food Chemistry* **2012**, 134, 2030-2039.
- Leitinger, N., Cholesteryl Ester Oxidation Products in Atherosclerosis. *Molecular Aspects of Medicine* **2003**, 24, 239-250.
- Lercker, G.; Rodriguez-Estrada, M. T., Chromatographic Analysis of Unsaponifiable Compounds of Olive Oils and Fat-Containing Foods. *Journal of Chromatography A* **2000**, 881, 105–129.
- Lercker, G.; Rodriguez-Estrada, M. T.; Bonoli, M., Analysis of the Oxidation Products of Cis- and Trans-Octadecenoate Methyl Esters by Capillary Gas Chromatography–Ion-Trap Mass Spectrometry I. Epoxide and Dimeric Compounds. *Journal of Chromatography A* **2002**, 985, 333–342.
- Lin, D.; Zhang, J.; Sayre, L. M., Synthesis of Six Epoxyketoctadecenoic Acid (EKODE) Isomers, Their Generation from Nonenzymatic Oxidation of Linoleic Acid, and their Reactivity with Imidazole Nucleophiles. *Journal of Organic Chemistry* **2007**, 72, 9471-9480.
- Makran, M.; Faubel, N.; Lopez-Garcia, G.; Cilla, A.; Barbera, R.; Alegria, A.; Garcia-Llatas, G., Sterol Bioaccessibility in a Plant Sterol-Enriched Beverage Using the INFOGEST Digestion Method: Influence of Gastric Lipase, Bile Salts and Cholesterol Esterase. *Food Chemistry* **2022**, 382, 132305.
- Marmesat, S.; Velasco, J.; Dobarganes, M. C., Quantitative Determination of Epoxy Acids, Keto Acids and Hydroxy Acids Formed in Fats and Oils at Frying Temperatures. *Journal of Chromatography A* **2008**, 1211, 129-134.
- Matissek, R.; Baltes, W., *Lebensmittelchemie*. 8th ed.; Springer-Verlag: Berlin, 2016.
- Mel'nikov, S. M.; Seijen ten Hoorn, J. W.; Eijkelenboom, A. P., Effect of Phytosterols and Phytostanols on the Solubilization of Cholesterol by Dietary Mixed Micelles: an In Vitro Study. *Chemistry and Physics of Lipids* **2004**, 127, 121-141.
- Menendez-Carreno, M.; Ansorena, D.; Astiasaran, I., Stability of Sterols in Phytosterol-Enriched Milk Under Different Heating Conditions. *Journal of Agricultural and Food Chemistry* **2008**, 56, 9997-10002.

- Miedes, D.; Makran, M.; Cilla, A.; Barbera, R.; Garcia-Llatas, G.; Alegria, A., Aging-Related Gastrointestinal Conditions Decrease the Bioaccessibility of Plant Sterols in Enriched Wholemeal Rye Bread: In Vitro Static Digestion. *Food and Function* **2023**, *14*, 6012-6022.
- Minekus, M.; Alminger, M.; Alvito, P.; Ballance, S.; Bohn, T.; Bourlieu, C.; Carriere, F.; Boutrou, R.; Corredig, M.; Dupont, D.; Dufour, C.; Egger, L.; Golding, M.; Karakaya, S.; Kirkhus, B.; Le Feunteun, S.; Lesmes, U.; Macierzanka, A.; Mackie, A.; Marze, S.; McClements, D. J.; Menard, O.; Recio, I.; Santos, C. N.; Singh, R. P.; Vegarud, G. E.; Wickham, M. S.; Weitschies, W.; Brodkorb, A., A Standardised Static In Vitro Digestion Method Suitable for Food - an International Consensus. *Food and Function* **2014**, *5*, 1113-1124.
- Miyoshi, N.; Iwasaki, N.; Tomono, S.; Higashi, T.; Ohshima, H., Occurrence of Cytotoxic 9-Oxononanoyl Secosterol Aldehydes in Human Low-Density Lipoprotein. *Free Radical Biology and Medicine* **2013**, *60*, 73-79.
- Morales, A.; Marmesat, S.; Ruiz-Méndez, M. V.; Márquez-Ruiz, G.; Velasco, J., Formation of Oxidation Products in Edible Vegetable Oils Analyzed as FAME Derivatives by HPLC-UV-ELSD. *Food Research International* **2014**, *62*, 1080-1086.
- Moran-Valero, M. I.; Martin, D.; Torrelo, G.; Reglero, G.; Torres, C. F., Phytosterols Esterified with Conjugated Linoleic Acid. In Vitro Intestinal Digestion and Interaction on Cholesterol Bioaccessibility. *Journal of Agricultural and Food Chemistry* **2012**, *60*, 11323-11330.
- Moreau, R. A.; Hicks, K. B., The In Vitro Hydrolysis of Phytosterol Conjugates in Food Matrices by Mammalian Digestive Enzymes. *Lipids* **2004**, *39*, 769-776.
- Moreau, R. A.; Whitaker, B. D.; Hicks, K. B., Phytosterols, Phytostanols, and Their Conjugates in Foods: Structural Diversity, Quantitative Analysis, and Health-Promoting Uses. *Progress in Lipid Research* **2002**, *41*, 457-500.
- Morlock, G. E.; Meyer, D., Designed Genotoxicity Profiling Detects Genotoxic Compounds in Staple Food Such as Healthy Oils. *Food Chemistry* **2023**, *408*, 135253.
- Moss, G. P., Nomenclature of Steroids (Recommendations 1989). *Pure and Applied Chemistry* **1989**, *61*, 1783-1822.

- Mozaffarian, D.; Aro, A.; Willett, W. C., Health Effects of Trans-Fatty Acids: Experimental and Observational Evidence. *European Journal of Clinical Nutrition* **2009**, *63*, S5-21.
- Mubiru, E.; Shrestha, K.; Papastergiadis, A.; De Meulenaer, B., Improved Gas Chromatography-Flame Ionization Detector Analytical Method for the Analysis of Epoxy Fatty Acids. *Journal of Chromatography A* **2013**, *1318*, 217-225.
- Neff, W. E.; Byrdwell, W. C., Characterization of Model Triacylglycerol (Triolein, Trilinolein and Trilinolenin) Autoxidation Products via High-Performance Liquid Chromatography Coupled with Atmospheric Pressure Chemical Ionization Mass Spectrometry. *Journal of Chromatography A* **1998**, *818*, 169–186.
- Nes, W. D., Biosynthesis of Cholesterol and Other Sterols. *Chemical Reviews* **2011**, *111*, 6423-6451.
- Noguchi, T.; Fujioaka, S.; Takatsuto, S.; Sakurai, A.; Yoshida, S.; Li, J.; Chory, J., Arabidopsis det2 is Defective in the Conversion of (24R)-24-Methylcholest-4-En-3-one to (24R)-24-Methyl-5alpha-cholestan-3-one in Brassinosteroid Biosynthesis. *Plant Physiology* **1999**, *120*, 833-840.
- Oelschlägel, S.; Menzel, C.; Speer, K., Phytosterols and Steryl Esters in Diverse Cucurbita, Cucumis and Citrullus Seed Oils. *Lipid Technology* **2012**, *24*, 181-184.
- Ostlund, R. E., Jr., Phytosterols in Human Nutrition. *Annual Review of Nutrition* **2002**, *22*, 533-549.
- Otaegui-Arrazola, A.; Menendez-Carreno, M.; Ansorena, D.; Astiasaran, I., Oxysterols: A world to explore. *Food Chem Toxicol* **2010**, *48*, 3289-303.
- Piironen, V.; Lindsay, D. G.; Miettinen, T. A.; Toivo, J.; Lampi, A.-M., Plant Sterols: Biosynthesis, Biological Function and Their Importance to Human Nutrition. *Journal of the Science of Food and Agriculture* **2000**, *80*, 939-966.
- Poudel, A.; Gachumi, G.; Purves, R.; Badea, I.; El-Aneed, A., Determination of Phytosterol Oxidation Products in Pharmaceutical Liposomal Formulations and Plant Vegetable Oil Extracts Using Novel Fast Liquid Chromatography - Tandem Mass Spectrometric Methods. *Analytica Chimica Acta* **2022**, *1194*, 339404.
- Raczyk, M.; Kmiecik, D.; Przybylski, R.; Rudzinska, M., Effect of Fatty Acid Unsaturation on Phytosteryl Ester Degradation. *Journal of the American Oil Chemists' Society* **2017**, *94*, 701-711.

- Ras, R. T.; Geleijnse, J. M.; Trautwein, E. A., LDL-Cholesterol-Lowering Effect of Plant Sterols and Stanols Across Different Dose Ranges: a Meta-Analysis of Randomised Controlled Studies. *British Journal of Nutrition* **2014**, *112*, 214-219.
- Rudzinska, M.; Przybylski, R.; Zhao, Y. Y.; Curtis, J. M., Sitosterol Thermo-Oxidative Degradation Leads to the Formation of Dimers, Trimers and Oligomers: a Study Using Combined Size Exclusion Chromatography/Mass Spectrometry. *Lipids* **2010**, *45*, 549-558.
- Schmarr, H.-G.; Gross, H. B.; Shibamoto, T., Analysis of Polar Cholesterol Oxidation Products: Evaluation of a New Method Involving Transesterification, Solid Phase Extraction, and Gas Chromatography. *Journal of Agricultural and Food Chemistry* **1996**, *44*, 512-517.
- Scholz, B.; Barnsteiner, A.; Feist, K.; Schmid, W.; Engel, K. H., Analysis of Phytostanyl Fatty Acid Esters in Enriched Foods via UHPLC-APCI-MS. *Journal of Agricultural and Food Chemistry* **2014**, *62*, 4268-4275.
- Scholz, B.; Guth, S.; Engel, K. H.; Steinberg, P., Phytosterol Oxidation Products in Enriched Foods: Occurrence, Exposure, and Biological Effects. *Molecular Nutrition and Food Research* **2015a**, *59*, 1339-1352.
- Scholz, B.; Menzel, N.; Lander, V.; Engel, K. H., An Approach Based on Ultrahigh Performance Liquid Chromatography-Atmospheric Pressure Chemical Ionization-Mass Spectrometry Allowing the Quantification of Both Individual Phytosteryl and Phytostanyl Fatty Acid Esters in Complex Mixtures. *Journal of Chromatography A* **2016a**, *1429*, 218-229.
- Scholz, B.; Menzel, N.; Lander, V.; Engel, K. H., Heating Two Types of Enriched Margarine: Complementary Analysis of Phytosteryl/Phytostanyl Fatty Acid Esters and Phytosterol/Phytostanol Oxidation Products. *Journal of Agricultural and Food Chemistry* **2016b**, *64*, 2699-2708.
- Scholz, B.; Stiegler, V.; Eisenreich, W.; Engel, K. H., Strategies for UHPLC-MS/MS-Based Analysis of Different Classes of Acyl Chain Oxidation Products Resulting from Thermo-Oxidation of Sitostanyl Oleate. *Journal of Agricultural and Food Chemistry* **2019**, *67*, 12072-12083.
- Scholz, B.; Weiherer, R.; Engel, K. H., Impact of Thermooxidation of Phytosteryl and Phytostanyl Fatty Acid Esters on Cholesterol Micellarization In Vitro. *Steroids* **2017**, *125*, 81-92.

- Scholz, B.; Wochezlander, S.; Lander, V.; Engel, K. H., On-line Liquid Chromatography-Gas Chromatography: A Novel Approach for the Analysis of Phytosterol Oxidation Products in Enriched Foods. *Journal of Chromatography A* **2015b**, 1396, 98-108.
- Schwartz, D. P.; Rady, A. H.; Castafieda, S., The Formation of Oxo- and Hydroxy-Fatty Acids in Heated Fats and Oils. *Journal of American Oil Chemistry Society* **1994**, 71, 441-444.
- Sgoutas, D. S., Comparative Studies on the Hydrolysis of Odd-Chain and Even-Chain Fatty Acid Cholesterol Esters by Rat Liver Sterol Ester Hydrolase. *Biochimica et Biophysica Acta* **1971**, 239, 469-474.
- Sgoutas, D. S., Hydrolysis of Synthetic Cholesterol Esters Containing Trans Fatty Acids. *Biochimica et Biophysica Acta* **1968**, 164, 317-326.
- Shing, T. K.; Yeung, Y. Y.; Su, P. L., Mild Manganese(III) Acetate Catalyzed Allylic Oxidation: Application to Simple and Complex Alkenes. *Organic Letters* **2006**, 8, 3149-3151.
- Soupas, L.; Huikko, L.; Lampi, A.-m.; Piironen, V., Pan-Frying May Induce Phytosterol Oxidation. *Food Chemistry* **2007**, 101, 286-297.
- Soupas, L.; Huikko, L.; Lampi, A. M.; Piironen, V., Esterification affects phytosterol oxidation. *European Journal of Lipid Science and Technology* **2005**, 107, 107-118.
- Soupas, L.; Juntunen, L.; Lampi, A. M.; Piironen, V., Effects of Sterol Structure, Temperature, and Lipid Medium on Phytosterol Oxidation. *Journal of Agricultural and Food Chemistry* **2004a**, 52, 6485-6491.
- Soupas, L.; Juntunen, L.; Säynäjoki, S.; Lampi, A.-M.; Piironen, V., GC-MS Method for Characterization and Quantification of Sitostanol Oxidation Products. *Journal of the American Oil Chemists' Society* **2004b**, 81, 135-141.
- Stern, H. S.; Treadwell, C. R., Cholesterol Esterases. VII. Hydrolysis of Branched Chain Esters by Pancreatic Cholesterol Esterase. *Proceedings of the Society for Experimental Biology and Medicine* **1958**, 97, 579-581.
- Swell, L.; Field, H., Jr.; Treadwell, C. R., Role of Bile Salts in Activity of Cholesterol Esterase. *Proceedings of the Society for Experimental Biology and Medicine* **1953**, 84, 417-420.

- Swell, L.; Field, H., Jr.; Treadwell, C. R., Sterol Specificity of Pancreatic Cholesterol Esterase. *Proceedings of the Society for Experimental Biology and Medicine* **1954**, *87*, 216-218.
- Swell, L.; Treadwell, C. R., Cholesterol Esterases: VI. Relative Specificity and Activity of Pancreatic Cholesterol Esterases. *Journal of Biological Chemistry* **1955**, *212*, 141-150.
- Swern, D.; Scanlan, J. T.; Knight, H. B., Mechanism of the Reactions of Oxygen with Fatty Materials. Advances from 1941 through 1946. *Journal of the American Oil Chemists Society* **1948**, *25*, 193-200.
- Toschi, T. G.; Costa, A.; Lercker, G., Gas Chromatographic Study on High-Temperature Thermal Degradation Products of Methyl Linoleate Hydroperoxides. *Journal of American Oil Chemistry Society* **1997**, *74*, 387-391.
- Trautwein, E. A.; Duchateau, G. S. M. J. E.; Lin, Y.; Mel'nikov, S. M.; Molhuizen, H. O. F.; Ntanos, F. Y., Proposed Mechanisms of Cholesterol-Lowering Action of Plant Sterols. *European Journal of Lipid Science and Technology* **2003**, *105*, 171-185.
- Vaghini, S.; Cilla, A.; Garcia-Llatas, G.; Lagarda, M. J., Bioaccessibility Study of Plant Sterol-Enriched Fermented Milks. *Food and Function* **2016**, *7*, 110-117.
- Vahouny, G. W.; Weersing, S.; Treadwell, C. R., Function of Specific Bile Acids in Cholesterol Esterase Activity In Vitro. *Biochimica et Biophysica Acta* **1965**, *98*, 607-616.
- Velasco, J.; Berdeaux, O.; Marquez-Ruiz, G.; Dobarganes, M. C., Sensitive and Accurate Quantitation of Monoepoxy Fatty Acids in Thermoxidized Oils by Gas-Liquid Chromatography. *Journal of Chromatography A* **2002**, *982*, 145-152.
- Velasco, J.; Marmesat, S.; Bordeaux, O.; Marquez-Ruiz, G.; Dobarganes, C., Formation and Evolution of Monoepoxy Fatty Acids in Thermoxidized Olive and Sunflower Oils and Quantitation in Used Frying Oils From Restaurants and Fried-Food Outlets. *Journal of Agricultural and Food Chemistry* **2004b**, *52*, 4438-4443.
- Velasco, J.; Marmesat, S.; Márquez-Ruiz, G.; Dobarganes, M. C., Formation of Short-Chain Glycerol-Bound Oxidation Products and Oxidised Monomeric

- Triacylglycerols during Deep-Frying and Occurrence in Used Frying Fats. *European Journal of Lipid Science and Technology* **2004a**, *106*, 728-735.
- Velasco, J.; Morales-Barroso, A.; Ruiz-Mendez, M. V.; Marquez-Ruiz, G., Quantitative Determination of Major Oxidation Products in Edible Oils by Direct NP-HPLC-DAD Analysis. *Journal of Chromatography A* **2018**, *1547*, 62-70.
- Vogelgesang, J.; Hädrich, J., Limits of Detection, Identification and Determination: a Statistical Approach for Practitioners. *Accreditation and Quality Assurance* **1998**, *3*, 242-255.
- von Bergmann, K.; Sudhop, T.; Lutjohann, D., Cholesterol and Plant Sterol Absorption: Recent Insights. *American Journal of Cardiology* **2005**, *96*, 10D-14D.
- Wang, T.; Ma, C.; Hu, Y.; Guo, S.; Bai, G.; Yang, G.; Yang, R., Effects of Food Formulation on Bioavailability of Phytosterols: Phytosterol Structures, Delivery Carriers, and Food Matrices. *Food and Function* **2023**, *14*, 5465-5477.
- Wocheslander, S.; Eisenreich, W.; Scholz, B.; Lander, V.; Engel, K. H., Identification of Acyl Chain Oxidation Products upon Thermal Treatment of a Mixture of Phytosteryl/-stanyl Linoleates. *Journal of Agricultural and Food Chemistry* **2016**, *64*, 9214-9223.
- Wocheslander, S.; Gross, F.; Scholz, B.; Engel, K. H., Quantitation of Acyl Chain Oxidation Products Formed upon Thermo-oxidation of Phytosteryl/-stanyl Oleates and Linoleates. *Journal of Agricultural and Food Chemistry* **2017**, *65*, 2435-2442.
- Xia, W.; Budge, S. M., GC-MS Characterization of Hydroxy Fatty Acids Generated From Lipid Oxidation in Vegetable Oils. *European Journal of Lipid Science and Technology* **2017**, *120*, 1700313.
- Xia, W.; Budge, S. M., Simultaneous Quantification of Epoxy and Hydroxy Fatty Acids as Oxidation Products of Triacylglycerols in Edible Oils. *Journal of Chromatography A* **2018**, *1537*, 83-90.
- Xu, G.; Sun, J.; Liang, Y.; Yang, C.; Chen, Z.-Y., Interaction of Fatty Acids with Oxidation of Cholesterol and β -Sitosterol. *Food Chemistry* **2011**, *124*, 162-170.
- Yanishlieva, N.; Schiller, H.; Marinova, E., Autoxidation of Sitosterol. II: Main Oxidation Products Formed at Ambident and High Temperature Treatment with Oxygen. *Rivista Italiana delle Sostanze Grasse* **1980**, *57*, 572-576.

- Yokoi, H.; Mizukami, H.; Nagatsu, A.; Tanabe, H.; Inoue, M., Hydroxy Monounsaturated Fatty Acids as Agonists for Peroxisome Proliferator-Activated Receptors. *Biological and Pharmaceutical Bulletin* **2010**, *33*, 854—861.
- Young, R. S. E.; Flakelar, C. L.; Narreddula, V. R.; Jekimovs, L. J.; Menzel, J. P.; Poad, B. L. J.; Blanksby, S. J., Identification of Carbon-Carbon Double Bond Stereochemistry in Unsaturated Fatty Acids by Charge-Remote Fragmentation of Fixed-Charge Derivatives. *Analytical Chemistry* **2022**, *94*, 16180-16188.
- Zhou, Z.; Li, Y. L.; Zhao, F.; Xin, R.; Huang, X. H.; Zhang, Y. Y.; Zhou, D.; Qin, L., Unraveling the Thermal Oxidation Products and Peroxidation Mechanisms of Different Chemical Structures of Lipids: An Example of Molecules Containing Oleic Acid. *Journal of Agricultural and Food Chemistry* **2022**, *70*, 16410-16423.
- Zhuang, Y.; Dong, J.; He, X.; Wang, J.; Li, C.; Dong, L.; Zhang, Y.; Zhou, X.; Wang, H.; Yi, Y.; Wang, S., Impact of Heating Temperature and Fatty Acid Type on the Formation of Lipid Oxidation Products During Thermal Processing. *Frontiers in Nutrition* **2022**, *9*, 913297.

8. PUBLICATIONS AND PRESENTATIONS

Reich, D.; Wurzer, A.; Wirtz, M.; Stiegler, V.; Spatz, P.; Pollmann, J.; Wester, H.; Notni, J., Dendritic poly-chelator frameworks for multimeric bioconjugation. *Chemical Communication*, **2017**, *17*, 2586-2589. DOI: 10.1039/C6CC10169K

Scholz, B.; Stiegler, V.; Eisenreich, W.; Engel, K. H., Strategies for UHPLC-MS/MS-Based Analysis of Different Classes of Acyl Chain Oxidation Products Resulting from Thermo-Oxidation of Sitostanyl Oleate. *Journal of Agricultural and Food Chemistry* **2019**, *67*, 12072-12083. DOI: 10.1021/acs.jafc.9b05197

Stiegler, V.; Scholz, B.; Engel, K.-H., Acyl Chain Oxidation Products Formed Upon Heat Treatment of Phytosteryl and Phytostanyl Fatty Acid Esters. *4th International Symposium on Lipid Oxidation and Antioxidants* **2022**, Vigo, Spain.